Quadratic Spline Based Numerical Schemes for Different Classes of Singularly Perturbed Problems

THESIS

Submitted in partial fulfillment of the requirements

for the degree of

DOCTOR OF PHILOSOPHY

by

Satpal Singh

ID No. 2019PHXF0425P

Under the Supervision of

Prof. Devendra Kumar

Birla Institute of Technology and Science, Pilani, Pilani Campus, India

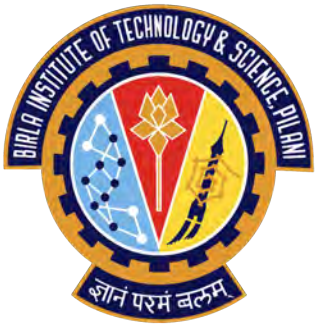

BIRLA INSTITUTE OF TECHNOLOGY AND SCIENCE, PILANI

Pilani Campus, Rajasthan, India

[2024]

BIRLA INSTITUTE OF TECHNOLOGY AND SCIENCE, PILANI

PILANI CAMPUS, RAJASTHAN, INDIA

CERTIFICATE

This is to certify that the thesis entitled, **"Quadratic Spline Based Numerical Schemes for Different Classes of Singularly Perturbed Problems"** and submitted by **Mr. Satpal Singh** ID No. **2019PHXF0425P** for the award of Ph.D. degree of the institute embodies original work done by her under my supervision.

_____

Signature of the Supervisor

Name : **PROF. DEVENDRA KUMAR**

Designation : **Professor, Department of Mathematics, BITS**

Pilani, Pilani Campus

Date: __/__/____

Dedicated to
My Beloved Family

ACKNOWLEDGEMENTS

It is said that if good people are found in the journey, even the most difficult journey becomes easy. Based on my experiences in my Ph.D. journey, this saying is absolutely true. In this journey, I have met very lovely and encouraging people. There can't be a better time and opportunity to thank them from the bottom of my heart.

I would like to express my deepest thanks and admiration to my respected thesis supervisor, Prof. Devendra Kumar. Throughout this time, his incalculably helpful direction and unflagging support have been indispensable. Under the guidance of my acclaimed mentor, I have experienced a broadening of my thinking abilities and improved my ability to think innovatively. He has shown me tremendous patience and encouragement while also allowing me entire creative freedom in my work. His vast knowledge and unwavering commitment to improving himself have been a driving force in my own quest for perfection. His kindness, generosity, thoroughness, diligence, and perseverance have made an everlasting imprint on me, and he has inspired me to push myself to be a better person.

In addition, I am grateful to all of the professors in the Mathematics Department at the Pilani Campus of BITS Pilani for their assistance and insightful recommendations throughout my research work. I consider myself extremely lucky to have Dr. Ashish Tiwari and Dr. Rajesh Kumar as members of my Doctoral Advisory Committee (DAC), since their consistent support as well as encouragement, allowed me to concentrate on my work. My work has been improved at various phases as a direct result of their comments and ideas.

I also express my deep appreciation to UGC, New Delhi, India, for providing financial assistance and facilities that enabled me to successfully complete the requirements for my doctoral degree. I would also like to express my gratitude to the members of the department office who assisted me during these years for every kind of help.

We thank Prof. Jesus Vigo-Aguiar and Prof. Higinio Ramos of Universidad de Salamanca, Salamanca, Spain, and Dr.Vembu Shanthi of National Institute of Technology, Tiruchirappalli for essential guidance whenever it was needed.

This undertaking would not have been feasible without the unwavering ethical backing and steadfast trust exhibited by my parents (Late Shri Ramkishan and Smt. Saraswati Devi), which has provided me with energy throughout this endeavor. I lost my father during this time, but I still remember his teachings and will try to glorify his name in my future life. My brother, Mainpal Singh, is also an equal share in my achievement. His way of seeing life and dutifulness always motivated me. I want to express my profound appreciation to my friends, whose constant encouragement and friendship have enriched my educational experience. I sincerely appreciate the humor, company, and maturity they have added to my life; their

appearance has served as a continual reminder that life beyond academics is just as vital as the quest for knowledge.

I would like to extend my gratitude to all individuals who have provided assistance, whether directly or indirectly, throughout my tenure at BITS PILANI, Pilani Campus. Ultimately, I express reverence towards the omnipotent deity who facilitated the realization of all my endeavors.

Place: BITS Pilani, Pilani Campus
Date: __/__/____ **(Satpal Singh)**

ABSTRACT

The fundamental objective of this thesis is to introduce numerical methods based on quadratic spline techniques, focusing primarily on attaining uniform convergence. The approaches presented in this study are specifically developed to tackle a diverse range of singularly perturbed problems (SPPs). These issues include various scenarios such as degenerate parabolic problems, systems of SPPs, and higher-order SPPs. These problems make their existence known in various physical phenomena found in research and engineering. Two noteworthy examples are the investigation of the behavior of DC motors and the chemical flow reactor theory field. In the upsurge, their influence may be seen in areas such as lubrication theory, the investigation of transport phenomena encountered in chemistry and biology, population dynamics, neural networks, and the study of fluid flow via unsaturated absorbent media. The presence of differential equations in which the higher-order spatial derivative(s) is/are scaled by very small parameters allows for identifying such problems. Indeed, any ordinary/partial differential equations (ODEs/PDEs) that display rapid changes in some provinces of their specified domain are called SPPs. As a development, the presence of boundary layers is a distinctive attribute, leading to the formation of narrow regions near the domain's boundary. In these specified zones, when the perturbation parameter tends toward zero, there is a prominent increase in the steepness of the solution's gradient. The standard numerical methods are inadequate in capturing the layer behavior of the solution and fail to give satisfactory results.

This thesis aims to make progress in the design, analysis, and advancement of numerical methods that exhibit parameter uniformity, particularly in their use for solving SPPs. There are two commonly employed ways of addressing these issues. One approach involves using fitted-operator techniques, which effectively capture the characteristics of the solution inside the boundary layers and can be easily implemented on a mesh with equidistant spacing. In contrast, the other approach involves the utilization of layer-adapted meshes. Fitted operator approaches employ a uniform mesh, rendering them easily implementable and facilitating a more straightforward convergence analysis than methods relying on non-uniform meshes. One of the primary limitations of these approaches is the inability to establish a ε-uniform

fitted operator method on an equidistant mesh in the presence of parabolic boundary layers inside the solution. A further aspect that needs refinement in this technique is the challenges of applying these strategies to multidimensional problems inside intricate domains. In addition, the utilization of fitted mesh techniques necessitates acquiring information about the precise positioning and thickness of the boundary layers to build non-uniform grids that are suitably tailored for the given application. This phenomenon governs the progression of numerical techniques that exhibit parameter uniformity, meaning that the error constant is unaffected by variations in the perturbation parameter ε and the mesh parameter. Within this particular context, the mesh is generated by utilizing pre-established knowledge of the behavior of the solution. The exponentially graded mesh (eXp mesh) is characterized by its unique approach of not explicitly identifying transition points during changes in the layer's behavior, differentiating it from Bakhvalov and Shishkin meshes.

The thesis commences with a brief introduction that outlines the objectives and explains the motivation for studying SPPs. At first, a numerical scheme is developed to solve singularly perturbed convection-diffusion type degenerates parabolic problems. As the perturbation parameter approaches zero, the solution to this problem exhibits a parabolic boundary layer in the neighborhood of the left end side of the domain. The proposed approach employs the Crank-Nicolson methodology on a uniformly distributed temporal mesh and the quadratic spline collocation method on an eXp mesh in space. Later, we presented the analysis for singularly perturbed arbitrary systems of ODEs/PDEs. We derived the robust error estimates to establish the optimal order of convergence. The findings from numerical investigations provide empirical evidence that supports the theoretical conclusions and validates the efficiency and correctness of the suggested method.

Extending our work from second-order problems to higher-order problems, we present spline-based techniques for fourth-order convection-diffusion/reaction-diffusion type problems. The associated DE is converted into a strong/weakly coupled system of two singularly perturbed ODEs with Dirichlet boundary conditions to solve the problem numerically. One of the equations in the system is independent of the perturbation parameter. The calculated theoretical bounds on the spline interpolation error show that the method is second-order parameter-uniformly convergent. In the final section of the thesis, we examine possible paths

for further expanding the research undertaken in this study.

Contents

List of Tables

List of Figures

Chapter 1

Introduction

1.1 Singular perturbation problems

Numerous scientific and technological domains are plagued by singular perturbation problems (SPPs), a class of mathematical complications. The SPPs field has developed throughout its history, boasting a substantial historical context, and it persists in harboring considerable promise for generating beneficial advancements in diverse scientific and technical fields. This discussion pertains to the extensive range of applications within several domains of applied mathematics, including but not limited to fluid dynamics, the characterization of fluctuations arising from turbulent motion in waves and currents, heat and mass transfer in the fields of nuclear and chemical engineering, quantum physics, and electroanalytic chemistry. The presence of differential equations in which very small parameters scale the highest-order spatial derivative allows for identifying such problems. These issues manifest themselves in mathematical models with steep gradients, quick transitions, and the interplay of numerous scales due to the enormous diversity in the scales of the controlling processes. Among the many applications of SPPs, the Navier-Stokes equation in fluid dynamics stands out as an especially striking example

$$\frac{\partial U}{\partial t} + U\frac{\partial U}{\partial x} + V\frac{\partial U}{\partial y} + \frac{\partial P}{\partial x} = \frac{1}{Re}\left(\frac{\partial^2 U}{\partial x^2} + \frac{\partial^2 U}{\partial y^2}\right), \tag{1.1.1}$$

with the appropriate set of conditions. P is the pressure, and U, V represents the velocity in the x and y directions, respectively. '*Re*' is the well-known 'Reynolds number', which shifts in a manner that is inversely proportional to the fluid's kinematic viscosity and fluctuates directly in proportion to the characteristic length and the characteristic velocity. Taking very large value ($\gg 1$) of '*Re*', Equation (1.1.1) becomes singularly perturbed. Other interesting examples include systems of parabolic singularly perturbed convection-diffusion issues, including the enzyme model with diffusion and convection, the neutron transport phenomenon with sufficiently relatively small diffusion coefficients, and the tubular model in chemical reactor theory. For illustration, think of an enzyme-substrate model with convection-diffusion as follows:

$$\begin{aligned}
&\mathbb{T}_t - \mathbb{D}_1\nabla^2\mathbb{T} + \vec{b}\cdot\nabla\mathbb{T} = \mathcal{K}_{-1}\mathbb{R} - \mathcal{K}_1\mathbb{E}\mathbb{T},\\
&\mathbb{R}_t - \mathbb{D}_2\nabla^2\mathbb{R} + \vec{b}\cdot\nabla\mathbb{R} = \mathcal{K}_1\mathbb{E}\mathbb{T} - (\mathcal{K}_{-1}+\mathcal{K}_2)\mathbb{R},\\
&\mathbb{E}_t - \mathbb{D}_2'\nabla^2\mathbb{E} + \vec{b}\cdot\nabla\mathbb{E} = (\mathcal{K}_{-1}+\mathcal{K}_2)\mathbb{R} - \mathcal{K}_1\mathbb{E}\mathbb{T},\\
&\mathbb{P}_t - \mathbb{D}_3\nabla^2\mathbb{P} + \vec{b}\cdot\nabla\mathbb{P} = \mathcal{K}_2\mathbb{R},
\end{aligned}$$

where $\mathbb{T}$, $\mathbb{P}$, $\mathbb{E}$ represent substrate, enzyme and product, respectively and $\mathcal{K}_{-1}$, $\mathcal{K}_1$ and $\mathcal{K}_2$ are reaction rates. The enzyme-substrate complex is denoted by $\mathbb{R} = \mathbb{T}\mathbb{E}$ and $\vec{b}$ is the velocity of the convecting fluid. Further developments on this model can be seen in [1, 2]. We also talk about a Turing model given by Dillon *et al.* [3] that features pattern formation using reaction-diffusion equations with Robin boundary conditions

$$\begin{cases}
\dfrac{\partial\mathbb{Y}}{\partial t} = \mathcal{Y}\nabla^2\mathbb{Y} + \widetilde{R}(\mathbb{Y},\tilde{p}) \ \text{ on } \mathcal{S},\\
n\cdot\mathcal{Y}\nabla\mathbb{Y} = \mathbb{H}(\mathbb{Y}^* - \mathbb{Y}) \ \text{ on } \partial\mathcal{S},\\
\mathbb{Y}(r,0) = \mathbb{Y}_0(r).
\end{cases} \tag{1.1.2}$$

Equation (1.1.2) is transformed into the following equation introducing non-dimensionalization parameters and linearization (see [3])

$$\begin{cases} \dfrac{\partial \chi}{\partial \tau} = \mu \mathcal{D} \nabla^2 \chi + \mathbb{K}\chi \ \text{ on } \mathcal{S}, \\ n \cdot \nabla \chi = -\mathcal{Q}\chi \ \text{ on } \partial\mathcal{S}, \\ \chi(\eta, 0) = \chi_0(\eta), \end{cases} \tag{1.1.3}$$

where $\mathbb{Y}$ and $\mathbb{Y}^*$ are vectors of varying and fixed chemical concentrations. $\mathcal{Y}$ and $\mathbb{H}$ are diagonal matrices, where $\mathcal{Y}$ is positive definite and $\mathbb{H}$ includes mass transfer coefficients, and resultant production rate is denoted by $\widetilde{R}$. Deflection due to the tensile force of a load is another noteworthy example, and it occurs when a defined load is delivered to a flexible beam (with limited flexural stiffness). The modeling of these problems leads to the Orr-Sommerfield equation [4, 5]

$$\mathcal{E}\mathcal{I} z^{(4)}(x) - \left(\mathcal{N}_0 \frac{\mathcal{E}\mathcal{A}}{2L} \int_0^L (z'(x))^2 dx \right) z'' = f(x), \ 0 \leq x \leq L,$$

where $\mathcal{A}$, $L \rightarrow$ cross-sectional area and length of the beam, $E \rightarrow$ Young's modulus, $I \rightarrow$ moment of inertia, $N_0 \rightarrow$ initial axial tension in the beam. Books by Morton [6], O' Malley [4], Pao [7], Linß [8] and Roos *et al.* [9] provide more information on the practical use of singularly perturbed differential equations.

During the Third International Congress of Mathematicians in Heidelberg in 1904, Prandtl [10] came up with the concept that was later be known as the "boundary layer". Prandtl dug into the substantial influence that even minute variables like viscosity have in ordinary fluids such as water and air, highlighting their importance in flow dynamics in his seven-page study on boundary layer theory. The paper was thorough and covered all aspects of the idea. This ground-breaking theory served as the foundation for developing contemporary fluid dynamics. Although Prandtl was the one who initially presented the concept of a "boundary layer", Wasow [11], who made significant contributions, is mainly credited with bringing to light the term's broader relevance. After that, the phrase "singular perturbation" was first used in 1946 in Friedrichs and Wasow's work, described in their article [12] presented at New York University.

In the subsequent section, we will provide a concise overview of the concept of the

singular perturbation issue, as it is frequently formulated in its most straightforward and widely employed structure. Singular perturbations occur in differential equations due to small parameter(s) in the product of higher-order spatial derivative(s). The term 'singular' perturbation emerges when these parameter(s) approaches zero, resulting in an ill-posedness to the problem as the order of the differential equation reduces by at least one. At the same time, the boundary conditions (BCs) stay the same. The presence of these parameter(s) causes the solution to be multiscale. Narrow sections are termed layer areas, and they emerge where the solution changes abruptly due to high gradients while the solution continues smoothly in the remaining domain. In most cases, boundary/interior layers are present when addressing issues involving such equations.

Mathematically, first, we consider a singularly perturbed boundary value problem; say T_ε,

$$\begin{aligned} -\varepsilon y''(x) + a(x)y'(x) + b(x)y(x) &= f(x), \quad c < x < d, \\ y(c) = \alpha, \quad y(d) &= \beta. \end{aligned} \tag{1.1.4}$$

where $0 < \varepsilon \ll 1$, $a(x)$, $b(x)$, and $f(x)$ are sufficiently smooth functions. Assuming that, for each ε, the problem T_ε has a unique smooth solution $y_\varepsilon(x)$, we aim to construct approximations of $y_\varepsilon(x)$ for small values of ε. The solution $y_\varepsilon(x)$ of T_ε depends on ε and BCs as well. Now we obtain the 'reduced problem' T_0 having the solution y_0, by putting $\varepsilon = 0$ in (1.1.4)

$$\begin{aligned} -a(x)y'(x) + b(x)y(x) &= f(x), \quad c < x < d, \\ y(c) = \alpha, \quad y(d) &= \beta, \end{aligned} \tag{1.1.5}$$

Now, y_0, the solution to the reduced problem (1.1.5) need not necessarily satisfy all the BCs. For a layperson, these questions can arise

- Does the problem (1.1.4) has a limiting solution as $\varepsilon \to 0$, *i.e.,* does $\lim_{\varepsilon \to 0} y_\varepsilon(x)$ exist?
- If yes, then
  - (i) Does this solution satisfy the Equation (1.1.5), *i.e.,* does $\lim_{\varepsilon \to 0} y_\varepsilon(x) = y_0(x)$ hold true?

(ii) Which of the BC(s) will be satisfied by the limiting solution?

The problem T_ε is called regularly perturbed if the solution $y_\varepsilon(x)$ approaches uniformly to $y_0(x)$ as $\varepsilon \to 0$, otherwise, T_ε is said to be singularly perturbed. In the literature, some researchers deliver the subsequent characterization of SPPs

- Miller *et al.* [13] :

  The justification for the name 'singular perturbation' is that the nature of the differential equations changes completely in the limit case when the singular perturbation parameter is equal to zero.

- Roos *et al.* [14] :

  They are differential equations (ordinary or partial) that depend on a small positive parameter ε and whose solutions (or their derivatives) approach a discontinuous limit as ε approaches zero. Such problems are said to be singularly perturbed, where we regard ε as a perturbation parameter.

- Linß [8] :

  Let B be a function space with norm $\|\cdot\|_B$. Let $D \subset \mathbb{R}^d$ be a parameter domain. The continuous function $u : D \to B$, $\varepsilon \mapsto u(\varepsilon)$ is said to be regular for $\varepsilon \to \varepsilon^* \in \partial D$ if there exists a function $u^* \in B$ such that:

$$\lim_{\varepsilon \to \varepsilon^*} \|u_\varepsilon - u^*\|_B = 0,$$

  otherwise u_ε is said to be singular for $\varepsilon \to \varepsilon^*$.

Considering (1.1.4) as our reference problem, we see the summary of various linear problems that will be very helpful in our further study.

Table 1.1: Different classes of SPPs

Conditions on $a(x)$	Position of layer
$a(x) \neq 0$ on $c \leq x \leq d$:	
$a(x) < 0$	Boundary layer at $x = c$
$a(x) > 0$	Boundary layer at $x = d$
$a(x) = 0$:	
$b(x) > 0$	Boundary layers at $x = c$ and $x = d$
$b(x) < 0$	Oscillatory solution
$b(x)$ changes sign	Classical turning point
$a'(x_0) \neq b(x_0)$, $a(x_0) = 0$:	
$a'(x_0) < 0$	Only interior layer at x_0
$a'(x_0) > 0$	Boundary layers at $x = c$ and $x = d$

Let us take one example to confirm the previous analogy.

Example 1.1.1. $-\varepsilon y'' + y' = 1$ *on* $(0, 1), \quad y(0) = y(1) = 0$, *with exact solution* $y(x) = x - \dfrac{e^{-\frac{1-x}{\varepsilon}} - e^{-1/\varepsilon}}{1 - e^{-1/\varepsilon}}$.

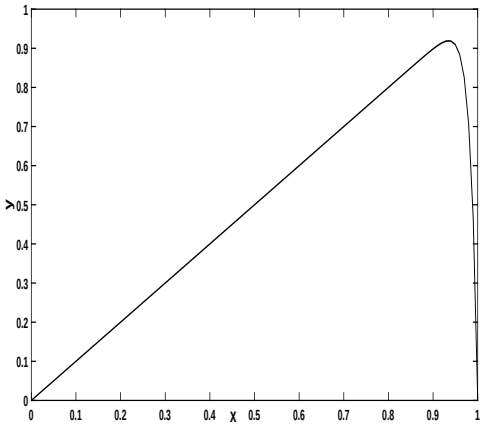

Figure 1.1: Exact Solution for $\varepsilon = 2^{-8}$

For any $a \in [0, 1)$,

$$\lim_{x \to a} \lim_{\varepsilon \to 0} y(x) = a = \lim_{\varepsilon \to 0} \lim_{x \to a} y(x),$$

but

$$1 = \lim_{x \to 1} \lim_{\varepsilon \to 0} y(x) \neq \lim_{\varepsilon \to 0} \lim_{x \to 1} y(x) = 0.$$

The phenomenon known as the appearance of an unequality, which may be observed at a specific moment (for example, when $x = 1$ in this scenario), indicates that the problem is singularly perturbed. The unequality implies that the solution $y(x)$ changes abruptly as x approaches 1; we say there is a boundary layer at $x = 1$.

There are two distinct layers, namely, the parabolic and regular layers, discussed in the academic literature. If the characteristic of the reduced problem is parallel to the boundary, it is called parabolic; otherwise, it is regular. It is possible for a layer to appear at the intersection or corner of the domain, in which case it is called a "corner layer". Standard numerical methods on an equidistant mesh fail to produce satisfactory approximations because large oscillations appear near the layer region(s). In other words, we can generate a scheme on an equidistant mesh that converges at all mesh points uniformly in the diffusion parameter unless an unacceptably large number of mesh points are used. It is not practical at all; thus, to resolve the layer(s), a non-uniform mesh is required. Because of these difficulties, researchers across applied mathematics and engineering disciplines have been more interested in finding numerical solutions for singularly perturbed problems.

1.2 Challenges in solving the singularly perturbed problems

Explaining singularly perturbed situations presents a formidable undertaking because of the distinctive attributes inherent in these problems. Below is a pointwise representation enumerating many significant obstacles commonly encountered in solving singularly perturbed problems:

- **Stiffness and Rapid Changes.** These problems frequently encompass rapidly changing or steep gradients, making numerical approaches susceptible to stability concerns and oscillatory behavior. Standard numerical methods might result in omitting crucial data while estimating the solution in areas characterized by fast change.

- **Multiple Scales.** The issues mentioned above demonstrate the presence of various scales, posing a significant challenge in effectively capturing them. Traditional approaches often require highly refined grids and expensive computational resources.

- **Layers.** Layers are commonly observed in singular perturbation problems, characterized by fast variations in the solution at specified boundaries and/ or the domain's interior. Effectively resolving these layers can provide a significant challenge.

- **Scaling Parameters.** The selection of scaling parameters can have a substantial influence on the numerical solution, and the process of choosing suitable scales is frequently challenging.

- **Mesh Selection.** The selection of mesh, referring to the spatial discretization technique, has the potential to impact both the precision and stability of the solution. Choosing the most suitable mesh can sometimes provide a significant challenge.

- **Oscillatory Solutions.** Fluctuations in the solution, especially around transition areas, can be introduced by numerical techniques and mask the system's actual behavior.

- **Sensitivity of the Parameter.** Identifying robust numerical algorithms that may effectively address various circumstances can be challenging because of the high sensitivity of the solution to parameter changes.

- **Confirmation and Verification.** Validating the correctness of numerical solutions can be difficult, mainly when a comparable analytical solution is not readily accessible for comparison.

To effectively address these obstacles, one must have a comprehensive knowledge of the mathematical and physical concepts behind them and the ability to create and implement specialized numerical algorithms customized to the particular qualities of singularly perturbed systems.

1.3 Concise literature survey on proposed model problems

The investigation of SPPs may be broken down into two separate classes: the first is through the many landscapes of asymptotic analysis, which provides insights into the qualitative core of the problem. Due to the inherent challenges associated with asymptotic analysis, researchers often seek alternate methodologies. Consequently, numerical analysis has emerged

as a viable tool for addressing SPPs, which reveals the quantitative complexities and necessitates an in-depth understanding of the solution's complexities to succeed. It is a dual voyage in which one participant obtains profound knowledge while the other separates the complexities with the desire for a deep understanding.

In the context of asymptotic analysis, the primary aim is to develop a refined analytical approximation for solving a differential equation that cannot be explicitly solved. It is accomplished through the skillful application of asymptotic expansion techniques. A differential equation of lower order is obtained through a straightforward asymptotic expansion using a sequence dependent on the perturbation parameter. This results in an eventual consequence: the asymptotic expansions might not satisfy all initial or boundary requirements. The approach entails decomposing the expansion inside the initial variables' domain, sometimes called the "*outer expansion*". The validity of this expansion remains independent of the boundary layers. Nevertheless, the true phenomenon occurs when we effectively incorporate the "*inner expansion*" strategically located in the layer region. The enigmatic BCs find their counterpart within this domain that closely adheres to its boundaries, culminating in the complicated interplay of these dual expansions. The inner expansion elegantly manifests through stretched variables, imparting a certain rhythmic quality to the equation. Simultaneously, in a distinct rhythm, the outer expansion gradually reveals itself through the recognizable manners of the first independent variable. The matching of these expansions reaches its pinnacle through an agreeable convergence, carefully managed at the boundary layer's periphery. The approach of *matched asymptotic expansion* can be likened to a lyrical dance, wherein the inner and outer expansions achieve a state of harmony. This technique transforms mathematical steps into a harmonious tango of variables. For a comprehensive introduction to asymptotic techniques, see Nayfeh [15], O'Malley [16, 17], Bellman [18], Smith [19] and reference therein.

When solving SPPs on a uniform grid, traditional computational methods such as regular finite difference, finite element, or finite volume approaches have constraints. A large number of mesh points are required to achieve the needed accuracy as $\varepsilon \to 0$, corresponding in magnitude to the perturbation parameter, significantly increasing the system size and causing inadequate performance. The set of algebraic equations necessarily grows more prominent as the problem's dimension increases, which raises computation costs proportionally. This

problem emphasizes the need for uniform numerical methods, which reduce the negative effects of computational complexity by maintaining the independence of the convergence order and error constants from the perturbation parameter.

SPPs can be solved using various numerical approaches available in numerical analysis. Beginning with Pearson's contributions [20, 21], Kadalbajoo *et al.* [22–25] published a comprehensive analysis of numerical approaches for dealing with SPPs from 1980 to 2009. These survey articles help to understand the development of various numerical techniques developed for SPPs.

Various articles have been published on the numerical findings of singularly perturbed turning point problems (SP-TPPs). We cite some of those (for further results, the readers are referred to the references therein). In 1993, Vulanović and Farrell [26] proposed a first-order exponentially fitted scheme for SPBVP with multiple turning points at a boundary. They also presented an improved modification on a special discretization mesh. Natesan and Ramanujam [27] used a combination of classical numerical methods and exponentially fitted difference schemes for solving SP-TPPs exhibiting twin boundary layers. Later, in 2003, Natesan *et al.* [28] suggested an almost first-order robust numerical method on a Shishkin mesh to solve SP-TPPs exhibiting two exponential boundaries. A literature review between 1970 and 2011 on asymptotic and numerical analysis of SP-TPPs can be seen in [29]. Kumar [30] proposed an almost second-order parameter-uniform scheme comprising cubic B-spline basis functions on a Shishkin mesh to solve differential-difference SP-TPPs whose solutions exhibit interior or twin boundary layers. In [31], he constructed a quintic B-spline parameter-uniform scheme for SP-TPPs showing interior or twin boundary layers. Recently, Alam *et al.* [32] proposed a parameter-uniform trigonometric quintic B-spline collocation method to solve SP-TPPs whose solutions exhibit interior/twin boundary layers.

Starting in the late 1960s, in this evolution process, several numerical methods (independent of ε) have been constructed for a scalar reaction-diffusion equation (see, [33–35] and the references therein). On the other hand, less effort has been devoted to systems of reaction-diffusion boundary value problems. For a system of two coupled singularly perturbed reaction-diffusion equations, with diffusion coefficients $\varepsilon_1, \varepsilon_2$, depending on the relation and values of ε_1 and ε_2 three cases are of interest (i) $\varepsilon_1, \varepsilon_2$ arbitrary, (ii) $\varepsilon_1 = \varepsilon, \varepsilon_2 = 1$, and (iii)

$\varepsilon_1 = \varepsilon_2 = \varepsilon$ (see [36]). Some schemes and their corresponding convergence analyses for these particular cases can be seen in [37–39], where a parameter-uniform convergence of the first order was established. We cite some works about systems of SPBVPs: Matthews *et al.* [40] proposed classical finite difference operators with special piecewise-uniform meshes to solve a system of two coupled reaction-diffusion equations. Madden and Stynes [41] suggested the first-order parameter-uniform central difference scheme with a variant of Shishkin mesh for a coupled system of two singularly perturbed linear reaction-diffusion equations. Using the basic ideas of the perturbation method, Valanarasu and Ramanujam [42] suggested exponentially fitted FDMs to solve a class of weakly coupled systems of singularly perturbed reaction-diffusion equations. For a coupled system of equations containing different magnitudes diffusion parameters, Linß and Madden [43] considered a central difference scheme on layer-adapted piecewise uniform meshes. They established that their scheme is almost second-order parameter-uniform convergent, which improves the scheme proposed in [41]. Linß and Madden [44] suggested a FEM on general layer-adapted meshes (Shishkin and Bakhvalov meshes) for a system of two coupled reaction-diffusion equations. They have shown that the method is of first-order and almost first-order (up to a logarithmic factor) parameter-uniform convergent with Bakhvalov and Shishkin meshes, respectively. Natesan and Deb [45] devised a second-order uniformly convergent hybrid scheme for a singularly perturbed system of reaction-diffusion equations. The scheme comprises a cubic spline scheme in the layer region and the classical central difference scheme elsewhere. Clavero *et al.* [46] presented a non-monotone FDM of HODIE type on a Shishkin mesh for the coupled systems of singularly perturbed reaction-diffusion equations. They have shown that the scheme is a parameter-uniform convergent of orders two and three in the cases of different and equal diffusion parameters, respectively. They have also addressed a hybrid FDM of HODIE type on a piecewise uniform Shishkin mesh for the coupled systems of singularly perturbed reaction-diffusion equations [47]. They have shown that the discretized operator satisfies the discrete maximum principle, and the scheme is almost a third-order parameter-uniform convergent (except for a logarithmic factor).

Das and Natesan [48] proposed a second-order central difference scheme with the adaptively generated graded mesh for a system of coupled singularly perturbed reaction-diffusion

equations. In the system, they have taken diffusion parameters with different magnitudes. Lin and Stynes [49] considered a FEM for a system of coupled reaction-diffusion equations, where each equation has the same diffusion coefficient. The method was used with a Shishkin mesh and showed an almost first-order convergent, independent of the magnitude of the diffusion parameter. Constructing an adaptive layer mesh using the equidistribution principle for a positive monitor function, Das and Aguiar [50] proposed an accurate second-order scheme for a system of reaction-diffusion equations. Singh and Natesan [51] applied the nonsymmetric discontinuous Galerkin FEM with interior penalties on a piecewise-uniform Shishkin mesh to obtain the numerical solution of a system of reaction-diffusion equations. They have shown that the method is k-th order uniformly convergent in the energy norm, where k is the polynomial degree. In some of the above articles, the equations have diffusion parameters of different magnitudes, while diffusion parameters of the same magnitudes were taken in some works.

Later on, an extension in terms of $\ell \geq 2$ (an arbitrary system) singularly perturbed equations were given by Linß and Madden [43, 52] in which they improved the accuracy from first-order to second-order. Gracia *et al.* [53] considered a singularly perturbed system with an arbitrary number of parabolic reaction-diffusion equations. For the arbitrary system of linear SPPs (reaction-diffusion type) in two space dimensions, the readers are referred to Kellogg *et al.* [54, 55]. Using the Bakhvalov and Shishkin meshes in their analysis, they obtained convergence of $O(N^{-2})$ and $O(N^{-2}\ln^2 N)$ respectively, where N is the degree of freedom. In the literature, we see posterior meshes whose construction does not require prior knowledge of layers like width and location. These meshes use the idea of equidistribution using a positive, strictly monotonically increasing monitor function. Das and Natesan [48] developed their numerical technique using adaptively generated mesh and proved second-order uniform convergence for systems of arbitrary size ($\ell \geq 2$). Das *et al.* [56] constructed a first-order accurate numerical technique on the equidistributed mesh using a combination of backward and forward difference schemes. Later, they enhanced the order of accuracy by two using spline approximations. Refer to [57–60] and references therein for more studies on equidistributed meshes for different types of SPPs. High-order numerical methods help to provide more precise numerical approximations using the equivalent computational cost

of other numerical schemes. Clavero *et al.* [47, 61] presented almost third-order parameter-uniform numerical methods for singularly perturbed systems of reaction-diffusion ordinary and parabolic partial differential equations. For an arbitrary singularly perturbed system of reaction-diffusion problems, a uniformly convergent Schwarz domain decomposition method (of almost fourth-order) was proposed by Rao and Kumar [62]. For a semilinear system of SPPs (reaction-diffusion type), Kumar and Kumar [63] developed a uniformly convergent (almost fourth-order) hybrid numerical method on a generalized Shishkin mesh. In [64], Das and Natesan proposed a hybrid scheme using cubic spline approximations for reaction-diffusion Robin-type BVPs. Interested readers may refer to different classes of singularly perturbed problems like a discontinuity in source and convection terms in two-parameter problems [65–67].

In the literature, a linear model is considered when a thin elastic plate is clamped under tension by a load applied vertically to the plane of the longitudinal axis. Semper [68] considered the following fourth-order elliptic PDE

$$\begin{aligned} &\varepsilon^2\Delta^2 Y - \nabla\cdot(a\nabla Y) = f(x,y),\ (x,y)\in\Omega\subseteq\mathbb{R}^2,\\ &Y = \frac{\partial Y}{\partial n} = 0,\ \text{on } \partial\Omega, \end{aligned}$$

where $\varepsilon = \dfrac{\text{bending rigidity of plate}}{\text{tensile stiffness in the plate}}$, $f(x,y)$ represents transverse load and the solution $Y(x,y)$ indicates the displacement of the plate. Franz and Roos [69] also considered fourth-order elliptic PDE concerning the plate bending problem

$$\begin{aligned} &\varepsilon^2\Delta^2 Y - b\Delta Y + (c\cdot\nabla)Y + dY = f(x,y),\ (x,y)\in\Omega=(0,1)^2,\\ &Y = \frac{\partial Y}{\partial n} = 0,\ \text{on } \partial\Omega. \end{aligned}$$

Using a non-uniform mesh (generated by the equidistribution principle), Gupta and Kaushik [70] proposed a higher-order hybrid numerical technique and proved optimal convergence (independent of any logarithmic factor). Different types of *hp* FEM were implemented by Panaseti *et al.* [71] and Constantinou *et al.* [72] on the Spectral Boundary Layer Mesh. In [73], Constantinou considered *h* version of FEM using Hermite polynomials on exponentially

graded mesh (eXp mesh) and showed uniformly convergent results in the energy norm and balanced norm.

1.4 Motivation

The widespread occurrence of singularly perturbed problems across various scientific and engineering subfields served as the impetus for the author of this thesis to delve into the world of singularly perturbed issues. Mathematical complexities that are difficult to solve using traditional computing methods frequently arise when there is a significant change in the scales of the phenomena regulating the situation. It can cause the challenges described above.

Understanding how to deal with singularly perturbed issues successfully is essential because these challenges encompass situations in which relatively few adjustments to a parameter can significantly affect the system's behavior. These phenomena are not only academic curiosities but also reflections of events that occur in the real world. Some examples include the boundary layer phenomena in fluid dynamics, the design of electronic circuits, and chemical processes. Therefore, becoming proficient in the numerical methods that may be used to tackle these issues is essential to the progression of knowledge and technology in various fields.

In addition, SPPs are commonly utilized as a crucible for the testing and improvement of numerical techniques. Our mathematical toolbox will be expanded due to successfully navigating these hurdles, and our ability to solve problems in more broad contexts will be enhanced due to this expansion. Our capability to deal with systems that contain elements on several scales is improved, which is necessary in today's technologically advanced society.

In conclusion, the desire to decipher the complexities of SPPs is the impetus for this thesis. These problems are intriguing not just from a theoretical standpoint but also for the practical insights they bring across a wide range of academic fields. By acting in this manner, we contribute to the overarching goal of overcoming complex challenges and effectively using the potential of numerical analysis to further scientific comprehension and technological innovation.

1.5 Model problems

We investigate five model problems numerically as part of this thesis, which are stated in the following manner.

1. We consider a degenerate parabolic convection-diffusion IBVP in the rectangular domain $\mathcal{G} = \mathcal{G}_x \times \mathcal{G}_t = (0,1) \times (0,T]$ for some finite positive T:

$$\mathcal{L}_{x,\varepsilon} u(x,t) \equiv \varepsilon \frac{\partial^2 u}{\partial x^2} + b(x,t)\frac{\partial u}{\partial x} - c(x,t)\frac{\partial u}{\partial t} - d(x,t)u = f(x,t),\ (x,t) \in \mathcal{G},$$

with the conditions

$$u(x,0) = \mathcal{V}(x),\ x \in [0,1],\ u(0,t) = p_0(t),\ u(1,t) = p_1(t),\ t \in [0,T],$$

where $0 < \varepsilon \ll 1$ is a perturbation parameter. The boundary of the domain $\mathcal{G}$ is defined as $\partial\mathcal{G} = \overline{\mathcal{G}} \backslash \mathcal{G}$. We assume that the coefficients $b(x,t)$, $c(x,t)$, and $d(x,t)$ satisfy

$$\begin{aligned} &b(x,t) = b_0(x,t)x^p,\ p \geq 1,\ (x,t) \in \overline{\mathcal{G}}, \\ &b_0(x,t) \geq \beta > 0,\ c(x,t) \geq \gamma > 0,\ d(x,t) \geq \delta \geq 0,\ (x,t) \in \overline{\mathcal{G}}. \end{aligned}$$

Generally, a parabolic boundary layer of width $O(\sqrt{\varepsilon})$ appears to solve the problem at the left lateral surface as ε approaches zero.

2. We consider a system of ℓ weakly coupled reaction-diffusion equations whose solution $\boldsymbol{u} \in (C^2(0,1) \cap C[0,1])^\ell$ satisfies

$$\begin{aligned} &\boldsymbol{\mathcal{L}u}(x) := -\boldsymbol{\mathcal{E}u}''(x) + \boldsymbol{B}(x)\boldsymbol{u}(x) = \boldsymbol{g}(x), \quad x \in (0,1), \\ &\boldsymbol{u}(0) = \boldsymbol{\varrho}_0, \quad \boldsymbol{u}(1) = \boldsymbol{\varrho}_1, \end{aligned}$$

where $\boldsymbol{\mathcal{L}} = (\mathcal{L}_1, \ldots, \mathcal{L}_\ell)^T$, $\boldsymbol{\mathcal{E}} = \text{diag}(\varepsilon_1^2, \varepsilon_2^2, \ldots, \varepsilon_\ell^2)$ with $\varepsilon_k = \varepsilon,\ k = 1,2,\ldots,\ell$, $\boldsymbol{B}(x) = (b_{ij}(x))_{\ell\times\ell}$, $\boldsymbol{g}(x) = (g_1(x), g_2(x), \ldots, g_\ell(x))^T$, $\boldsymbol{u}(x) = (u_1(x), u_2(x), \ldots, u_\ell(x))^T$, $\boldsymbol{\varrho}_0 = (\varrho_{0,1}, \ldots, \varrho_{0,\ell})^T$, and $\boldsymbol{\varrho}_1 = (\varrho_{1,1}, \ldots, \varrho_{1,\ell})^T$. We assume that each column of the coupling matrix $\boldsymbol{B} : [0,1] \to \mathbb{R}^{(\ell,\ell)}$ and the function $\boldsymbol{g} : [0,1] \to \mathbb{R}^\ell$ belong to $C^4[0,1]^\ell$. We

assume that the following inequality holds to fulfill the condition of the strongly diagonally dominant matrix along with the nonsingularity of $\boldsymbol{B}(x)\ \forall x \in [0,1]$

$$\sum_{\substack{k=1\\k\neq i}}^{\ell} \left\| \frac{b_{ik}}{b_{ii}} \right\| < 1, \quad \text{for } i = 1, 2, \ldots, \ell.$$

The solution components exhibit boundary layers at $x = 0$ and $x = 1$ of width $O(\varepsilon)$.

3. Next, we have a general weakly-coupled reaction-diffusion system (m number of equations) of parabolic IBVPs

$$\mathfrak{L}\boldsymbol{y} := \frac{\partial \boldsymbol{y}}{\partial t} - \boldsymbol{\mathcal{E}}\frac{\partial^2 \boldsymbol{y}}{\partial x^2} + \boldsymbol{A}(x,t)\boldsymbol{y} = \boldsymbol{f}(x,t),\ (x,t) \in \mathcal{Q} = \mathcal{Q}_x \times \mathcal{Q}_t,$$
$$\boldsymbol{y}(0,t) = \boldsymbol{q}(t) \text{ in } \mathcal{Q}_l, \quad \boldsymbol{y}(1,t) = \boldsymbol{r}(t) \text{ in } \mathcal{Q}_r, \quad \boldsymbol{y}(x,0) = \boldsymbol{0} \text{ in } \mathcal{Q}_b,$$

where $\mathcal{Q}_l = \{(0,t)|\ 0 \le t \le \mathcal{T}\},\ \mathcal{Q}_r = \{(1,t)|\ 0 \le t \le \mathcal{T}\},\ \mathcal{Q}_b = \{(x,0)|\ 0 \le x \le 1\}$, $\mathfrak{L} = (\mathfrak{L}_1, \mathfrak{L}_2, \ldots, \mathfrak{L}_m)^T, \boldsymbol{\mathcal{E}} = \text{diag}(\varepsilon, \varepsilon, \ldots, \varepsilon), \boldsymbol{f}(x,t) = (f_1(x,t), f_2(x,t), \ldots, f_m(x,t))^T$, $\boldsymbol{A} = \{a_{ij}(x,t)\}_{i,j=1}^m, \boldsymbol{y}(x,t) = (y_1(x,t), y_2(x,t), \ldots, y_m(x,t))^T, \boldsymbol{q} = (q_1, q_2, \ldots, q_m)^T$, $\boldsymbol{r} = (r_1, r_2, \ldots, r_m)^T$. The boundary of $\mathcal{Q}$ denoted by $\partial\mathcal{Q} = \overline{\mathcal{Q}}\backslash\mathcal{Q}$ includes initial ($\mathcal{Q}_b$) and lateral boundaries ($\mathcal{Q}_l$ and $\mathcal{Q}_r$) of the domain. The operator $\mathfrak{L}_k$ can be defined as

$$\mathfrak{L}_k\boldsymbol{y} = \frac{\partial y_k}{\partial t} - \varepsilon\frac{\partial^2 y_k}{\partial x^2} + \sum_{j=1}^{m} a_{kj}y_j.$$

In general, boundary layers of width $O(\sqrt{\varepsilon})$ appear in the solution components at the left and right lateral surfaces as ε approaches zero.

4. We consider the following singularly perturbed fourth-order differential equation

$$-\mu z^{(4)}(t) + a(t)z''(t) - b(t)z(t) = -f(t), \quad t \in \mathcal{D} = (0,1),$$

subject to the following boundary conditions (BCs)

$$z(0) = q_1,\ z(1) = q_3,\ z''(0) = -q_2,\ z''(1) = -q_4,$$

where $0 < \mu \ll 1$ is referred to as the perturbation parameter. We consider a particular type of BCs influenced by [35], which helps us to set up uniform stability estimates and other results. We assume $a(t)$, $b(t)$ and $f(t)$ to be sufficiently smooth that satisfy the following conditions

$$\zeta^* \geqslant a(t) \geqslant \zeta > 0, \quad 0 \geqslant b(t) \geqslant -\beta,\ \beta > 0,$$
$$\zeta - 2\beta \geqslant \eta > 0, \text{ for some } \eta.$$

5. The following singularly perturbed convection-diffusion type fourth-order boundary value problem (BVP) will be in consideration

$$-\varepsilon y^{(4)}(x) - a(x)y'''(x) + b(x)y''(x) + c(x)y'(x) - d(x)y(x) = -f(x), \quad x \in \mathfrak{D} = (0,1),$$

subject to the following BCs

$$y(0) = q_1,\ y(1) = q_3,\ y''(0) = -q_2,\ y''(1) = -q_4.$$

We assume $a(x)$, $b(x)$, $c(x)$, $d(x)$ and $f(x)$ to be sufficiently smooth that satisfy the following conditions

$$a(x) \geqslant \alpha^* > 0,\ b(x) \geqslant \beta^* > 0,$$
$$c(x) \geqslant \gamma^* > 0,\ 0 \geqslant d(x) \geqslant -\delta^*,\ \delta^* > 0,$$
$$\alpha^* - \delta^*(1 + \zeta^*) \geqslant \eta^* > 0, \text{ for some } \eta^* \text{ and } \zeta^* > 0,$$

for $x \in \overline{\mathfrak{D}}$.

1.6 Thesis contribution

The creation and detailed examination of a novel quadratic spline-based numerical approach is the basis for this thesis's significant contribution to numerical analysis and the study of singularly perturbed problems. This novel technique has several significant contributions, including the following:

- **Robust Nature of the Technique.** The thesis offers a robust numerical approach to address issues caused by singular perturbations. In computational mathematics and engineering, tackling issues like these, characterized by steep gradients and many scales, has been a struggle for a long time. The quadratic spline approach that has been offered provides an efficient manner of responding to the issues that have been presented.

- **Accuracy and Convergence.** Demonstrating the accuracy and convergence qualities of the proposed approach constitutes an essential contribution. Exhaustive mathematical study and computing experimentation show second-order convergence even in singularities and fast changes. This understanding benefits practitioners looking for trustworthy numerical tools to solve situations with steep gradients in the real world.

- **Independency on Mesh.** The approach is a significant improvement since it can work well on eXp mesh without requiring any prior knowledge of transition parameters. This proficiency to use any mesh refinement technique improves the method's flexibility and makes it easier to apply to new types of issues.

- **Versatility.** By putting it to use in a variety of different model situations, the thesis demonstrates the adaptability of the technique that is based on quadratic splines. Problems with various physical understandings, parameter sensitivities, and transition factors are included in this category.

- **Verification and Benchmarking.** The suggested method's numerical findings are thoroughly checked against theoretical constraints and compared to established approaches. The outcomes of the benchmarks show that the technique outperforms the alternatives, giving it a viable option for resolving singularly perturbed cases.

- **Applications to Diverse Fields.** In addition to the theoretical assistance, the thesis strongly emphasizes the practical usefulness of the technique across a wide range of applications in various academic disciplines. It illustrates the approach's potential in numerous fields, from fluid dynamics to electrical engineering. Additionally, it highlights the importance of the method in solving real-world issues.

- **Future Research Suggestions.** In addition to this, the thesis outlines potential directions for further investigation. It involves applying the method to issues with a higher dimension, fractional PDEs, and integro differential equations and investigating how it might be integrated with uncertainty quantification techniques, which will pave the way for more research and development in the field.

In conclusion, the thesis's presented numerical approach is essential to the arsenal of academics and researchers who work with singularly perturbed problems. Because of its accuracy, convergence features, adaptability, and independence from mesh details, it is an encouraging option for a wide range of applications, and it has the potential to stimulate innovation and advancement in computational mathematics and engineering.

1.7 Plan of the thesis

Consisting of a total of seven chapters, this thesis starts with **Chapter 1**, which provides a thorough overview and the historical backdrop of previous research in the field of singular perturbation. Moreover, it provides the justification and objectives that underlie the resolution of singularly perturbed systems of differential equations and higher-order problems. The succeeding portions of this thesis consist of six chapters and are arranged in the following manner:

In **Chapter 2**, a numerical scheme is developed to solve singularly perturbed convection-diffusion type degenerate parabolic problems. The degenerative nature of the problem is due to the coefficient of the convection term. The problem is semi-discretized using the Crank-Nicolson scheme, and then the quadratic spline basis functions are used to discretize the semi-discrete problem. A priori bounds for the solution and its derivatives of the continuous problem are given, which are necessary to analyze the error. A rigorous error analysis shows that the proposed method is boundary layer resolving and second-order parameter uniformly convergent. Some numerical experiments have been devised to support the proposed scheme's theoretical findings and effectiveness.

Chapter 3 is dedicated to analyzing a parameter-uniform numerical scheme for a system of weakly coupled singularly perturbed reaction-diffusion equations of arbitrary size with appropriate boundary conditions. More precisely, quadratic B-spline basis functions with an

eXp mesh are used to solve a $\ell \times \ell$ system whose solution exhibits parabolic (or exponential) boundary layers at both endpoints of the domain. A convergence analysis is addressed, which shows a uniform convergence of the second order. To validate the theoretical findings, test problems are solved numerically.

Chapter 4 presents a uniformly convergent numerical technique for a time-dependent reaction-dominated singularly perturbed system, including the same diffusion parameters multiplied with second-order spatial derivatives in all equations. The proposed numerical approach consists of the Crank-Nicolson scheme in the temporal direction over a uniform mesh and quadratic $\mathbb{B}$-splines collocation technique over an eXp mesh in the spatial direction. We derived the robust error estimates to establish the optimal order of convergence. Numerical investigations confirm the theoretical determinations and the proposed method's efficiency and accuracy.

A numerical study for the fourth-order singularly perturbed boundary value problems (SP-BVPs) is carried out in **Chapter 5**. The associated differential equation is converted into a weakly coupled system of two singularly perturbed ordinary differential equations (SP-ODEs) with Dirichlet boundary conditions to solve the problem numerically. One of the equations in the system is independent of the perturbation parameter. To solve this system, we present a numerical technique of quadratic B-splines on an eXp mesh. The established results show that the scheme is second-order uniformly convergent in the discrete maximum norm. The theoretical results are validated using the proposed method on two test problems.

Chapter 6 contemplates a numerical investigation of the convection-diffusion type's fourth-order singularly perturbed linear and nonlinear boundary value problems. First, the considered linear fourth-order differential equation is converted into a strongly/weakly coupled singularly perturbed system (depending on the coefficient of the first-order derivative) of two ordinary differential equations with Dirichlet boundary conditions to solve the problem numerically. To obtain the solution for this system, we propose a numerical method of quadratic $\mathfrak{B}$-splines on an eXp mesh. Convergence analysis shows that the proposed numerical scheme is second-order uniformly convergent in the discrete maximum norm. The nonlinear differential equation is linearized using the quasilinearization technique, and then the proposed approach is applied to the linearized problem. The theoretical outcomes are validated by

executing the proposed method on three test problems.

In conclusion, **Chapter 7** provides a concise recapitulation of the outcomes, highlighting the different contributions generated as a result of this thesis. In furtherance of this, it presents a variety of opportunities for future research that might be conducted with the intention of building upon already established theoretical findings.

Comprehensive numerical findings have been offered to support the theoretical discoveries and to demonstrate the accuracy of the advised computational methods. The numerical outcomes corresponding to the various illustrations have been brought out in the numerical section of each chapter. Each chapter is supplemented by appropriate graphs and tables, which support the analytical findings obtained from the chapter.

Chapter 2

A uniformly convergent quadratic B-spline based scheme for singularly perturbed degenerate parabolic problems

---

The fundamental motivation behind this work is to provide a numerical scheme for singularly perturbed degenerate parabolic PDEs that is robust and accurate over a broad range of parameter values. Chemical kinetics, biological pattern formation, heat conduction in materials with sharp surfaces, thin-film flows, and the modeling of semiconductor devices are just a few examples of many scientific and technical fields where these equations are frequently used. In the framework of PDEs, degeneracy is when some coefficients or terms become zero or explode at some points in the domain. Thus, the typical solutions fail, and the analysis becomes more complicated.

The work of this chapter has been published in the following publication:

S. Singh, D. Kumar, H. Ramos, "A uniformly convergent quadratic B-spline based scheme for singularly perturbed degenerate parabolic problems." Math. Comput. Simul., 195 (2022), 88–106.

The combined effect of singular perturbation and degeneracy renders these problems difficult and intriguing to investigate. Using standard computational techniques may result in an excessive amount of errors or the requirement of fine grids, which leads to inefficiency in the computation. The analysis of such issues calls for advanced mathematical methods that consider the relationship between singular perturbations and degeneracy.

2.1 Problem statement

In this study, we consider the following parabolic singularly perturbed (PSP) initial-boundary value problem (IBVP) named as degenerate parabolic convection-diffusion IBVP in the rectangular domain $\mathcal{G} = \mathcal{G}_x \times \mathcal{G}_t = (0,1) \times (0,T]$ for some finite positive T:

$$\mathcal{L}_{x,\varepsilon} u(x,t) \equiv \varepsilon \frac{\partial^2 u}{\partial x^2} + b(x,t)\frac{\partial u}{\partial x} - c(x,t)\frac{\partial u}{\partial t} - d(x,t)u = f(x,t),\ (x,t) \in \mathcal{G}, \quad \text{(2.1.1a)}$$

with the initial condition

$$u(x,0) = \mathcal{V}(x) \text{ on } P_x = [0,1] \times \{0\}, \quad \text{(2.1.1b)}$$

and the boundary conditions

$$u(0,t) = p_0(t) \text{ on } P_0 = \{0\} \times [0,T], \quad \text{(2.1.1c)}$$

$$u(1,t) = p_1(t) \text{ on } P_1 = \{1\} \times [0,T], \quad \text{(2.1.1d)}$$

where $0 < \varepsilon \ll 1$ is a perturbation parameter; P_0, P_1, and P_x are the left, right, and the bottom sides of the domain $\mathcal{G}$, respectively. The boundary of the domain $\mathcal{G}$ is defined as $\partial\mathcal{G} = P_x \cup P_0 \cup P_1$. We assume that the coefficients $b(x,t)$, $c(x,t)$, and $d(x,t)$ satisfy

$$\begin{aligned} &b(x,t) = b_0(x,t)x^p,\ p \geq 1,\ (x,t) \in \overline{\mathcal{G}}, \\ &b_0(x,t) \geq \beta > 0,\ c(x,t) \geq \gamma > 0,\ d(x,t) \geq \delta \geq 0,\ (x,t) \in \overline{\mathcal{G}}. \end{aligned} \quad \text{(2.1.2)}$$

Problem (2.1.1) is related to the flow problem when directed towards the left side P_0 of the domain, and the flow stops at this boundary. These problems arise in modeling heat flow

and mass transport near an oceanic rise [74] and developing the models of thermal boundary layers in laminar flow [75].

As the coefficient $b(x,t)$ of the convection term vanishes at $x = 0$, the problem (2.1.1) is called a problem with a boundary turning point. It covers two aspects: the turning point for $p = 1$ is referred to as a simple turning point (assuming the linear velocity distribution [74]), and it is a multiple turning point when $p > 1$ (for higher orders of velocity distribution [75], Chapter 12). The reduced problem obtained by taking $\varepsilon = 0$ in (2.1.1) is the following first-order hyperbolic PDE

$$\begin{aligned} &b(x,t)(u_0)_x(x,t) - c(x,t)(u_0)_t(x,t) - d(x,t)u_0(x,t) = f(x,t),\ (x,t) \in \mathcal{G}, \\ &u_0(x,t) = u(x,t),\ (x,t) \in P_x \cup P_1. \end{aligned} \tag{2.1.3}$$

The left side P_0 and all other lines parallel to P_0 are the characteristic curves of the reduced problem when $b(0,t) = 0$, $c(0,t) > 0$. Consequently, the resulting boundary layer functions are called the parabolic boundary layer functions. These are characterized by the boundary values $u(0,t)$ at the left side P_0. It has been observed that the left lateral surface and the characteristic curve of (2.1.3) do not have any intersection. However, their deviation increases vertically, far from the lateral boundary (see [76, 77]). They have also observed the exponential (regular) boundary layer function as a result of the inconsistency between the boundary value $p_0(t)$ and the value being transported along the characteristic at the intersection point (if $b(x,t) > 0,\ \forall (x,t) \in \overline{\mathcal{G}}$ then every characteristic intersects P_0 at one point). In general, a parabolic boundary layer of width $O(\sqrt{\varepsilon})$ appears in the solution to the problem (2.1.1) in the neighbourhood of P_0 as ε approaches zero.

2.1.1 Literature of the problem

To solve the problem (2.1.1), Dunne *et al.* [78] proposed an almost first-order parameter-uniform upwind finite-difference scheme on a Shishkin mesh. Christara *et al.* [79] proposed quadratic-spline collocation for the space discretization and classical finite differences for the time discretization. They have also introduced adaptive mesh techniques providing competitive results to solve the American put option pricing problems, giving very competitive

results. Viscor and Stynes [80] used a standard implicit central difference scheme to solve the degenerate parabolic problem and showed that the method is dependent on the degeneracy parameter but is independent of the singular perturbation parameter. To solve (2.1.1), Gupta and Kadalbajoo [76] proposed a B-spline collocation method in space combined with the implicit Euler scheme in time. To solve singularly perturbed degenerate convection-diffusion problems with discontinuity in the source term, Clavero *et al.* [81] constructed a parameter-uniform scheme. They used an upwind finite difference scheme with a Shishkin mesh in the spatial direction and the implicit Euler method on a uniform mesh in the temporal direction. The discontinuity originates from the presence of an interior layer in the solution to the problem. Majumdar and Natesan [82] proposed an almost first-order convergent in space and first-order convergent in time parameter-uniform numerical scheme consisting of the implicit-Euler scheme for the time derivative and an upwind finite difference scheme for the spatial derivatives. They have used the Richardson extrapolation scheme to increase the order of accuracy to $O(N^{-2}\ln^2 N + (\Delta t)^2)$. Majumdar and Natesan [83] proposed a hybrid scheme comprising a central difference scheme in the inner region and the midpoint upwind scheme in the outer region. They proved the second-order (more precisely, second-order in the outer region and almost second-order in the inner region) parameter-uniform convergence in space. Yadav *et al.* [84] proposed an implicit Euler difference formula and a hybrid scheme in the temporal and spatial directions, respectively. To resolve the boundary layer, they have used a generalized Shishkin mesh. Moreover, they have used the Richardson extrapolation in the time direction to increase time accuracy. Recently, Kumar and Aguiar [85] constructed a parameter-uniform method of order one for the solution of (2.1.1). Their discretization consists of the implicit Euler method in the temporal direction and an upwind finite difference scheme in the spatial direction. The boundary layer is resolved using an adaptive mesh generated using the equidistribution principle. In this chapter, we aim to construct a parameter-uniform numerical scheme for the problem (2.1.1). We use the Crank-Nicolson scheme to get the semi-discrete problem, and then the quadratic B-spline basis functions are used for the full discretization. An exponentially graded mesh is constructed in the spatial direction to resolve the boundary layer.

The following outline constitutes the chapter's structure: Section 2.2 offers some essential

preliminary findings on the solution and its derivatives. The proposed numerical approach is described thoroughly in Section 2.3, which includes time and spatial discretizations. In Section 2.4, we thoroughly examine the scheme's convergence. To ascertain the efficacy of our methodology, we undertake numerical simulations and subsequently analyze the outcomes in Section 2.5. Finally, in Section 2.6, the chapter is concluded with final remarks and recommendations for potential avenues of future research within this domain.

Throughout the chapter, C is a positive generic constant independent of the perturbation and mesh parameters and can take different values at different places. Furthermore, we denote the maximum norm by $\|.\|$ e.g., for a function w defined on a domain $\mathcal{D}$, we define $\|w\|_{\mathcal{D}} = \max_{\mathcal{D}} |w|$.

2.2 Properties of the solution of the continuous problem

In the numerical study of SPPs, analytical results play an important role in finding the bounds for the exact solution to the continuous problem, the solution, and the derivatives to the semi-discrete and fully discretized problems. We assume that $b(x,t)$, $c(x,t)$, and $d(x,t)$ are Hölder continuous in both space and time with exponent $\lambda \in (0,1)$. We further assume that the functions $b_0(x,t)$, $c(x,t)$, $d(x,t)$, and $f(x,t)$ on $\overline{\mathcal{G}}$, and $\mathcal{V}$, p_0, and p_1 on $\partial\mathcal{G}$ are sufficiently smooth, which guarantee the essential smoothness of the solution on $\overline{\mathcal{G}}$. The following conditions are also made on the problem data given in (2.1.1) (see [84, 86] for definitions of Hölder continuous function and the space C_λ^K):

$$
\begin{aligned}
&b(x,t), c(x,t), d(x,t), f(x,t) \in C_\lambda^q(\overline{\mathcal{G}}),\ \mathcal{V}(x) \in C_\lambda^{q+2}[0,1],\\
&p_0(t) \in C_\lambda^{q/2+1}[0,T],\ p_1(t) \in C_\lambda^{q/2+1}[0,T],\ q \geq 0,\ \lambda \in (0,1).
\end{aligned}
$$

Furthermore, at the corner points $P^c = (P_0 \cup P_1) \cap P_x = \{(0,0),(1,0)\}$, the problem data satisfy the compatibility conditions (see [84]) for time derivatives up to order $q_0 = [q/2] + 1$. The following compatibility conditions ensure the existence of a unique solution to the problem (2.1.1)

$$
\mathcal{V}(0) = p_0(0), \quad \mathcal{V}(1) = p_1(0), \tag{2.2.1a}
$$

$$-c(0,0)\frac{\partial p_0(0,0)}{\partial t} = f(0,0) - \left(\varepsilon\frac{\partial^2}{\partial x^2} + b(0,0)\frac{\partial}{\partial x} - d(0,0)\right)\mathcal{V}(0), \tag{2.2.1b}$$

$$-c(1,0)\frac{\partial p_1(1,0)}{\partial t} = f(1,0) - \left(\varepsilon\frac{\partial^2}{\partial x^2} + b(1,0)\frac{\partial}{\partial x} - d(1,0)\right)\mathcal{V}(1). \tag{2.2.1c}$$

Results given in [87] directly imply that the solution to the IBVP (2.1.1) satisfies the following bounds:

$$|u(x,0) - \mathcal{V}(x)| \leq Ct,$$
$$|u(1,t) - p_1(t)| \leq C(1-x).$$

Furthermore, it can be noted that the solution $u(x,t)$ to the problem (2.1.1) is bounded, *i.e.,* $\|u(x,t)\|_{\overline{\mathcal{G}}} \leq C$.

Lemma 2.2.1 (Continuous minimum principle)**.** *Let* $W(x,t) \in C^{2,1}(\overline{\mathcal{G}})$. *If* $W(x,t) \geq 0,\ \forall\,(x,t) \in \partial\mathcal{G}$ *and* $\mathcal{L}_{x,\varepsilon}W(x,t) \leq 0,\ \forall\,(x,t) \in \mathcal{G}$, *then* $W(x,t) \geq 0,\ \forall\,(x,t) \in \overline{\mathcal{G}}$.

Proof. For the proof, the readers are referred to [82]. □

The stability bound for the solution to the problem (2.1.1) given in the following lemma can be obtained using Lemma 2.2.1.

Lemma 2.2.2 (Stability bound)**.** *For all* $\varepsilon > 0$, *the solution* $u(x,t)$ *of the IBVP (2.1.1) satisfies the following bound*

$$\|u\|_{\overline{\mathcal{G}}} \leq \|u\|_{\partial\mathcal{G}} + \frac{T}{\gamma}\|f\|_{\overline{\mathcal{G}}}.$$

Proof. Let us construct the barrier functions

$$\Phi^{\pm}(x,t) = \|u\|_{\partial\mathcal{G}} + \frac{t}{\gamma}\|f\|_{\overline{\mathcal{G}}} \pm u(x,t),\ (x,t) \in \overline{\mathcal{G}}.$$

From above we find $\Phi^{\pm}(x,t) > 0,\ \forall\,(x,t) \in \partial\mathcal{G}$. Also, as $c(x,t) \geq \gamma > 0$ and $\|f\| \geq f(x,t),\ \forall\,(x,t) \in \overline{\mathcal{G}}$, so $-c(x,t)\gamma^{-1}\|f\| \pm f(x,t) \leq 0$. Using the above inequalities, we obtain

$$\mathcal{L}_{x,\varepsilon}\Phi^{\pm}(x,t) \leq 0,\ \forall\,(x,t) \in \mathcal{G}.$$

Therefore, direct use of Lemma 2.2.1 gives $\Phi^{\pm}(x,t) \geq 0,\ \forall\,(x,t) \in \overline{\mathcal{G}}$, which leads to the desired bound. □

The following theorem gives the bounds for the mixed derivatives of u.

Theorem 2.2.1. *For all $i, j \geq 0$ satisfying $0 \leq i + 2j \leq 4$, the solution $u(x,t)$ of the IBVP (2.1.1) satisfies*

$$\left\| \frac{\partial^{i+j} u}{\partial x^i \partial t^j} \right\|_{\overline{\mathcal{G}}} \leq C(1 + \varepsilon^{-i/2} \exp(-x\sqrt{\delta/\varepsilon})).$$

Proof. For the proof, the readers are referred to [83]. □

The estimates obtained in Theorem 2.2.1 are weak from the convergence point of view, and these bounds are insufficient to get parameter-uniform results. To obtain stronger error bounds on $u(x,t)$ and its derivatives, we decompose the solution $u(x,t)$ into two parts as $u(x,t) = y(x,t) + z(x,t),\ \forall\,(x,t) \in \overline{\mathcal{G}}$, where $y(x,t)$ and $z(x,t)$ represent the regular (smooth) and singular components, respectively. The regular component is the solution to the following non-homogeneous problem

$$\begin{aligned} \mathcal{L}_{x,\varepsilon} y(x,t) &= f(x,t),\ (x,t) \in \mathcal{G}, \\ y(x,t) &= u(x,t),\ (x,t) \in P_x \cup P_1, \end{aligned}$$

and the singular component is the solution to the following homogeneous problem

$$\begin{aligned} \mathcal{L}_{x,\varepsilon} z(x,t) &= 0,\ (x,t) \in \mathcal{G}, \\ z(x,t) &= 0,\ (x,t) \in P_x \cup P_1, \\ z(x,t) &= u(x,t) - y(x,t),\ (x,t) \in P_0. \end{aligned}$$

The following theorem gives the bounds of the mixed derivatives of the regular and singular components.

Theorem 2.2.2. *For all $i, j \geq 0$ satisfying $0 \leq i + 2j \leq 6$, the regular and singular components satisfy*

$$\left\| \frac{\partial^{i+j} y}{\partial x^i \partial t^j} \right\|_{\overline{\mathcal{G}}} \leq C(1 + \varepsilon^{3-\frac{i}{2}}),$$

$$\left\| \frac{\partial^{i+j} z}{\partial x^i \partial t^j} \right\|_{\overline{\mathcal{G}}} \leq C(\varepsilon^{-i/2} \exp(-x\sqrt{\delta/\varepsilon})).$$

Proof. Let us assume an asymptotic expansion for the regular component given by

$$y(x,t) = y_0(x,t) + \varepsilon y_1(x,t) + \varepsilon^2 y_2(x,t) + \varepsilon^3 y_3(x,t) + \cdots = v(x,t) + r_y(x,t),\ (x,t) \in \overline{\mathcal{G}}, \tag{2.2.2}$$

where $v(x,t) = y_0(x,t) + \varepsilon y_1(x,t) + \varepsilon^2 y_2(x,t)$, and $r_y(x,t)$ denotes the remainder term (contribution of the higher order terms). The solution $y_0(x,t)$ satisfies the following reduced hyperbolic problem

$$\begin{aligned} \left(b\frac{\partial y_0}{\partial x} - c\frac{\partial y_0}{\partial t} - dy_0\right)(x,t) &= f(x,t),\ (x,t) \in \mathcal{G}, \\ y_0(x,t) &= u(x,t),\ (x,t) \in P_x \cup P_1. \end{aligned} \tag{2.2.3}$$

Also, $y_k(x,t)$ (for $k = 1, 2$) satisfy the following equations

$$\begin{aligned} \left(b\frac{\partial y_k}{\partial x} - c\frac{\partial y_k}{\partial t} - dy_k\right)(x,t) &= -\left(\frac{\partial^2 y_{k-1}}{\partial x^2}\right)(x,t),\ (x,t) \in \mathcal{G}, \\ y_k(x,t) &= 0,\ (x,t) \in P_x \cup P_1, \end{aligned} \tag{2.2.4}$$

and

$$\begin{aligned} \mathcal{L}_{x,\varepsilon} r_y(x,t) &= -\varepsilon^3 \left(\frac{\partial^2 y_2}{\partial x^2}\right)(x,t),\ (x,t) \in \mathcal{G}, \\ r_y(x,t) &= 0,\ (x,t) \in \partial\mathcal{G}. \end{aligned} \tag{2.2.5}$$

Thus, $v(x,t)$ satisfies

$$\begin{aligned} \mathcal{L}_{x,\varepsilon} v(x,t) &= f(x,t),\ (x,t) \in \mathcal{G}, \\ v(x,t) &= u(x,t),\ (x,t) \in P_x \cup P_1. \end{aligned} \tag{2.2.6}$$

Since $y_k(x,t)$, for $k = 0, 1, 2$ are ε free solutions of the first-order reduced hyperbolic PDEs (2.2.3) and (2.2.4) with bounded coefficients. So for all $i, j \geq 0$ satisfying $0 \leq i + 2j \leq 6$,

we have

$$\left\| \frac{\partial^{i+j} y_k}{\partial x^i \partial t^j} \right\|_{\overline{\mathcal{G}}} \leq C, \quad k = 0, 1, 2. \tag{2.2.7}$$

Also, as $r_y(x,t)$ is a solution of (2.2.5) (a problem similar to the problem (2.1.1)), proceeding similarly as in [84] for all $i, j \geq 0$, satisfying $0 \leq i + 2j \leq 6$ gives

$$\left\| \frac{\partial^{i+j} r_y}{\partial x^i \partial t^j} \right\|_{\overline{\mathcal{G}}} \leq C\varepsilon^{-i/2}. \tag{2.2.8}$$

Using the estimates of (2.2.7) and (2.2.8), we get the desired bounds for the regular component. Now, to get the bounds for the singular component $z(x,t)$, we consider the following barrier functions

$$\Phi^{\pm}(x,t) = C \exp\left(-x\sqrt{\frac{\delta}{\varepsilon}}\right) \exp(t) \pm z(x,t), \ (x,t) \in \overline{\mathcal{G}}, \tag{2.2.9}$$

where C is chosen in such a way that

$$\Phi^{\pm}(x,0) \geq 0, \ (x,0) \in P_x,$$
$$\Phi^{\pm}(0,t) \geq 0, \ (0,t) \in P_0,$$
$$\Phi^{\pm}(1,t) \geq 0, \ (1,t) \in P_1.$$

Then, $\Phi^{\pm}(x,t) \geq 0, \ \forall\, (x,t) \in \partial\mathcal{G}$ and $\mathcal{L}_{x,\varepsilon}\Phi^{\pm}(x,t) \leq 0, \ \forall (x,t) \in \overline{\mathcal{G}}$ (as $d(x,t) \geq \delta > 0$). Thus, using Lemma 2.2.1, we get

$$|z(x,t)| \leq C \exp\left(-x\sqrt{\frac{\delta}{\varepsilon}}\right) \exp(t) \leq C \exp\left(-x\sqrt{\frac{\delta}{\varepsilon}}\right), \ (x,t) \in \overline{\mathcal{G}}. \tag{2.2.10}$$

Using a similar approach to that given in [88], we can find the bounds on the $z(x,t)$ derivatives. Hence, the proof is completed. □

2.3 The discrete problem

In this section, we discretize the continuous problem (2.1.1). First, it is discretized in the temporal direction using the Crank-Nicolson scheme on a uniform mesh. Some essential properties of the solution to the semi-discrete problem are given. Then, after constructing

a piecewise uniform exponentially graded mesh in the spatial direction, a quadratic spline collocation method (QSCM) is used to find the solution at the collocation points.

2.3.1 Temporal semi-discretization

To get a uniform partition $\Omega_t^{N_t} = \{t_j = j\Delta t,\ j = 0, 1, \ldots, N_t\}$ of the domain $\mathcal{G}_t = [0, T]$ in the temporal direction, we divide $[0, T]$ into N_t mesh subintervals with step length $\Delta t = \frac{T}{N_t}$. At $(j + \frac{1}{2})$-th time level, the problem (2.1.1) is discretized as

$$\widetilde{u}^0(x) = \mathcal{V}(x),\ x \in \overline{\mathcal{G}}_x, \tag{2.3.1a}$$

$$\begin{aligned} L\widetilde{u}^{j+1}(x) &\equiv \frac{\varepsilon}{2}\widetilde{u}_{xx}^{j+1}(x) + \frac{b^{j+\frac{1}{2}}(x)}{2}\widetilde{u}_x^{j+1}(x) - \left(\frac{c^{j+\frac{1}{2}}(x)}{\Delta t} + \frac{d^{j+\frac{1}{2}}(x)}{2}\right)\widetilde{u}^{j+1}(x) \\ &= g^{j+1}(x),\ x \in \mathcal{G}_x,\ j \geq 0, \end{aligned} \tag{2.3.1b}$$

$$\widetilde{u}^{j+1}(0) = p_0(t_{j+1}),\ \widetilde{u}^{j+1}(1) = p_1(t_{j+1}),\ j \geq 0, \tag{2.3.1c}$$

where $\widetilde{u}^{j+1} \approx u(x, t_{j+1})$ is the solution to (2.3.1) at $(j + 1)$-th time level, and

$$g^{j+1}(x) = \frac{1}{2}(f^{j+1}(x) + f^j(x)) - \frac{\varepsilon}{2}\widetilde{u}_{xx}^j(x) - \frac{b^{j+\frac{1}{2}}(x)}{2}\widetilde{u}_x^j(x) - \left(\frac{c^{j+\frac{1}{2}}(x)}{\Delta t} - \frac{d^{j+\frac{1}{2}}(x)}{2}\right)\widetilde{u}^j(x).$$

To establish the convergence, we represent the local truncation error (LTE) as $e_{j+1} = L\nu^{j+1}(x) - g^{j+1}$, where ν^{j+1} is the approximate solution of (2.3.1). We also define the global error as follows, which is the sum of all LTEs at each time level

$$E_j = \sum_{n=0}^{j} e_n.$$

The proof of the following lemmas, which estimate the LTE and the global truncation error, can be seen in [89].

Lemma 2.3.1. *Under the assumption*

$$\left|\frac{\partial^j u(x,t)}{\partial t^j}\right| \leq C,\ \forall\,(x,t) \in \overline{\mathcal{G}},\ 0 \leq j \leq 3,$$

the LTE e_{j+1} for the scheme (2.3.1) in the temporal direction satisfies

$$\|e_{j+1}\| \leq C(\Delta t)^3.$$

Lemma 2.3.2. *Under the assumption of Lemma 2.3.1, the global error E_j of the discretized scheme (2.3.1) satisfies the bound*

$$\sup_{j \leq \frac{T}{\Delta t}} \|E_j\| \leq C(\Delta t)^2.$$

The above results conclude that the semi-discrete scheme (2.3.1) is second-order convergent in time. The solution $\widetilde{u}^{j+1}(x)$ to the problem (2.3.1) can also be decomposed into regular and singular component as $\widetilde{u}^{j+1}(x) = \widetilde{y}^{j+1}(x) + \widetilde{z}^{j+1}(x)$. The bounds on these components are given in the following theorem (refer to [90]).

Theorem 2.3.1. *The solution $\widetilde{u}^{j+1}(x)$ and its derivatives satisfy the following bounds*

$$\left|\frac{d^k \widetilde{u}^{j+1}(x)}{dx^k}\right| \leq C(1 + \varepsilon^{-k/2} \exp(-x\sqrt{\delta/\varepsilon})),\ x \in \overline{\mathcal{G}}_x,\ 0 \leq k \leq 4,$$

where the regular and singular components satisfy the following bounds

$$\left|\frac{d^k \widetilde{y}^{j+1}(x)}{dx^k}\right| \leq C(1 + \varepsilon^{(3-\frac{k}{2})}),\ x \in \overline{\mathcal{G}}_x,\ 0 \leq k \leq 4,$$
$$\left|\frac{d^k \widetilde{z}^{j+1}(x)}{dx^k}\right| \leq C(\varepsilon^{-k/2} \exp(-x\sqrt{\delta/\varepsilon})),\ x \in \overline{\mathcal{G}}_x,\ 0 \leq k \leq 4.$$

2.3.2 Spatial mesh generation

To obtain an exponentially graded mesh $\Omega_x^{N_x} = \{x_i |\ 0 \leq i \leq N_x\}$ divide the interval $(0, 1)$ into $N_x > 2$ (multiple of 2) subintervals $I_i = [x_{i-1}, x_i]$. Let $\mathbb{P}_k$ be the space of all polynomials of degree $\leq k$. We generate these points with the help of the mesh generating function $\Psi(\rho)$, which is monotonically increasing, continuous, and piecewise continuously differentiable, given by

$$\Psi(\rho) = -\ln(1 - 2\mathcal{C}_{k,\varepsilon}\rho),\ \rho \in [0, 1/2 - 1/N_x], \tag{2.3.2}$$

where $\mathcal{C}_{k,\varepsilon} = 1 - \exp\left(-\frac{1}{(k+1)\sqrt{\varepsilon}}\right) \in \mathbb{R}^+$. We split the interval $[0,1]$ as a union of two subintervals $[0, x_{\frac{N_x}{2}-1}]$ and $[x_{\frac{N_x}{2}-1}, 1]$, where $x_{\frac{N_x}{2}-1}$ is the transition point of the mesh. The mesh points in these subintervals are defined as

$$x_i = \begin{cases} (k+1)\sqrt{\varepsilon}\Psi(\rho_i), & i = 0, 1, \ldots, \frac{N_x}{2} - 1, \\ x_{\frac{N_x}{2}-1} + \left(\frac{1 - x_{\frac{N_x}{2}-1}}{\frac{N_x}{2}+1}\right), & i = \frac{N_x}{2}, \ldots, N_x, \end{cases} \tag{2.3.3}$$

where $\rho_i = \frac{i}{N_x}$ for $i = 0, 1, \ldots, N_x$ and $\widetilde{h}_i = x_i - x_{i-1}$ for $i = 1, 2, \ldots, N_x$. The mesh points are distributed equidistantly in $[x_{\frac{N_x}{2}-1}, 1]$ and exponentially graded in $[0, x_{\frac{N_x}{2}-1}]$ with $N_x/2 + 1$, $N_x/2 - 1$ elements, respectively. Using the mesh characterizing function $\Phi = \exp(-\Psi)$ defined in [91], the mesh spacing satisfies

$$\widetilde{h}_i \leq \begin{cases} C(k+1)\sqrt{\varepsilon}N_x^{-1} \max \Psi'(\rho_i) \leq C\sqrt{\varepsilon}N_x^{-1}, & i = 1, 2, \ldots, \frac{N_x}{2} - 1, \\ CN_x^{-1}, & i = \frac{N_x}{2}, \ldots, N_x, \end{cases} \tag{2.3.4}$$

and also they satisfy the following estimate [91, 92]

$$|\widetilde{h}_{i+1} - \widetilde{h}_i| = C \begin{cases} \sqrt{\varepsilon}N_x^{-2}, & i = 1, 2, \ldots, \frac{N_x}{2} - 1, \\ 0, & i = N_x/2, \ldots, N_x. \end{cases} \tag{2.3.5}$$

2.3.3 Implementation of QSCM

In this section, by using QSCM in the spatial direction on an exponentially graded mesh, we convert the semi-discrete scheme (2.3.1) into a fully discrete scheme. For $m, k \in \mathbb{N}\,(m < k)$ we define the polynomial space S_k^m as

$$S_k^m(\Omega_x^{N_x}) = \{r \in C^m[0,1] : \ r|_{I_i} \in \mathbb{P}_k, \text{ for } i = 1, 2, \ldots, N_x\}.$$

We further define the quadratic B-spline functions $\mathcal{B}_i(x) \in S_2^1(\Omega_x^{N_x})$ for $i = 0, 1, 2, \ldots, N_x, N_x+1$ as follows

$$\mathcal{B}_0(x) = \begin{cases} \dfrac{(x_1 - x)^2}{\widetilde{h}_1^2}, & x_0 \le x \le x_1, \\ 0, & \text{otherwise}, \end{cases}$$

$$\mathcal{B}_1(x) = \begin{cases} \dfrac{\widetilde{h}_1^2 - (x_1 - x)^2}{\widetilde{h}_1^2} - \dfrac{(x - x_0)^2}{\widetilde{h}_1(\widetilde{h}_1 + \widetilde{h}_2)}, & x_0 \le x \le x_1, \\ \dfrac{(x_2 - x)^2}{\widetilde{h}_1(\widetilde{h}_1 + \widetilde{h}_2)}, & x_1 \le x \le x_2, \\ 0, & \text{otherwise}, \end{cases}$$

and for $i = 2, 3, \ldots, N_x - 1$

$$\mathcal{B}_i(x) = \begin{cases} \dfrac{(x - x_{i-2})^2}{\widetilde{h}_{i-1}(\widetilde{h}_{i-1} + \widetilde{h}_i)}, & x_{i-2} \le x \le x_{i-1}, \\ \dfrac{(x - x_{i-2})(x_i - x)}{\widetilde{h}_i(\widetilde{h}_{i-1} + \widetilde{h}_i)} + \dfrac{(x_{i+1} - x)(x - x_{i-1})}{\widetilde{h}_i(\widetilde{h}_i + \widetilde{h}_{i+1})}, & x_{i-1} \le x \le x_i, \\ \dfrac{(x_{i+1} - x)^2}{\widetilde{h}_{i+1}(\widetilde{h}_i + \widetilde{h}_{i+1})}, & x_i \le x \le x_{i+1}, \\ 0, & \text{otherwise}, \end{cases}$$

while for $i = N_x,\ N_x + 1$ these are given as

$$\mathcal{B}_{N_x}(x) = \begin{cases} \dfrac{(x_{N_x-2} - x)^2}{\widetilde{h}_{N_x-1}(\widetilde{h}_{N_x-1} + \widetilde{h}_{N_x})}, & x_{N_x-2} \le x \le x_{N_x-1}, \\ \dfrac{\widetilde{h}_{N_x}^2 - (x_{N_x-1} - x)^2}{\widetilde{h}_{N_x}^2} - \dfrac{(x - x_{N_x})^2}{\widetilde{h}_{N_x}(\widetilde{h}_{N_x-1} + \widetilde{h}_{N_x})}, & x_{N_x-1} \le x \le x_{N_x}, \\ 0, & \text{otherwise}, \end{cases}$$

$$\mathcal{B}_{N_x+1}(x) = \begin{cases} \dfrac{(x_{N_x-1} - x)^2}{\widetilde{h}_{N_x}^2}, & x_{N_x-1} \le x \le x_{N_x}, \\ 0, & \text{otherwise}. \end{cases}$$

Now we define the collocation points (mid points of I_i) as $x_{i-1/2} = \frac{x_i + x_{i-1}}{2} = x_{i-1} + \frac{\widetilde{h}_i}{2} = x_i - \frac{\widetilde{h}_i}{2},\ i = 1, 2, \ldots, N_x$. We seek an approximate solution at the $(j+1)$-th time level at

these collocation points as

$$\mathcal{S}^{j+1}(x) = \sum_{k=0}^{N_x+1} w_k^{j+1} \mathcal{B}_k(x),\ j = 0, 1, \ldots, N_t - 1, \tag{2.3.6}$$

where w_k^{j+1} are the coefficients at the $(j+1)$-th time level. The conversion of the semi-discrete scheme (2.3.1) into a fully discrete scheme using this collocation method results in

$$\begin{aligned} \mathcal{S}_{i-1/2}^0 &= \mathcal{V}(x_{i-1/2}), \\ L\mathcal{S}_{i-1/2}^{j+1} &= g^{j+1}(x_{i-1/2}),\ \text{for } i = 1, 2, \ldots, N_x, \\ \mathcal{S}_0^{j+1} &= p_0(t_{j+1}),\ \mathcal{S}_{N_x}^{j+1} = p_1(t_{j+1}). \end{aligned} \tag{2.3.7}$$

At each time level, the values of $\mathcal{S},\ \mathcal{S}',\ \mathcal{S}''$ at the mid-points are given by

$$\begin{aligned} \mathcal{S}^{j+1}(x_{i-1/2}) &= \left(\frac{\widetilde{h}_i}{4(\widetilde{h}_i + \widetilde{h}_{i-1})}\right) w_{i-1}^{j+1} + \left(1 - \frac{\widetilde{h}_i}{4(\widetilde{h}_i + \widetilde{h}_{i-1})} - \frac{\widetilde{h}_i}{4(\widetilde{h}_i + \widetilde{h}_{i+1})}\right) w_i^{j+1} \\ &\quad + \left(\frac{\widetilde{h}_i}{4(\widetilde{h}_i + \widetilde{h}_{i+1})}\right) w_{i+1}^{j+1}, \\ (\mathcal{S}')^{j+1}(x_{i-1/2}) &= \left(\frac{-1}{\widetilde{h}_i + \widetilde{h}_{i-1}}\right) w_{i-1}^{j+1} + \left(\frac{1}{\widetilde{h}_i + \widetilde{h}_{i-1}} - \frac{1}{\widetilde{h}_i + \widetilde{h}_{i+1}}\right) w_i^{j+1} \\ &\quad + \left(\frac{1}{\widetilde{h}_i + \widetilde{h}_{i+1}}\right) w_{i+1}^{j+1}, \\ (\mathcal{S}'')^{j+1}(x_{i-1/2}) &= \left(\frac{2}{\widetilde{h}_i(\widetilde{h}_i + \widetilde{h}_{i-1})}\right) w_{i-1}^{j+1} + \left(-\frac{2}{\widetilde{h}_i(\widetilde{h}_i + \widetilde{h}_{i-1})} - \frac{2}{\widetilde{h}_i(\widetilde{h}_i + \widetilde{h}_{i+1})}\right) w_i^{j+1} \\ &\quad + \left(\frac{2}{\widetilde{h}_i(\widetilde{h}_i + \widetilde{h}_{i+1})}\right) w_{i+1}^{j+1}. \end{aligned} \tag{2.3.8}$$

The values of w_i^{j+1} for $i = 0, 1, \ldots, N_x + 1$ are calculated by solving the following system

$$\begin{aligned} w_0^{j+1} &= p_0(t_{j+1}), \\ [\mathcal{L}^{N_x} \mathbf{w}^{j+1}]_{i-1/2} &= g^{j+1}(x_{i-1/2}),\ i = 1, 2, \ldots, N_x, \\ w_{N_x+1}^{j+1} &= p_1(t_{j+1}), \end{aligned} \tag{2.3.9}$$

where $\mathbf{w}^{j+1} = (w_0^{j+1}, \ldots, w_{N_x+1}^{j+1})^T \in \mathbb{R}^{N_x+2}$. The operator $\mathcal{L}^{N_x}$ and $g^{j+1}(x_{i-1/2})$ in (2.3.9) are defined as

$$
\begin{aligned}
[\mathcal{L}^{N_x}\mathbf{w}^{j+1}]_{i-1/2} = \frac{\varepsilon}{2}\left[\frac{2(w_{i+1}^{j+1}-w_i^{j+1})}{\widetilde{h}_i(\widetilde{h}_i+\widetilde{h}_{i+1})} - \frac{2(w_i^{j+1}-w_{i-1}^{j+1})}{\widetilde{h}_i(\widetilde{h}_i+\widetilde{h}_{i-1})}\right] + \frac{b_{i-1/2}^{j+\frac{1}{2}}}{2}\left[\frac{w_{i+1}^{j+1}-w_i^{j+1}}{\widetilde{h}_i+\widetilde{h}_{i+1}}\right. \\
\left. + \frac{w_i^{j+1}-w_{i-1}^{j+1}}{\widetilde{h}_i+\widetilde{h}_{i-1}}\right] - \left(\frac{c_{i-1/2}^{j+\frac{1}{2}}}{\Delta t} + \frac{d_{i-1/2}^{j+\frac{1}{2}}}{2}\right)\left[\frac{\widetilde{h}_i w_{i-1}^{j+1}}{4(\widetilde{h}_i+\widetilde{h}_{i-1})}\right. \\
\left. + \left(1 - \frac{\widetilde{h}_i}{4(\widetilde{h}_i+\widetilde{h}_{i-1})} - \frac{\widetilde{h}_i}{4(\widetilde{h}_i+\widetilde{h}_{i+1})}\right)w_i^{j+1} + \frac{\widetilde{h}_i w_{i+1}^{j+1}}{4(\widetilde{h}_i+\widetilde{h}_{i+1})}\right],
\end{aligned}
$$

and

$$
\begin{aligned}
g^{j+1}(x_{i-1/2}) = \frac{1}{2}(f^{j+1}(x_{i-1/2}) + f^j(x_{i-1/2})) - \frac{\varepsilon}{2}\left[\frac{2(w_{i+1}^j-w_i^j)}{\widetilde{h}_i(\widetilde{h}_i+\widetilde{h}_{i+1})} - \frac{2(w_i^j-w_{i-1}^j)}{\widetilde{h}_i(\widetilde{h}_i+\widetilde{h}_{i-1})}\right] \\
- \frac{b_{i-1/2}^{j+\frac{1}{2}}}{2}\left[\frac{w_{i+1}^j-w_i^j}{\widetilde{h}_i+\widetilde{h}_{i+1}} + \frac{w_i^j-w_{i-1}^j}{\widetilde{h}_i+\widetilde{h}_{i-1}}\right] - \left(\frac{c_{i-1/2}^{j+\frac{1}{2}}}{\Delta t} - \frac{d_{i-1/2}^{j+\frac{1}{2}}}{2}\right) \\
\times \left[\frac{\widetilde{h}_i w_{i-1}^j}{4(\widetilde{h}_i+\widetilde{h}_{i-1})} + \left(1 - \frac{\widetilde{h}_i}{4(\widetilde{h}_i+\widetilde{h}_{i-1})} - \frac{\widetilde{h}_i}{4(\widetilde{h}_i+\widetilde{h}_{i+1})}\right)w_i^j + \frac{\widetilde{h}_i w_{i+1}^j}{4(\widetilde{h}_i+\widetilde{h}_{i+1})}\right],
\end{aligned}
$$

where $b_{i-1/2}^{j+\frac{1}{2}} = b(x_{i-1/2}, t_{j+1/2})$, $c_{i-1/2}^{j+\frac{1}{2}} = c(x_{i-1/2}, t_{j+1/2})$, and $d_{i-1/2}^{j+\frac{1}{2}} = d(x_{i-1/2}, t_{j+1/2})$. We fix $\widetilde{h}_0 = \widetilde{h}_{N_x+1} = 0$. It gives rise to a linear system of the form

$$
A_i w_{i-1}^{j+1} + B_i w_i^{j+1} + C_i w_{i+1}^{j+1} = g^{j+1}(x_{i-1/2}),
$$

where

$$
\begin{aligned}
A_i &= \frac{\varepsilon}{\widetilde{h}_i(\widetilde{h}_i+\widetilde{h}_{i-1})} - \frac{b_{i-1/2}^{j+\frac{1}{2}}}{2(\widetilde{h}_i+\widetilde{h}_{i-1})} - \left(\frac{c_{i-1/2}^{j+\frac{1}{2}}}{\Delta t} + \frac{d_{i-1/2}^{j+\frac{1}{2}}}{2}\right)\frac{\widetilde{h}_i}{4(\widetilde{h}_i+\widetilde{h}_{i-1})}, \\
B_i &= -\varepsilon\left[\frac{1}{\widetilde{h}_i(\widetilde{h}_i+\widetilde{h}_{i+1})} + \frac{1}{\widetilde{h}_i(\widetilde{h}_i+\widetilde{h}_{i-1})}\right] + \frac{b_{i-1/2}^{j+\frac{1}{2}}}{2}\left[\frac{-1}{\widetilde{h}_i+\widetilde{h}_{i+1}} + \frac{1}{\widetilde{h}_i+\widetilde{h}_{i-1}}\right] \\
&\quad - \left(\frac{c_{i-1/2}^{j+\frac{1}{2}}}{\Delta t} + \frac{d_{i-1/2}^{j+\frac{1}{2}}}{2}\right)\left(1 - \frac{\widetilde{h}_i}{4(\widetilde{h}_i+\widetilde{h}_{i-1})} - \frac{\widetilde{h}_i}{4(\widetilde{h}_i+\widetilde{h}_{i+1})}\right),
\end{aligned}
$$

$$C_i = \frac{\varepsilon}{\widetilde{h}_i(\widetilde{h}_i + \widetilde{h}_{i+1})} + \frac{b_{i-1/2}^{j+\frac{1}{2}}}{2(\widetilde{h}_i + \widetilde{h}_{i+1})} - \left(\frac{c_{i-1/2}^{j+\frac{1}{2}}}{\Delta t} + \frac{d_{i-1/2}^{j+\frac{1}{2}}}{2}\right)\frac{\widetilde{h}_i}{4(\widetilde{h}_i + \widetilde{h}_{i+1})}.$$

2.4 Convergence analysis

In this section, we shall develop the parameter-uniform convergence of the proposed method. We find $\widetilde{v}^{j+1} \in S_2^1(\Omega_x^{N_x})$ such that

$$[L\widetilde{v}^{j+1}]_{i-1/2} = g^{j+1}(x_{i-1/2}),\ i = 1, 2, \ldots, N_x,\ \widetilde{v}_0^{j+1} = p_0(t_{j+1}),\ \widetilde{v}_{N_x}^{j+1} = p_1(t_{j+1}). \quad (2.4.1)$$

We represent $\widetilde{v}^{j+1}(x)$ as

$$\widetilde{v}^{j+1}(x) = \sum_{k=0}^{N_x+1} \widetilde{w}_k^{j+1}\mathcal{B}_k(x), \quad j = 0, 1, \ldots, N_t - 1.$$

Applying the collocation scheme at each time level, the coefficients $\widetilde{w}_k^{j+1}$ are determined by solving the equivalent system

$$[\mathcal{L}^{N_x}\widetilde{\mathbf{w}}^{j+1}]_{i-1/2} = g^{j+1}(x_{i-1/2}),\ i = 1, 2, \ldots, N_x,\ \widetilde{w}_0^{j+1} = p_0(t_{j+1}),\ \widetilde{w}_{N_x+1}^{j+1} = p_1(t_{j+1}), \quad (2.4.2)$$

where $\widetilde{\mathbf{w}}^{j+1} = (\widetilde{w}_0^{j+1}, \ldots, \widetilde{w}_{N_x+1}^{j+1}) \in \mathbb{R}^{N_x+2}$. Now, first, we discuss the error estimates in S_2^0-interpolation, which will be used to prove error estimates in S_2^1-interpolation. After concluding all these estimates, we can easily prove the uniform convergence of the proposed method.

2.4.1 S_2^0-interpolation

To find a piecewise quadratic function $I_2^0 v^{j+1} \in S_2^0(\Omega_x^{N_x})$ for an arbitrary function $v^{j+1} \in C^0(\overline{\mathcal{G}}_x)$, consider the following interpolation problem

$$(I_2^0 v^{j+1})_i = v_i^{j+1},\ i = 0, 1, \ldots, N_x, \quad \text{and} \quad (I_2^0 v^{j+1})_{i-1/2} = v_{i-1/2}^{j+1},\ i = 1, 2, \ldots, N_x,$$

where $v_i^{j+1} = v(x_i, t_{j+1}),\ v_{i-1/2}^{j+1} = v(x_{i-1/2}, t_{j+1})$.

Theorem 2.4.1. *Assuming $b^{j+1}, c^{j+1}, d^{j+1}, f^{j+1} \in C^4(\overline{\mathcal{G}}_x)$, the interpolating error $\widetilde{u}^{j+1} - I_2^0\widetilde{u}^{j+1}$ for the semi-discrete solution $\widetilde{u}^{j+1}$ of (2.3.1) at each time level satisfies the following bounds*

$$\begin{aligned}
\|\widetilde{u}^{j+1} - I_2^0\widetilde{u}^{j+1}\| &\leq CN_x^{-3},\\
\max_{i=1,2,\ldots,N_x} |(\widetilde{u}^{j+1} - I_2^0\widetilde{u}^{j+1})'_{i-1/2}| &\leq CN_x^{-2},\\
\sqrt{\varepsilon}\max_{i=1,2,\ldots,N_x} |(\widetilde{u}^{j+1} - I_2^0\widetilde{u}^{j+1})''_{i-1/2}| &\leq CN_x^{-2}.
\end{aligned}$$

Proof. The interpolating error in the solution and its derivatives satisfy the following bounds [92]

$$\|\widetilde{u}^{j+1} - I_2^0\widetilde{u}^{j+1}\|_{I_i} \leq C\widetilde{h}_i^3\|(\widetilde{u}^{j+1})'''\|_{I_i}, \tag{2.4.3a}$$

$$|(\widetilde{u}^{j+1} - I_2^0\widetilde{u}^{j+1})'_{i-1/2}| \leq C\widetilde{h}_i^2\|(\widetilde{u}^{j+1})'''\|_{I_i}, \tag{2.4.3b}$$

$$|(\widetilde{u}^{j+1} - I_2^0\widetilde{u}^{j+1})''_{i-1/2}| \leq C\widetilde{h}_i^2\|(\widetilde{u}^{j+1})^{(4)}\|_{I_i}. \tag{2.4.3c}$$

Applying the decomposition of $\widetilde{u}^{j+1}$ and the linearity property of I_2^0, the interpolating error in $\widetilde{u}^{j+1}$ can be decomposed in the following manner

$$\widetilde{u}^{j+1} - I_2^0\widetilde{u}^{j+1} = (\widetilde{y}^{j+1} - I_2^0\widetilde{y}^{j+1}) + (\widetilde{z}^{j+1} - I_2^0\widetilde{z}^{j+1}). \tag{2.4.4}$$

The above decomposition encourages us to separately compute the error estimates for regular and singular components. For the regular component, the use of Theorem 2.3.1 and inequality (2.3.4) give

$$\begin{aligned}
\|\widetilde{y}^{j+1} - I_2^0\widetilde{y}^{j+1}\|_{I_i} &\leq C\widetilde{h}_i^3\|(\widetilde{y}^{j+1})'''\|_{I_i} \leq CN_x^{-3},\\
\max_{i=1,2,\ldots,N_x} |(\widetilde{y}^{j+1} - I_2^0\widetilde{y}^{j+1})'_{i-1/2}| &\leq C\widetilde{h}_i^2\|(\widetilde{y}^{j+1})'''\|_{I_i} \leq CN_x^{-2},\\
\max_{i=1,2,\ldots,N_x} |(\widetilde{y}^{j+1} - I_2^0\widetilde{y}^{j+1})''_{i-1/2}| &\leq C\widetilde{h}_i^2\|(\widetilde{y}^{j+1})^{(4)}\|_{I_i} \leq CN_x^{-2}.
\end{aligned}$$

We analyze the errors of the singular component in layer region and uniform region using Theorem 2.3.1 and the inequality (2.3.4).

Case 1. For $I_i \subset [0, x_{\frac{N_x}{2}-1}]$, we have

$$\|\widetilde{z}^{j+1} - I_2^0 \widetilde{z}^{j+1}\|_{I_i} \leq C\widetilde{h}_i^3 \|(\widetilde{z}^{j+1})'''\|_{I_i} \leq CN_x^{-3}.$$

Case 2. For $I_i \subset [x_{\frac{N_x}{2}-1}, 1]$, we have

$$\|\widetilde{z}^{j+1} - I_2^0 \widetilde{z}^{j+1}\|_{I_i} \leq C\widetilde{h}_i^3 \|(\widetilde{z}^{j+1})'''\|_{I_i} \leq CN_x^{-3}.$$

The required result is obtained using the triangle inequality in (2.4.4). Using the same approach, one can obtain bounds for $(\widetilde{u}^{j+1} - I_2^0 \widetilde{u}^{j+1})'_{i-1/2}$ and $(\widetilde{u}^{j+1} - I_2^0 \widetilde{u}^{j+1})''_{i-1/2}$. □

Lemma 2.4.1. *Assume $r \in S_2^0(\Omega_x^{N_x})$ such that $r_{i-1/2} = 0,\ i = 1, 2, \ldots, N_x$, then*

$$\|r\|_{I_i} \leq \max_i\{|r_{i-1}|, |r_i|\}, \quad \|r'\|_{I_i} \leq \frac{4}{\widetilde{h}_i} \max_i\{|r_{i-1}|, |r_i|\}, \quad \|r''\|_{I_i} \leq \frac{8}{\widetilde{h}_i^2} \max_i\{|r_{i-1}|, |r_i|\}.$$

Proof. Refer to Lemma 3.2 given in [92]. □

2.4.2 S_2^1-interpolation

To find a piecewise quadratic function $I_2^1 v^{j+1} \in S_2^1(\Omega_x^{N_x})$ for an arbitrary function $v^{j+1} \in C^1(\overline{\mathcal{G}}_x)$, consider the following interpolation problem

$$(I_2^1 v^{j+1})_{i-1/2} = v_{i-1/2}^{j+1},\ i = 1, 2, \ldots, N_x, (I_2^1 v^{j+1})_0 = v_0^{j+1},\ (I_2^1 v^{j+1})_{N_x} = v_{N_x}^{j+1}. \quad (2.4.5)$$

For the quadratic spline $r(x)$, for $i = 1, 2, \ldots, N_x$, we set $r_i = r(x_i), r_{i-1/2} = r(x_i - \widetilde{h}_i/2), a_i = \frac{\widetilde{h}_{i+1}}{\widetilde{h}_i + \widetilde{h}_{i+1}}$, and $c_i = 1 - a_i = \frac{\widetilde{h}_i}{\widetilde{h}_i + \widetilde{h}_{i+1}}$. Let $G : S_2^1(\Omega_x^{N_x}) \to \mathbb{R}^{N_x+1}$ be the operator defined by

$$[Gr]_i = a_i r_{i-1} + 3r_i + c_i r_{i+1},$$

then because of continuity, the parameters r_{i-1}, r_i, and $r_{i-1/2}$ must satisfy the consistency relation [93]

$$a_i r_{i-1} + 3r_i + c_i r_{i+1} = 4a_i r_{i-1/2} + 4c_i r_{i+1/2},\ i = 1, 2, \ldots, N_x - 1. \quad (2.4.6)$$

Lemma 2.4.2 (Stability of the operator G)**.** *Assuming that* $r_0 = r_{N_x} = 0$ *for all* $r_i \in \mathbb{R}^{N_x+1}$, *the operator* G *satisfies the following stability bound*

$$\max_{i=1,2,\ldots,N_x-1} |r_i| \leq \frac{1}{2} \max_{i=1,2,\ldots,N_x-1} |[Gr]_i|.$$

Proof. Refer to [94] for the proof. □

Theorem 2.4.2. *Assuming that* $b^{j+1}, c^{j+1}, d^{j+1}, f^{j+1} \in C^4(\overline{\mathcal{G}}_x)$ *the interpolating errors* $\widetilde{u}^{j+1} - I_2^1 \widetilde{u}^{j+1}$ *for the semi-discrete solution* $\widetilde{u}^{j+1}$ *of (2.3.1) at each time level satisfy the following bounds*

$$\max_{i=0,1,\ldots,N_x} |(\widetilde{u}^{j+1} - I_2^1 \widetilde{u}^{j+1})_i| \leq C N_x^{-4}, \tag{2.4.7}$$

$$\|\widetilde{u}^{j+1} - I_2^1 \widetilde{u}^{j+1}\| \leq C N_x^{-3}, \tag{2.4.8}$$

$$\max_{i=1,2,\ldots,N_x} |(\widetilde{u}^{j+1} - I_2^1 \widetilde{u}^{j+1})'_{i-1/2}| \leq C N_x^{-2}, \tag{2.4.9}$$

$$\sqrt{\varepsilon} \max_{i=1,2,\ldots,N_x} |(\widetilde{u}^{j+1} - I_2^1 \widetilde{u}^{j+1})''_{i-1/2}| \leq C N_x^{-2}. \tag{2.4.10}$$

Proof. The interpolating error of an arbitrary function $v^{j+1} \in C^4(\overline{\mathcal{G}}_x)$ satisfies

$$(v^{j+1} - I_2^1 v^{j+1})_0 = (v^{j+1} - I_2^1 v^{j+1})_{N_x} = 0.$$

Truncation error is given by using (2.4.5) and (2.4.6)

$$\tau_{v,i}^{j+1} = [G(v^{j+1} - I_2^1 v^{j+1})]_i = a_i v_{i-1}^{j+1} - 4a_i v_{i-1/2}^{j+1} + 3v_i^{j+1} - 4c_i v_{i+1/2}^{j+1} + c_i v_{i+1}^{j+1}, \quad i = 1, 2, \ldots, N_x. \tag{2.4.11}$$

The use of Taylor series expansion in (2.4.11) implies

$$|\tau_{v,i}^{j+1}| \leq \frac{1}{12} \widetilde{h}_i \widetilde{h}_{i+1} |\widetilde{h}_{i+1} - \widetilde{h}_i| \|(v^{j+1})'''\|_{I_i} + \frac{5}{96} \max\{\widetilde{h}_i^4, \widetilde{h}_{i+1}^4\} \|(v^{j+1})^{(4)}\|_{I_i \cup I_{i+1}}. \tag{2.4.12}$$

Again the truncation error $\tau_{\widetilde{u},i}^{j+1}$ can be decomposed as

$$\tau_{\widetilde{u},i}^{j+1} = \tau_{\widetilde{y},i}^{j+1} + \tau_{\widetilde{z},i}^{j+1}.$$

Using Theorem 2.3.1 and the inequality (2.4.12), the regular component $\tau_{\widetilde{y},i}^{j+1}$ can be bounded as follows

$$|\tau_{\widetilde{y},i}^{j+1}| \leq C(\widetilde{h}_i\widetilde{h}_{i+1}|\widetilde{h}_{i+1} - \widetilde{h}_i| + \max\{\widetilde{h}_i^4, \widetilde{h}_{i+1}^4\}).$$

In the layer region $[0, x_{\frac{N_x}{2}-1}]$, it is $\widetilde{h}_{i+1} < \widetilde{h}_i$, and thus

$$|\tau_{\widetilde{y},i}^{j+1}| \leq C(\widetilde{h}_i^2|\widetilde{h}_{i+1} - \widetilde{h}_i| + \widetilde{h}_i^4).$$

Now using (2.3.4) and (2.3.5), we have

$$|\tau_{\widetilde{y},i}^{j+1}| \leq CN_x^{-4}.$$

Following the approach of Lemma 2.4.2, we find

$$\max_{i=0,1,\ldots,N_x} |(\widetilde{y}^{j+1} - I_2^1\widetilde{y}^{j+1})_i| \leq CN_x^{-4}. \tag{2.4.13}$$

A similar procedure can be used to find the following bounds for $\tau_{\widetilde{z},i}^{j+1}$ for $i = 1, 2, \ldots, \frac{N_x}{2} - 1$.

$$\begin{aligned}
|\tau_{\widetilde{z},i}^{j+1}| &\leq \frac{1}{12}\widetilde{h}_i\widetilde{h}_{i+1}|\widetilde{h}_{i+1} - \widetilde{h}_i|\|(\widetilde{z}^{j+1})'''\|_{I_i} + \frac{5}{96}\max\{\widetilde{h}_i^4, \widetilde{h}_{i+1}^4\}\|(\widetilde{z}^{j+1})^{(4)}\|_{I_i\cup I_{i+1}} \\
&\leq CN_x^{-4}\left\|\exp\left(-x\sqrt{\frac{\delta}{\varepsilon}}\right)\right\|_{I_i} \\
&\leq CN_x^{-4}.
\end{aligned}$$

For $i = \frac{N_x}{2}, \frac{N_x}{2} + 1, \ldots, N_x$,

$$\begin{aligned}
|\tau_{\widetilde{z},i}^{j+1}| &\leq \frac{1}{12}\widetilde{h}_i\widetilde{h}_{i+1}|\widetilde{h}_{i+1} - \widetilde{h}_i|\|(\widetilde{z}^{j+1})'''\|_{I_i} + \frac{5}{96}\max\{\widetilde{h}_i^4, \widetilde{h}_{i+1}^4\}\|(\widetilde{z}^{j+1})^{(4)}\|_{I_i\cup I_{i+1}} \\
&\leq CN_x^{-4}\varepsilon^{-2}\left\|\exp\left(-x\sqrt{\frac{\delta}{\varepsilon}}\right)\right\|_{I_i} \\
&\leq CN_x^{-4}.
\end{aligned}$$

Using the approach of Lemma 2.4.2, we get

$$\max_{i=0,1,\ldots,N_x} |(\widetilde{z}^{j+1} - I_2^1 \widetilde{z}^{j+1})_i| \leq C N_x^{-4}. \tag{2.4.14}$$

From the inequalities (2.4.13) and (2.4.14), we can obtain the estimate (2.4.7). To prove (2.4.8), we use the triangle inequality to obtain

$$\begin{aligned} \|\widetilde{u}^{j+1} - I_2^1 \widetilde{u}^{j+1}\| &\leq \|\widetilde{u}^{j+1} - I_2^0 \widetilde{u}^{j+1}\| + \|I_2^0 \widetilde{u}^{j+1} - I_2^1 \widetilde{u}^{j+1}\| \\ &\leq \|\widetilde{u}^{j+1} - I_2^0 \widetilde{u}^{j+1}\| + \max_{i=0,1,\ldots,N_x} |(\widetilde{u}^{j+1} - I_2^1 \widetilde{u}^{j+1})_i|. \end{aligned}$$

From S_0^2-interpolation, we know $(I_2^0 \widetilde{u}^{j+1})_i = \widetilde{u}_i^{j+1},\ i = 0, 1, \ldots, N_x$. Using Theorem 2.4.1 and estimate (2.4.7), we obtain (2.4.8). To obtain the estimate (2.4.9), we use Lemma 2.4.1, Theorem 2.4.1, (2.4.7), and the triangle inequality

$$\begin{aligned} |(\widetilde{u}^{j+1} - I_2^1 \widetilde{u}^{j+1})'_{i-1/2}| &\leq |(\widetilde{u}^{j+1} - I_2^0 \widetilde{u}^{j+1})'_{i-1/2}| + |(I_2^0 \widetilde{u}^{j+1} - I_2^1 \widetilde{u}^{j+1})'_{i-1/2}| \\ &\leq |(\widetilde{u}^{j+1} - I_2^0 \widetilde{u}^{j+1})'_{i-1/2}| + \frac{4}{\widetilde{h}_i} \max_{i=0,1,\ldots,N_x} |(\widetilde{u}^{j+1} - I_2^1 \widetilde{u}^{j+1})_i|. \end{aligned}$$

A simple use of the triangle inequality again gives

$$\begin{aligned} \sqrt{\varepsilon}|(\widetilde{u}^{j+1} - I_2^1 \widetilde{u}^{j+1})''_{i-1/2}| &\leq \sqrt{\varepsilon}|(\widetilde{u}^{j+1} - I_2^0 \widetilde{u}^{j+1})''_{i-1/2}| + \sqrt{\varepsilon}|(I_2^0 \widetilde{u}^{j+1} - I_2^1 \widetilde{u}^{j+1})''_{i-1/2}| \\ &\leq \sqrt{\varepsilon}|(\widetilde{u}^{j+1} - I_2^0 \widetilde{u}^{j+1})'_{i-1/2}| + \frac{8}{\widetilde{h}_i^2} \max_{i=0,1,\ldots,N_x} \sqrt{\varepsilon}|(\widetilde{u}^{j+1} - I_2^1 \widetilde{u}^{j+1})_i|. \end{aligned}$$

Now, using a procedure similar to the one we use to prove (2.4.9), we obtain (2.4.10). Hence, the proof is completed. □

Theorem 2.4.3 (Stability of the operator $\mathcal{L}^{N_x}$)**.** *The operator $\mathcal{L}^{N_x}$ satisfies the following stability bound in the maximum-norm*

$$\|\Theta\| \leq \frac{4\Delta t}{\delta \Delta t + 1} \|\mathcal{L}^{N_x}\Theta\|,\ \textit{for all}\ \Theta \in \mathbb{R}_0^{N_x+2},$$

where $\mathbb{R}_0^{N_x+2} = \{s \in \mathbb{R}^{N_x+2} : s_0 = s_{N_x+1} = 0\}$.

Proof. Refer to [94]. □

Theorem 2.4.4. *The semi-discrete solution $\widetilde{u}^{j+1}(x)$ of the problem (2.3.1) and the solution $\widetilde{v}^{j+1}(x)$ of the problem (2.4.1) satisfy*

$$\|\widetilde{u}^{j+1} - \widetilde{v}^{j+1}\| \leq CN_x^{-2},$$
$$\|\widetilde{u}^{j+1}_{i-1/2} - \widetilde{v}^{j+1}_{i-1/2}\| \leq CN_x^{-2}, \text{ for } i = 1, 2, \ldots, N_x.$$

Proof. Using the triangle inequality, we get

$$\|\widetilde{u}^{j+1} - \widetilde{v}^{j+1}\| \leq \|\widetilde{u}^{j+1} - I_2^1\widetilde{u}^{j+1}\| + \|I_2^1\widetilde{u}^{j+1} - \widetilde{v}^{j+1}\|.$$

As $I_2^1\widetilde{u}^{j+1}$ is the interpolant of $\widetilde{u}^{j+1}$, it can be written as

$$I_2^1\widetilde{u}^{j+1}(x) = \sum_{k=0}^{N_x+1} \widetilde{\beta}_k^{j+1}\mathcal{B}_k(x).$$

Thus,

$$[\mathcal{L}^{N_x}(\widetilde{\mathbf{w}}^{j+1} - \widetilde{\boldsymbol{\beta}}^{j+1})]_{i-1/2} = L(\widetilde{v}^{j+1} - I_2^1\widetilde{u}^{j+1})_{i-1/2},\ i = 1, 2, \ldots, N_x.$$

Since $\widetilde{\mathbf{w}}^{j+1} - \widetilde{\boldsymbol{\beta}}^{j+1} \in \mathbb{R}_0^{N_x+2}$, the application of Theorems 2.4.2 and 2.4.3 gives

$$\|I_2^1\widetilde{u}^{j+1} - \widetilde{v}^{j+1}\| \leq \|\widetilde{\mathbf{w}}^{j+1} - \widetilde{\boldsymbol{\beta}}^{j+1}\| \leq CN_x^{-2}.$$

The second estimate can be obtained by using the same procedure as in Theorem 2.4.4. □

Corollary 2.4.1. *Assuming that $N_x^{-l} \leq C\Delta t,\ 0 < l < 1$, then*

$$|\widetilde{u}^{j+1}_{i-1/2} - \widetilde{v}^{j+1}_{i-1/2}| \leq C\Delta t N_x^{-2+l},\ i = 1, 2, \ldots, N_x.$$

This bound is required to prove the parameter-uniform convergence of the fully discrete scheme.

Theorem 2.4.5. *For $N_x^{-l} \leq C\Delta t,\ 0 < l < 1$, we have*

$$\|u(x_{i-1/2}, t_j) - \mathcal{S}^j_{i-1/2}\| \leq C((\Delta t)^2 + N_x^{-2+l}).$$

Proof. Let $\xi_i^j = u(x_{i-1/2}, t_j) - \mathcal{S}_{i-1/2}^j$ be the error at j-th time level. We split ξ_i^j by the triangle inequality, as

$$\|\xi_i^j\| \leq \|u(x_{i-1/2}, t_j) - \widetilde{u}_{i-1/2}^j\| + \|\widetilde{u}_{i-1/2}^j - \widetilde{v}_{i-1/2}^j\| + \|\widetilde{v}_{i-1/2}^j - \mathcal{S}_{i-1/2}^j\|.$$

Using the corollary 2.4.1 and the boundedness of the time derivative, we get

$$\|\xi_i^j\| \leq C\Delta t((\Delta t)^2 + N_x^{-2+l}) + \|\widetilde{v}_{i-1/2}^j - \mathcal{S}_{i-1/2}^j\|.$$

Using the stability estimate given in Theorem 2.4.3, it can be proved that

$$\|\widetilde{v}_{i-1/2}^j - \mathcal{S}_{i-1/2}^j\| \leq \|u(x_{i-1/2}, t_{j-1}) - \mathcal{S}_{i-1/2}^{j-1}\|,$$

this recurrence follows at each time level, and finally, we deduce our required estimate

$$\|\xi_i^j\| \leq C\Delta t((\Delta t)^2 + N_x^{-2+l}) + \|\xi_i^{j-1}\|.$$

Using the inequality repeatedly, we get the required result. □

2.5 Numerical simulations and discussion

In this section, to validate the theoretical findings and assess the performance of the proposed scheme, we have applied our numerical scheme to solve two test problems. For the first problem, the readers are referred to [76, 78, 84, 85], and for the second problem, the readers are referred to [82–84]). The numerical results for different values of p are compared with the existing results. As the exact solutions of the test problems are unknown, the double mesh principle estimates the errors and convergence orders. To measure the accuracy of the method, the error estimates are devised in the discrete maximum norm defined as

$$e_\varepsilon^{N_x,N_t} = \max_j \left(\max_i |U^{2N_x,2N_t}(x_{2i-1}, t_{2j-1}) - U^{N_x,N_t}(x_{i-1/2}, t_j)| \right),$$

where $U^{N_x,N_t}(x_i,t_j)$ and $U^{2N_x,2N_t}(x_{2i-1},t_{2j-1})$ are the numerical solutions to the given problem by taking (N_x,N_t) and $(2N_x,2N_t)$ partitions, respectively. Also, the corresponding order of convergence is defined as

$$\rho_{\varepsilon}^{N_x,N_t}=\frac{\ln(e_{\varepsilon}^{N_x,N_t}/e_{\varepsilon}^{2N_x,2N_t})}{\ln 2}.$$

Furthermore, we calculate the ε-uniform maximum pointwise error e^{N_x,N_t} and the corresponding ε-uniform order of convergence ρ^{N_x,N_t} as follows

$$\begin{aligned}e^{N_x,N_t}&=\max_{\varepsilon}e_{\varepsilon}^{N_x,N_t},\\ \rho^{N_x,N_t}&=\frac{\ln(e^{N_x,N_t}/e^{2N_x,2N_t})}{\ln 2}.\end{aligned}$$

Example 2.5.1. *Consider the following SP degenerate parabolic IBVP:*

$$\varepsilon\frac{\partial^2u}{\partial x^2}+x^p\frac{\partial u}{\partial x}-\frac{\partial u}{\partial t}-u=x^2-1,\ (x,t)\in\mathcal{G}=(0,1)\times(0,1],$$

subject to

$$u(0,t)=1+t^2,\ t\in P_0,\quad u(1,t)=0,\ t\in P_1,\quad u(x,0)=(1-x)^2,\ x\in P_x.$$

Example 2.5.2. *Consider the following SP degenerate parabolic IBVP:*

$$\varepsilon\frac{\partial^2u}{\partial x^2}+x^p\frac{\partial u}{\partial x}-\frac{\partial u}{\partial t}-(x+p)u=p(x^2-1)\exp(-t),\ (x,t)\in\mathcal{G}=(0,1)\times(0,1],$$

subject to

$$u(0,t)=1+t^2,\ t\in P_0,\quad u(1,t)=0,\ t\in P_1,\quad u(x,0)=(1-x)^2,\ x\in P_x.$$

The solutions to these problems exhibit a boundary layer of width $O(\sqrt{\varepsilon})$, so while solving these problems numerically, we face the difficulty on a uniform mesh (in the spatial direction) when ε tends to zero. We discretize the spatial domain using an exponentially graded mesh to overcome this difficulty. Using exponentially graded mesh increases the mesh point density

Table 2.1: $e_{\varepsilon}^{N_x,N_t}$, $\rho_{\varepsilon}^{N_x,N_t}$, e^{N_x,N_t}, and ρ^{N_x,N_t} for Example 2.5.1 for $p = 1$

	N_x				
ε	8	16	32	64	128
2^{-8}	$9.6503e-03$	$2.8447e-03$	$7.0104e-04$	$1.7688e-04$	$4.4147e-05$
	1.7623	2.0207	1.9866	2.0024	
2^{-16}	$9.7260e-03$	$2.8849e-03$	$7.0998e-04$	$1.7933e-04$	$4.4779e-05$
	1.7533	2.0227	1.9852	2.0018	
2^{-24}	$9.7269e-03$	$2.8849e-03$	$7.0999e-04$	$1.7934e-04$	$4.4780e-05$
	1.7533	2.0227	1.9852	2.0018	
2^{-32}	$9.7269e-03$	$2.8849e-03$	$7.0999e-04$	$1.7934e-04$	$4.4780e-05$
	1.7533	2.0227	1.9852	2.0018	
e^{N_x,N_t} (PM)	$9.7269e-03$	$2.8849e-03$	$7.0999e-04$	$1.7934e-04$	$4.4780e-05$
ρ^{N_x,N_t} (PM)	1.7533	2.0227	1.9852	2.0018	
e^{N_x,N_t} ([78])	$6.29e-02$	$3.61e-02$	$1.94e-02$	$9.94e-03$	$4.79e-03$
ρ^{N_x,N_t} ([78])	0.677	0.811	0.885	0.935	
e^{N_x,N_t} ([76])	–	$2.6631e-02$	$1.4511e-03$	$7.5647e-02$	$3.8609e-03$
ρ^{N_x,N_t} ([76])	–	0.8759	0.9398	0.9703	
e^{N_x,N_t} ([84])	$1.593e-02$	$3.887e-03$	$9.449e-04$	$2.345e-04$	$6.424e-5$
ρ^{N_x,N_t} ([84])	2.035	2.040	2.011	1.868	

within the layer region and resolves the boundary layer efficiently.

The numerical results of Example 2.5.1 for different values of ε, p, and N_x are given in Tables 2.1–2.2. The numerical results ($e_{\varepsilon}^{N_x,N_t}$ and $\rho_{\varepsilon}^{N_x,N_t}$) for $p = 1$ are presented in Table 2.1. A comparison with the schemes proposed by Yadav *et al.* [84], Dunne *et al.* [78], and Gupta and Kadalbajoo [76] is given at the end of Table 2.1. Table 2.2 provides the comparison of ε-uniform maximum pointwise errors e^{N_x,N_t} and the corresponding ε-uniform orders of convergence ρ^{N_x,N_t} between the proposed scheme and the schemes considered in [76, 78, 84] for various values of $p > 1$. It can be observed that the error bounds do not depend on p. We have used $N_x = N_t$ to compute the results presented in the tables. These tables show that the proposed scheme is better than the schemes proposed in [76, 78, 84] regarding the parameter-uniform error estimates and the order of convergence.

The results obtained for Example 2.5.2 for different values of ε, p, and N_x are given in Tables 2.3–2.4. A comparative study for $p = 1$ between the proposed scheme and the scheme given by Majumdar and Natesan [82] is given in Table 2.3. From these results, it can be seen that the proposed scheme performs better than the one in [82]. A comparison of $e_{\varepsilon}^{N_x,N_t}$ between the schemes given in [82–84] and the proposed scheme for $\varepsilon = 2^{-20}$ and for different values of p (2, 6, and 10) are given in Table 2.4.

For Example 2.5.1, a comparison of the results between our scheme and the scheme given

Table 2.2: Comparison of e^{N_x,N_t} and ρ^{N_x,N_t} for the Example 2.5.1 associated to different values of p

		N_x				
p	Scheme	8	16	32	64	128
2	[78]	$5.67e-02$	$4.09e-02$	$2.28e-02$	$1.21e-02$	$5.96e-03$
		0.388	0.744	0.825	0.895	
	[76]	–	$8.1465e-03$	$5.2846e-03$	$2.9479e-03$	$1.5508e-03$
		–	0.6244	0.8421	0.9267	
	[84]	$2.889e-02$	$7.860e-03$	$2.567e-03$	$7.124e-04$	$2.299e-04$
		1.878	1.614	1.849	1.832	
	PM	$7.8402e-03$	$1.8698e-03$	$5.5839e-04$	$1.5843e-04$	$4.7157e-05$
		2.0680	1.7436	1.8174	1.7483	
6	[76]	–	$1.0568e-02$	$5.4783e-03$	$2.9877e-03$	$1.5596e-03$
		–	0.9479	0.8747	0.9379	
	[84]	$4.743e-02$	$2.330e-02$	$7.745e-03$	$2.649e-03$	$8.419e-04$
		1.025	1.589	1.548	1.654	
	PM	$3.5792e-02$	$1.6816e-02$	$4.5071e-03$	$1.2934e-03$	$4.3795e-04$
		1.0875	1.9005	1.8026	1.5624	
10	[78]	$4.39e-02$	$3.72e-02$	$2.83e-02$	$1.65e-02$	$8.36e-03$
		0.115	0.511	0.594	0.734	
	[76]	–	$1.7124e-02$	$5.4782e-03$	$2.9877e-03$	$1.5595e-03$
		–	1.6442	0.8747	0.9379	
	[84]	$1.934e-01$	$6.003e-02$	$1.607e-02$	$4.713e-03$	$1.347e-03$
		1.688	1.901	1.770	1.806	
	PM	$6.4141e-03$	$1.7347e-02$	$9.4634e-03$	$2.6238e-03$	$8.2703e-04$
			0.8743	1.8507	1.6657	

Table 2.3: $e_\varepsilon^{N_x,N_t}$, e^{N_x,N_t}, and ρ^{N_x,N_t} for Example 2.5.2 for $p=1$

	N_x				
ε	8	16	32	64	128
2^{-10}	$1.1916e-02$	$3.4849e-03$	$8.6107e-04$	$2.1667e-04$	$5.4298e-05$
2^{-15}	$1.1961e-02$	$3.5096e-03$	$8.6690e-04$	$2.1810e-04$	$5.4348e-05$
2^{-20}	$1.1977e-02$	$3.5129e-03$	$8.6766e-04$	$2.1829e-04$	$5.4394e-05$
2^{-25}	$1.1980e-02$	$3.5134e-03$	$8.6778e-04$	$2.1832e-04$	$5.4401e-05$
2^{-30}	$1.1981e-02$	$3.5135e-03$	$8.6780e-04$	$2.1832e-04$	$5.4402e-05$
2^{-35}	$1.1982e-02$	$3.5136e-03$	$8.6780e-04$	$2.1832e-04$	$5.4402e-05$
e^{N_x,N_t} (PM)	$1.1982e-02$	$3.5136e-03$	$8.6780e-04$	$2.1832e-04$	$5.4402e-05$
ρ^{N_x,N_t} (PM)	1.7533	2.0227	1.9852	2.0018	
e^{N_x,N_t} ([82])	–	–	$1.0568e-03$	$3.3876e-04$	$1.0496e-04$
ρ^{N_x,N_t} ([82])	–	–	1.6413	1.6904	

Table 2.4: Comparison of $e_{\varepsilon}^{N_x,N_t}$ for Example 2.5.2 for $\varepsilon = 2^{-20}$ associated with the different values of p

p	Scheme	N_x			
		32	64	128	256
2	[83] with $N_t = N_x^2$	$6.8958e-03$	$2.6028e-03$	$8.9736e-04$	$2.9563e-04$
	[84]	$1.522e-03$	$5.568e-04$	$1.925e-04$	$6.408e-05$
	PM	$6.7777e-04$	$2.7015e-04$	$1.0613e-04$	$4.1748e-05$
6	[83] with $N_t = N_x^2$	$1.4830e-02$	$5.6392e-03$	$1.9744e-04$	$6.4986e-04$
	[84]	$3.309e-03$	$1.222e-03$	$4.230e-04$	$1.412e-04$
	PM	$2.1981e-04$	$8.7937e-04$	$3.3182e-04$	$1.2664e-04$
10	[83] with $N_t = N_x^2$	$2.1820e-02$	$8.1427e-03$	$2.9871e-03$	$1.0048e-03$
	[84]	$5.117e-03$	$1.886e-03$	$6.550e-04$	$2.189e-04$
	PM	$3.0652e-03$	$1.2367e-03$	$4.6664e-04$	$1.7464e-04$

in [76, 78, 84] are also shown graphically (see Figure 2.1(a)). In Figure 2.1(a), e^{N_x,N_t} are plotted for $p = 1$ by taking N_x from 16 to 256. It clearly shows that e^{N_x,N_t} of our scheme are lower than those considered in [76, 78, 84]. In Figure 2.1(b), we have shown that e^{N_x,N_t} of our scheme for $p = 3$ are lower than those considered in [83, 84]. To show the physical phenomenon of the solution to the problems, the surface plots (refer Figure 2.2) for different values of p and ε are drawn. From these graphs, it can be observed that for small ε (close to zero), the solution to these problems exhibits a boundary layer at the left lateral surface. It can also be observed that the width of the boundary layer continuously depends on ε, and it decreases as ε decreases.

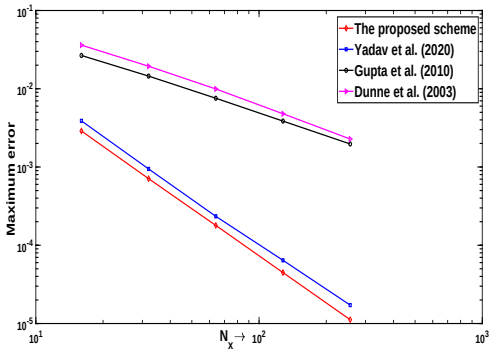

(a) Comparison of e^{N_x,N_t} for Example 2.5.1 for $p = 1$, $\varepsilon = 2^{-32}$ from $N_x = 16$ to $N_x = 256$

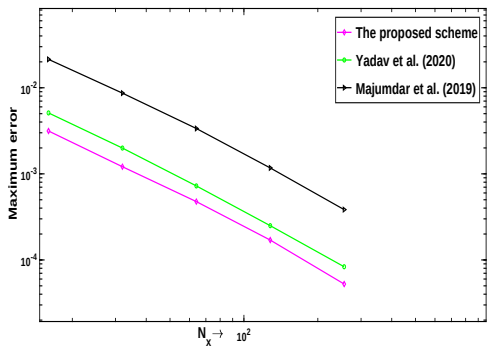

(b) Log-log plot of e^{N_x,N_t} for Example 2.5.2 for $p = 3$, $\varepsilon = 2^{-32}$ from $N_x = 16$ to $N_x = 256$

Figure 2.1: Maximum absolute error comparison plots

Remark 2.5.1. *Numerical experiments carried out in this section do not require any restric-*

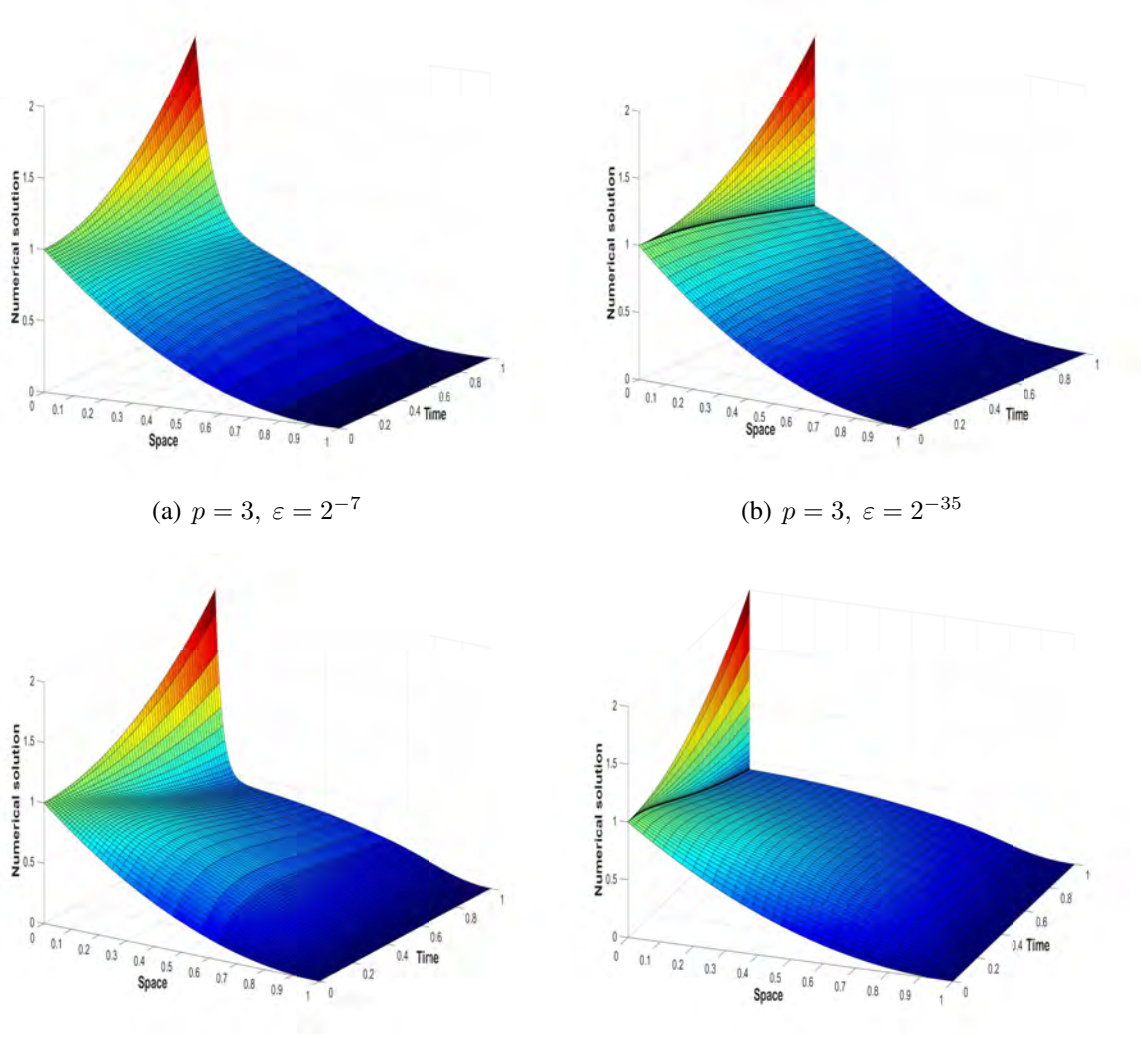

(a) $p = 3,\ \varepsilon = 2^{-7}$

(b) $p = 3,\ \varepsilon = 2^{-35}$

(c) $p = 6,\ \varepsilon = 2^{-8}$

(d) $p = 6,\ \varepsilon = 2^{-28}$

Figure 2.2: Surface plots of numerical solution of the Example 2.5.1 ((a) and (b)) and Example 2.5.2 ((c) and (d)) by using $N_x = N_t = 64$

tion like $N_x^{-l} \leq C\Delta t,\ 0 < l < 1$ *to achieve parameter-uniform estimates.*

2.6 Conclusion

A numerical scheme comprising the Crank-Nicolson scheme in the temporal direction and the quadratic spline collocation method in the spatial direction is developed to solve the singularly perturbed convection-diffusion type degenerated parabolic problems. An exponentially graded mesh is used to resolve the boundary layer. The scheme is shown to be second-order parameter-uniformly convergent through rigorous error analysis. The numerical results for two test

problems validate the theoretical error bounds and show a better performance of the proposed scheme than some existing methods. For future work, we aim to extend the present method for higher-dimensional PDEs and systems of PDEs.

Chapter 3

An efficient parameter uniform spline-based technique for singularly perturbed weakly coupled reaction-diffusion systems

---

Many different scientific and practical applications call for a specific category of mathematical models known as a singularly perturbed weakly coupled reaction-diffusion system of ODEs. The interaction among diffusion and reaction components in singularly perturbed BVPs can rise to intriguing pattern generation and spatial organization phenomena in chemical kinetics and reaction-diffusion systems. These systems typically result in double-layer structures because of parameters (commonly denoted by ε) that multiply the highest-order derivative term.

The work of this chapter has been published in the following publication:

S. Singh, D. Kumar, H. Ramos, "An efficient parameter uniform spline-based technique for singularly perturbed weakly coupled reaction-diffusion systems." J. Appl. Anal. Comput., 13 (2023), 2203–2228.

Because of this property, the system behaves excitingly and is challenging to examine, necessitating specialized analysis techniques such as adaptive mesh refinement, domain decomposition, and higher-order numerical schemes.

3.1 Problem statement

We consider the following singularly perturbed problem, which involves a system of ℓ weakly coupled reaction-diffusion equations. We seek a solution $\boldsymbol{u} \in (C^2(0,1) \cap C[0,1])^\ell$ that satisfies

$$\boldsymbol{\mathcal{L}u}(x) := -\boldsymbol{\mathcal{E}u}''(x) + \boldsymbol{B}(x)\boldsymbol{u}(x) = \boldsymbol{g}(x), \quad x \in (0,1), \tag{3.1.1a}$$

subject to the Dirichlet boundary conditions

$$\boldsymbol{u}(0) = \boldsymbol{\varrho}_0, \quad \boldsymbol{u}(1) = \boldsymbol{\varrho}_1, \tag{3.1.1b}$$

where $\boldsymbol{\mathcal{L}} = (\mathcal{L}_1, \ldots, \mathcal{L}_\ell)^T$, $\boldsymbol{\mathcal{E}} = \text{diag}(\varepsilon_1^2, \varepsilon_2^2, \ldots, \varepsilon_\ell^2)$ with $\varepsilon_k = \varepsilon,\ k = 1, 2, \ldots, \ell$, $\boldsymbol{B}(x) = (b_{ij}(x))_{\ell\times\ell}$, $\boldsymbol{g}(x) = (g_1(x), g_2(x), \ldots, g_\ell(x))^T$, $\boldsymbol{u}(x) = (u_1(x), u_2(x), \ldots, u_\ell(x))^T$, $\boldsymbol{\varrho}_0 = (\varrho_{0,1}, \ldots, \varrho_{0,\ell})^T$, and $\boldsymbol{\varrho}_1 = (\varrho_{1,1}, \ldots, \varrho_{1,\ell})^T$. We assume that each column of the coupling matrix $\boldsymbol{B} : [0,1] \to \mathbb{R}^{(\ell,\ell)}$ and the function $\boldsymbol{g} : [0,1] \to \mathbb{R}^\ell$ belong to $C^4[0,1]^\ell$. We assume that the following inequality holds to fulfill the condition of the strongly diagonally dominant matrix along with the nonsingularity of $\boldsymbol{B}(x)\ \forall x \in [0,1]$

$$\sum_{\substack{k=1 \\ k\neq i}}^{\ell} \left\| \frac{b_{ik}}{b_{ii}} \right\| < 1, \quad \text{for } i = 1, 2, \ldots, \ell. \tag{3.1.2}$$

3.1.1 Brief literature survey and motivation

These systems of equations frequently arise in several applications in science and engineering, as in electroanalytical chemistry [36], predator-prey population dynamics [95], the turbulent interaction of waves and currents [96, 97], chemical reactor theory [98], the classical linear double-diffusion model for saturated flow in fractured porous media [99], modelling of the diffusion process in bones [100], and control theory [101]. Only a few articles have appeared

dealing with systems of arbitrary size; to cite a few, Linß and Madden [52] proposed a parameter-uniform central difference scheme on layer-adapted meshes (Shishkin, Bakhvalov, and Equidistribution meshes). They have shown that the method is second-order accurate on the Bakhvalov and Equidistribution meshes, while it is almost second-order accurate up to a logarithmic factor on a Shishkin mesh. Linß suggested a FEM on arbitrary meshes (layer-adapted meshes) for a system of $\ell \geqslant 2$ singularly perturbed reaction-diffusion equations. Theoretically, he has shown that the error bounds for the Shishkin meshes are sharper than those on the Bakhvalov meshes. Stephens and Madden [102] developed the discrete Schwarz method on three overlapping subdomains for arbitrarily sized coupled singularly perturbed systems. They have used standard FDM on a uniform mesh on each subdomain and proved that the technique is parameter-uniform when appropriate subdomains are used. In this chapter, we consider a $\ell \times \ell$ system of singularly perturbed reaction-diffusion equations in which the equations have diffusion parameters of the same magnitudes. We use an exponentially graded mesh for the discretization, which results in a second-order (without logarithmic factor) parameter-uniform convergence. The proposed scheme extends the method developed for a single singularly perturbed reaction-diffusion BVP [94] to a system of reaction-diffusion equations.

We propose and analyze a parameter-uniform numerical method that uses quadratic B-spline basis functions with a special non-uniform exponentially graded mesh [91, 103–105]. In [91], Constantinou and Xenophontos analyzed h version FEM in the natural energy norm for the singularly perturbed class of reaction-diffusion and convection-diffusion problems. Shivhare *et al.* [103] constructed a quadratic B-spline-based parameter uniform numerical scheme of second order in space and first order in time for two parameter singularly perturbed PDEs. Exploring the degenerate parabolic problems, Singh *et al.* [105] proposed a uniformly convergent method and proved second-order convergence on the exponentially graded mesh. Zarin [104] developed the h-version of the standard Galerkin method using higher order polynomials and proved its robust convergence in the energy norm.

The chapter is organized as follows: Section 3.2 gives preliminary results on the solution and its derivatives. A decomposition of the exact solution is also provided in this section. The scheme is proposed in Section 3.3, divided into two subsections: in subsection 3.3.1, an

exponentially graded mesh is constructed, and the collocation scheme is given in subsection 3.3.2. The comprehensive convergence analysis is provided in Section 3.4. Numerical simulations and discussion of the results are exemplified in Section 3.5, while some concluding comments and further research in this direction are included in Section 3.6.

Throughout the chapter, matrices and vectors will be denoted by bold letters, while we use plain letters for scalars. A superscript T will be used to transpose a vector/matrix. When the domain $\mathcal{D}$ is obvious, the standard notation $\|.\|$ will be used (instead of $\|.\|_{\mathcal{D}}$) for the infinity-norm ($L^\infty-$norm) e.g., for a scalar function U defined on an interval I, we define $\|U\| = \max_{x\in I} |U(x)|$ while for a vector valued function $\boldsymbol{U} = (U_1, U_2, \ldots, U_\ell)^T \in \mathbb{R}^\ell$, defined on I, the infinity-norm is defined as $\|\boldsymbol{U}\| = \max_{x\in I}\{|U_1(x)|, |U_2(x)|, \ldots, |U_\ell(x)|\}$. For simplicity, for any function U, we use U_j for $U(x_j)$ and $\tilde{U}_j$ for an approximation of U at x_j. For a vector valued function $\boldsymbol{U} = (U_1, U_2, \ldots, U_\ell)^T \in \mathbb{R}^\ell$ applied to x_j we use the notation $(U_1, U_2, \ldots, U_\ell)^T(x_j) = (U_{1,j}, U_{2,j}, \ldots, U_{\ell,j})^T$. Furthermore, $\boldsymbol{C} = (C, C, \ldots, C)^T$ denotes a generic positive constant vector independent of the perturbation parameter ε, the nodal points x_j, and the mesh parameter N_x. A subscripted C (e.g., C_1) is also a constant independent of ε, x_j, and N_x, but whose value is fixed. Furthermore, we use $C^0(\mathcal{D})$ for the set of continuous functions in $\mathcal{D}$, and $C^k(\mathcal{D})$ for k times continuously differentiable functions in $\mathcal{D}$. Moreover, $C^k(\mathcal{D})^\ell$ is used for k times continuously differentiable vector-valued functions (with ℓ components) in $\mathcal{D}$.

3.2 Preliminary: properties of the exact solution

In this section, we present some bounds on the solution $\boldsymbol{u}$ and its derivatives, which will be used in the convergence analysis.

Theorem 3.2.1. *Assume that $\boldsymbol{B}$ satisfies the following conditions to be a strongly diagonally dominant matrix*

$$b_{ii} > 0, \text{ and } \sum_{\substack{k=1\\k\neq i}}^{\ell} \left\| \frac{b_{ik}}{b_{ii}} \right\| < \xi < 1, \quad \xi \in (0,1), \quad \text{for } i = 1, 2, \ldots, \ell.$$

Then

$$|u_i^{(k)}(x)| \leqslant C\left\{1+\varepsilon^{-k}\left(e^{-\lambda x/\varepsilon}+e^{-\lambda(1-x)/\varepsilon}\right)\right\}, \quad \textit{for } k=0,1,2;\ i=1,2,\ldots,\ell,$$

where $\lambda=\lambda(\xi)>0$ *is given by*

$$\lambda^2=(1-\xi)\min_{i=1,2,\ldots,\ell}\left\{\min_{x\in[0,1]} b_{ii}(x)\right\}.$$

Proof. Refer to the proof of Theorem 2.4 given in [52]. □

In the study of numerical simulation of SPBVPs, stability estimates ensure the boundedness of the solution. We assumed that the coupling matrix $\boldsymbol{B}$ is an arbitrary matrix with positive diagonal entries. We give the following stability criterion using the maximum principle (refer to Protter and Weinberger [106]).

Lemma 3.2.1 (Stability Estimate)**.** *Consider the differential operator*

$$\widetilde{\mathcal{L}}u:=-\nu^2u''+c(x)u'+b(x)u,$$

with $\nu>0$*,* $b,c\in C[0,1]$ *and* $b(x)>0$ *on* $[0,1]$*. Then*

$$\|\mathcal{V}\|\leqslant\max\left\{\left\|\frac{\widetilde{\mathcal{L}}\mathcal{V}}{b}\right\|,|\mathcal{V}(0)|,|\mathcal{V}(1)|\right\},\ \textit{for all } \mathcal{V}\in C^2(0,1)\cap C[0,1].$$

We decompose the solution of problem (3.1.1) as $\boldsymbol{u}=\boldsymbol{\varphi}+\boldsymbol{\eta}$, with $\boldsymbol{\varphi}=(\varphi_1,\ldots,\varphi_\ell)^T$, and $\boldsymbol{\eta}=(\eta_1,\ldots,\eta_\ell)^T$, where the components satisfy the following BVPs, respectively

$$-\varepsilon^2\varphi_i''(x)+b_{ii}(x)\varphi_i(x)=g_i(x),\ 0<x<1,\quad \varphi_i(0)=\varrho_{0,i},\ \varphi_i(1)=\varrho_{1,i},\ i=1,2,\ldots,\ell,$$

and

$$-\varepsilon^2\eta_i''(x)+b_{ii}(x)\eta_i(x)=-\sum_{\substack{k=1\\k\neq i}}^{\ell}b_{ik}(x)u_k(x),\ 0<x<1,\ \eta_i(0)=\eta_i(1)=0,\ i=1,2,\ldots,\ell.$$

Using Lemma 3.2.1, we obtain

$$\|\varphi_i\| \leqslant \max\left\{\left\|\frac{g_i}{b_{ii}}\right\|, |\varrho_{0,i}|, |\varrho_{1,i}|\right\}, \quad \text{and} \quad \|\eta_i\| \leqslant \sum_{\substack{k=1\\k\neq i}}^{\ell}\left\|\frac{b_{ik}}{b_{ii}}\right\|\|u_k\| \quad \text{for } i = 1, 2, \ldots, \ell.$$

Now, since $\|u_i\| \leqslant \|\varphi_i\| + \|\eta_i\|$, we have

$$\|u_i\| - \sum_{\substack{k=1\\k\neq i}}^{\ell}\left\|\frac{b_{ik}}{b_{ii}}\right\|\|u_k\| \leqslant \max\left\{\left\|\frac{g_i}{b_{ii}}\right\|, |\varrho_{0,i}|, |\varrho_{1,i}|\right\} \quad \text{for } i = 1, 2, \ldots, \ell.$$

We consider the matrix

$$\boldsymbol{G} = \begin{bmatrix} 1 & -\|b_{12}/b_{11}\| & \ldots & -\|b_{1\ell}/b_{11}\| \\ -\|b_{21}/b_{22}\| & 1 & \ldots & -\|b_{2\ell}/b_{22}\| \\ \vdots & \vdots & \ddots & \vdots \\ -\|b_{\ell 1}/b_{\ell\ell}\| & -\|b_{\ell 2}/b_{\ell\ell}\| & \ldots & 1 \end{bmatrix}, \tag{3.2.1}$$

such that all entries of $\boldsymbol{G}^{-1}$ are non-negative, then u is bounded for the given data.

Theorem 3.2.2. *Assuming that the coupling matrix B has positive diagonal entries, the matrix $\boldsymbol{G}$ is inverse monotone. Then the solution $\boldsymbol{u}$ of (3.1.1) satisfies*

$$\|u_i\| \leqslant \sum_{k=1}^{\ell}(\boldsymbol{G}^{-1})_{ik} \max\left\{\left\|\frac{g_i}{b_{ii}}\right\|, |\varrho_{0,i}|, |\varrho_{1,i}|\right\}, \quad \textit{for } i = 1, 2, \ldots, \ell.$$

Proof. The condition (3.1.2) implies that the matrix $\boldsymbol{G}$ is a strictly diagonally dominant L_0-matrix, and the inverse monotonicity of $\boldsymbol{G}$ is directed by the M-matrix criterion. The proof follows using Lemma 3.2.1 (see [52, 107, 108] for the details). □

Remark 3.2.1. *In general, the operator $\boldsymbol{\mathcal{L}}$ does not satisfy the maximum principle, but Theorem 3.2.2 suggests that $\boldsymbol{\mathcal{L}}$ is stable in the maximum-norm.*

Remark 3.2.2. *The existence and uniqueness of the solution $\boldsymbol{u} \in C^4[0,1]^\ell$ is guaranteed by the following arguments:*

(a) The stability estimates of the vector-differential operator $\boldsymbol{\mathcal{L}}$ using the standard arguments

given in [109].

(b) The coupling matrix $\boldsymbol{B}$ and the vector-valued function $\boldsymbol{g}$ belong to the space of twice continuously differentiable functions.

Due to the presence of boundary layers, we need to examine the solution in regular and layer regions. So, we decompose $\boldsymbol{u}$ into three parts as follows:

$$\boldsymbol{u} = \boldsymbol{v} + \boldsymbol{w}_L + \boldsymbol{w}_R,$$

where $\boldsymbol{v}$ is the regular component, $\boldsymbol{w}_L$ and $\boldsymbol{w}_R$ are termed as the left and right singular components, respectively. These components are the solutions of the following BVPs for $x \in (0,1)$, respectively:

$$-\boldsymbol{\mathcal{E}}\boldsymbol{v}''(x) + \boldsymbol{B}(x)\boldsymbol{v}(x) = \boldsymbol{g}(x), \quad \boldsymbol{v}(0) = \boldsymbol{B}(0)^{-1}\boldsymbol{g}(0), \quad \boldsymbol{v}(1) = \boldsymbol{B}(1)^{-1}\boldsymbol{g}(1), \tag{3.2.2a}$$

$$-\boldsymbol{\mathcal{E}}\boldsymbol{w}_L''(x) + \boldsymbol{B}(x)\boldsymbol{w}_L(x) = 0, \quad \boldsymbol{w}_L(0) = \boldsymbol{\varrho}_0 - \boldsymbol{v}(0), \quad \boldsymbol{w}_L(1) = 0, \tag{3.2.2b}$$

and

$$-\boldsymbol{\mathcal{E}}\boldsymbol{w}_R''(x) + \boldsymbol{B}(x)\boldsymbol{w}_R(x) = 0, \quad \boldsymbol{w}_R(0) = 0, \quad \boldsymbol{w}_R(1) = \boldsymbol{\varrho}_1 - \boldsymbol{v}(1). \tag{3.2.2c}$$

Theorem 3.2.3. *The components $\boldsymbol{v}$, $\boldsymbol{w}_L$, and $\boldsymbol{w}_R$ satisfy*

$$|v_i^{(k)}| \leqslant C, \quad \textit{for } k = 0, 1, \ldots, 4;\ i = 1, 2, \ldots, \ell, \tag{3.2.3a}$$

$$|(w_L)_i^{(k)}| \leqslant C\varepsilon^{-k}e^{-\lambda x/\varepsilon}, \quad \textit{for } k = 0, 1, \ldots, 4;\ i = 1, 2, \ldots, \ell, \tag{3.2.3b}$$

$$|(w_R)_i^{(k)}| \leqslant C\varepsilon^{-k}e^{-\lambda(1-x)/\varepsilon}, \quad \textit{for } k = 0, 1, \ldots, 4;\ i = 1, 2, \ldots, \ell. \tag{3.2.3c}$$

Proof. An explanatory proof is given in [47]. □

3.3 The proposed scheme

In this section, first, we give the details of the construction of the non-uniform mesh. Then, we introduce and implement the proposed scheme for the problem (3.1.1).

3.3.1 Mesh construction

It is well-known that standard numerical schemes on an equidistant mesh fail to solve SPBVPs, and unexpectedly large oscillations appear near the layer region(s) when we use a classical numerical technique. In other words, we can generate a scheme on an equidistant mesh that converges at all mesh points uniformly in the diffusion parameter unless an unacceptably large number of mesh points are used. It is not practical at all; thus, to resolve the layer(s), a non-uniform mesh is required. In this section, we construct an exponentially graded mesh that generates more mesh points in the layer region than in the other part of the domain.

To construct the exponentially graded mesh $\Delta = \{x_j |\ 0 \leqslant j \leqslant N_x\}$, we split the interval $[0, 1]$ into $N_x > 4$ (with N_x a multiple of 4) subintervals $I_j = [x_{j-1}, x_j]$. We denote by $\mathcal{P}_p$, the space of all polynomials of degree $\leqslant p$. In the construction of the mesh, we require a mesh generating function $\Psi(\rho)$, which belongs to a class of piecewise continuously differentiable functions, monotonically increasing in nature, and defined as

$$\Psi(\rho) = -\ln(1 - 2\mathfrak{C}_{p,\varepsilon}\rho),\ \rho \in [0, 1/2 - 1/N_x], \tag{3.3.1}$$

where $\mathfrak{C}_{p,\varepsilon} = 1 - \exp\left(-\frac{1}{(p+1)\varepsilon}\right) \in \mathbb{R}^+$. With the help of the transition points $x_{\frac{N_x}{4}-1}$ and $x_{\frac{3N_x}{4}+1}$, we split the interval $[0, 1]$ into three subintervals such that $[0, 1] = [0, x_{\frac{N_x}{4}-1}] \cup [x_{\frac{N_x}{4}-1}, x_{\frac{3N_x}{4}+1}] \cup [x_{\frac{3N_x}{4}+1}, 1]$. The nodal points can be written in the following form

$$x_j = \begin{cases} (p+1)\varepsilon\Psi(\rho_j), & j = 0, 1, \ldots, \frac{N_x}{4} - 1, \\ x_{\frac{N_x}{4}-1} + \left(\dfrac{x_{\frac{3N_x}{4}+1} - x_{\frac{N_x}{4}-1}}{\frac{N_x}{2}+2}\right)(j - N_x/4 + 1), & j = \frac{N_x}{4}, \ldots, \frac{3N_x}{4}, \\ 1 - (p+1)\varepsilon\Psi(1-\rho_j), & j = \frac{3N_x}{4} + 1, \ldots, N_x, \end{cases}$$

where $\rho_j = \frac{j}{N_x}$ for $j = 0, 1, \ldots, N_x$, and $\widetilde{h}_j = x_j - x_{j-1}$ for $j = 1, 2, \ldots, N_x$. The mesh points are distributed equidistantly in $[x_{\frac{N_x}{4}-1}, x_{\frac{3N_x}{4}+1}]$ with $N_x/2 + 2$ subintervals, and exponentially graded in $[0, x_{\frac{N_x}{4}-1}]$ and $[x_{\frac{3N_x}{4}+1}, 1]$ with $N_x/4 - 1$ subintervals in each. The mesh step lengths $\widetilde{h}_j$ satisfy the following inequalities utilizing the mesh characterizing

function $\Phi = \exp(-\Psi)$ (see [91] for more details)

$$\widetilde{h}_j \leqslant \begin{cases} C(p+1)\varepsilon N_x^{-1} \max \Psi'(\rho_j), & j = 1, 2, \ldots, \frac{N_x}{4} - 1, \\ C N_x^{-1}, & j = \frac{N_x}{4}, \ldots, \frac{3N_x}{4} + 1, \\ C(p+1)\varepsilon N_x^{-1} \max \Psi'(1-\rho_j), & j = \frac{3N_x}{4} + 2, \ldots, N_x, \end{cases}$$

which can be further simplified as

$$\widetilde{h}_j \leqslant \begin{cases} C(p+1)\varepsilon N_x^{-1} \max |\Phi'(\rho_j)| \exp\left(\frac{x_j}{(p+1)\varepsilon}\right), & j = 1, 2, \ldots, \frac{N_x}{4} - 1, \\ C N_x^{-1}, & j = \frac{N_x}{4}, \ldots, \frac{3N_x}{4} + 1, \\ C(p+1)\varepsilon N_x^{-1} \max |\Phi'(1-\rho_j)| \exp\left(\frac{1-x_j}{(p+1)\varepsilon}\right), & j = \frac{3N_x}{4} + 2, \ldots, N_x. \end{cases}$$

Since $\max |\Phi^{'}| < 2$, we can simply write the above inequalities as

$$\widetilde{h}_j \leqslant \begin{cases} C\varepsilon N_x^{-1} \exp\left(\frac{x_j}{(p+1)\varepsilon}\right), & j = 1, 2, \ldots, \frac{N_x}{4} - 1, \\ C N_x^{-1}, & j = \frac{N_x}{4}, \ldots, \frac{3N_x}{4} + 1, \\ C\varepsilon N_x^{-1} \exp\left(\frac{1-x_j}{(p+1)\varepsilon}\right), & j = \frac{3N_x}{4} + 2, \ldots, N_x, \end{cases} \tag{3.3.2}$$

and the step lengths of this adaptive mesh satisfy the following estimates

$$|\widetilde{h}_{j+1} - \widetilde{h}_j| \leqslant C \begin{cases} \varepsilon N_x^{-2}, & j = 1, 2, \ldots, \frac{N_x}{4} - 1, \\ 0, & j = \frac{N_x}{4}, \ldots, \frac{3N_x}{4}, \\ \varepsilon N_x^{-2}, & j = \frac{3N_x}{4} + 1, \ldots, N_x. \end{cases} \tag{3.3.3}$$

Remark 3.3.1. *Near the transition points, the Shishkin and Bakhvalov meshes do not satisfy the inequality $|\tilde{h}_{i+1} - \tilde{h}_i| \leq C N_x^{-2}$. Thus, we cannot extend our analysis to these meshes.*

3.3.2 Discretization of the problem

In this section, considering the collocation approach, we discretize the problem (3.1.1) using piecewise quadratic C^1-splines. We denote the mesh intervals by $I_j = [x_{j-1}, x_j]$, and the

collocation points are chosen as midpoints of these intervals *i.e.,*

$$X_j = x_{j-1/2} := \frac{x_{j-1}+x_j}{2} = x_{j-1} + \frac{\widetilde{h}_j}{2} = x_j - \frac{\widetilde{h}_j}{2}, \quad \text{for } j = 1, 2, \ldots, N_x.$$

For $m, p \in \mathbb{N}\,(m < p)$, we define

$$S_p^m(\Delta) := \{r \in C^m[0,1] : \ r|_{I_j} \in \mathcal{P}_p, \text{ for } j = 1, 2, \ldots, N_x\}.$$

To discretize (3.1.1), we consider a vector of splines whose components are in $S_2^1(\Delta)$ and satisfies the BVP (3.1.1) at certain points. It is known that the midpoints of $I_j,\ j = 1, 2, \ldots, N_x$, are the best choice for collocation with quadratic C^1-splines for regularly perturbed BVPs (see [110]). Next, we define the quadratic nonuniform and nonsmooth splines $\mathfrak{B}_j(x) \in S_2^1(\Delta)$ for $j = 0, 1, 2, \ldots, N_x, N_x + 1$ as follows:

$$\mathfrak{B}_0(x) = \begin{cases} \dfrac{(x_1 - x)^2}{\widetilde{h}_1^2}, & x_0 \leqslant x \leqslant x_1, \\ 0, & \text{otherwise}, \end{cases}$$

$$\mathfrak{B}_1(x) = \begin{cases} \dfrac{\widetilde{h}_1^2 - (x_1 - x)^2}{\widetilde{h}_1^2} + \dfrac{(x - x_0)^2}{\widetilde{h}_1(\widetilde{h}_1 + \widetilde{h}_2)}, & x_0 \leqslant x \leqslant x_1, \\ \dfrac{(x_2 - x)^2}{\widetilde{h}_1(\widetilde{h}_1 + \widetilde{h}_2)}, & x_1 \leqslant x \leqslant x_2, \\ 0, & \text{otherwise}, \end{cases}$$

and for $j = 2, 3, \ldots, N_x - 1$,

$$\mathfrak{B}_j(x) = \begin{cases} \dfrac{(x - x_{j-2})^2}{\widetilde{h}_{j-1}(\widetilde{h}_{j-1} + \widetilde{h}_j)}, & x_{j-2} \leqslant x \leqslant x_{j-1}, \\ \dfrac{(x - x_{j-2})(x_j - x)}{\widetilde{h}_j(\widetilde{h}_{j-1} + \widetilde{h}_j)} + \dfrac{(x_{j+1} - x)(x - x_{j-1})}{\widetilde{h}_j(\widetilde{h}_j + \widetilde{h}_{j+1})}, & x_{j-1} \leqslant x \leqslant x_j, \\ \dfrac{(x_{j+1} - x)^2}{\widetilde{h}_{j+1}(\widetilde{h}_j + \widetilde{h}_{j+1})}, & x_j \leqslant x \leqslant x_{j+1}, \\ 0, & \text{otherwise}, \end{cases}$$

while for $j = N_x,\ N_x + 1$ these are given as

$$\mathfrak{B}_{N_x}(x) = \begin{cases} \dfrac{(x - x_{N_x-2})^2}{\widetilde{h}_{N_x-1}(\widetilde{h}_{N_x-1} + \widetilde{h}_{N_x})}, & x_{N_x-2} \leqslant x \leqslant x_{N_x-1}, \\ \dfrac{\widetilde{h}_{N_x}^2 - (x - x_{N_x-1})^2}{\widetilde{h}_{N_x}^2} + \dfrac{(x_{N_x} - x)^2}{\widetilde{h}_{N_x}(\widetilde{h}_{N_x-1} + \widetilde{h}_{N_x})}, & x_{N_x-1} \leqslant x \leqslant x_{N_x}, \\ 0, & \text{otherwise}, \end{cases}$$

$$\mathfrak{B}_{N_x+1}(x) = \begin{cases} \dfrac{(x - x_{N_x-1})^2}{\widetilde{h}_{N_x}^2}, & x_{N_x-1} \leqslant x \leqslant x_{N_x}, \\ 0, & \text{otherwise}. \end{cases}$$

The discretization consists of finding $\tilde{\boldsymbol{u}}$ whose components are in $S_2^1(\Delta)$ such that

$$\tilde{\boldsymbol{u}}_0 = \tilde{\boldsymbol{u}}(0) = \boldsymbol{\varrho}_0, \quad (\boldsymbol{\mathcal{L}}\tilde{\boldsymbol{u}})_{j-1/2} = \boldsymbol{g}_{j-1/2}, \quad \tilde{\boldsymbol{u}}_{N_x} = \tilde{\boldsymbol{u}}(1) = \boldsymbol{\varrho}_1, \quad j = 1, 2, \ldots, N_x. \tag{3.3.4}$$

Using the component-wise form, for $k = 1, 2, \ldots, \ell$ it can be written as

$$(\tilde{u}_k)_0 = \varrho_{0,k}, \quad (\mathcal{L}_k\tilde{u}_k)_{j-1/2} = (g_k)_{j-1/2}, \quad (\tilde{u}_k)_{N_x} = \varrho_{1,k},\ j = 1, 2, \ldots, N_x. \tag{3.3.5}$$

We represent each component of the collocation solution $\tilde{\boldsymbol{u}}$ as

$$\tilde{u}_k(x) = \sum_{j=0}^{N_x+1} \alpha_{j,k}\mathfrak{B}_j(x), \quad k = 1, 2, \ldots, \ell, \tag{3.3.6}$$

where the coefficients $\alpha_{j,k}$ can be determined by solving the following system obtained by using (3.3.6) in (3.3.4). This system can be written in the form

$$\alpha_{0,k} = \varrho_{0,k}, \quad [\boldsymbol{L}\boldsymbol{\alpha}_k]_{j-1/2} = \boldsymbol{g}_{j-1/2},\ j = 1, 2, \ldots, N_x, \quad \alpha_{N_x+1,k} = \varrho_{1,k},\ k = 1, 2, \ldots, \ell, \tag{3.3.7}$$

where $[\boldsymbol{L}\boldsymbol{\alpha}_k]_{j-1/2}$ comes from the discretization of $(\boldsymbol{\mathcal{L}}\tilde{\boldsymbol{u}})_{j-1/2}$ and is given by

$$[\boldsymbol{L}\boldsymbol{\alpha}_k]_{j-1/2} := -\varepsilon^2\left[\frac{2(\alpha_{j+1,k} - \alpha_{j,k})}{\widetilde{h}_j(\widetilde{h}_j + \widetilde{h}_{j+1})} - \frac{2(\alpha_{j,k} - \alpha_{j-1,k})}{\widetilde{h}_j(\widetilde{h}_j + \widetilde{h}_{j-1})}\right]$$

$$+\sum_{m=1}^{\ell}(b_{km})_{j-1/2}\left[q_j^+\alpha_{j+1,k}+\left(1-q_j^+-q_j^-\right)\alpha_{j,k}+q_j^-\alpha_{j-1,k}\right],\ j=1,2,\ldots,N_x,$$

where $q_j^+ := \frac{\widetilde{h}_j}{4(\widetilde{h}_j+\widetilde{h}_{j+1})}$ and $q_j^- := \frac{\widetilde{h}_j}{4(\widetilde{h}_j+\widetilde{h}_{j-1})}$. Combining all the equations, we get the system

$$\boldsymbol{A}\boldsymbol{\wp} = \mathfrak{G},$$

where

$$\mathfrak{G} = \Bigg(\underbrace{\varrho_{0,1}, g_1(X_1),\ldots,g_1(X_{N_x}),\varrho_{1,1}}_{1^{\text{st}}\text{component}},\underbrace{\varrho_{0,2}, g_2(X_1),\ldots,g_2(X_{N_x}),\varrho_{1,2}}_{2^{\text{nd}}\text{component}},\ldots\ldots,$$
$$\underbrace{\varrho_{0,\ell}, g_\ell(X_1),\ldots,g_\ell(X_{N_x}),\varrho_{1,\ell}}_{\ell^{\text{th}}\text{component}}\Bigg)^T,$$
$$\boldsymbol{\wp} = \Bigg(\underbrace{\alpha_{0,1},\alpha_{1,1},\ldots,\alpha_{N_x,1},\alpha_{N_x+1,1}}_{1^{\text{st}}\text{component}},\underbrace{\alpha_{0,2},\alpha_{1,2},\ldots,\alpha_{N_x,2},\alpha_{N_x+1,2}}_{2^{\text{nd}}\text{component}},\ldots\ldots,$$
$$\underbrace{\alpha_{0,\ell},\alpha_{1,\ell},\ldots,\alpha_{N_x,\ell},\alpha_{N_x+1,\ell}}_{\ell^{\text{th}}\text{component}}\Bigg)^T.$$

The matrix $\boldsymbol{A}$ is given as

$$\boldsymbol{A} = \begin{bmatrix} A_{11} & A_{12} & \ldots & A_{1\ell} \\ A_{21} & A_{22} & \ldots & A_{2\ell} \\ \vdots & \vdots & \ddots & \vdots \\ A_{\ell 1} & A_{\ell 2} & \ldots & A_{\ell\ell} \end{bmatrix},$$

where each A_{km} is a submatrix of order $(N_x+2)\times(N_x+2)$. These submatrices are given by

$$A_{kk} = \begin{bmatrix} 1 & 0 & 0 & 0 & \ldots & \ldots & 0 \\ a_{21,kk} & a_{22,kk} & a_{23,kk} & 0 & \ldots & \ldots & 0 \\ 0 & a_{32,kk} & a_{33,kk} & a_{34,kk} & \ldots & \ldots & 0 \\ \vdots & \ddots & \ddots & \ddots & \vdots & \vdots & \vdots \\ \ldots & \ldots & \ldots & 0 & a_{N_x+1N_x,kk} & a_{N_x+1N_x+1,kk} & a_{N_x+1N_x+2,kk} \\ \ldots & \ldots & \ldots & 0 & 0 & 0 & 1 \end{bmatrix},$$

where

$$
\begin{aligned}
a_{ii-1,kk} &= -\frac{8\varepsilon^2 q_{i-1}^-}{\widetilde{h}_{i-1}^2} + b_{kk}(X_{i-1})q_{i-1}^-, \\
a_{ii,kk} &= \frac{8\varepsilon^2 q_{i-1}^+}{\widetilde{h}_{i-1}^2} - \frac{8\varepsilon^2 q_{i-1}^-}{\widetilde{h}_{i-1}^2} + b_{kk}(X_{i-1})\left(1 - q_{i-1}^+ - q_{i-1}^-\right), \\
a_{ii+1,kk} &= -\frac{8\varepsilon^2 q_{i-1}^+}{\widetilde{h}_{i-1}^2} + b_{kk}(X_{i-1})q_{i-1}^+,
\end{aligned}
$$

for $i = 2, 3, \ldots, N_x + 1$. Furthermore, for $m \neq k,\ m = 1, 2, \ldots, \ell;\ k = 1, 2, \ldots, \ell$, the submatrix A_{km} is

$$
A_{km} = \begin{bmatrix}
0 & 0 & 0 & 0 & \ldots & \ldots & 0 \\
a_{21,km} & a_{22,km} & a_{23,km} & 0 & \ldots & \ldots & 0 \\
0 & a_{32,km} & a_{33,km} & a_{34,km} & \ldots & \ldots & 0 \\
\vdots & \ddots & \ddots & \ddots & \vdots & \vdots & \vdots \\
\ldots & \ldots & \ldots & 0 & a_{N_x+1N_x,km} & a_{N_x+1N_x+1,km} & a_{N_x+1N_x+2,km} \\
\ldots & \ldots & \ldots & 0 & 0 & 0 & 0
\end{bmatrix},
$$

where

$$
\begin{aligned}
a_{ii-1,km} &= b_{km}(X_{i-1})q_{i-1}^-, \\
a_{ii,km} &= b_{km}(X_{i-1})\left(1 - q_{i-1}^+ - q_{i-1}^-\right), \\
a_{ii+1,km} &= b_{km}(X_{i-1})q_{i-1}^+,
\end{aligned}
$$

for $i = 2, 3, \ldots, N_x + 1$.

3.4 Convergence analysis

3.4.1 S_2^0-interpolation

To find the interpolation $I_2^0\boldsymbol{y}$ whose components are in $S_2^0(\Delta)$, we solve the following interpolation problem assuming that $y_k \in C^0[0,1]$:

$$(I_2^0 y_k)_j = (y_k)_j,\ j = 0, 1, \ldots, N_x, \quad \text{and} \quad (I_2^0 y_k)_{j-1/2} = (y_k)_{j-1/2},\ j = 1, 2, \ldots, N_x,$$

where $(y_k)_j = y_k(x_j),\ (y_k)_{j-1/2} = y_k(X_j),\ k = 1, 2, \ldots, \ell.$

Theorem 3.4.1. *Assuming $b_{ij}(x), g_j(x) \in C^4[0,1]$, for $i,\ j = 1, 2, \ldots, \ell$, the interpolation error $\boldsymbol{u} - I_2^0\boldsymbol{u}$ of the solution $\boldsymbol{u}$ of (3.1.1) satisfies the following bounds:*

$$\|\boldsymbol{u} - I_2^0\boldsymbol{u}\| \leqslant CN_x^{-3}, \quad \textit{and} \quad \boldsymbol{\mathcal{E}} \max_{j=1,2,\ldots,N_x} |(\boldsymbol{u} - I_2^0\boldsymbol{u})''_{j-1/2}| \leqslant \boldsymbol{C}N_x^{-2}.$$

Proof. First, we make use of the Lagrange representation of the interpolation polynomial and Taylor expansions to verify that for any $\boldsymbol{y} \in C^4[0,1]^\ell$, the interpolation error on each I_j satisfies

$$\left\|y_k - I_2^0 y_k\right\|_{I_j} \leqslant \frac{\widetilde{h}_j^3}{24}\left\|y_k^{(3)}\right\|_{I_j}, \quad \left|(y_k - I_2^0 y_k)''_{j-1/2}\right| \leqslant \frac{\widetilde{h}_j^2}{48}\left\|y_k^{(4)}\right\|_{I_j}, \quad k = 1, 2, \ldots, \ell. \tag{3.4.1}$$

Using the linear property of I_2^0, the solution components u_k can be decomposed as

$$u_k - I_2^0 u_k = (v_k - I_2^0 v_k) + \Big((w_L)_k - I_2^0(w_L)_k\Big) + \Big((w_R)_k - I_2^0(w_R)_k\Big).$$

We start this analysis by finding the interpolation error in the regular component. For $I_j \subset [x_0, x_{N_x/4-1}]$, we use the bounds given in Theorem 3.2.3, to obtain

$$\begin{aligned}\frac{\widetilde{h}_j^3}{24}\left|v_k^{(3)}\right|_{I_j} &\leqslant C\varepsilon^3 N_x^{-3}\exp\left(\frac{3x_j}{(p+1)\varepsilon}\right)\\ &\leqslant CN_x^{-3}\exp\left(\frac{x_j}{\varepsilon}\right)\end{aligned}$$

$$\leqslant CN_x^{-3}\exp\Big((p+1)\Psi(\rho_j)\Big)$$
$$\leqslant CN_x^{-3}.$$

Similarly, using the same analysis in the right layer region $I_j \subset [x_{3N_x/4+2}, x_{N_x}]$, we obtain $\|v_k - I_2^0 v_k\|_{I_j} \leqslant CN_x^{-3}$. Also, for $I_j \subset [x_{N_x/4}, x_{3N_x/4+1}]$, the bounds for $\widetilde{h}_j$ (using Equation (3.3.2)) trivially give $\|v_k - I_2^0 v_k\|_{I_j} \leqslant CN_x^{-3}$. Thus, by combining all the estimates for the regular component, we get

$$\|v_k - I_2^0 v_k\| \leqslant CN_x^{-3}.$$

Next, we consider the left singular component $(w_L)_k$ in $I_j \subset [x_0, x_{N_x/4-1}]$. Using Theorem 3.2.3 and the inequality given in (3.3.2), we get

$$\begin{aligned}
\frac{\widetilde{h}_j^3}{24}\Big|(w_L)_k^{(3)}\Big|_{I_j} &\leqslant C\varepsilon^3 N_x^{-3}\exp\left(\frac{3x_j}{(p+1)\varepsilon}\right)\varepsilon^{-3}|e^{-\lambda x/\varepsilon}|_{I_j} \\
&\leqslant CN_x^{-3}\exp\left(\frac{x_j}{\varepsilon} - \frac{x_{j-1}}{\varepsilon}\right) \\
&\leqslant CN_x^{-3}\exp\left(\frac{\widetilde{h}_j}{\varepsilon}\right) \\
&\leqslant CN_x^{-3}\exp\Big((p+1)N_x^{-1}\max\Psi'(\rho_j)\Big) \\
&\leqslant CN_x^{-3}.
\end{aligned}$$

Now for $I_j \subset [x_{N_x/4}, x_{3N_x/4+1}]$, we obtain

$$\begin{aligned}
\frac{\widetilde{h}_j^3}{24}\Big|(w_L)_k^{(3)}\Big|_{I_j} &\leqslant CN_x^{-3}\varepsilon^{-3}|e^{-\lambda x/\varepsilon}|_{I_j} \\
&\leqslant CN_x^{-3}\varepsilon^{-3}\exp\left(-\frac{\lambda x_{j-1}}{\varepsilon}\right).
\end{aligned}$$

Using L'Hôpital's rule, it is easy to see that the term $\varepsilon^{-3}\exp\left(-\frac{\lambda x_{j-1}}{\varepsilon}\right)$ is bounded in $[x_{N_x/4}, x_{3N_x/4+1}]$. Thus, the above inequality gives

$$\frac{\widetilde{h}_j^3}{24}\Big|(w_L)_k^{(3)}\Big|_{I_j} \leqslant CN_x^{-3}.$$

Similar bounds can be obtained for $I_j \subset [x_{3N_x/4+2}, x_{N_x}]$ using the same arguments as for $[x_0, x_{N_x/4-1}]$. Thus, we get

$$\|(w_L)_k - I_2^0(w_L)_k\| \leqslant CN_x^{-3}.$$

Now for the right singular component $(w_R)_k$ in $I_j \subset [x_0, x_{N_x/4-1}]$ (using Theorem 3.2.3 and the inequality in (3.3.2)), we get

$$\begin{aligned}
\frac{\widetilde{h}_j^3}{24}\left|(w_R)_k^{(3)}\right|_{I_j} &\leqslant C\varepsilon^3 N_x^{-3}\exp\left(\frac{3x_j}{(p+1)\varepsilon}\right)\varepsilon^{-3}|e^{-\lambda(1-x)/\varepsilon}|_{I_j} \\
&\leqslant C\varepsilon^3 N_x^{-3}\exp\left(\frac{C_1 x_j}{\varepsilon}\right)\varepsilon^{-3}\exp\left(-\frac{C_2(1-x_{j-1})}{\varepsilon}\right) \\
&\leqslant CN_x^{-3}\exp\left(C_3\frac{x_j-(1-x_{j-1})}{\varepsilon}\right) \\
&\leqslant CN_x^{-3}\exp\left(C_3\frac{\widetilde{h}_j-1-2x_{j-1}}{\varepsilon}\right) \\
&\leqslant CN_x^{-3}\exp\left(C_3(p+1)N_x^{-1}\max\Psi'(\rho_j)\right) \\
&\leqslant CN_x^{-3}.
\end{aligned}$$

Following the same approach as we have done for $(w_L)_k$ in the intervals $[x_{N_x/4}, x_{3N_x/4+1}]$ and $[x_{3N_x/4+2}, x_{N_x}]$, we obtain

$$\|(w_R)_k - I_2^0(w_R)_k\| \leqslant CN_x^{-3}.$$

Next, we find the bounds for $\max\limits_{j=1,2,\ldots,N_x}|(u_k - I_2^0 u_k)''_{j-1/2}|$. For this purpose, first, we consider v_k in $I_j \subset [x_0, x_{N_x/4-1}]$ as follows

$$\begin{aligned}
\frac{\widetilde{h}_j^2}{48}\left|v_k^{(4)}\right|_{I_j} &\leqslant C\varepsilon^2 N_x^{-2}\exp\left(\frac{2x_j}{(p+1)\varepsilon}\right) \text{ (using Theorem 3.2.3 and the inequality in (3.3.2))} \\
&\leqslant CN_x^{-2}\exp\left(\frac{2x_j}{(p+1)\varepsilon}\right) \\
&\leqslant CN_x^{-2}\exp\left(2\Psi(\rho_j)\right) \\
&\leqslant CN_x^{-2}.
\end{aligned}$$

Similar results can be obtained for the intervals $[x_{N_x/4}, x_{3N_x/4+1}]$ and $[x_{3N_x/4+2}, x_{N_x}]$. Now for the left singular component in $I_j \subset [x_0, x_{N_x/4-1}]$, we have

$$\begin{aligned}
\frac{\widetilde{h}_j^2}{48}\left|(w_L)_k^{(4)}\right|_{I_j} &\leqslant C\varepsilon^2 N_x^{-2}\exp\left(\frac{2x_j}{(p+1)\varepsilon}\right)\varepsilon^{-4}|e^{-\lambda x/\varepsilon}|_{I_j} \\
&\leqslant C\varepsilon^2 N_x^{-2}\exp\left(\frac{C_1 x_j}{\varepsilon}\right)\varepsilon^{-4}\exp\left(\frac{-C_2 x_{j-1}}{\varepsilon}\right) \\
&\leqslant C\varepsilon^{-2} N_x^{-2}\exp\left(\frac{C_3(x_j - x_{j-1})}{\varepsilon}\right) \\
&\leqslant C\varepsilon^{-2} N_x^{-2}\exp\left(\frac{C_3\widetilde{h}_j}{\varepsilon}\right) \\
&\leqslant C\varepsilon^{-2} N_x^{-2}\exp\left(C_3(p+1)N_x^{-1}\max\Psi'(\rho_j)\right) \\
&\leqslant C\varepsilon^{-2} N_x^{-2}.
\end{aligned}$$

A similar procedure can obtain the same bounds for the intervals $[x_{N_x/4}, x_{3N_x/4+1}]$ and $[x_{3N_x/4+2}, x_{N_x}]$. Thus, we have

$$\max_{j=1,2,\ldots,N_x} |((w_L)_k - I_2^0(w_L)_k)''_{j-1/2}| \leqslant C\varepsilon^{-2}N_x^{-2}.$$

Furthermore, one can use a similar analogy to find the bounds for the right singular component $(w_R)_k$. Finally, using the triangle inequality leads us to complete the proof. □

Lemma 3.4.1. *Let* $s_k \in S_2^0(\Delta)$ *with* $(s_k)_{j-1/2} = 0,\ j = 1, 2, \ldots, N_x;\ k = 1, 2, \ldots, \ell$, *then*

$$\|s_k\|_{I_j} \leqslant \max_j\{|(s_k)_{j-1}|, |(s_k)_j|\}, \quad \|s_k''\|_{I_j} \leqslant \frac{8}{\widetilde{h}_j^2}\max_j\{|(s_k)_{j-1}|, |(s_k)_j|\}.$$

Proof. Refer to [103] for a complete proof. □

3.4.2 S_2^1-interpolation

To find the interpolation $I_2^1 y_k \in S_2^1(\Delta)$ assuming that $y_k \in C^1[0,1]$, we solve the following interpolation problem:

$$(I_2^1 y_k)_0 = (y_k)_0, \quad (I_2^1 y_k)_{j-1/2} = (y_k)_{j-1/2},\ j = 1, 2, \ldots, N_x, \quad (I_2^1 y_k)_{N_x} = (y_k)_{N_x}, \tag{3.4.2}$$

where $(y_k)_{j-1/2} = y_k(X_j),\ \text{for } k = 1, 2, \ldots, \ell.$

Let $\Lambda : S_2^1(\Delta) \to \mathbb{R}^{N_x+1}$ be the operator defined by

$$[\Lambda s_k]_j = a_j(s_k)_{j-1} + 3(s_k)_j + c_j(s_k)_{j+1},$$

where $a_j = \frac{\widetilde{h}_{j+1}}{\widetilde{h}_j+\widetilde{h}_{j+1}}$ and $c_j = 1 - a_j = \frac{\widetilde{h}_j}{\widetilde{h}_j+\widetilde{h}_{j+1}}$. Then from [93, 111], we have

$$[\Lambda s_k]_j \equiv a_j(s_k)_{j-1}+3(s_k)_j+c_j(s_k)_{j+1} = 4a_j(s_k)_{j-1/2}+4c_j(s_k)_{j+1/2},\ j = 1, 2, \ldots, N_x-1, \tag{3.4.3}$$

Lemma 3.4.2. *The operator Λ in (3.4.3) is stable, with $(s_k)_0 = (s_k)_{N_x} = 0$,*

$$\max_{j=1,2,\ldots,N_x-1} |(s_k)_j| \leqslant \frac{1}{2}\left\{\max_{j=1,2,\ldots,N_x-1} |[\Lambda s_k]_j|\right\}, \quad k = 1, 2, \ldots, \ell,$$

for $s_k \in \mathbb{R}^{N_x+1}$.

Proof. Refer to Lemma 3 given in [94]. □

Theorem 3.4.2. *Assume that $b_{ij}(x), g_j(x) \in C^4[0, 1],\ for\ i,\ j = 1, 2, \ldots, \ell$, then the interpolation error $\boldsymbol{u} - I_2^1\boldsymbol{u}$ of the solution $\boldsymbol{u}$ of (3.1.1) satisfies the following bounds*

$$\max_{j=0,1,\ldots,N_x} |(\boldsymbol{u} - I_2^1\boldsymbol{u})_j| \leqslant \boldsymbol{C}N_x^{-4}, \tag{3.4.4a}$$

$$\|\boldsymbol{u} - I_2^1\boldsymbol{u}\| \leqslant CN_x^{-3}, \tag{3.4.4b}$$

$$\boldsymbol{\mathcal{E}} \max_{j=1,2,\ldots,N_x} |(\boldsymbol{u} - I_2^1\boldsymbol{u})''_{j-1/2}| \leqslant \boldsymbol{C}N_x^{-2}. \tag{3.4.4c}$$

Proof. For the interpolation error $y_k - I_2^1 y_k$, we consider an arbitrary function y_k that satisfies

$$(y_k - I_2^1 y_k)_0 = (y_k - I_2^1 y_k)_{N_x} = 0, \quad k = 1, 2, \ldots, \ell.$$

Using the definitions of S_2^1-interpolation and the operator Λ given by (3.4.2) and (3.4.3), respectively, we have

$$\tau_{y_k,j} = [\Lambda(y_k - I_2^1 y_k)]_j = a_j(y_k)_{j-1} - 4a_j(y_k)_{j-1/2} + 3(y_k)_j - 4c_j(y_k)_{j+1/2} + c_j(y_k)_{j+1}, \tag{3.4.5}$$

for $j = 1, 2, \ldots, N_x,\ k = 1, 2, \ldots, \ell$. Furthermore, we use the Taylor series expansions to get

$$|\tau_{y_k,j}| \leqslant \frac{1}{12}\widetilde{h}_j\widetilde{h}_{j+1}|\widetilde{h}_{j+1} - \widetilde{h}_j||(y_k''')_j|_{I_j} + \frac{5}{96}\max\{\widetilde{h}_j^4, \widetilde{h}_{j+1}^4\}\|(y_k^{(4)})_j\|_{I_j\cup I_{j+1}}. \tag{3.4.6}$$

Now, the interpolation error can be decomposed as

$$u_k - I_2^1 u_k = (v_k - I_2^1 v_k) + \Big((w_L)_k - I_2^1(w_L)_k\Big) + \Big((w_R)_k - I_2^1(w_R)_k\Big),$$

or

$$\tau_{u_k,j} = \tau_{v_k,j} + \tau_{(w_L)_k,j} + \tau_{(w_R)_k,j}.$$

To find the error, we start considering the regular component. For $I_j \subset [x_0, x_{N_x/4-1}]$, we use Theorem 3.2.3 and the inequality (3.4.6), to get

$$|\tau_{v_k,j}| \leqslant C\Big(\widetilde{h}_j\widetilde{h}_{j+1}|\widetilde{h}_{j+1} - \widetilde{h}_j| + \max\{\widetilde{h}_j^4, \widetilde{h}_{j+1}^4\}\Big).$$

Now as $\widetilde{h}_j < \widetilde{h}_{j+1}$ holds in $[x_0, x_{N_x/4-1}]$, so

$$\begin{aligned}
|\tau_{v_k,j}| &\leqslant C\Big(\widetilde{h}_{j+1}^2|\widetilde{h}_{j+1} - \widetilde{h}_j| + \widetilde{h}_{j+1}^4\Big)\\
&\leqslant C\left(\varepsilon^3 N_x^{-4}\exp\left(\frac{2x_{j+1}}{(p+1)\varepsilon}\right) + \varepsilon^4 N_x^{-4}\exp\left(\frac{4x_{j+1}}{(p+1)\varepsilon}\right)\right)\\
&\leqslant CN_x^{-4}\exp\left(\frac{4x_{j+1}}{(p+1)\varepsilon}\right)\\
&\leqslant CN_x^{-4}\exp\Big(4\Psi(\rho_{j+1})\Big)\\
&\leqslant CN_x^{-4}.
\end{aligned}$$

Moreover, for $x_j \in [x_{N_x/4}, x_{3N_x/4+1}]$, it is obvious to prove that $|\tau_{v_k,j}| \leqslant CN_x^{-4}$. A similar bound can be proved for $x_j \in [x_{3N_x/4+2}, x_{N_x}]$. Therefore, using Lemma 3.4.2, we get

$$\max_{j=0,1,\ldots,N_x} |(v_k - I_2^1 v_k)_j| \leqslant CN_x^{-4}.$$

Now in the process of finding the bounds for $(w_L)_k$, we use the fact that $\widetilde{h}_j < \widetilde{h}_{j+1}$ for $x_j \in [x_0, x_{N_x/4-1}]$, which yields

$$\begin{aligned}
|\tau_{(w_L)_k,j}| &\leqslant \frac{1}{12}\widetilde{h}_j\widetilde{h}_{j+1}|\widetilde{h}_{j+1}-\widetilde{h}_j||(w_L''')_{k,j}|_{I_j} + \frac{5}{96}\max\{\widetilde{h}_j^4, \widetilde{h}_{j+1}^4\}\|(w_L^{(4)})_{k,j}\|_{I_j\cup I_{j+1}} \\
&\leqslant C\left(\widetilde{h}_{j+1}^2|\widetilde{h}_{j+1}-\widetilde{h}_j|\varepsilon^{-3}|e^{-\lambda x/\varepsilon}|_{I_j} + \widetilde{h}_{j+1}^4\varepsilon^{-4}|e^{-\lambda x/\varepsilon}|_{I_j\cup I_{j+1}}\right) \\
&\leqslant C\left(N_x^{-4}\exp\left(\frac{2x_{j+1}}{(p+1)\varepsilon}\right)|e^{-\lambda x/\varepsilon}|_{I_j} + N_x^{-4}\exp\left(\frac{4x_{j+1}}{(p+1)\varepsilon}\right)|e^{-\lambda x/\varepsilon}|_{I_j\cup I_{j+1}}\right) \\
&\leqslant CN_x^{-4}\exp\left(\frac{C_1\widetilde{h}_{j+1}}{\varepsilon}\right) \\
&\leqslant CN_x^{-4}\exp\left(C_1(p+1)N_x^{-1}\max\Psi'(\rho_{j+1})\right) \\
&\leqslant CN_x^{-4}.
\end{aligned}$$

Similar bounds can be obtained in $[x_{3N_x/4+2}, x_{N_x}]$. Moreover, it is easy to prove $\tau_{(w_L)_k,j} \leqslant CN_x^{-4}$ for $x_j \in [x_{N_x/4}, x_{3N_x/4+1}]$. Therefore, using Lemma 3.4.2, we get

$$\max_{j=0,1,\ldots,N_x}|((w_L)_k - I_2^1(w_L)_k)_j| \leqslant CN_x^{-4}.$$

Similar arguments can be used to derive the bounds for the right singular component $(w_R)_k$ (we skip the analysis here). The estimate in (3.4.4a) can be attained directly by combining all the interpolation errors for three components. To prove (3.4.4b), we use the triangle inequality as

$$\begin{aligned}
\|\boldsymbol{u} - I_2^1\boldsymbol{u}\| &\leqslant \|\boldsymbol{u} - I_2^0\boldsymbol{u}\| + \|I_2^0\boldsymbol{u} - I_2^1\boldsymbol{u}\| \\
&\leqslant \|\boldsymbol{u} - I_2^0\boldsymbol{u}\| + \max_{j=0,1,\ldots,N_x}|(\boldsymbol{u} - I_2^1\boldsymbol{u})_j|.
\end{aligned}$$

Now using the fact $(I_2^1\boldsymbol{u})_j = \boldsymbol{u}_j,\ j = 0, 1, \ldots, N_x$, Lemma 3.4.1, Theorem 3.4.1, and (3.4.4a), we obtain the estimate (3.4.4b). Furthermore, to obtain the inequality (3.4.4c), we use the same approach as we have used for (3.4.4b). For this purpose, we write

$$|(u_k - I_2^1u_k)''_{j-1/2}| \leqslant |(u_k - I_2^0u_k)''_{j-1/2}| + |(I_2^0u_k - I_2^1u_k)''_{j-1/2}|$$

$$\leqslant |(u_k - I_2^0 u_k)''_{j-1/2}| + \max_{j=0,1,\ldots,N_x} \frac{8}{\widetilde{h}_j^2} |(u_k - I_2^1 u_k)_j|.$$

Hence, the proof is completed using Theorem 3.4.1 and inequality (3.4.4a). □

Theorem 3.4.3. *We assume that there exists a constant $\mu > 0$ such that*

$$\max\{\widetilde{h}_{j+1}, \widetilde{h}_{j-1}\} \geqslant \mu \widetilde{h}_j, \quad j = 1, 2, \ldots, N_x - 1, \ \widetilde{h}_1 \geqslant \mu \widetilde{h}_2, \ \textit{and} \ \widetilde{h}_{N_x} \geqslant \mu \widetilde{h}_{N_x - 1}.$$

Then the operator L_k is stable in the maximum-norm being

$$\|\boldsymbol{\gamma}_k\| \leqslant 3 \max_{j=1,2,\ldots,N_x} \left| \frac{[L_k \boldsymbol{\gamma}_k]_{j-1/2}}{n_{j-1/2,k}} \right|, \ \ k = 1, 2, \ldots, \ell,$$

for all $\boldsymbol{\gamma}_k \in \mathbb{R}_0^{N_x+2} = \{r \in \mathbb{R}^{N_x+2} : r_0 = r_{N_x+1} = 0\}$, where $n_{j-1/2,k} := \sum_{m=1}^{\ell} (b_{km})_{j-1/2} \Big(1 - q_j^+ - q_j^- \Big)$, $j = 1, 2, \ldots, N_x$, $k = 1, 2, \ldots, \ell$.

Proof. Note that $q_j^+, \ q_j^- \in (0, 1/4)$, therefore $n_{j,k} > 0, \ j = 1, 2, \ldots, N_x$. For arbitrary vectors $\boldsymbol{\gamma}_k \in \mathbb{R}_0^{N_x+2}$, we define the operators $\boldsymbol{\Lambda}_k$ by

$$[\boldsymbol{\Lambda}_k \boldsymbol{\gamma}_k]_{j-1/2} = -\frac{\varepsilon^2}{n_{j-1/2,k}} \left[\frac{2(\gamma_{j+1,k} - \gamma_{j,k})}{\widetilde{h}_j (\widetilde{h}_j + \widetilde{h}_{j+1})} - \frac{2(\gamma_{j,k} - \gamma_{j-1,k})}{\widetilde{h}_j (\widetilde{h}_j + \widetilde{h}_{j-1})} \right] + \gamma_{j,k}, \quad j = 1, 2, \ldots, N_x.$$

The operators $\boldsymbol{\Lambda}_k$ are well defined due to the positivity of all $n_{j-1/2,k}$. We get the required result as in [94]. □

Theorem 3.4.4. *Let $\boldsymbol{u}$ be the exact solution to (3.1.1) and $\tilde{\boldsymbol{u}}$ is its approximation on the exponentially graded mesh, then*

$$\|\boldsymbol{u} - \tilde{\boldsymbol{u}}\| \leqslant C N_x^{-2}.$$

Proof. We generalize the approach given in [105] for a scalar problem to a system. Using the triangle inequality, we have

$$\|u_k - \tilde{u}_k\| \leqslant \|u_k - I_2^1 u_k\| + \|I_2^1 u_k - \tilde{u}_k\|,$$

for $k = 1, 2, \ldots, \ell$. Making use of B-spline functions, we write the interpolant $I_2^1 u_k$ as

$$I_2^1 u_k(x) = \sum_{j=0}^{N_x+1} \beta_{j,k} \mathfrak{B}_j(x), \quad \text{for } k = 1, 2, \ldots, \ell.$$

$$[\boldsymbol{L}(\boldsymbol{\alpha}_k - \boldsymbol{\beta}_k)]_{j-1/2} = L_k(\tilde{u}_k - I_2^1 u_k)_{j-1/2} = \varepsilon^2 (I_2^1 u_k - u_k)_{j-1/2}, \ j = 1, 2, \ldots, N_x.$$

Finally, Theorems 3.4.2 and 3.4.3 give

$$\|\boldsymbol{\alpha}_k - \boldsymbol{\beta}_k\| \leqslant C N_x^{-2}.$$

Since each $\mathfrak{B}_j \geqslant 0$ and the sum of all basis functions equals 1, so

$$\|I_2^1 \boldsymbol{u} - \tilde{\boldsymbol{u}}\| \leqslant \|\boldsymbol{\alpha}_k - \boldsymbol{\beta}_k\| \leqslant C N_x^{-2}.$$

We now apply Theorem 3.4.2 to complete the proof. □

3.5 Numerical outcomes and discussion

In this section, we examine the verification of the theoretical estimates provided in the previous section by considering two numerical examples. The error estimates (in the maximum norm) are obtained using the double mesh principle [112]. The maximum pointwise error is computed as

$$e_{k,\varepsilon}^{N_x} = \max_j |\tilde{u}_k(x_{2j-1}) - \hat{u}_k(x_{j-1/2})|,$$

where $\hat{u}_k$ and $\tilde{u}_k$ represent the computed solutions by considering N_x and $2N_x$ mesh partitions, respectively. We also compute the corresponding order of convergence as

$$\eta_{k,\varepsilon}^{N_x} = \frac{\ln(e_{k,\varepsilon}^{N_x} / e_{k,\varepsilon}^{2N_x})}{\ln 2}.$$

Furthermore, we calculate the ε-uniform maximum pointwise error $e_k^{N_x}$ and the corresponding ε-uniform order of convergence $\eta_k^{N_x}$ as follows

$$e_k^{N_x} = \max_\varepsilon e_{k,\varepsilon}^{N_x},$$

$$\eta_k^{N_x} = \frac{\ln(e_k^{N_x}/e_k^{2N_x})}{\ln 2}.$$

Remark 3.5.1. *All the above estimates are calculated for* $k = 1, 2, \ldots, \ell$.

We have also calculated the overall error $\boldsymbol{e}^{N_x}$ as follows:

$$\boldsymbol{e}^{N_x} = \max_k(\max_\varepsilon e_{k,\varepsilon}^{N_x}).$$

Finally, the corresponding orders of convergence are given by

$$\boldsymbol{\eta}^{N_x} = \frac{\ln(\boldsymbol{e}^{N_x}/\boldsymbol{e}^{2N_x})}{\ln 2}.$$

From a practical point of view, we have calculated the uniform errors over a finite range of ε values ($\varepsilon = 1, 10^{-1}, \ldots, 10^{-10}$).

In the test problems, for simplicity, we take $\ell = 2$ in the first problem and $\ell = 3$ in the second problem. The solution components are denoted as u_k (exact solution) and $\tilde{u}_k$ (numerical solution), respectively. Moreover, the solution in vector form is denoted by bold letters.

Example 3.5.1. *In this example, we consider the following system of two equations:*

$$\begin{aligned}
&-\varepsilon^2 u_1'' + 2(1+x)^2 u_1 - (1+x^3)u_2 = 2e^x,\\
&-\varepsilon^2 u_2'' - 2\cos\left(\frac{\pi x}{4}\right)u_1 + (1+\sqrt{2})e^{1-x}u_2 = 10x+1,\\
&u_1(0) = u_1(1) = 0, \quad u_2(0) = u_2(1) = 0.
\end{aligned}$$

For this example, the matrix $\boldsymbol{B}$, $\boldsymbol{g}(x)$, $\boldsymbol{\varrho}_0$, and $\boldsymbol{\varrho}_1$ are as given below

$$\boldsymbol{B} = \begin{bmatrix} 2(1+x)^2 & -(1+x^3) \\ -2\cos\left(\frac{\pi x}{4}\right) & (1+\sqrt{2})e^{1-x} \end{bmatrix}, \ \boldsymbol{g}(x) = (2e^x, 10x+1)^T, \ \boldsymbol{\varrho}_0 = (0,0)^T, \quad \boldsymbol{\varrho}_1 = (0,0)^T.$$

Example 3.5.2. *In this example, we consider the following system of three equations:*

$$
\begin{aligned}
&-\varepsilon^2 u_1'' + 3u_1 + (1-x)(u_2 - u_3) = e^x,\\
&-\varepsilon^2 u_2'' + 2u_1 + (4+x)u_2 - u_3 = \cos x,\\
&-\varepsilon^2 u_3'' + 2u_1 + 3u_3 = 1 + x^2,\\
&u_1(0) = u_1(1) = 0, \quad u_2(0) = u_2(1) = 0, \quad u_3(0) = u_3(1) = 0.
\end{aligned}
$$

For this example, the matrix $\boldsymbol{B}$, $\boldsymbol{g}(x)$, $\boldsymbol{\varrho}_0$, and $\boldsymbol{\varrho}_1$ are as given below

$$
\boldsymbol{B} = \begin{bmatrix} 3 & 1-x & -(1-x) \\ 2 & 4+x & -1 \\ 2 & 0 & 3 \end{bmatrix}, \boldsymbol{g}(x) = (e^x, \cos x, 1+x^2)^T, \boldsymbol{\varrho}_0 = (0,0,0)^T, \quad \boldsymbol{\varrho}_1 = (0,0,0)^T.
$$

The solution of the system exhibits twin boundary layers in the neighborhoods of $x = 0$ and $x = 1$. As explained above, the uniform mesh is unsuitable for resolving these layers, and one cannot obtain parameter-uniform estimates on this mesh. So, the numerical results for both examples are obtained using the exponentially graded mesh (eXp mesh). Tables 3.1 and 3.2 show the second-order parameter-uniform results for the solutions $\tilde{u}_1$ and $\tilde{u}_2$ for Example 3.5.1. Similarly, for Example 3.5.2, we obtain the parameter-uniform estimates of order $O(N_x^{-2})$ for $\tilde{u}_1$, $\tilde{u}_2$, and $\tilde{u}_3$, respectively (refer to Tables 3.3, 3.4, and 3.5). We have also computed the results for the Shishkin mesh and Bakhvalov-Shishkin (B-S) mesh and compared the results on these meshes in Tables 3.6 and 3.7. This comparison suggests a parameter-uniform convergence of orders $O(N_x^{-2})$, $O(N_x^{-2}\ln^2 N_x)$, and $O(N_x^{-2})$, respectively. To support this, we have also calculated ε-uniform orders of convergence and ε-uniform error constants (see [113] for the computation of C^{N_x}).

Furthermore, we combine the mesh plots of the considered meshes (eXp, Shishkin, and B-S) in a single plot showing the distribution of mesh points in the layer and regular regions. Since the eXp and the B-S mesh differ by slightly changing the choice of the mesh generating function $\Psi(\rho)$, the mesh points coincide in the plot. We have displayed the presence of boundary layers in the solution by plotting the 2-D graphs. From Fig. 3.2 it is observed that the boundary layers for $\varepsilon = 10^{-4}$ are stiffer (see Figs. 3.2(b) and 3.2(d)) as compared to the

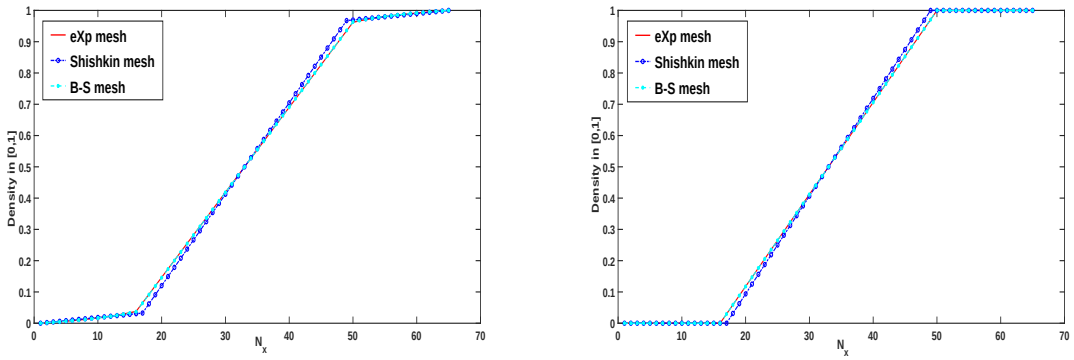

(a) $\varepsilon = 2^{-8}$ (b) $\varepsilon = 2^{-20}$

Figure 3.1: Mesh comparison of eXp mesh, Shishkin mesh, B-S mesh for $N_x = 64$

boundary layers for $\varepsilon = 10^{-2}$ (see Figs. 3.2(a) and 3.2(c)) which confirms the theory that for SPBVPs the width of the boundary layer decreases as ε decreases.

Remark 3.5.2. *In Fig. 3.2, $u_{\Delta;k}$ represents the k^{th} component of the numerical solution on the partition Δ.*

3.6 Concluding remarks

A numerical scheme that uses the quadratic B-spline functions on an exponentially graded mesh has been developed for a weakly coupled system of ℓ singularly perturbed reaction-diffusion equations. The main reason to choose the exponentially graded mesh is its advantage over other meshes like Shishkin and Bakhvalov-type meshes, as it does not require prior information about the transition parameter *i.e.,* it is independent of the transition point(s). The estimated theoretical bounds on the spline interpolation error show that the method is second-order convergent irrespective of the $\mathcal{E}$ value. The numerical results in the tables validate the theoretical estimates regarding the orders of convergence and the errors estimated in Section 3.4.

Table 3.1: Maximum pointwise errors $e_{1,\varepsilon}^{N_x}$ in the solution $\tilde{u}_1$ for Example 3.5.1

	N_x						
ε	64	128	256	512	1024	2048	4096
10^{-2}	$3.4414e-03$	$8.7439e-04$	$2.1556e-04$	$5.2958e-05$	$1.3095e-05$	$3.2550e-06$	$8.1124e-07$
	1.9766	2.0202	2.0252	2.0158	2.0083	2.0045	
10^{-4}	$3.4571e-03$	$8.7821e-04$	$2.1656e-04$	$5.3212e-05$	$1.3159e-05$	$3.2708e-06$	$8.1520e-07$
	1.9769	2.0198	2.0249	2.0157	2.0083	2.0045	
10^{-6}	$3.4573e-03$	$8.7825e-04$	$2.1658e-04$	$5.3215e-05$	$1.3159e-05$	$3.2710e-06$	$8.1529e-07$
	1.9769	2.0198	2.0249	2.0158	2.0083	2.0045	
10^{-8}	$3.4573e-03$	$8.7826e-04$	$2.1658e-04$	$5.3215e-05$	$1.3159e-05$	$3.2760e-06$	$8.2269e-07$
	1.9769	2.0198	2.0249	2.0158	2.0083	2.0045	
10^{-10}	$3.4573e-03$	$8.7826e-04$	$2.1658e-04$	$5.3215e-05$	$1.3159e-05$	$3.2765e-06$	$8.2278e-07$
	1.9769	2.0198	2.0249	2.0158	2.0083	2.0045	
$e_1^{N_x}$	$3.4573e-03$	$8.7826e-04$	$2.1658e-04$	$5.3215e-05$	$1.3159e-05$	$3.2765e-06$	$8.2278e-07$
$\eta_1^{N_x}$	1.9769	2.0202	2.0252	2.0158	2.0083	2.0045	
$C_1^{N_x}$	14.16	14.38	14.19	13.95	13.79	13.74	13.75

Table 3.2: Maximum pointwise errors $e_{2,\varepsilon}^{N_x}$ in the solution $\tilde{u}_2$ for Example 3.5.1

	N_x						
ε	64	128	256	512	1024	2048	4096
10^{-2}	$7.0349e-03$	$1.7946e-03$	$4.4247e-04$	$1.0926e-04$	$2.7095e-05$	$6.7447e-06$	$1.6824e-06$
	1.9709	2.0200	2.0178	2.0117	2.0062	2.0032	
10^{-4}	$7.1101e-03$	$1.8146e-03$	$4.4739e-04$	$1.1048e-04$	$2.7400e-05$	$6.8205e-06$	$1.7013e-06$
	1.9702	2.0200	2.0177	2.0115	2.0062	2.0032	
10^{-6}	$7.1109e-03$	$1.8148e-03$	$4.4744e-04$	$1.1049e-04$	$2.7403e-05$	$6.8213e-06$	$1.7016e-06$
	1.9702	2.0200	2.0177	2.0115	2.0062	2.0032	
10^{-8}	$7.1109e-03$	$1.8148e-03$	$4.4746e-04$	$1.1048e-04$	$2.7411e-05$	$6.8213e-06$	$1.7160e-06$
	1.9702	2.0200	2.0177	2.0115	2.0062	2.0032	
10^{-10}	$7.1109e-03$	$1.8148e-03$	$4.4746e-04$	$1.1048e-04$	$2.7414e-05$	$6.8220e-06$	$1.7169e-06$
	1.9702	2.0200	2.0177	2.0115	2.0062	2.0032	
$e_2^{N_x}$	$7.1109e-03$	$1.8148e-03$	$4.4746e-04$	$1.1048e-05$	$2.7414e-05$	$6.8220e-06$	$1.7169e-06$
$\eta_2^{N_x}$	1.9702	2.0200	2.0178	2.0117	2.0062	2.0032	
$C_2^{N_x}$	29.12	29.73	29.32	28.96	28.74	28.61	28.60

Table 3.3: Maximum pointwise errors $e_{1,\varepsilon}^{N_x}$ in the solution $\tilde{u}_1$ for Example 3.5.2

	N_x						
ε	64	128	256	512	1024	2048	4096
10^{-2}	$1.8695e-03$	$4.7469e-04$	$1.1770e-04$	$2.9012e-05$	$7.1840e-06$	$1.7866e-06$	$4.4546e-07$
	1.9776	2.0119	2.0204	2.0138	2.0076	2.0038	
10^{-4}	$1.8675e-03$	$4.7416e-04$	$1.1756e-04$	$2.8978e-05$	$7.1757e-06$	$1.7845e-06$	$4.4494e-07$
	1.9777	2.0120	2.0204	2.0138	2.0076	2.0038	
10^{-6}	$1.8675e-03$	$4.7416e-04$	$1.1756e-04$	$2.8978e-05$	$7.1757e-06$	$1.7845e-06$	$4.4496e-07$
	1.9776	2.0120	2.0204	2.0138	2.0076	2.0038	
10^{-8}	$1.8675e-03$	$4.7416e-04$	$1.1756e-04$	$2.8978e-05$	$7.1757e-06$	$1.7845e-06$	$4.4496e-07$
	1.9776	2.0120	2.0204	2.0138	2.0076	2.0038	
10^{-10}	$1.8675e-03$	$4.7416e-04$	$1.1756e-04$	$2.8978e-05$	$7.1757e-06$	$1.7845e-06$	$4.4496e-07$
	1.9776	2.0120	2.0204	2.0138	2.0076	2.0038	
$e_1^{N_x}$	$1.8675e-03$	$4.7469e-04$	$1.1770e-04$	$2.9012e-05$	$7.1840e-06$	$1.7845e-06$	$4.4496e-06$
$\eta_1^{N_x}$	1.9776	2.0120	2.0204	2.0138	2.0076	2.0038	
$C_1^{N_x}$	7.64	7.76	7.70	7.59	7.52	7.48	7.49

Table 3.4: Maximum pointwise errors $e_{2,\varepsilon}^{N_x}$ in the solution $\tilde{u}_2$ for Example 3.5.2

	N_x						
ε	64	128	256	512	1024	2048	4096
10^{-2}	$7.2661e-04$	$1.9713e-04$	$4.8933e-05$	$1.2064e-05$	$2.9843e-06$	$7.4152e-07$	$1.8478e-07$
	1.8820	2.0103	2.0201	2.0152	2.0088	2.0047	
10^{-4}	$7.2739e-04$	$1.9735e-04$	$4.8989e-05$	$1.2078e-05$	$2.9877e-06$	$7.4238e-07$	$1.8500e-07$
	1.8820	2.0102	2.0201	2.0153	2.0088	2.0046	
10^{-6}	$7.2740e-04$	$1.9735e-04$	$4.8989e-05$	$1.2078e-05$	$2.9878e-06$	$7.4239e-07$	$1.8500e-07$
	1.8820	2.0102	2.0201	2.0153	2.0088	2.0046	
10^{-8}	$7.2740e-04$	$1.9735e-04$	$4.8989e-05$	$1.2078e-05$	$2.9878e-06$	$7.4239e-07$	$1.8500e-07$
	1.8820	2.0102	2.0201	2.0153	2.0088	2.0046	
10^{-10}	$7.2740e-04$	$1.9735e-04$	$4.8989e-05$	$1.2078e-05$	$2.9878e-06$	$7.4239e-07$	$1.8500e-07$
	1.8820	2.0102	2.0201	2.0153	2.0088	2.0046	
$e_2^{N_x}$	$7.2740e-04$	$1.9735e-04$	$4.8989e-05$	$1.2078e-05$	$2.9878e-06$	$7.4239e-07$	$1.8500e-07$
$\eta_2^{N_x}$	1.9702	2.0200	2.0178	2.0117	2.0062	2.0032	
$C_2^{N_x}$	2.97	3.23	3.21	3.16	3.13	3.11	3.10

Table 3.5: Maximum pointwise errors $e_{3,\varepsilon}^{N_x}$ in the solution $\tilde{u}_3$ for Example 3.5.2

	N_x						
ε	64	128	256	512	1024	2048	4096
10^{-2}	$1.4829e-03$	$4.1205e-04$	$1.0335e-04$	$2.5429e-05$	$6.2959e-06$	$1.5641e-06$	$3.8974e-07$
	1.8475	1.9953	2.0230	2.0140	2.0091	2.0047	
10^{-4}	$1.4837e-03$	$4.1227e-04$	$1.0340e-04$	$2.5442e-05$	$6.2991e-06$	$1.5648e-06$	$3.8993e-07$
	1.8475	1.9954	2.0230	2.0140	2.0091	2.0047	
10^{-6}	$1.4838e-03$	$4.1227e-04$	$1.0340e-04$	$2.5442e-05$	$6.2991e-06$	$1.5648e-06$	$3.8993e-07$
	1.8475	1.9954	2.0230	2.0140	2.0091	2.0047	
10^{-8}	$1.4837e-03$	$4.1227e-04$	$1.0340e-04$	$2.5442e-05$	$6.2991e-06$	$1.5648e-06$	$3.8993e-07$
	1.8475	1.9954	2.0230	2.0140	2.0091	2.0047	
10^{-10}	$1.4837e-03$	$4.1227e-04$	$1.0340e-04$	$2.5442e-05$	$6.2991e-06$	$1.5648e-06$	$3.8993e-07$
	1.8475	1.9954	2.0230	2.0140	2.0091	2.0047	
$e_3^{N_x}$	$1.4837e-03$	$4.1227e-03$	$1.0340e-04$	$2.5442e-05$	$6.2991e-06$	$1.5648e-06$	$3.8993e-07$
$\eta_3^{N_x}$	1.8475	1.9954	2.0230	2.0140	2.0091	2.0047	
$C_3^{N_x}$	6.07	6.75	6.77	6.66	6.60	6.56	6.55

Table 3.6: Uniform maximum pointwise errors comparison in the solution for Example 3.5.1

	eXp mesh			Shishkin mesh			B-S mesh		
N_x	$\boldsymbol{e}^{N_x}$	$\boldsymbol{\eta}^{N_x}$	C^{N_x}	$\boldsymbol{e}^{N_x}$	$\boldsymbol{\eta}^{N_x}$	C^{N_x}	$\boldsymbol{e}^{N_x}$	$\boldsymbol{\eta}^{N_x}$	C^{N_x}
128	$1.814(-3)$	2.019	29.73	$6.114(-3)$	1.622	16.41	$1.784(-3)$	2.006	29.23
256	$4.474(-4)$	2.018	29.32	$1.986(-3)$	1.672	16.42	$4.440(-4)$	2.013	29.10
512	$1.104(-4)$	2.010	28.96	$6.232(-4)$	1.706	15.86	$1.100(-4)$	2.008	28.84
1024	$2.741(-5)$	2.006	28.74	$1.910(-4)$	1.774	14.97	$2.734(-5)$	2.001	28.67
2048	$6.821(-6)$	1.990	28.61	$5.584(-5)$	1.921	13.47	$6.828(-6)$	1.994	28.64
4096	$1.716(-6)$	-	28.60	$1.474(-5)$	-	10.95	$1.714(-7)$	-	28.61

Table 3.7: Uniform maximum pointwise errors comparison in the solution for Example 3.5.2

	eXp mesh			Shishkin mesh			B-S mesh		
N_x	$\boldsymbol{e}^{N_x}$	$\boldsymbol{\eta}^{N_x}$	C^{N_x}	$\boldsymbol{e}^{N_x}$	$\boldsymbol{\eta}^{N_x}$	C^{N_x}	$\boldsymbol{e}^{N_x}$	$\boldsymbol{\eta}^{N_x}$	C^{N_x}
128	$4.741(-4)$	2.012	7.76	$1.442(-3)$	1.563	2.92	$4.672(-4)$	2.002	7.65
256	$1.175(-4)$	2.020	7.70	$4.878(-4)$	1.672	2.92	$1.166(-4)$	2.014	7.64
512	$2.897(-5)$	2.013	7.59	$1.530(-4)$	1.707	2.71	$2.886(-5)$	2.010	7.56
1024	$7.175(-6)$	2.007	7.52	$4.685(-5)$	1.768	2.45	$7.161(-6)$	2.004	7.50
2048	$1.784(-6)$	2.003	7.48	$1.375(-5)$	1.891	2.12	$1.785(-6)$	1.994	7.48
4096	$4.449(-7)$	-	7.49	$3.706(-6)$	-	1.70	$4.446(-7)$	-	7.49

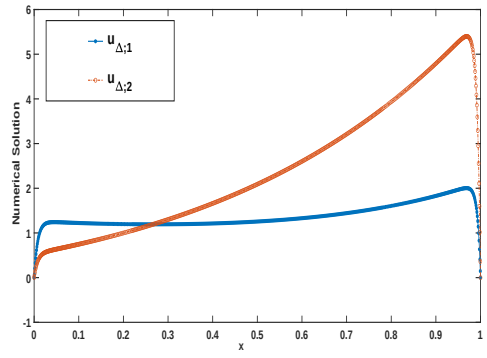

(a) $\varepsilon = 10^{-2}$

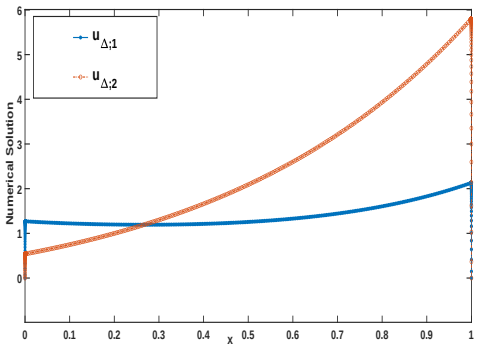

(b) $\varepsilon = 10^{-4}$

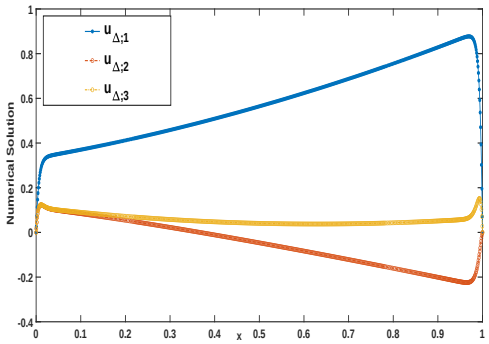

(c) $\varepsilon = 10^{-2}$

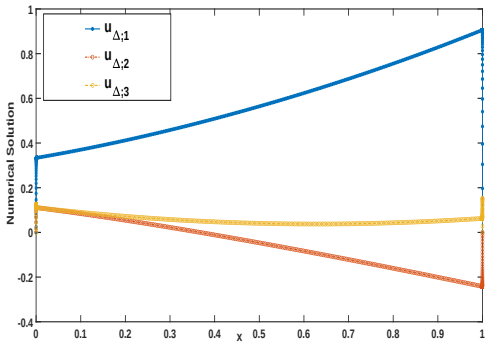

(d) $\varepsilon = 10^{-4}$

Figure 3.2: Numerical solution plots of Example 3.5.1 (subfigures (a) and (b)), and Example 3.5.2 (subfigures (c) and (d))

Chapter 4

A robust numerical technique for a weakly coupled system of parabolic singularly perturbed reaction-diffusion equations

---

In mathematics, a class of models known as weakly coupled systems of parabolic singularly perturbed reaction-diffusion equations is a model that can be used to illustrate the complicated dynamic relationship between diffusion and reaction processes in complex systems. The phrase "weakly coupled" denotes that the interconnections among the variables are relatively unnoticeable compared to their dynamics. Nevertheless, despite their limited strength, these couplings can still give rise to complex dynamics and impact the collective behaviour of the system as a whole, hence facilitating the creation of patterns and spatial organization.

The work of this chapter has been published in the following publication:

S. Singh, D. Kumar, J Vigo-Aguiar, " A robust numerical technique for a weakly coupled system of parabolic singularly perturbed reaction-diffusion equations." J. Math. Chem., 61 (2023), 1313–1350.

The system exhibits a singularly perturbed characteristic, resulting in the emergence of boundary layers. These boundary layers are narrow regions where variables undergo fast fluctuations. The layers mentioned above are of utmost importance in determining the comprehensive behavior of the solution.

4.1 Problem statement

Time-dependent singularly perturbed problems (SPPs) can be described by the Burgers' and Navier Stokes equations. These problems occur in several models, like for saturated flow in fractured porous media [99], the well-known linear double-diffusion model [99], and the bone diffusion process [100]. First, we consider the following singularly perturbed parabolic reaction-diffusion initial boundary value problem (IBVP) on $\mathcal{Q} = \mathcal{Q}_x \times \mathcal{Q}_t = (0,1) \times (0, \mathcal{T}]$

$$\mathfrak{L}y := \frac{\partial y}{\partial t} - \varepsilon \frac{\partial^2 y}{\partial x^2} + a(x,t)y = f(x,t), \ (x,t) \in \mathcal{Q}, \tag{4.1.1a}$$

$$y(0,t) = q(t) \text{ in } \mathcal{Q}_l, \quad y(1,t) = r(t) \text{ in } \mathcal{Q}_r, \quad y(x,0) = 0 \text{ in } \mathcal{Q}_b, \tag{4.1.1b}$$

where $\mathcal{Q}_l = \{(0,t) |\ 0 \leq t \leq \mathcal{T}\}$, $\mathcal{Q}_r = \{(1,t) |\ 0 \leq t \leq \mathcal{T}\}$, $\mathcal{Q}_b = \{(x,0) |\ 0 \leq x \leq 1\}$. The boundary of $\mathcal{Q}$ denoted by $\partial\mathcal{Q} = \overline{\mathcal{Q}} \backslash \mathcal{Q}$ includes initial ($\mathcal{Q}_b$) and lateral boundaries ($\mathcal{Q}_l$ and $\mathcal{Q}_r$) of the domain. Mainly in this chapter, we are concerned with a general weakly-coupled reaction-diffusion system (m number of equations) of the following type

$$\boldsymbol{\mathfrak{L}y} := \frac{\partial \boldsymbol{y}}{\partial t} - \boldsymbol{\mathcal{E}} \frac{\partial^2 \boldsymbol{y}}{\partial x^2} + \boldsymbol{A}(x,t)\boldsymbol{y} = \boldsymbol{f}(x,t), \ (x,t) \in \mathcal{Q} = \mathcal{Q}_x \times \mathcal{Q}_t, \tag{4.1.2a}$$

$$\boldsymbol{y}(0,t) = \boldsymbol{q}(t) \text{ in } \mathcal{Q}_l, \quad \boldsymbol{y}(1,t) = \boldsymbol{r}(t) \text{ in } \mathcal{Q}_r, \quad \boldsymbol{y}(x,0) = \boldsymbol{0} \text{ in } \mathcal{Q}_b, \tag{4.1.2b}$$

where $\boldsymbol{\mathfrak{L}} = (\mathfrak{L}_1, \mathfrak{L}_2, \ldots, \mathfrak{L}_m)^T$, $\boldsymbol{\mathcal{E}} = \text{diag}(\varepsilon, \varepsilon, \ldots, \varepsilon)$, $\boldsymbol{f}(x,t) = (f_1(x,t), f_2(x,t), \ldots, f_m(x,t))^T$, $\boldsymbol{A} = \{a_{ij}(x,t)\}_{i,j=1}^m$, $\boldsymbol{y}(x,t) = (y_1(x,t), y_2(x,t), \ldots, y_m(x,t))^T$, $\boldsymbol{q} = (q_1, q_2, \ldots, q_m)^T$, $\boldsymbol{r} = (r_1, r_2, \ldots, r_m)^T$. The operator $\mathfrak{L}_k$ can be defined as

$$\mathfrak{L}_k \boldsymbol{y} = \frac{\partial y_k}{\partial t} - \varepsilon \frac{\partial^2 y_k}{\partial x^2} + \sum_{j=1}^{m} a_{kj} y_j.$$

This kind of system is pervasive in modeling chemical reactor theory, turbulence in water

waves, and control theory. The entries $a_{ij}(x,t)$ of the coefficient matrix $\boldsymbol{A}$ are assumed to satisfy the following positivity condition

$$\begin{cases} \sum_{j=1}^{m} a_{ij} \geq \alpha > 0, \quad a_{ii} > 0,\ 1 \leq i \leq m, \\ a_{ij} \leq 0, \qquad\qquad \text{for } i \neq j. \end{cases} \tag{4.1.3}$$

We also assume that $\boldsymbol{A}$ is a diagonally dominant matrix. Otherwise, we can apply the transformation $\boldsymbol{v}(x,t) = \boldsymbol{y}(x,t)e^{-\alpha t}$ with sufficiently large α to transform the diagonal entries in such a way that they satisfy first condition of the Equation (4.1.3) (see [114]). We assume that a unique solution $\boldsymbol{y} \in (C^{(2,2)}(\overline{\mathcal{Q}}) \cap C^{(4,2)}(\mathcal{Q}))^m$ exist by assuming sufficient smooth and regular data of the problem (4.1.2). The following conditions are also assumed on the boundary conditions and source functions

$$\begin{cases} \boldsymbol{q}^{(l)}(0) = \boldsymbol{r}^{(l)}(0) = \boldsymbol{0}, & l = 0, 1, 2, \\ \left.\dfrac{\partial^{i+i_0}\boldsymbol{f}}{\partial x^i \partial t^{i_0}}\right|_{(0,0)} = \left.\dfrac{\partial^{i+i_0}\boldsymbol{f}}{\partial x^i \partial t^{i_0}}\right|_{(1,0)} = \boldsymbol{0}, & 0 \leq i + 2i_0 \leq 4, \end{cases} \tag{4.1.4}$$

which are inspired by the compatibility conditions required for the equations of type (4.1.1). Several ways can affect the numerical analysis of SPPs depending on how the magnitude of the parameter varies. For example, for two equations ($m = 2$), we have the following cases (i) $0 < \varepsilon_1 = \varepsilon_2 \leq 1$, (ii) $0 < \varepsilon_1 \leq 1$, $\varepsilon_2 = 1$, (iii) ε_1 and ε_2 are arbitrary. These cases can be generalized for the system containing the m number of equations. The analysis for cases (i) and (ii) is more straightforward than case (iii) because in case (iii), the solution components may possess a sublayer for each of the perturbation parameters.

4.1.1 Literature survey

A sufficient amount of literature is available for singularly perturbed systems (for $m = 2$) containing the above three cases. For $m = 2$, Madden and Stynes [41] developed a first-order uniformly convergent scheme for singularly perturbed BVPs. Later, improved order of convergence (from first-order to second-order) was established by Linß and Madden in [43] concerned with the same equation as in [41]. In [52], Linß and Madden considered a system

of $m \geq 2$ equations assuming the coupling matrix is strongly diagonally dominant with the conditions

$$a_{ii}(x) > 0, \ \sum_{\substack{k=1 \\ k \neq i}}^{m} \max_{x \in [0,1]} \left| \frac{a_{ik}}{a_{ii}} \right| < 1, \ i = 1, 2, \ldots, m.$$

Their work used Shishkin, Bakhvalov, and equidistribution meshes to compare their parameter uniform results. Taking $\varepsilon_k = \varepsilon, \ \forall k$ and a coercive coupling matrix $\boldsymbol{A}$, Bakhvalov [33] established second-order convergence in his paper. Das and Natesan [64] dealt with a system of BVPs with Robin-type boundary conditions using a hybrid scheme that combines central difference and cubic spline approximations in different regions. Das and Vigo-Aguiar [50] proposed a second-order uniformly convergent technique on a layer adaptive mesh whose construction uses the equidistribution of a positive valued monitor function. For $m = 2$, a system of parabolic IBVPs with the same diffusion parameters was considered by Shishkina and Shishkin in [115]. They used classical finite difference schemes and obtained almost second-order ε-uniform estimates in the spatial direction. Clavero *et al.* [116] proposed a numerical method combining Crank-Nicolson discretization in time with the central finite difference in space on the Shishkin mesh. Kumar and Rao [117] devised a method based on Schwarz domain decomposition for singularly perturbed reaction-diffusion IBVPs. Then, they extended this method for a system ($m \geq 2$) of IBVPs. Singh and Natesan [51] studied a system of two reaction-diffusion BVPs applying the nonsymmetric discontinuous Galerkin finite element method (NIPG method). They proved the first and second-order uniform convergence depending on the degree of the piecewise polynomial used in finite element space. Recently, Shakti *et al.* [59] proposed an optimal numerical technique using adaptive mesh by taking different diffusion parameters and comparing the uniform, Shishkin, and adaptive mesh accuracy. Further, one can review the references in the above-cited articles for more numerical methods.

The chapter is organized as follows: In Section 4.2, some basic properties and bounds on the exact solution and its derivatives are established. The numerical scheme, including the mesh construction and the temporal and spatial discretization, is developed in Section 4.3. The error estimates through $\mathbb{S}_2^0$ and $\mathbb{S}_2^1$ interpolations are obtained in Section 4.4. To validate the theoretical findings, two test problems are considered in Section 4.5. Finally,

some concluding remarks are included in Section 4.6.

Throughout the chapter, we have used C as a positive generic constant independent of the perturbation and mesh parameters, which can take different values at different places, and $\boldsymbol{C} = (C, C, \ldots, C)$ is used for a positive generic constant vector. Moreover, a subscripted C (e.g., C_1) is used for a constant.

4.2 Continuous problem

This section deduces some bounds on the exact solution and its derivatives to the problem (4.1.2). The coupling matrix $\boldsymbol{A}$ is assumed to satisfy the condition (4.1.3). Under these assumptions, we establish the maximum principle for the differential operator $\boldsymbol{\mathfrak{L}}$ and prove that it satisfies the stability results in the maximum norm.

Lemma 4.2.1. *Assume that* $\boldsymbol{y} \in (C^{(2,1)}(\mathcal{Q}) \cap C^{(0,0)}(\overline{\mathcal{Q}}))^m$ *such that* $\boldsymbol{y}(x,0) \geq 0$ *on* $(0,1)$ *and* $\boldsymbol{y}(0,t) \geq 0,\ \boldsymbol{y}(1,t) \geq 0$ *on* $(0,T]$. *Then* $\boldsymbol{\mathfrak{L}y} \geq 0,\ \forall\,(x,t) \in \mathcal{Q}$ *implies that* $\boldsymbol{y} \geq 0,\ \forall\,(x,t) \in \overline{\mathcal{Q}}$.

Proof. We contradict the statement by assuming that there is a point $(\hat{x},\hat{t}) \in \overline{\mathcal{Q}} \backslash \partial\mathcal{Q}$ such that

$$\min\{y_1(\hat{x},\hat{t}), \ldots, y_m(\hat{x},\hat{t})\} = \min\left\{ \min_{(x,t)\in\overline{\mathcal{Q}}} y_1(x,t),\ \min_{(x,t)\in\overline{\mathcal{Q}}} y_2(x,t), \ldots,\ \min_{(x,t)\in\overline{\mathcal{Q}}} y_m(x,t) \right\} < 0.$$

Without loss of generality, suppose that $y_1(\hat{x},\hat{t}) \leq y_2(\hat{x},\hat{t}) \leq \cdots \leq y_m(\hat{x},\hat{t})$. At the point $(\hat{x},\hat{t})$, we have the following conditions

$$\left.\frac{\partial y_1}{\partial x}\right|_{(\hat{x},\hat{t})} = 0, \quad \left.\frac{\partial y_1}{\partial t}\right|_{(\hat{x},\hat{t})} = 0, \quad \left.\frac{\partial^2 y_1}{\partial x^2}\right|_{(\hat{x},\hat{t})} \geq 0,$$

and from the first equation of $\boldsymbol{\mathfrak{L}y}$, we obtain

$$\begin{aligned}
\mathfrak{L}_1\boldsymbol{y}(\hat{x},\hat{t}) &= \left(\frac{\partial y_1}{\partial t} - \varepsilon\frac{\partial^2 y_1}{\partial x^2} + \sum_{\ell=1}^{m} a_{1m}(x,t)y_\ell(x,t)\right)_{(\hat{x},\hat{t})}, \\
&\leq \sum_{\ell=1}^{m} a_{1\ell}(\hat{x},\hat{t})y_1(\hat{x},\hat{t}) + \sum_{\ell=2}^{m} a_{1\ell}(\hat{x},\hat{t})(y_\ell(\hat{x},\hat{t}) - y_1(\hat{x},\hat{t})), \\
&\leq \sum_{\ell=1}^{m} a_{1\ell}(\hat{x},\hat{t})y_1(\hat{x},\hat{t}) < 0.
\end{aligned}$$

Therefore, we have

$$\mathfrak{L}_1 \boldsymbol{y}(\hat{x}, \hat{t}) < 0,$$

which contradicts the hypothesis. Hence, we conclude the result. □

Lemma 4.2.2. *The solution $\boldsymbol{y}$ to the problem (4.1.2) satisfies*

$$\|\boldsymbol{y}\|_{\overline{\mathcal{Q}}} \leq \frac{1}{\alpha}\|\boldsymbol{f}\|_{\overline{\mathcal{Q}}} + \max\{\|\boldsymbol{q}\|_{\overline{\mathcal{Q}}_t}, \|\boldsymbol{r}\|_{\overline{\mathcal{Q}}_t}\}.$$

Proof. This lemma can be easily proved by implementing the maximum principle on the barrier functions $\boldsymbol{\Phi}^{\pm}(x,t) = \frac{1}{\alpha}\|\boldsymbol{f}\|_{\overline{\mathcal{Q}}} + \max\{\|\boldsymbol{q}\|_{\overline{\mathcal{Q}}_t}, \|\boldsymbol{r}\|_{\overline{\mathcal{Q}}_t}\} \pm \boldsymbol{y}(x,t),\ (x,t) \in \overline{\mathcal{Q}}$. □

Lemma 4.2.3. *The solution $\boldsymbol{y}$ to the problem (4.1.2) satisfies*

$$\left\| \frac{\partial^l \boldsymbol{y}}{\partial t^l} \right\|_{\overline{\mathcal{Q}}} \leq C, \quad l = 0, 1, 2.$$

Proof. We use the barrier function $\boldsymbol{\psi} = (1+t)\boldsymbol{C}$ to prove the result. First, to prove the result for $\boldsymbol{y}_t$, assume $\boldsymbol{p} = \boldsymbol{y}_t$. On $\mathcal{Q}_l \cup \mathcal{Q}_r$, $\boldsymbol{p}$ satisfies

$$|\boldsymbol{p}(x,t)| \leq \max_{t \in \overline{\mathcal{Q}}_t}\{|\boldsymbol{q}_t'|, |\boldsymbol{r}_t'|\} \leq \boldsymbol{C},$$

and on $\mathcal{Q}_b$ taking continuity of initial condition, we get

$$\|\boldsymbol{p}(x,0)\|_{\overline{\mathcal{Q}}_x} = \|\boldsymbol{f}(x,0)\|_{\overline{\mathcal{Q}}_x} \leq C.$$

Differentiating (4.1.2a) w.r.t. t, to get

$$\boldsymbol{\mathfrak{L}p} = \boldsymbol{f}_t - \boldsymbol{A}_t \boldsymbol{y},\ (x,t) \in \mathcal{Q},$$

where $\boldsymbol{A}_t = \left(\frac{\partial a_{ij}}{\partial t}\right)$. We use previously defined barrier function $\boldsymbol{\psi} = (1+t)\boldsymbol{C}$ to prove $\|\boldsymbol{p}\|_{\overline{\mathcal{Q}}} = \|\boldsymbol{y}_t\|_{\overline{\mathcal{Q}}} \leq C$. The analysis for $\boldsymbol{q} = \boldsymbol{y}_{tt}$ follows

$$\begin{aligned}
&|\boldsymbol{q}(x,t)| \leq \boldsymbol{C}, \quad (x,t) \in \mathcal{Q}_l \cup \mathcal{Q}_r, \\
&\|\boldsymbol{q}(x,0)\|_{\overline{\mathcal{Q}}_x} = \|\boldsymbol{f}_t(x,0) - \boldsymbol{A}_t \boldsymbol{y} + \boldsymbol{\mathcal{E}} \boldsymbol{f}_{xx}(x,0) - \boldsymbol{A}\boldsymbol{f}(x,0)\|_{\overline{\mathcal{Q}}_x} \leq C,
\end{aligned}$$

$$\mathfrak{L}\boldsymbol{q} = \boldsymbol{f}_{tt} - \boldsymbol{A}_{tt}\boldsymbol{y} - 2\boldsymbol{A}_t\boldsymbol{y}_t,\ (x,t) \in \mathcal{Q},$$

where $\boldsymbol{A}_{tt} = \left(\frac{\partial^2 a_{ij}}{\partial t^2}\right)$. Again, using $\boldsymbol{\psi} = (1+t)\boldsymbol{C}$, we have $\|\boldsymbol{q}\|_{\overline{\mathcal{Q}}} = \|\boldsymbol{y}_{tt}\|_{\overline{\mathcal{Q}}} \leq C$. □

Now, we decompose the exact solution as

$$\boldsymbol{y} = \underbrace{\boldsymbol{\nu}}_{\text{regular component}} + \underbrace{\boldsymbol{w} = \boldsymbol{w}_l + \boldsymbol{w}_r}_{\text{singular component}},$$

where the regular component $\boldsymbol{\nu}$ satisfies

$$\begin{cases} \mathfrak{L}\boldsymbol{\nu} = \boldsymbol{f},\ \text{in } \mathcal{Q}, \\ \boldsymbol{\nu}(x,0) = \boldsymbol{0},\ \text{on } \mathcal{Q}_b, \\ \boldsymbol{\nu} = \boldsymbol{z},\ \text{on } \mathcal{Q}_l \cup \mathcal{Q}_r, \end{cases} \tag{4.2.1}$$

and $\boldsymbol{z}$ is the solution of

$$\begin{cases} \boldsymbol{z}_t + \boldsymbol{A}\boldsymbol{z} = \boldsymbol{f}, \quad (x,t) \in (\mathcal{Q}_l \cup \mathcal{Q}_r)\backslash\{(0,0),(1,0)\}, \\ \boldsymbol{z}(x,0) = \boldsymbol{0}, \qquad x \in \{0,1\}. \end{cases} \tag{4.2.2}$$

The left and right components of $\boldsymbol{w}$ are the solutions to the following problems

$$\begin{cases} \mathfrak{L}\boldsymbol{w}_l = \boldsymbol{0},\ \text{in } \mathcal{Q}, \\ \boldsymbol{w}_l(x,0) = \boldsymbol{0},\ \text{on } \mathcal{Q}_b, \\ \boldsymbol{w}_l(0,t) = \boldsymbol{q}(t) - \boldsymbol{\nu}(0,t) - \boldsymbol{w}_r(0,t),\ \boldsymbol{w}_l(1,t) = \boldsymbol{0},\ t \in \overline{\mathcal{Q}}_t. \end{cases} \tag{4.2.3}$$

$$\begin{cases} \mathfrak{L}\boldsymbol{w}_r = \boldsymbol{0},\ \text{in } \mathcal{Q}, \\ \boldsymbol{w}_r(x,0) = \boldsymbol{0},\ \text{on } \mathcal{Q}_b, \\ \boldsymbol{w}_r(0,t) = \boldsymbol{0},\ \boldsymbol{w}_r(1,t) = \boldsymbol{r}(t) - \boldsymbol{\nu}(1,t),\ t \in \overline{\mathcal{Q}}_t. \end{cases} \tag{4.2.4}$$

Theorem 4.2.1. *The solutions of (4.2.1), (4.2.3) and (4.2.4) satisfy the following bounds*

$$\left|\frac{\partial^{i+j}\nu_k}{\partial x^i \partial t^j}\right| \leq C(1+\varepsilon^{1-i/2}), \quad \text{for } 0 \leq i \leq 4,\ 1 \leq k \leq m, \tag{4.2.5a}$$

$$\left|\frac{\partial^{i+j}w_{l;k}}{\partial x^i \partial t^j}\right| \leq C\varepsilon^{-i/2}e^{-x\sqrt{\alpha/\varepsilon}}, \quad \text{for } 0 \leq i \leq 4,\ 1 \leq k \leq m, \tag{4.2.5b}$$

$$\left|\frac{\partial^{i+j}w_{r;k}}{\partial x^i \partial t^j}\right| \leq C\varepsilon^{-i/2}e^{-(1-x)\sqrt{\alpha/\varepsilon}}, \quad \text{for } 0 \leq i \leq 4,\ 1 \leq k \leq m. \tag{4.2.5c}$$

Proof. The bounds can be easily obtained using the similar ideas of [116]. □

4.3 The proposed scheme

This section presents the construction of the mesh and brings into effect the offered numerical scheme to the problem (4.1.2).

4.3.1 Discretization in time

This discretization process of the problem (4.1.2) includes the Crank-Nicolson technique on an equidistant mesh. We divide $[0, \mathcal{T}]$ into M_t subintervals with step size $\delta t = \frac{\mathcal{T}}{M_t}$ and consider a uniform partition $\Omega_t^{M_t} = \{t_j = j\delta t,\ j = 0, 1, \ldots, M_t\}$ of $\overline{\mathcal{Q}}_t = [0, \mathcal{T}]$ in the time direction. At the $(j+\frac{1}{2})$-th time level, Equation (4.1.2) is discretized as

$$\widetilde{\boldsymbol{y}}^0(x) = \mathbf{0},\ x \in \overline{\mathcal{Q}}_x, \tag{4.3.1a}$$

$$\mathbb{L}\widetilde{\boldsymbol{y}}^{j+1}(x) \equiv -\frac{\boldsymbol{\mathcal{E}}}{2}\widetilde{\boldsymbol{y}}_{xx}^{j+1}(x) + \left(\frac{1}{\delta t}\boldsymbol{I} + \frac{\boldsymbol{A}^{j+\frac{1}{2}}(x)}{2}\right)\widetilde{\boldsymbol{y}}^{j+1}(x) = \boldsymbol{g}^{j+1}(x),\ x \in \mathcal{Q}_x,\ j \geq 0, \tag{4.3.1b}$$

$$\widetilde{\boldsymbol{y}}^{j+1}(0) = \boldsymbol{q}(t_{j+1}),\ \widetilde{\boldsymbol{y}}^{j+1}(1) = \boldsymbol{r}(t_{j+1}),\ j \geq 0, \tag{4.3.1c}$$

where $\boldsymbol{I}$ is the identity matrix of order $m \times m$, $\boldsymbol{A}^{j+\frac{1}{2}}(x) = (a_{kl}(x, t_{j+\frac{1}{2}}))_{1\leq k,l\leq m}$, $\widetilde{\boldsymbol{y}}^{j+1} \approx \boldsymbol{y}(x, t_{j+1})$ represents the solution of the Equation (4.3.1) at the $(j+1)$-th time level, and

$$\boldsymbol{g}^{j+1}(x) = \boldsymbol{f}^{j+\frac{1}{2}}(x) + \frac{\boldsymbol{\mathcal{E}}}{2}\widetilde{\boldsymbol{y}}_{xx}^{j}(x) + \left(\frac{1}{\delta t}\boldsymbol{I} - \frac{\boldsymbol{A}^{j+\frac{1}{2}}(x)}{2}\right)\widetilde{\boldsymbol{y}}^{j}(x).$$

For the components $\widetilde{y}_k^{j+1},\ k=1,2,\ldots,m$ the above equation can be written as

$$\widetilde{y}_k^0(x)=0, \tag{4.3.2a}$$

$$\mathbb{L}_k\widetilde{\boldsymbol{y}}^{j+1}(x)\equiv-\frac{\varepsilon}{2}(\widetilde{y}_{xx}^{j+1})_k(x)+\left(\frac{1}{\delta t}+\frac{a_{kk}^{j+\frac{1}{2}}(x)}{2}\right)\widetilde{y}_k^{j+1}(x)+\frac{1}{2}\sum_{\substack{l=1\\l\neq k}}^{m}a_{lk}^{j+\frac{1}{2}}(x)\widetilde{y}_l^{j+1}(x)=g_k^{j+1}(x), \tag{4.3.2b}$$

$$\widetilde{y}_k^{j+1}(0)=q_k(t_{j+1}),\ \widetilde{y}_k^{j+1}(1)=r_k(t_{j+1}),\ j\geq 0, \tag{4.3.2c}$$

where

$$g_k^{j+1}(x)=f_k^{j+\frac{1}{2}}(x)+\frac{\varepsilon}{2}(\widetilde{y}_{xx}^{j})_k(x)+\left(\frac{1}{\delta t}-\frac{a_{kk}^{j+\frac{1}{2}}(x)}{2}\right)\widetilde{y}_k^{j}(x)-\frac{1}{2}\sum_{\substack{l=1\\l\neq k}}^{m}a_{lk}^{j+\frac{1}{2}}(x)\widetilde{y}_l^{j}(x).$$

The study of local truncation error (LTE) requires the solution of the following auxiliary problem

$$\mathbb{L}\widehat{\boldsymbol{y}}^{j+1}(x)\equiv-\frac{\boldsymbol{\mathcal{E}}}{2}\widehat{\boldsymbol{y}}_{xx}^{j+1}(x)+\left(\frac{1}{\delta t}\boldsymbol{I}+\frac{\boldsymbol{A}^{j+\frac{1}{2}}(x)}{2}\right)\widehat{\boldsymbol{y}}^{j+1}(x)=\boldsymbol{g}^{j+1}(x),\ x\in\mathcal{Q}_x,\ j\geq 0, \tag{4.3.3a}$$

$$\widehat{\boldsymbol{y}}^{j+1}(0)=\boldsymbol{q}(t_{j+1}),\ \widehat{\boldsymbol{y}}^{j+1}(1)=\boldsymbol{r}(t_{j+1}),\ j\geq 0. \tag{4.3.3b}$$

Lemma 4.3.1. *The LTE associated to the Equation (4.3.1), defined as* $\boldsymbol{e}^{j+1}=\boldsymbol{y}(x,t_{j+1})-\widehat{\boldsymbol{y}}^{j+1}(x)$, *satisfies* $\|\boldsymbol{e}^{j+1}\|\leq C(\delta t)^3$.

Proof. The proof is analogous to the proof of Lemma 2.3 given in [89]. □

Lemma 4.3.2. *We define the global error by* $\boldsymbol{E}^j=\sum_{n=0}^{j}\boldsymbol{e}^n$, *which satisfy the following bound*

$$\|\boldsymbol{E}^j\|\leq C(\delta t)^2,\ j\leq\frac{\mathcal{T}}{\delta t}.$$

Proof. We have

$$\begin{aligned}\|\boldsymbol{E}^j\| &= \left\| \sum_{k=1}^{j} \boldsymbol{e}^k \right\|, \; j \leq \frac{\mathcal{T}}{\delta t} \\ &\leq \|\boldsymbol{e}^1\| + \|\boldsymbol{e}^2\| + \cdots + \|\boldsymbol{e}^j\|.\end{aligned}$$

The use of estimate given in Lemma 4.3.1 gives

$$\begin{aligned}\|\boldsymbol{E}^j\| &\leq Cj(\delta t)^3 \\ &= C(\delta t)^2(j\delta t) \\ &\leq C(\delta t)^2\mathcal{T}, \text{ since } j \leq M_t \\ &\leq C(\delta t)^2.\end{aligned}$$

□

From the Lemma 4.3.2, it is evident that the semi-discretized scheme (4.3.1) is convergent of second-order in time. We can decompose the k-th solution component $\widetilde{y}_k^{j+1}(x)$ as $\widetilde{y}_k^{j+1}(x) = \nu_k^{j+1}(x) + w_{l;k}^{j+1}(x) + w_{r;k}^{j+1}(x)$, where the components derivatives satisfy the following bounds (see [50, 89, 116] for detailed analysis)

$$\left|\frac{d^i \nu_k^{j+1}(x)}{dx^i}\right| \leq C(1+\varepsilon^{1-i/2}), \; x \in \overline{\mathcal{Q}}_x, \; 0 \leq i \leq 4, \tag{4.3.4a}$$

$$\left|\frac{d^i w_{l;k}^{j+1}(x)}{dx^i}\right| \leq C(\varepsilon^{-i/2}e^{-x\sqrt{\alpha/\varepsilon}}), \; x \in \overline{\mathcal{Q}}_x, \; 0 \leq i \leq 4, \tag{4.3.4b}$$

$$\left|\frac{d^i w_{r;k}^{j+1}(x)}{dx^i}\right| \leq C(\varepsilon^{-i/2}e^{-(1-x)\sqrt{\alpha/\varepsilon}}), \; x \in \overline{\mathcal{Q}}_x, \; 0 \leq i \leq 4, \tag{4.3.4c}$$

for $k = 0, 1, \ldots, m$.

4.3.2 Exponentially graded mesh (eXp mesh) construction

A well-known fact from the literature tells us that traditional numerical techniques using uniform mesh are insufficient to solve singularly perturbed IBVPs because they produce abruptly extensive oscillations near the layer(s). In additional terms, we can modify this statement as a method can only be developed by using many nodal points on a uniform mesh that gives a uniform approximation at all mesh points and does not depend on the diffusion

parameter. From the application perspective, this goal could be more attainable. Therefore, the situation demands a nonuniform mesh to determine the uniform approximation in the layer region. This subsection mainly focused on constructing an exponentially graded mesh that quickly resolves the layer part by introducing more mesh points in the layer part.

First, the interval $[0,1]$ is divided into $M_x > 4$ (divisible by 4) subintervals $I_i^* = [x_{i-1}^*, x_i^*]$ to construct the eXp mesh $\Delta^{M_x} = \{x_i^* |\ 0 \le i \le M_x\}$. The polynomial space Π_s is defined as $\Pi_s = \{r(x) |\, deg(r(x)) \le s\}$, where $deg(r(x))$ denotes the degree of a polynomial $r(x)$. The mesh generating function $\Psi(\eta)$, which is a piecewise continuously differentiable and monotonically increasing function, is defined by

$$\Psi(\eta) = -\ln(1 - 2\mathfrak{C}_{s,\varepsilon}\eta),\ \eta \in [0, 1/2 - 1/M_x], \tag{4.3.5}$$

where $\mathfrak{C}_{s,\varepsilon} = 1 - \exp\left(-\frac{1}{(s+1)\sqrt{\varepsilon}}\right) \in \mathbb{R}^+$. The interval $[0,1]$ can be split into three subintervals as $[0,1] = [0, x^*_{\frac{M_x}{4}-1}] \cup [x^*_{\frac{M_x}{4}-1}, x^*_{\frac{3M_x}{4}+1}] \cup [x^*_{\frac{3M_x}{4}+1}, 1]$. The nodal points are given as

$$x_i^* = \begin{cases} (s+1)\sqrt{\varepsilon}\Psi(\eta_i), & i = 0, 1, \ldots, \frac{M_x}{4} - 1, \\ x^*_{\frac{M_x}{4}-1} + \left(\dfrac{x^*_{\frac{3M_x}{4}+1} - x^*_{\frac{M_x}{4}-1}}{\frac{M_x}{2}+2}\right)(i - M_x/4 + 1), & i = \frac{M_x}{4}, \ldots, \frac{3M_x}{4}, \\ 1 - (s+1)\sqrt{\varepsilon}\Psi(1-\eta_i), & i = \frac{3M_x}{4} + 1, \ldots, M_x, \end{cases}$$

where $\eta_i = \frac{i}{M_x}$ for $i = 0, 1, \ldots, M_x$, and $\hat{h}_i = x_i^* - x_{i-1}^*$ for $i = 1, 2, \ldots, M_x$. The interval $[x^*_{\frac{M_x}{4}-1}, x^*_{\frac{3M_x}{4}+1}]$ (with $M_x/2 + 2$ partitions) contains equidistant mesh points and the union $[0, x^*_{\frac{M_x}{4}-1}] \cup [x^*_{\frac{3M_x}{4}+1}, 1]$ (with $M_x/4 - 1$ partitions in each subinterval) contain exponentially graded distribution of mesh points. The estimates on $\hat{h}_i$ can be evaluated using the mesh characterizing function $\Phi = \exp(-\Psi)$ (see [91] for more details)

$$\hat{h}_i \le \begin{cases} C(s+1)\sqrt{\varepsilon}M_x^{-1}\max\Psi'(\eta_i), & i = 1, 2, \ldots, \frac{M_x}{4} - 1, \\ CM_x^{-1}, & i = \frac{M_x}{4}, \ldots, \frac{3M_x}{4} + 1, \\ C(s+1)\sqrt{\varepsilon}M_x^{-1}\max\Psi'(1-\eta_i), & i = \frac{3M_x}{4} + 2, \ldots, M_x, \end{cases}$$

which can be further simplified as

$$\hat{h}_i \leq \begin{cases} C(s+1)\sqrt{\varepsilon}M_x^{-1}\max|\Phi'|\exp\left(\frac{x_i^*}{(s+1)\sqrt{\varepsilon}}\right), & i=1,2,\ldots,\frac{M_x}{4}-1,\\ CM_x^{-1}, & i=\frac{M_x}{4},\ldots,\frac{3M_x}{4}+1,\\ C(s+1)\sqrt{\varepsilon}M_x^{-1}\max|\Phi'|\exp\left(\frac{1-x_i^*}{(s+1)\sqrt{\varepsilon}}\right), & i=\frac{3M_x}{4}+2,\ldots,M_x. \end{cases}$$

Using $\max|\Phi'| \leq 2$, the above estimates can be simplified as

$$\hat{h}_i \leq \begin{cases} C\sqrt{\varepsilon}M_x^{-1}\exp\left(\frac{x_i^*}{(s+1)\sqrt{\varepsilon}}\right), & i=1,2,\ldots,\frac{M_x}{4}-1,\\ CM_x^{-1}, & i=\frac{M_x}{4},\ldots,\frac{3M_x}{4}+1,\\ C\sqrt{\varepsilon}M_x^{-1}\exp\left(\frac{1-x_i^*}{(s+1)\sqrt{\varepsilon}}\right), & i=\frac{3M_x}{4}+2,\ldots,M_x. \end{cases} \tag{4.3.6}$$

Additionally, the eXp mesh satisfies

$$|\hat{h}_{i+1}-\hat{h}_i| \leq C\begin{cases} \sqrt{\varepsilon}M_x^{-2}, & i=1,2,\ldots,\frac{M_x}{4}-1,\\ 0, & i=\frac{M_x}{4},\ldots,\frac{3M_x}{4},\\ \sqrt{\varepsilon}M_x^{-2}, & i=\frac{3M_x}{4}+1,\ldots,M_x. \end{cases} \tag{4.3.7}$$

4.3.3 Execution of the collocation technique

In this section, we execute our collocation technique to find the solution of the Equation (4.3.1) by converting the semi-discretized form to a fully discrete form with the use of piecewise quadratic C^1-splines. The collocation points are denoted by χ_i^*

$$\chi_i^* = x_{i-1/2}^* := \frac{x_{i-1}^*+x_i^*}{2} = x_{i-1}^* + \frac{\hat{h}_i}{2} = x_i^* - \frac{\hat{h}_i}{2}, \quad \text{for } i=1,2,\ldots,M_x.$$

For $\mathfrak{m}, s \in \mathbb{N}\cup\{0\}$ $(\mathfrak{m} < s)$, we define the following spaces

$$\mathbb{S}_s^{\mathfrak{m}}(\Delta^{M_x}) := \{r \in C^{\mathfrak{m}}[0,1] :\ r|_{I_i^*} \in \Pi_s,\ \text{for } i=1,2,\ldots,M_x\},$$
$$\mathbb{S}_{s,0}^{\mathfrak{m}}(\Delta^{M_x}) := \{r \in S_s^{\mathfrak{m}}(\Delta^{M_x}) :\ r(0)=r(1)=0\}.$$

The quadratic splines $\mathbb{B}_i(x) \in \mathbb{S}_2^1(\Delta^{M_x}),\ i = 0, 1, \ldots, M_x + 1$ defined below constitute the solution basis for IBVP (4.3.1)

$$\mathbb{B}_0(x) = \begin{cases} \dfrac{(x_1^* - x)^2}{\hat{h}_1^2}, & x_0^* \le x \le x_1^*, \\ 0, & \text{otherwise}, \end{cases}$$

$$\mathbb{B}_1(x) = \begin{cases} \dfrac{\hat{h}_1^2 - (x_1^* - x)^2}{\hat{h}_1^2} - \dfrac{(x - x_0^*)^2}{\hat{h}_1(\hat{h}_1 + \hat{h}_2)}, & x_0^* \le x \le x_1^*, \\ \dfrac{(x_2^* - x)^2}{\hat{h}_1(\hat{h}_1 + \hat{h}_2)}, & x_1^* \le x \le x_2^*, \\ 0, & \text{otherwise}, \end{cases}$$

and for $i = 2, 3, \ldots, M_x - 1$,

$$\mathbb{B}_i(x) = \begin{cases} \dfrac{(x - x_{i-2}^*)^2}{\hat{h}_{i-1}(\hat{h}_{i-1} + \hat{h}_i)}, & x_{i-2}^* \le x \le x_{i-1}^*, \\ \dfrac{(x - x_{i-2}^*)(x_i^* - x)}{\hat{h}_i(\hat{h}_{i-1} + \hat{h}_i)} + \dfrac{(x_{i+1}^* - x)(x - x_{i-1}^*)}{\hat{h}_i(\hat{h}_i + \hat{h}_{i+1})}, & x_{i-1}^* \le x \le x_i^*, \\ \dfrac{(x_{i+1}^* - x)^2}{\hat{h}_{i+1}(\hat{h}_i + \hat{h}_{i+1})}, & x_i^* \le x \le x_{i+1}^*, \\ 0, & \text{otherwise}, \end{cases}$$

while for $i = M_x,\ M_x + 1$ these are defined as

$$\mathbb{B}_{M_x}(x) = \begin{cases} \dfrac{(x - x_{M_x-2}^*)^2}{\hat{h}_{M_x-1}(\hat{h}_{M_x-1} + \hat{h}_{M_x})}, & x_{M_x-2}^* \le x \le x_{M_x-1}^*, \\ \dfrac{\hat{h}_{M_x}^2 - (x - x_{M_x-1}^*)^2}{\hat{h}_{M_x}^2} - \dfrac{(x_{M_x}^* - x)^2}{\hat{h}_{M_x}(\hat{h}_{M_x-1} + \hat{h}_{M_x})}, & x_{M_x-1}^* \le x \le x_{M_x}^*, \\ 0, & \text{otherwise}, \end{cases}$$

$$\mathbb{B}_{M_x+1}(x) = \begin{cases} \dfrac{(x - x_{M_x-1}^*)^2}{\hat{h}_{M_x}^2}, & x_{M_x-1}^* \le x \le x_{M_x}^*, \\ 0, & \text{otherwise}. \end{cases}$$

The approximate solution for the k-th component at the $(j+1)$-th time level is taken as

$$\mathscr{S}_k^{j+1}(x) = \sum_{l=0}^{M_x+1} \alpha_{l;k}^{j+1} \mathbb{B}_l(x),\ j = 0, 1, \ldots, M_t - 1, \tag{4.3.8}$$

where $\alpha_{l;k}^{j+1}$ are the unknowns at the $(j+1)$-th time level. The component-wise (for $k = 1, 2, \ldots, m$) form of fully discrete scheme can be written as

$$\begin{aligned} \mathscr{S}_{i-1/2;k}^{0} &= 0, \\ \mathbb{L}_k \boldsymbol{\mathscr{S}}_{i-1/2}^{j+1} &= g_k^{j+1}(\chi_i^*),\ \text{for } i = 1, 2, \ldots, M_x, \\ \mathscr{S}_{0;k}^{j+1} &= q_k(t_{j+1}),\ \mathscr{S}_{M_x;k}^{j+1} = r_k(t_{j+1}). \end{aligned} \tag{4.3.9}$$

At each time level, the values of $\mathscr{S}_k$ and $\mathscr{S}_k''$ at χ_i^* are given by

$$\begin{aligned} \mathscr{S}_k^{j+1}(\chi_i^*) &= \left(\frac{\hat{h}_i}{4(\hat{h}_i + \hat{h}_{i-1})}\right)\alpha_{i-1;k}^{j+1} + \left(1 - \frac{\hat{h}_i}{4(\hat{h}_i + \hat{h}_{i-1})} - \frac{\hat{h}_i}{4(\hat{h}_i + \hat{h}_{i+1})}\right)\alpha_{i;k}^{j+1} \\ &\quad + \left(\frac{\hat{h}_i}{4(\hat{h}_i + \hat{h}_{i+1})}\right)\alpha_{i+1;k}^{j+1}, \\ (\mathscr{S}_k'')^{j+1}(\chi_i^*) &= \left(\frac{2}{\hat{h}_i(\hat{h}_i + \hat{h}_{i-1})}\right)\alpha_{i-1;k}^{j+1} + \left(-\frac{2}{\hat{h}_i(\hat{h}_i + \hat{h}_{i-1})} - \frac{2}{\hat{h}_i(\hat{h}_i + \hat{h}_{i+1})}\right)\alpha_{i;k}^{j+1} \\ &\quad + \left(\frac{2}{\hat{h}_i(\hat{h}_i + \hat{h}_{i+1})}\right)\alpha_{i+1;k}^{j+1}. \end{aligned} \tag{4.3.10}$$

Substituting these values in (4.3.2b), the L.H.S. becomes

$$\begin{aligned} \mathbb{L}_k^{M_x}\boldsymbol{\alpha}_k^{j+1} = &-\frac{\varepsilon}{2}\left[\left(\frac{2\alpha_{i-1;k}^{j+1}}{\hat{h}_i(\hat{h}_i + \hat{h}_{i-1})}\right) + \left(-\frac{2}{\hat{h}_i(\hat{h}_i + \hat{h}_{i-1})} - \frac{2}{\hat{h}_i(\hat{h}_i + \hat{h}_{i+1})}\right)\alpha_{i;k}^{j+1}\right. \\ &\left. + \left(\frac{2\alpha_{i+1;k}^{j+1}}{\hat{h}_i(\hat{h}_i + \hat{h}_{i+1})}\right)\right] + \left(\frac{1}{\delta t} + \frac{a_{kk}^{j+\frac{1}{2}}(x)}{2}\right)\left[\hat{\mathfrak{q}}_i^{-}\alpha_{i-1;k}^{j+1} + (1 - \hat{\mathfrak{q}}_i^{-} - \hat{\mathfrak{q}}_i^{+})\alpha_{i;k}^{j+1}\right. \\ &\left. + \hat{\mathfrak{q}}_i^{+}\alpha_{i+1;k}^{j+1}\right] + \frac{1}{2}\sum_{l\neq k, l=1}^{m} (a_{lk})_{i-1/2}^{j+\frac{1}{2}}\left[\hat{\mathfrak{q}}_i^{-}\alpha_{i-1;k}^{j+1} + (1 - \hat{\mathfrak{q}}_i^{-} - \hat{\mathfrak{q}}_i^{+})\alpha_{i;k}^{j+1} + \hat{\mathfrak{q}}_i^{+}\alpha_{i+1;k}^{j+1}\right], \end{aligned}$$

where $\mathfrak{q}_i^+ := \frac{\hat{h}_i}{4(\hat{h}_i+\hat{h}_{i+1})}$ and $\mathfrak{q}_i^- := \frac{\hat{h}_i}{4(\hat{h}_i+\hat{h}_{i-1})}$. In the R.H.S., we have

$$\begin{aligned} g_k^{j+1}(x) =& \frac{\varepsilon}{2}\Bigg[\left(\frac{2\alpha_{i-1;k}^j}{\hat{h}_i(\hat{h}_i+\hat{h}_{i-1})}\right) + \left(-\frac{2}{\hat{h}_i(\hat{h}_i+\hat{h}_{i-1})} - \frac{2}{\hat{h}_i(\hat{h}_i+\hat{h}_{i+1})}\right)\alpha_{i;k}^j \\ &+ \left(\frac{2\alpha_{i+1;k}^j}{\hat{h}_i(\hat{h}_i+\hat{h}_{i+1})}\right)\Bigg] + \left(\frac{1}{\delta t} - \frac{a_{kk}^{j+\frac{1}{2}}(x)}{2}\right)\Bigg[\hat{\mathfrak{q}}_i^-\alpha_{i-1;k}^j + (1-\hat{\mathfrak{q}}_i^- - \hat{\mathfrak{q}}_i^+)\alpha_{i;k}^j \\ &+ \hat{\mathfrak{q}}_i^+\alpha_{i+1;k}^j\Bigg] - \frac{1}{2}\sum_{l\neq k, l=1}^{m}(a_{lk})_{i-1/2}^{j+\frac{1}{2}}\Bigg[\hat{\mathfrak{q}}_i^-\alpha_{i-1;k}^j + (1-\hat{\mathfrak{q}}_i^- - \hat{\mathfrak{q}}_i^+)\alpha_{i;k}^j + \hat{\mathfrak{q}}_i^+\alpha_{i+1;k}^j\Bigg] \\ &+ f_k^{j+\frac{1}{2}}(\chi_i^*). \end{aligned}$$

We combine all the equations and form a system of the type

$$\mathbb{A}\boldsymbol{\alpha}^{j+1} = \mathbb{B}\boldsymbol{\alpha}^j + \mathbb{G},$$

where

$$\begin{aligned} \mathbb{G} =& \Bigg(\underbrace{q_1, f_1^{j+\frac{1}{2}}(\chi_1^*), \ldots, f_1^{j+\frac{1}{2}}(\chi_{M_x}^*), r_1}_{1^{\text{st}}\text{component}}, \underbrace{q_2, f_2^{j+\frac{1}{2}}(\chi_1^*), \ldots, f_2^{j+\frac{1}{2}}(\chi_{M_x}^*), r_2}_{2^{\text{nd}}\text{component}}, \ldots, \\ &\underbrace{q_m, f_m^{j+\frac{1}{2}}(\chi_1^*), \ldots, f_m^{j+\frac{1}{2}}(\chi_{M_x}^*), r_m}_{m^{\text{th}}\text{component}}\Bigg)^T, \\ \boldsymbol{\alpha}^{j+1} =& \Bigg(\underbrace{\alpha_{0;1}^{j+1}, \alpha_{1;1}^{j+1}, \ldots, \alpha_{M_x+1;1}^{j+1}}_{1^{\text{st}}\text{component}}, \underbrace{\alpha_{0;2}^{j+1}, \alpha_{1;2}^{j+1}, \ldots, \alpha_{M_x+1;2}^{j+1}}_{2^{\text{nd}}\text{component}}, \ldots, \\ &\underbrace{\alpha_{0;m}^{j+1}, \alpha_{1;m}^{j+1}, \ldots, \alpha_{M_x+1;m}^{j+1}}_{m^{\text{th}}\text{component}}\Bigg)^T. \end{aligned}$$

The matrices $\mathbb{A}$ and $\mathbb{B}$ are given by

$$\mathbb{A} = \begin{bmatrix} \mathbb{A}_{11} & \mathbb{A}_{12} & \ldots & \mathbb{A}_{1m} \\ \mathbb{A}_{21} & \mathbb{A}_{22} & \ldots & \mathbb{A}_{2m} \\ \vdots & \vdots & \ddots & \vdots \\ \mathbb{A}_{m1} & \mathbb{A}_{m2} & \ldots & \mathbb{A}_{mm} \end{bmatrix}, \quad \mathbb{B} = \begin{bmatrix} \mathbb{B}_{11} & \mathbb{B}_{12} & \ldots & \mathbb{B}_{1m} \\ \mathbb{B}_{21} & \mathbb{B}_{22} & \ldots & \mathbb{B}_{2m} \\ \vdots & \vdots & \ddots & \vdots \\ \mathbb{B}_{m1} & \mathbb{B}_{m2} & \ldots & \mathbb{B}_{mm} \end{bmatrix}.$$

Each $\mathbb{A}_{lk}$ is also a matrix of order $(M_x+2)\times(M_x+2)$. The matrix $\mathbb{A}_{kk}$ is given as

$$\mathbb{A}_{kk}=\begin{bmatrix} 1 & 0 & 0 & 0 & \dots & \dots & 0 \\ \mathfrak{a}_{21;kk} & \mathfrak{a}_{22;kk} & \mathfrak{a}_{23;kk} & 0 & \dots & \dots & 0 \\ 0 & \mathfrak{a}_{32;kk} & \mathfrak{a}_{33;kk} & \mathfrak{a}_{34;kk} & \dots & \dots & 0 \\ \vdots & \ddots & \ddots & \ddots & \vdots & \vdots & \vdots \\ \dots & \dots & \dots & 0 & \mathfrak{a}_{M_x+1M_x;kk} & \mathfrak{a}_{M_x+1M_x+1;kk} & \mathfrak{a}_{M_x+1M_x+2;kk} \\ \dots & \dots & \dots & 0 & 0 & 0 & 1 \end{bmatrix},$$

where

$$\begin{aligned}
\mathfrak{a}_{ii-1;kk} &= -\frac{4\varepsilon\hat{\mathfrak{q}}^{-}_{i-1}}{\hat{h}^2_{i-1}}+\left(\frac{1}{\delta t}+\frac{a^{j+\frac{1}{2}}_{kk}(\chi^*_{i-1})}{2}\right)\hat{\mathfrak{q}}^{-}_{i-1},\\
\mathfrak{a}_{ii;kk} &= \frac{4\varepsilon\hat{\mathfrak{q}}^{+}_{i-1}}{\hat{h}^2_{i-1}}+\frac{4\varepsilon\hat{\mathfrak{q}}^{-}_{i-1}}{\hat{h}^2_{i-1}}+\left(\frac{1}{\delta t}+\frac{a^{j+\frac{1}{2}}_{kk}(\chi^*_{i-1})}{2}\right)\left(1-\hat{\mathfrak{q}}^{+}_{i-1}-\hat{\mathfrak{q}}^{-}_{i-1}\right),\\
\mathfrak{a}_{ii+1;kk} &= -\frac{4\varepsilon\hat{\mathfrak{q}}^{+}_{i-1}}{\hat{h}^2_{i-1}}+\left(\frac{1}{\delta t}+\frac{a^{j+\frac{1}{2}}_{kk}(\chi^*_{i-1})}{2}\right)\hat{\mathfrak{q}}^{+}_{i-1},
\end{aligned}$$

for $i=2,3,\dots,M_x+1$. Furthermore, for $l\neq k,\ l=1,2,\dots,m,\ k=1,2,\dots,m$ the matrix $\mathbb{A}_{lk}$ is given as

$$\mathbb{A}_{lk}=\begin{bmatrix} 0 & 0 & 0 & 0 & \dots & \dots & 0 \\ \mathfrak{a}_{21;lk} & \mathfrak{a}_{22;lk} & \mathfrak{a}_{23;lk} & 0 & \dots & \dots & 0 \\ 0 & \mathfrak{a}_{32;lk} & \mathfrak{a}_{33;lk} & \mathfrak{a}_{34;lk} & \dots & \dots & 0 \\ \vdots & \ddots & \ddots & \ddots & \vdots & \vdots & \vdots \\ \dots & \dots & \dots & 0 & \mathfrak{a}_{M_x+1M_x;lk} & \mathfrak{a}_{M_x+1M_x+1;lk} & \mathfrak{a}_{M_x+1M_x+2;lk} \\ \dots & \dots & \dots & 0 & 0 & 0 & 0 \end{bmatrix},$$

where

$$\begin{aligned}
\mathfrak{a}_{ii-1,lk} &= \frac{1}{2}a^{j+\frac{1}{2}}_{lk}(\chi^*_{i-1})\hat{\mathfrak{q}}^{-}_{i-1},\\
\mathfrak{a}_{ii,lk} &= \frac{1}{2}a^{j+\frac{1}{2}}_{lk}(\chi^*_{i-1})\left(1-\hat{\mathfrak{q}}^{+}_{i-1}-\hat{\mathfrak{q}}^{-}_{i-1}\right),
\end{aligned}$$

$$\mathfrak{a}_{ii+1,lk} = \frac{1}{2} a_{lk}^{j+\frac{1}{2}}(\chi_{i-1}^{*})\hat{\mathfrak{q}}_{i-1}^{+},$$

for $i = 2, 3, \ldots, M_x + 1$. Again, each $\mathbb{B}_{lk}$ is also a matrix of order $(M_x + 2) \times (M_x + 2)$. The matrix $\mathbb{B}_{kk}$ is given as

$$\mathbb{B}_{kk} = \begin{bmatrix} 0 & 0 & 0 & 0 & \ldots & \ldots & 0 \\ \mathfrak{b}_{21;kk} & \mathfrak{b}_{22;kk} & \mathfrak{b}_{23;kk} & 0 & \ldots & \ldots & 0 \\ 0 & \mathfrak{b}_{32;kk} & \mathfrak{b}_{33;kk} & \mathfrak{b}_{34;kk} & \ldots & \ldots & 0 \\ \vdots & \ddots & \ddots & \ddots & \vdots & \vdots & \vdots \\ \ldots & \ldots & \ldots & 0 & \mathfrak{b}_{M_x+1M_x;kk} & \mathfrak{b}_{M_x+1M_x+1;kk} & \mathfrak{b}_{M_x+1M_x+2;kk} \\ \ldots & \ldots & \ldots & 0 & 0 & 0 & 0 \end{bmatrix},$$

where

$$\begin{aligned} \mathfrak{b}_{ii-1;kk} =& \frac{4\varepsilon\hat{\mathfrak{q}}_{i-1}^{-}}{\hat{h}_{i-1}^{2}} + \left(\frac{1}{\delta t} - \frac{a_{kk}^{j+\frac{1}{2}}(\chi_{i-1}^{*})}{2}\right)\hat{\mathfrak{q}}_{i-1}^{-}, \\ \mathfrak{b}_{ii;kk} =& -\frac{4\varepsilon\hat{\mathfrak{q}}_{i-1}^{+}}{\hat{h}_{i-1}^{2}} - \frac{4\varepsilon\hat{\mathfrak{q}}_{i-1}^{-}}{\hat{h}_{i-1}^{2}} + \left(\frac{1}{\delta t} - \frac{a_{kk}^{j+\frac{1}{2}}(\chi_{i-1}^{*})}{2}\right)\left(1 - \hat{\mathfrak{q}}_{i-1}^{+} - \hat{\mathfrak{q}}_{i-1}^{-}\right), \\ \mathfrak{b}_{ii+1;kk} =& \frac{4\varepsilon\hat{\mathfrak{q}}_{i-1}^{+}}{\hat{h}_{i-1}^{2}} + \left(\frac{1}{\delta t} - \frac{a_{kk}^{j+\frac{1}{2}}(\chi_{i-1}^{*})}{2}\right)\hat{\mathfrak{q}}_{i-1}^{+}, \end{aligned}$$

for $i = 2, 3, \ldots, M_x + 1$. Furthermore, for $l \neq k,\ l = 1, 2, \ldots, m,\ k = 1, 2, \ldots, m$ the matrix $\mathbb{B}_{lk}$ is given as

$$\mathbb{B}_{lk} = \begin{bmatrix} 0 & 0 & 0 & 0 & \ldots & \ldots & 0 \\ \mathfrak{b}_{21;lk} & \mathfrak{b}_{22;lk} & \mathfrak{b}_{23;lk} & 0 & \ldots & \ldots & 0 \\ 0 & \mathfrak{b}_{32;lk} & \mathfrak{b}_{33;lk} & \mathfrak{b}_{34;lk} & \ldots & \ldots & 0 \\ \vdots & \ddots & \ddots & \ddots & \vdots & \vdots & \vdots \\ \ldots & \ldots & \ldots & 0 & \mathfrak{b}_{M_x+1M_x;lk} & \mathfrak{b}_{M_x+1M_x+1;lk} & \mathfrak{b}_{M_x+1M_x+2;lk} \\ \ldots & \ldots & \ldots & 0 & 0 & 0 & 0 \end{bmatrix},$$

where

$$\begin{aligned}\mathfrak{b}_{ii-1,lk} &= -\frac{1}{2}a_{lk}^{j+\frac{1}{2}}(\chi_{i-1}^{*})\hat{\mathfrak{q}}_{i-1}^{-},\\ \mathfrak{b}_{ii,lk} &= -\frac{1}{2}a_{lk}^{j+\frac{1}{2}}(\chi_{i-1}^{*})\Big(1-\hat{\mathfrak{q}}_{i-1}^{+}-\hat{\mathfrak{q}}_{i-1}^{-}\Big),\\ \mathfrak{b}_{ii+1,lk} &= -\frac{1}{2}a_{lk}^{j+\frac{1}{2}}(\chi_{i-1}^{*})\hat{\mathfrak{q}}_{i-1}^{+},\end{aligned}$$

for $i = 2, 3, \ldots, M_x + 1$.

4.4 Convergence and error analysis

In this section, first we find $\mathbb{Y}_k^{j+1} \in \mathbb{S}_2^1(\Delta^{M_x})$ such that

$$[\mathbb{L}_k\mathbf{Y}^{j+1}]_{i-1/2} = g_k^{j+1}(\chi_i^{*}),\ i = 1, 2, \ldots, M_x,\ (\mathbf{Y}^{j+1})_0 = \boldsymbol{q}(t_{j+1}),\ (\mathbf{Y}^{j+1})_{M_x} = \boldsymbol{r}(t_{j+1}), \tag{4.4.1}$$

where the components $\mathbb{Y}_k^{j+1}$ are represented as

$$\mathbb{Y}_k^{j+1}(x) = \sum_{l=0}^{M_x+1} \varsigma_{l;k}^{j+1}\mathbb{B}_l(x),\ j = 0, 1, \ldots, M_t - 1.$$

We apply our collocation technique on each component at each time step to get the following system

$$[\mathbb{L}_k^{M_x}\boldsymbol{\varsigma}_k^{j+1}]_{i-1/2} = g_k^{j+1}(\chi_i^{*}),\ i = 1, 2, \ldots, M_x,\ \varsigma_{0;k}^{j+1} = q_k(t_{j+1}),\ \varsigma_{M_x+1;k}^{j+1} = r_k(t_{j+1}), \tag{4.4.2}$$

then, to prove the parameter-uniform convergence, we need error estimates in $\mathbb{S}_2^0$ and $\mathbb{S}_2^1$-interpolations.

4.4.1 $\mathbb{S}_2^0$-interpolation

To find an interpolating function $\mathbb{I}_2^0\mathbb{Y}_k^{j+1} \in \mathbb{S}_2^0(\Delta^{M_x})$ for the function $\mathbb{Y}_k^{j+1} \in C^0(\overline{\mathcal{Q}}_x)$, we need to solve the following interpolation problem

$$(\mathbb{I}_2^0\mathbb{Y}_k^{j+1})_i = (\mathbb{Y}_k^{j+1})_i,\ i = 0, 1, \ldots, M_x, \text{ and } \quad (\mathbb{I}_2^0\mathbb{Y}_k^{j+1})_{i-1/2} = (\mathbb{Y}_k^{j+1})_{i-1/2},\ i = 1, 2, \ldots, M_x,$$

where $(\mathbb{Y}_k^{j+1})_i = \mathbb{Y}_k(x_i^*, t_{j+1}),\ (\mathbb{Y}_k^{j+1})_{i-1/2} = \mathbb{Y}_k(\chi_i^*, t_{j+1}), \quad k = 1, 2, \ldots, m.$

Theorem 4.4.1. *Assuming $a_{pq}^{j+1}, f_k^{j+1} \in C^4(\overline{\mathcal{Q}}_x)$, the interpolating error $\widetilde{\boldsymbol{y}}^{j+1} - \mathbb{I}_2^0\widetilde{\boldsymbol{y}}^{j+1}$ in the semi-discretized solution $\widetilde{\boldsymbol{y}}^{j+1}$ of equation (4.3.1) at each time step satisfies*

$$\|\widetilde{\boldsymbol{y}}^{j+1} - \mathbb{I}_2^0\widetilde{\boldsymbol{y}}^{j+1}\| \leq CM_x^{-3},$$
$$\boldsymbol{\mathcal{E}} \max_{i=1,2,\ldots,M_x} |(\widetilde{\boldsymbol{y}}^{j+1} - \mathbb{I}_2^0\widetilde{\boldsymbol{y}}^{j+1})''_{i-1/2}| \leq \boldsymbol{C}M_x^{-2}.$$

Proof. First, using the Lagrange representation and Taylor expansions for interpolating polynomial, we verify that for any $\widetilde{\boldsymbol{y}}^{j+1} \in C^4[0,1]^m$,

$$\left\|\widetilde{y}_k^{j+1} - \mathbb{I}_2^0\widetilde{y}_k^{j+1}\right\|_{I_i^*} \leq \frac{\hat{h}_i^3}{24}\left\|(\widetilde{y}_k^{j+1})^{(3)}\right\|_{I_i^*}, \quad \left|(\widetilde{y}_k^{j+1} - \mathbb{I}_2^0\widetilde{y}_k^{j+1})''_{i-1/2}\right| \leq \frac{\hat{h}_i^2}{48}\left\|(\widetilde{y}_k^{j+1})^{(4)}\right\|_{I_i^*}. \quad (4.4.3)$$

Solution components $\widetilde{y}_k^{j+1}$ can be decomposed by making use of the linear property of $\mathbb{I}_2^0$ as

$$\widetilde{y}_k^{j+1} - \mathbb{I}_2^0\widetilde{y}_k^{j+1} = (\nu_k^{j+1} - \mathbb{I}_2^0\nu_k^{j+1}) + \left(w_{l;k}^{j+1} - \mathbb{I}_2^0 w_{l;k}^{j+1}\right) + \left(w_{r;k}^{j+1} - \mathbb{I}_2^0 w_{r;k}^{j+1}\right).$$

First, we analyze the regular component as follows. For $I_i^* \subset [0, x^*_{\frac{M_x}{4}-1}]$, using the bounds of the Equation (4.3.4), we obtain

$$\begin{aligned}
\frac{\hat{h}_i^3}{24}\left|(\nu_k^{j+1})^{(3)}\right|_{I_i^*} &\leq C\varepsilon^{3/2}M_x^{-3}\exp\left(\frac{3x_i^*}{(s+1)\sqrt{\varepsilon}}\right)(1+\varepsilon^{-1/2}) \\
&\leq CM_x^{-3}\exp\left(\frac{x_i^*}{\sqrt{\varepsilon}}\right) \\
&\leq CM_x^{-3}\exp\Big((s+1)\Psi(\eta_i)\Big) \\
&\leq CM_x^{-3}.
\end{aligned}$$

Using the bounds for $\hat{h}_i$ from Equation (4.3.6), we get $\|\nu_k^{j+1} - \mathbb{I}_2^0\nu_k^{j+1}\|_{I_i^*} \leq CM_x^{-3}$ for the right layer region ($I_i^* \subset [x^*_{\frac{3M_x}{4}+2}, 1]$) and regular region ($I_i^* \subset [x^*_{\frac{M_x}{4}}, x^*_{\frac{3M_x}{4}+1}]$). Thus, for regular component ν_k^{j+1} in all the three regions, we have

$$\|\nu_k^{j+1} - \mathbb{I}_2^0\nu_k^{j+1}\| \leq CM_x^{-3}.$$

For the left singular component $w_{l;k}^{j+1}$ in $I_i^* \subset [0, x^*_{\frac{M_x}{4}-1}]$, using the bounds and inequality of Equations (4.3.4) and (4.3.6), we get

$$\begin{aligned}
\frac{\hat{h}_i^3}{24}\left|(w_{l;k}^{j+1})^{(3)}\right|_{I_i^*} &\leq C\varepsilon^{3/2}M_x^{-3}\exp\left(\frac{3x_i^*}{(s+1)\sqrt{\varepsilon}}\right)\varepsilon^{-3/2}\left|e^{-x\sqrt{\alpha/\varepsilon}}\right|_{I_i^*} \\
&\leq CM_x^{-3}\exp\left(\frac{x_i^*}{\sqrt{\varepsilon}}-\frac{x_{i-1}^*}{\sqrt{\varepsilon}}\right) \\
&\leq CM_x^{-3}\exp\left(\frac{\hat{h}_i}{\sqrt{\varepsilon}}\right) \\
&\leq CM_x^{-3}\exp\left((s+1)M_x^{-1}\max\Psi'(\eta_i)\right) \\
&\leq CM_x^{-3}.
\end{aligned}$$

Now for $I_i^* \subset [x^*_{\frac{M_x}{4}}, x^*_{\frac{3M_x}{4}+1}]$, we obtain

$$\begin{aligned}
\frac{\hat{h}_i^3}{24}\left|(w_{l;k}^{j+1})^{(3)}\right|_{I_i^*} &\leq CM_x^{-3}\varepsilon^{-3/2}\left|e^{-x\sqrt{\alpha/\varepsilon}}\right|_{I_i^*} \\
&\leq CM_x^{-3}\varepsilon^{-3/2}\exp\left(-x_{i-1}^*\sqrt{\frac{\alpha}{\varepsilon}}\right).
\end{aligned}$$

Here we use L'Hôpital rule (as limit of $\varepsilon \to 0$) to show that the term $\varepsilon^{-3/2}\exp\left(-x_{i-1}^*\sqrt{\frac{\alpha}{\varepsilon}}\right)$ is bounded in $[x^*_{\frac{M_x}{4}}, x^*_{\frac{3M_x}{4}+1}]$. Thus

$$\frac{\hat{h}_i^3}{24}\left|(w_{l;k}^{j+1})^{(3)}\right|_{I_i^*} \leq CM_x^{-3}.$$

Following the analogy of the subinterval $[0, x^*_{\frac{M_x}{4}-1}]$, one can easily get the bounds in $I_i^* \subset [x^*_{\frac{3M_x}{4}+2}, 1]$. Combining all these estimates, we have

$$\|w_{l;k}^{j+1} - \mathbb{I}_2^0 w_{l;k}^{j+1}\| \leq CM_x^{-3}.$$

For the right singular component $w_{r;k}^{j+1}$ in $I_i^* \subset [0, x^*_{\frac{M_x}{4}-1}]$, using the bounds and inequality of

Equations (4.3.4) and (4.3.6), we get

$$\begin{aligned}
\frac{\hat{h}_i^3}{24}\left|(w_{r;k}^{j+1})^{(3)}\right|_{I_i^*} &\leq C\varepsilon^{3/2}M_x^{-3}\exp\left(\frac{3x_i^*}{(s+1)\sqrt{\varepsilon}}\right)\varepsilon^{-3/2}\left|e^{-(1-x)\sqrt{\alpha/\varepsilon}}\right|_{I_i^*} \\
&\leq C\varepsilon^{3/2}M_x^{-3}\exp\left(\frac{C_1x_i^*}{\sqrt{\varepsilon}}\right)\varepsilon^{-3/2}\exp\left(-\frac{C_2(1-x_{i-1}^*)}{\sqrt{\varepsilon}}\right) \\
&\leq CM_x^{-3}\exp\left(C_3\frac{x_i^*-(1-x_{i-1}^*)}{\sqrt{\varepsilon}}\right) \\
&\leq CM_x^{-3}\exp\left(C_3\frac{\hat{h}_i-1-2x_{i-1}^*}{\sqrt{\varepsilon}}\right) \\
&\leq CM_x^{-3}\exp\left(C_3(s+1)M_x^{-1}\max\Psi'(\eta_i)\right) \\
&\leq CM_x^{-3}.
\end{aligned}$$

The bounds in the intervals $[x^*_{\frac{3M_x}{4}+2}, 1]$ and $[x^*_{\frac{M_x}{4}}, x^*_{\frac{3M_x}{4}+1}]$ can easily be obtained by following the previously used approach for $w_{l;k}^{j+1}$. Thus, we get

$$\|w_{r;k}^{j+1} - \mathbb{I}_2^0 w_{r;k}^{j+1}\| \leq CM_x^{-3}.$$

In the next step we obtain the bounds for $\max\limits_{i=1,2,\ldots,M_x}|(y_k^{j+1} - \mathbb{I}_2^0 y_k^{j+1})''_{i-1/2}|$. For this, first consider ν_k in $I_i^* \subset [0, x^*_{\frac{M_x}{4}-1}]$ as follows

$$\begin{aligned}
\frac{\hat{h}_i^2}{48}\left|(\nu_k^{j+1})^{(4)}\right|_{I_i^*} &\leq C\varepsilon M_x^{-2}\exp\left(\frac{2x_i^*}{(s+1)\sqrt{\varepsilon}}\right)(1+\varepsilon^{-1}) \text{ (using Equations (4.3.4) and (4.3.6))} \\
&\leq CM_x^{-2}\exp\left(\frac{2x_i^*}{(s+1)\sqrt{\varepsilon}}\right) \\
&\leq CM_x^{-2}\exp\left(2\Psi(\eta_i)\right) \\
&\leq CM_x^{-2}.
\end{aligned}$$

Similar results can be obtained for the intervals $[x^*_{\frac{M_x}{4}}, x^*_{\frac{3M_x}{4}+1}]$ and $[x^*_{\frac{3M_x}{4}+2}, 1]$. Now for the left singular component in $I_i^* \subset [0, x^*_{\frac{M_x}{4}-1}]$, we have

$$\frac{\hat{h}_i^2}{48}\left|(w_{l;k}^{j+1})^{(4)}\right|_{I_i^*} \leq C\varepsilon M_x^{-2}\exp\left(\frac{2x_i^*}{(s+1)\sqrt{\varepsilon}}\right)\varepsilon^{-2}\left|e^{-x\sqrt{\alpha/\varepsilon}}\right|_{I_i^*}$$

$$
\begin{aligned}
&\leq C\varepsilon M_x^{-2}\exp\left(\frac{C_4 x_i^*}{\sqrt{\varepsilon}}\right)\varepsilon^{-2}\exp\left(\frac{-C_5 x_{i-1}^*}{\sqrt{\varepsilon}}\right)\\
&\leq C\varepsilon^{-1}M_x^{-2}\exp\left(\frac{C_6(x_i^*-x_{i-1}^*)}{\sqrt{\varepsilon}}\right)\\
&\leq C\varepsilon^{-1}M_x^{-2}\exp\left(\frac{C_6\hat{h}_i}{\sqrt{\varepsilon}}\right)\\
&\leq C\varepsilon^{-1}M_x^{-2}\exp\left(C_6(s+1)M_x^{-1}\max\Psi'(\eta_i)\right)\\
&\leq C\varepsilon^{-1}M_x^{-2}.
\end{aligned}
$$

Previously used approach led us to obtain the bounds for the intervals $[x^*_{\frac{M_x}{4}}, x^*_{\frac{3M_x}{4}+1}]$ and $[x^*_{\frac{3M_x}{4}+2}, 1]$. Thus,

$$
\max_{i=1,2,\ldots,M_x}|(w_{l;k}^{j+1}-\mathbb{I}_2^0 w_{l;k}^{j+1})''_{i-1/2}|\leq C\varepsilon^{-1}M_x^{-2}.
$$

For the right singular component $w_{r;k}^{j+1}$ in $I_i^*\subset[0,x^*_{\frac{M_x}{4}-1}]$, using the bounds and inequality of Equations (4.3.4) and (4.3.6), we get

$$
\begin{aligned}
\frac{\hat{h}_i^2}{48}\left|(w_{r;k}^{j+1})^{(4)}\right|_{I_i^*}&\leq C\varepsilon M_x^{-2}\exp\left(\frac{3x_i^*}{(s+1)\sqrt{\varepsilon}}\right)\varepsilon^{-2}\left|e^{-(1-x)\sqrt{\alpha/\varepsilon}}\right|_{I_i^*}\\
&\leq C\varepsilon^{-1}M_x^{-2}\exp\left(\frac{C_7 x_i^*}{\sqrt{\varepsilon}}\right)\exp\left(-\frac{C_8(1-x_{i-1}^*)}{\sqrt{\varepsilon}}\right)\\
&\leq C\varepsilon^{-1}M_x^{-2}\exp\left(C_9\frac{x_i^*-(1-x_{i-1}^*)}{\sqrt{\varepsilon}}\right)\\
&\leq C\varepsilon^{-1}M_x^{-2}\exp\left(C_9\frac{\hat{h}_i-1-2x_{i-1}^*}{\sqrt{\varepsilon}}\right)\\
&\leq C\varepsilon^{-1}M_x^{-2}\exp\left(C_9(s+1)M_x^{-1}\max\Psi'(\eta_i)\right)\\
&\leq C\varepsilon^{-1}M_x^{-2}.
\end{aligned}
$$

Previously used approach led us to obtain the bounds for the intervals $[x^*_{\frac{M_x}{4}}, x^*_{\frac{3M_x}{4}+1}]$ and $[x^*_{\frac{3M_x}{4}+2}, 1]$. Thus,

$$
\max_{i=1,2,\ldots,M_x}|(w_{r;k}^{j+1}-\mathbb{I}_2^0 w_{r;k}^{j+1})''_{i-1/2}|\leq C\varepsilon^{-1}M_x^{-2}.
$$

As discussed earlier, $\mathbb{I}_2^0\widetilde{y}_k^{j+1}$ satisfy linearity, so using the triangle inequality, the proof is completed. □

Lemma 4.4.1. *Let* $\phi_k \in \mathbb{S}_2^0(\Delta^{M_x})$ *with* $(\phi_k)_{i-1/2} = 0,\ i = 1, 2, \ldots, M_x,\ k = 1, 2, \ldots, m,$ *then*

$$\|\phi_k\|_{I_i^*} \leq \max_i\{|(\phi_k)_{i-1}|, |(\phi_k)_i|\}, \quad \|\phi_k''\|_{I_i^*} \leq \frac{8}{\hat{h}_i^2}\max_i\{|(\phi_k)_{i-1}|, |(\phi_k)_i|\}.$$

Proof. Refer to [94]. □

4.4.2 $\mathbb{S}_2^1$-interpolation

To find an interpolating function $\mathbb{I}_2^1\mathbb{Y}_k^{j+1} \in \mathbb{S}_2^1(\Delta^{M_x})$ for the function $\mathbb{Y}_k^{j+1} \in C^1(\overline{\mathcal{Q}}_x)$, we need to solve the following interpolation problem

$$\begin{aligned}&(\mathbb{I}_2^1\mathbb{Y}_k^{j+1})_{i-1/2} = (\mathbb{Y}_k^{j+1})_{i-1/2},\ i = 1, 2, \ldots, M_x,\\ &(\mathbb{I}_2^1\mathbb{Y}_k^{j+1})_0 = (\mathbb{Y}_k^{j+1})_0,\ (\mathbb{I}_2^1\mathbb{Y}_k^{j+1})_{M_x} = (\mathbb{Y}_k^{j+1})_{M_x},\end{aligned} \tag{4.4.4}$$

where $(\mathbb{Y}_k^{j+1})_{i-1/2} = \mathbb{Y}_k(\chi_i^*, t_{j+1}), \quad k = 1, 2, \ldots, m$. From [93, 111], we have

$$[\Lambda\phi_k]_i \equiv a_i(\phi_k)_{i-1}+3(\phi_k)_i+c_i(\phi_k)_{i+1} = 4a_i(\phi_k)_{i-1/2}+4c_i(\phi_k)_{i+1/2},\ i = 1, 2, \ldots, M_x-1, \tag{4.4.5}$$

where $a_i = \frac{\hat{h}_{i+1}}{\hat{h}_i+\hat{h}_{i+1}}$ and $c_i = 1 - a_i = \frac{\hat{h}_i}{\hat{h}_i+\hat{h}_{i+1}}$.

Lemma 4.4.2. *The operator* Λ *(refer Equation (4.4.5)) is stable, with* $(\phi_k)_0 = (\phi_k)_1 = 0,$

$$\max_{i=1,2,\ldots,M_x-1}|(\phi_k)_i| \leq \frac{1}{2}\max_{i=1,2,\ldots,M_x-1}|[\Lambda\phi_k]_i|, \quad k = 1, 2, \ldots, m,$$

for the vectors $\phi_k \in \mathbb{R}^{M_x+1}$.

Proof. Refer to [94]. □

Theorem 4.4.2. *Assuming* $a_{pq}^{j+1}, f_k^{j+1} \in C^4(\overline{\mathcal{Q}}_x)$*, the interpolating error* $\widetilde{\boldsymbol{y}}^{j+1} - \mathbb{I}_2^1\widetilde{\boldsymbol{y}}^{j+1}$ *in the*

semi-discretized solution $\widetilde{\boldsymbol{y}}^{j+1}$ *of equation (4.3.1) at each time step satisfies*

$$\max_{i=0,1,\ldots,M_x} |(\widetilde{\boldsymbol{y}}^{j+1} - \mathbb{I}_2^1 \widetilde{\boldsymbol{y}}^{j+1})_i| \leq \boldsymbol{C} M_x^{-4}, \tag{4.4.6a}$$

$$\|\widetilde{\boldsymbol{y}}^{j+1} - \mathbb{I}_2^1 \widetilde{\boldsymbol{y}}^{j+1}\| \leq C M_x^{-3}, \tag{4.4.6b}$$

$$\boldsymbol{\mathcal{E}} \max_{i=1,2,\ldots,M_x} |(\widetilde{\boldsymbol{y}}^{j+1} - \mathbb{I}_2^1 \widetilde{\boldsymbol{y}}^{j+1})''_{i-1/2}| \leq \boldsymbol{C} M_x^{-2}. \tag{4.4.6c}$$

Proof. For an arbitrary function $\psi_k^{j+1} \in C^4(\overline{\mathcal{Q}}_x)$, the interpolating error satisfies

$$(\psi_k^{j+1} - \mathbb{I}_2^1 \psi_k^{j+1})_0 = (\psi_k^{j+1} - \mathbb{I}_2^1 \psi_k^{j+1})_1 = 0.$$

We use Equations (4.4.4) and (4.4.5) to get the following expression for truncation error

$$\begin{aligned} \tau_{\psi_k,i}^{j+1} &= [\Lambda(\psi_k^{j+1} - \mathbb{I}_2^1 \psi_k^{j+1})]_i \\ &= a_i(\psi_k^{j+1})_{i-1} - 4a_i(\psi_k^{j+1})_{i-1/2} + 3(\psi_k^{j+1})_i - 4c_i(\psi_k^{j+1})_{i+1/2} + c_i(\psi_k^{j+1})_{i+1}, \end{aligned} \tag{4.4.7}$$

for $i = 1, 2, \ldots, M_x,\ k = 1, 2, \ldots, m$. Using the Taylor expansions in (4.4.7), we obtain

$$|\tau_{\psi_k,i}^{j+1}| \leq \frac{1}{12} \hat{h}_i \hat{h}_{i+1} |\hat{h}_{i+1} - \hat{h}_i| \|(\psi_k^{j+1})'''\|_{I_i^*} + \frac{5}{96} \max\{\hat{h}_i^4, \hat{h}_{i+1}^4\} \|(\psi_k^{j+1})^{(4)}\|_{I_i^* \cup I_{i+1}^*}. \tag{4.4.8}$$

Now, the decomposition of the interpolating error is given by

$$\widetilde{y}_k^{j+1} - \mathbb{I}_2^1 \widetilde{y}_k^{j+1} = (\nu_k^{j+1} - \mathbb{I}_2^1 \nu_k^{j+1}) + \left(w_{l;k}^{j+1} - \mathbb{I}_2^1 w_{l;k}^{j+1} \right) + \left(w_{r;k}^{j+1} - \mathbb{I}_2^1 w_{r;k}^{j+1} \right),$$

or

$$\tau_{y_k,i}^{j+1} = \tau_{\nu_k,i}^{j+1} + \tau_{w_{l;k},i}^{j+1} + \tau_{w_{r;k},i}^{j+1}.$$

We start with exploring the regular component in $I_i^* \subset [0, x^*_{\frac{M_x}{4}-1}]$. Using the inequality (4.4.8) and bounds of (4.3.4), we get

$$|\tau_{\nu_k,i}^{j+1}| \leq C \left(\hat{h}_i \hat{h}_{i+1} |\hat{h}_{i+1} - \hat{h}_i| (1 + \varepsilon^{-1/2}) + \max\{\hat{h}_i^4, \hat{h}_{i+1}^4\} (1 + \varepsilon^{-1}) \right).$$

Now as $\hat{h}_i < \hat{h}_{i+1}$ holds in $[0, x^*_{\frac{M_x}{4}-1}]$, so

$$\begin{aligned}
|\tau^{j+1}_{\nu_k,i}| &\leq C\left(\hat{h}^2_{i+1}|\hat{h}_{i+1}-\hat{h}_i|(1+\varepsilon^{-1/2}) + \hat{h}^4_{i+1}(1+\varepsilon^{-1})\right) \\
&\leq C\left(\varepsilon^{3/2}(1+\varepsilon^{-1/2})M_x^{-4}\exp\left(\frac{2x^*_{i+1}}{(s+1)\sqrt{\varepsilon}}\right) + \varepsilon^2(1+\varepsilon^{-1})M_x^{-4}\exp\left(\frac{4x^*_{i+1}}{(s+1)\sqrt{\varepsilon}}\right)\right) \\
&\leq CM_x^{-4}\exp\left(\frac{4x^*_{i+1}}{(s+1)\sqrt{\varepsilon}}\right) \\
&\leq CM_x^{-4}\exp\left(4\Psi(\eta_{i+1})\right) \\
&\leq CM_x^{-4}.
\end{aligned}$$

When $x^*_i \in [x^*_{\frac{M_x}{4}}, x^*_{\frac{3M_x}{4}+1}]$, it is easy to prove $|\tau^{j+1}_{\nu_k,i}| \leq CM_x^{-4}$. Similar result can be proved for $x^*_i \in [x^*_{\frac{3M_x}{4}+2}, 1]$. Therefore, applying Lemma 4.4.2, we get

$$\max_{i=0,1,\ldots,M_x} |(\nu^{j+1}_k - \mathbb{I}^1_2\nu^{j+1}_k)_i| \leq CM_x^{-4}.$$

Finding the bounds for $w^{j+1}_{l;k}$, use of the fact $\hat{h}_i < \hat{h}_{i+1}$ for $x^*_i \in [0, x^*_{\frac{M_x}{4}-1}]$ gives

$$\begin{aligned}
|\tau^{j+1}_{w_{l;k},i}| &\leq \frac{1}{12}\hat{h}_i\hat{h}_{i+1}|\hat{h}_{i+1}-\hat{h}_i|\|(w^{j+1}_{l;k})'''\|_{I^*_i} + \frac{5}{96}\max\{\hat{h}^4_i, \hat{h}^4_{i+1}\}\|(w^{j+1}_{l;k})^{(4)}\|_{I^*_i\cup I^*_{i+1}} \\
&\leq C\left(\hat{h}^2_{i+1}|\hat{h}_{i+1}-\hat{h}_i|\varepsilon^{-3/2}\left|e^{-x\sqrt{\alpha/\varepsilon}}\right|_{I^*_i} + \hat{h}^4_{i+1}\varepsilon^{-2}\left|e^{-x\sqrt{\alpha/\varepsilon}}\right|_{I^*_i\cup I^*_{i+1}}\right) \\
&\leq CM_x^{-4}\left(\exp\left(\frac{2x^*_{i+1}}{(s+1)\sqrt{\varepsilon}}\right)\left|e^{-x\sqrt{\alpha/\varepsilon}}\right|_{I^*_i} + \exp\left(\frac{4x^*_{i+1}}{(s+1)\sqrt{\varepsilon}}\right)\left|e^{-x\sqrt{\alpha/\varepsilon}}\right|_{I^*_i\cup I^*_{i+1}}\right) \\
&\leq CM_x^{-4}\exp\left(\frac{C_{10}\hat{h}_{i+1}}{\sqrt{\varepsilon}}\right) \\
&\leq CM_x^{-4}\exp\left(C_{10}(s+1)M_x^{-1}\max\Psi'(\eta_{i+1})\right) \\
&\leq CM_x^{-4}.
\end{aligned}$$

Similarly for $w^{j+1}_{r;k}$, we have

$$|\tau^{j+1}_{w_{r;k},i}| \leq \frac{1}{12}\hat{h}_i\hat{h}_{i+1}|\hat{h}_{i+1}-\hat{h}_i|\|(w^{j+1}_{r;k})'''\|_{I^*_i} + \frac{5}{96}\max\{\hat{h}^4_i, \hat{h}^4_{i+1}\}\|(w^{j+1}_{r;k})^{(4)}\|_{I^*_i\cup I^*_{i+1}}$$

$$
\begin{aligned}
&\leq C\left(\hat{h}_{i+1}^2|\hat{h}_{i+1}-\hat{h}_i|\varepsilon^{-3/2}\left|e^{-(1-x)\sqrt{\alpha/\varepsilon}}\right|_{I_i^*}+\hat{h}_{i+1}^4\varepsilon^{-2}\left|e^{-(1-x)\sqrt{\alpha/\varepsilon}}\right|_{I_i^*\cup I_{i+1}^*}\right)\\
&\leq CM_x^{-4}\left(\exp\left(\frac{2x_{i+1}^*}{(s+1)\sqrt{\varepsilon}}\right)\left|e^{-(1-x)\sqrt{\alpha/\varepsilon}}\right|_{I_i^*}+\exp\left(\frac{4x_{i+1}^*}{(s+1)\sqrt{\varepsilon}}\right)\left|e^{-(1-x)\sqrt{\alpha/\varepsilon}}\right|_{I_i^*\cup I_{i+1}^*}\right)\\
&\leq CM_x^{-4}\exp\left(C_{11}(s+1)M_x^{-1}\max\Psi'(\eta_{i+1})\right)\\
&\leq CM_x^{-4}.
\end{aligned}
$$

The similar approach can be followed in the subintervals $[x^*_{\frac{M_x}{4}}, x^*_{\frac{3M_x}{4}+1}]$ and $[x^*_{\frac{3M_x}{4}+2}, 1]$ for both the components. Therefore, applying Lemma 4.4.2, we get

$$
\max_{i=0,1,\ldots,M_x}\left|\left(w_{l;k}^{j+1}-\mathbb{I}_2^1 w_{l;k}^{j+1}\right)_i\right|\leq CM_x^{-4},\quad \text{and}\quad \max_{i=0,1,\ldots,M_x}\left|\left(w_{r;k}^{j+1}-\mathbb{I}_2^1 w_{r;k}^{j+1}\right)_i\right|\leq CM_x^{-4}.
$$

We skip some analysis as it is analogous to the previous one. We combine all the interpolating errors to obtain the bound (4.4.6a). To prove the bound (4.4.6b), we make use of triangle inequality as

$$
\begin{aligned}
\|\widetilde{\boldsymbol{y}}^{j+1}-\mathbb{I}_2^1\widetilde{\boldsymbol{y}}^{j+1}\|&\leq\|\widetilde{\boldsymbol{y}}^{j+1}-\mathbb{I}_2^0\widetilde{\boldsymbol{y}}^{j+1}\|+\|\mathbb{I}_2^0\widetilde{\boldsymbol{y}}^{j+1}-\mathbb{I}_2^1\widetilde{\boldsymbol{y}}^{j+1}\|\\
&\leq\|\widetilde{\boldsymbol{y}}^{j+1}-\mathbb{I}_2^0\widetilde{\boldsymbol{y}}^{j+1}\|+\max_{i=0,1,\ldots,M_x}|(\widetilde{\boldsymbol{y}}^{j+1}-\mathbb{I}_2^1\widetilde{\boldsymbol{y}}^{j+1})_i|.
\end{aligned}
$$

From $\mathbb{S}_2^0$-interpolation, we have $(\mathbb{I}_2^0\widetilde{\boldsymbol{y}}^{j+1})_i=\widetilde{\boldsymbol{y}}_i^{j+1},\ i=0,1,\ldots,M_x$. Using Lemma 4.4.1, Theorem 4.4.1, and Equation (4.4.6a), we get the estimate (4.4.6b). For Equation (4.4.6c), we use

$$
\begin{aligned}
|(\widetilde{y}_k^{j+1}-\mathbb{I}_2^1\widetilde{y}_k^{j+1})''_{i-1/2}|&\leq|(\widetilde{y}_k^{j+1}-\mathbb{I}_2^0\widetilde{y}_k^{j+1})''_{i-1/2}|+|(\mathbb{I}_2^0\widetilde{y}_k^{j+1}-\mathbb{I}_2^1\widetilde{y}_k^{j+1})''_{i-1/2}|\\
&\leq|(\widetilde{y}_k^{j+1}-\mathbb{I}_2^0\widetilde{y}_k^{j+1})''_{i-1/2}|+\max_{i=0,1,\ldots,M_x}\frac{8}{\hat{h}_i^2}|(\widetilde{y}_k^{j+1}-\mathbb{I}_2^1\widetilde{y}_k^{j+1})_i|.
\end{aligned}
$$

Finally, use Theorem 4.4.1 and inequality (4.4.6a) to complete the proof. □

Theorem 4.4.3. *Assume that μ is a positive constant such that*

$$
\max\{\hat{h}_{i+1},\hat{h}_{i-1}\}\geqslant\mu\hat{h}_i,\quad i=1,2,\ldots,M_x-1,\ \hat{h}_1\geqslant\mu\hat{h}_2,\ \textit{and}\ \hat{h}_{M_x}\geqslant\mu\hat{h}_{M_x-1}.
$$

Then the operator $\mathbb{L}_k$ *satisfies the following stability bound in the maximum-norm* i.e.,

$$\|\Theta_k\| \leq \frac{4\delta t}{\alpha\delta t + 1} \max_{i=1,2,\ldots,M_x} \left| \frac{[\mathbb{L}_k \Theta_k]_{i-1/2}}{n^{j+1}_{i-1/2;k}} \right|,$$

for all $\Theta_k \in \mathbb{R}_0^{M_x+2} = \{r \in \mathbb{R}^{M_x+2} : r_0 = r_{M_x+1} = 0\}$, *where*

$$n^{j+1}_{i-1/2;k} := \frac{1}{2} \sum_{l\neq k, l=1}^{m} (a_{lk})^{j+\frac{1}{2}}_{i-1/2} \left[\hat{\mathfrak{q}}^-_i \alpha^{j+1}_{i-1;k} + (1 - \hat{\mathfrak{q}}^-_i - \hat{\mathfrak{q}}^+_i)\alpha^{j+1}_{i;k} + \hat{\mathfrak{q}}^+_i \alpha^{j+1}_{i+1;k} \right],\ k = 1, 2, \ldots, m.$$

Proof. Refer to [94]. □

Theorem 4.4.4. *Let* $\widetilde{\boldsymbol{y}}^{j+1}(x)$ *and* $\mathbf{Y}^{j+1}(x)$ *are the solutions to the problems (4.3.1) and (4.4.1), respectively. Then*

$$\|\widetilde{\boldsymbol{y}}^{j+1} - \mathbf{Y}^{j+1}\| \leq C M_x^{-2},$$
$$\|\widetilde{\boldsymbol{y}}^{j+1}_{i-1/2} - \mathbf{Y}^{j+1}_{i-1/2}\| \leq C M_x^{-2}, \text{ for } i = 1, 2, \ldots, M_x.$$

Proof. To prove the first inequality, we use the triangle inequality

$$\|\widetilde{y}^{j+1}_k - \mathbb{Y}^{j+1}_k\| \leq \|\widetilde{y}^{j+1}_k - I^1_2 \widetilde{y}^{j+1}_k\| + \|\mathbb{I}^1_2 \widetilde{y}^{j+1}_k - \mathbb{Y}^{j+1}_k\|.$$

The interpolant $\mathbb{I}^1_2 \widetilde{y}^{j+1}_k$ of $\widetilde{y}^{j+1}_k$ can be defined as

$$\mathbb{I}^1_2 \widetilde{y}^{j+1}_k(x) = \sum_{l=0}^{M_x+1} \beta^{j+1}_{l;k} \mathbb{B}_l(x).$$

Thus,

$$[\mathbb{L}^{M_x}_k (\boldsymbol{\varsigma}^{j+1}_k - \boldsymbol{\beta}^{j+1}_k)]_{i-1/2} = \mathbb{L}_k (\mathbf{Y}^{j+1} - \mathbb{I}^1_2 \widetilde{\boldsymbol{y}}^{j+1})_{i-1/2},\ i = 1, 2, \ldots, M_x.$$

Since $\boldsymbol{\varsigma}^{j+1}_k - \boldsymbol{\beta}^{j+1}_k \in \mathbb{R}_0^{M_x+2}$, then we use Theorems 4.4.2 and 4.4.3 for

$$\|\mathbb{I}^1_2 \widetilde{y}^{j+1}_k - \mathbb{Y}^{j+1}_k\| \leq \|\boldsymbol{\varsigma}^{j+1}_k - \boldsymbol{\beta}^{j+1}_k\| \leq C M_x^{-2}.$$

The process of obtaining the second estimate is analogous to the first part. □

Corollary 4.4.1. *Assuming that* $M_x^{-p} \leq C\delta t,\ 0 < p < 1$, *then*

$$|\widetilde{y}_k^{j+1} - \mathbb{Y}_k^{j+1}| \leq C\delta t M_x^{-2+p},\ i = 1, 2, \ldots, M_x. \tag{4.4.9}$$

The bound given in the Equation (4.4.9) is needed for establishing the parameter-uniform convergence of the fully discretized scheme.

Theorem 4.4.5. *For* $M_x^{-p} \leq C\delta t,\ 0 < p < 1$, *we have*

$$\|\boldsymbol{y}(\chi_i^*, t_j) - \boldsymbol{\mathscr{I}}_{i-1/2}^j\| \leq C((\delta t)^2 + M_x^{-2+p}).$$

Proof. Let $\xi_{i;k}^j = y_k(\chi_i^*, t_j) - \mathscr{I}_{i-1/2;k}^j$ denotes the error in the k-th component at the j-th time step. Splitting $\xi_{i;k}^j$ using the triangle inequality

$$\|\xi_{i;k}^j\| \leq \|y_k(\chi_i^*, t_j) - \widetilde{y}_{i-1/2;k}^j\| + \|\widetilde{y}_{i-1/2;k}^j - \mathbb{Y}_{i-1/2;k}^j\| + \|\mathbb{Y}_{i-1/2;k}^j - \mathscr{I}_{i-1/2;k}^j\|.$$

Since the time derivatives of the solution are bounded, use of Corollary 4.4.1 gives

$$\|\xi_{i;k}^j\| \leq C\delta t((\delta t)^2 + M_x^{-2+p}) + \|\mathbb{Y}_{i-1/2;k}^j - \mathscr{I}_{i-1/2;k}^j\|.$$

Stability estimate of Theorem 4.4.3 provide the following result

$$\|\mathbb{Y}_{i-1/2;k}^j - \mathscr{I}_{i-1/2;k}^j\| \leq \|y_k(\chi_i^*, t_{j-1}) - \mathscr{I}_{i-1/2;k}^{j-1}\|,$$

and this recurrence occurs as we move to other time levels and finally, we have our required estimate

$$\|\xi_{i;k}^j\| \leq C\delta t((\delta t)^2 + M_x^{-2+p}) + \|\xi_{i;k}^{j-1}\|.$$

A repeated use of this inequality leads to the final result

$$\|\boldsymbol{y}(\chi_i^*, t_j) - \boldsymbol{\mathscr{I}}_{i-1/2}^j\| \leq C((\delta t)^2 + M_x^{-2+p}).$$

□

4.5 Computational experiments

This section delivers some numerical results, which verify our theoretical determinations. We consider the numerical investigations on three test problems to show the applicability and efficiency of the present method.

Remark 4.5.1. *Figures 4.1(f), 4.2(f), and 4.3(f) are drawn using* $M_x = M_t = 128$ *while other figures are drawn using* $M_x = M_t = 64$.

Example 4.5.1. *First, we consider the following one-dimensional reaction-diffusion parabolic problem:*

$$\frac{\partial y}{\partial t} - \varepsilon \frac{\partial^2 y}{\partial x^2} + (6 + x^2)y = t^3(1 + x),\ (x, t) \in (0, 1) \times (0, 1],$$

subject to

$$y(0, t) = 0,\ y(1, t) = 0,\ t \in [0, 1], \quad y(x, 0) = 0,\ x \in [0, 1].$$

Example 4.5.2. *Next, we consider the following weakly-coupled reaction-diffusion parabolic system of two equations:*

$$\frac{\partial \boldsymbol{y}}{\partial t} - \boldsymbol{\mathcal{E}} \frac{\partial^2 \boldsymbol{y}}{\partial x^2} + \boldsymbol{A}\boldsymbol{y} = \boldsymbol{f}(x, t),\ (x, t) \in (0, 1) \times (0, 1],$$

subject to

$$\boldsymbol{y}(0, t) = \boldsymbol{0},\ \boldsymbol{y}(1, t) = \boldsymbol{0},\ t \in [0, 1], \quad \boldsymbol{y}(x, 0) = \boldsymbol{0},\ x \in [0, 1],$$

where

$$\boldsymbol{A} = \begin{bmatrix} 2(1 + x^2) & -(1 + x^3) \\ -2\cos(\frac{\pi x}{4}) & 4\exp(1 - x) \end{bmatrix}, \quad \boldsymbol{f} = \begin{bmatrix} 2\exp(x)t(1 - t) \\ (10x + 1)t(1 - t) \end{bmatrix}.$$

Example 4.5.3. *In the end, we consider the following weakly-coupled reaction-diffusion parabolic system of three equations:*

$$\frac{\partial \boldsymbol{y}}{\partial t} - \boldsymbol{\mathcal{E}} \frac{\partial^2 \boldsymbol{y}}{\partial x^2} + \boldsymbol{A}\boldsymbol{y} = \boldsymbol{f}(x, t),\ (x, t) \in (0, 1) \times (0, 1],$$

subject to

$$\boldsymbol{y}(0,t)=\boldsymbol{0},\ \boldsymbol{y}(1,t)=\boldsymbol{0},\ t\in[0,1],\quad \boldsymbol{y}(x,0)=\boldsymbol{0},\ x\in[0,1],$$

where

$$\boldsymbol{A}=\begin{bmatrix} 2 & -(1-x) & -(1+x) \\ -x & 1+x & -x \\ -(2+x) & -(1-x) & 3+x \end{bmatrix},\quad \boldsymbol{f}=\begin{bmatrix} 16x^2(1-x)^2 \\ t^2 \\ -16x^2(1-x)^2 \end{bmatrix}.$$

The exact solutions are not available for the considered problems, so we employ the double mesh principle [112] to obtain the maximum pointwise error and associated convergence orders. We give the maximum pointwise errors by the following formula

$$e_{k,\varepsilon}^{M_x,M_t}=\max_j\left(\max_i|\tilde{y}_k(x_{2i-1}^*,t_{2j-1})-\tilde{y}_k(\chi_i^*,t_j)|\right),\quad k=1,2,\ldots,m,$$

where $\tilde{y}_k(\chi_i^*,t_j)$ and $\tilde{y}_k(x_{2i-1}^*,t_{2j-1})$ are the computed solutions of the k-th component using (M_x,M_t) and $(2M_x,2M_t)$ points, respectively. The associated orders of convergence are given as

$$\rho_{k,\varepsilon}^{M_x,M_t}=\log_2\left(e_{k,\varepsilon}^{M_x,M_t}/e_{k,\varepsilon}^{2M_x,2M_t}\right).$$

In continuation, we also calculate the parameter-uniform errors $e_k^{M_x,M_t}$ and the associated parameter-uniform orders of convergence $\rho_k^{M_x,M_t}$ as follows

$$e_k^{M_x,M_t}=\max_\varepsilon e_{k,\varepsilon}^{M_x,M_t},\quad \rho_k^{M_x,M_t}=\log_2\left(e_k^{M_x,M_t}/e_k^{2M_x,2M_t}\right),\quad k=1,2,\ldots,m.$$

We further calculate the overall uniform errors $\boldsymbol{e}^{M_x,M_t}$ and the associated orders of convergence $\boldsymbol{\rho}^{M_x,M_t}$ using the following formulas:

$$\boldsymbol{e}^{M_x,M_t}=\max_k(e_k^{M_x,M_t}),\quad \boldsymbol{\rho}^{M_x,M_t}=\log_2\left(\boldsymbol{e}^{M_x,M_t}/\boldsymbol{e}^{2M_x,2M_t}\right).$$

We find all these estimates over a finite range of ε values ($\varepsilon=2^{-6},2^{-10},\ldots,2^{-26}$).

Remark 4.5.2. *For Example 4.5.1, estimates are given by*

$$e_{\varepsilon}^{M_x,M_t} = \max_{j}\left(\max_{i}|\tilde{y}(x^{*}_{2i-1},t_{2j-1}) - \tilde{y}(\chi^{*}_{i},t_{j})|\right), \quad \rho_{\varepsilon}^{M_x,M_t} = \log_2\left(e_{\varepsilon}^{M_x,M_t}/e_{\varepsilon}^{2M_x,2M_t}\right),$$
$$e^{M_x,M_t} = \max_{\varepsilon} e_{\varepsilon}^{M_x,M_t}, \quad \rho^{M_x,M_t} = \log_2\left(e^{M_x,M_t}/e^{2M_x,2M_t}\right).$$

We have considered the scalar problem in Example 4.5.1 since there is no literature concerned with developing the numerical technique for singularly perturbed reaction-diffusion IBVP taken in Example 4.5.1 using quadratic $\mathbb{B}$-splines. In Table 4.1 we have presented the results of $e_{\varepsilon}^{M_x,M_t}$, $\rho_{\varepsilon}^{M_x,M_t}$, e^{M_x,M_t}, and ρ^{M_x,M_t} for Example 4.5.1. The results are parameter uniform and in line with theoretical estimates. Two surface plots of the numerical solution are displayed in subfigures 4.1(a) and 4.1(b) for different values of ε. It is evident from these plots that the solution exhibits boundary layers at both ends. Figures 4.1(c) and 4.1(d) portray the numerical solution at different time steps for $\varepsilon = 2^{-6}$ and $\varepsilon = 2^{-15}$, respectively. These subfigures show that reducing the ε values impacts the boundary layer width (it reduces when ε decreases). At the end of Figure 4.1, we have added error plots of numerical solution keeping ε fixed and changing the mesh points. We observed that errors in the boundary layer region dominate the errors in the regular region (can be seen through high tips).

Now we discuss the results of our problems in Examples 4.5.2 and 4.5.3. We have taken $m = 2$, $m = 3$, and variable coefficients in these examples, respectively. We display the results of $e_{k,\varepsilon}^{M_x,M_t}$, $\rho_{k,\varepsilon}^{M_x,M_t}$, $e_{k}^{M_x,M_t}$, $\rho_{k}^{M_x,M_t}$, and $C_{k}^{M_x,M_t}$ for $k = 1, 2$ in Tables 4.2 and 4.3 for the first and second solution component of Example 4.5.2, respectively. In both tables, the results are parameter uniform (in each column, errors are very close, independent of ε) and can be confirmed by the values of $C_{k}^{M_x,M_t}$ (see [113]). Figures 4.2 and 4.3 include surface plots of the numerical solution, 2D plots of the numerical solution at different time levels, and error plots of the first and second solution components of Example 4.5.2, respectively. Boundary layers at $x = 0$ and $x = 1$ can be easily observed in both solution components. High spikes are observed in the error plots at both endpoints. Keeping ε fixed and double the mesh points, in Figures 4.2(e) and 4.2(f), we observe that the height of spikes reduces *i.e.,* error decreases as we increase the number of points. We observed similar types of results for Example 4.5.3. In Table 4.7, we compare the results of $\boldsymbol{e}^{M_x,M_t}$, $\boldsymbol{\rho}^{M_x,M_t}$ and $\boldsymbol{C}^{M_x,M_t}$ by

Table 4.1: $e_{\varepsilon}^{M_x,M_t}$, $\rho_{\varepsilon}^{M_x,M_t}$, e^{M_x,M_t}, and ρ^{M_x,M_t} for Example 4.5.1

	Mesh points with $M_x = M_t$				
ε	16	32	64	128	256
2^{-6}	$1.3746e-03$	$5.2503e-04$	$1.3610e-04$	$3.3672e-05$	$8.2783e-06$
	1.3885	1.9477	2.0150	2.0241	
2^{-10}	$1.4474e-03$	$5.9209e-04$	$1.5636e-04$	$3.8496e-05$	$9.4898e-06$
	1.2896	1.9209	2.0221	2.0203	
2^{-14}	$1.4561e-03$	$5.9107e-04$	$1.5605e-04$	$3.8496e-05$	$9.4704e-06$
	1.3007	1.9213	2.0192	2.0232	
2^{-18}	$1.4626e-03$	$5.9084e-04$	$1.5598e-04$	$3.8399e-05$	$9.4651e-06$
	1.3077	1.9214	2.0222	2.0204	
2^{-22}	$1.4648e-03$	$5.9078e-04$	$1.5596e-04$	$3.8396e-05$	$9.4645e-06$
	1.3100	1.9214	2.0221	2.0204	
2^{-26}	$1.4654e-03$	$5.9077e-04$	$1.5596e-04$	$3.8395e-05$	$9.4645e-06$
	1.3106	1.9214	2.0221	2.0204	
e^{M_x,M_t}	$1.4654e-03$	$5.9209e-04$	$1.5636e-04$	$3.8496e-05$	$9.4898e-06$
ρ^{M_x,M_t}	1.3074	1.9209	2.0221	2.0203	

considering three different meshes, namely Shishkin [94], eXp [91], and Bakhvalov-Shishkin (B-S) [91] meshes.

Remark 4.5.3. *The restriction $M_x^{-p} \leq C\delta t,\ 0 < p < 1$ is imposed only to obtain parameter-uniform estimates; computational experiments are free from this restriction.*

4.6 Conclusion

A robust spline-based numerical technique is presented for the singularly perturbed system of $m \geq 2$ equations with the same diffusion parameter. It has been established theoretically that the suggested approach converges uniformly with second-order accuracy in space, along with second-order accuracy in time, using the Crank-Nicolson method. The execution of the proposed scheme demonstrates that theoretical bounds and tabular results are highly credible.

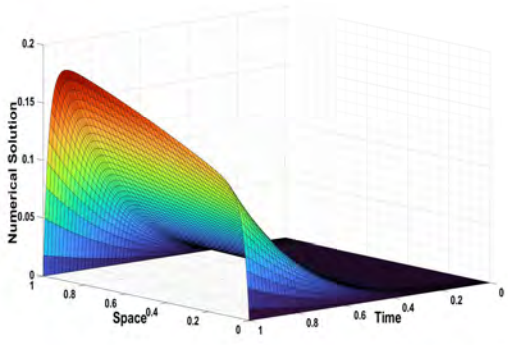

(a) $\varepsilon = 2^{-7}$

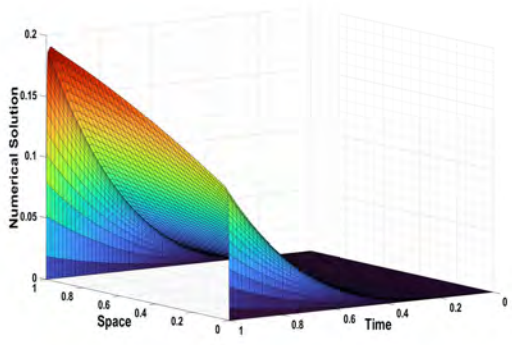

(b) $\varepsilon = 2^{-14}$

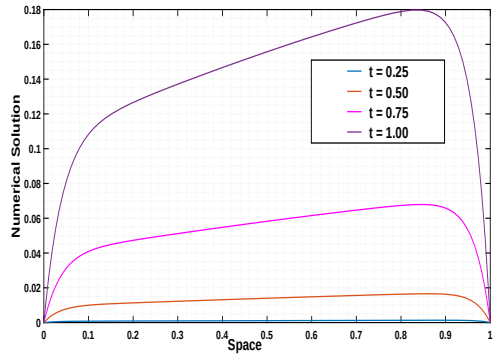

(c) $\varepsilon = 2^{-6}$

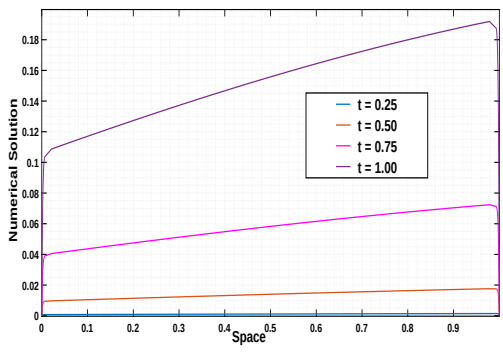

(d) $\varepsilon = 2^{-15}$

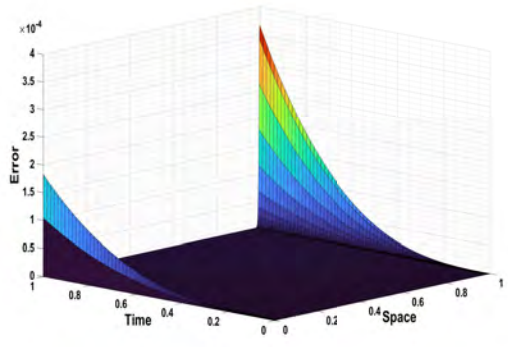

(e) $\varepsilon = 2^{-15}$ and $M_x = M_t = 64$

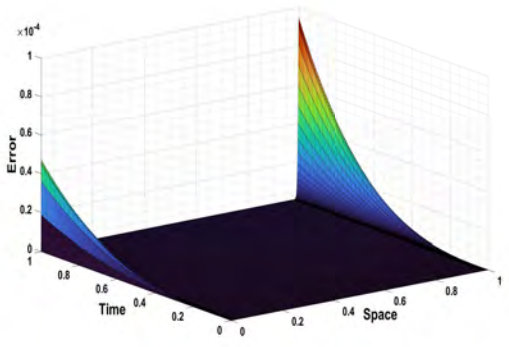

(f) $\varepsilon = 2^{-15}$ and $M_x = M_t = 128$

Figure 4.1: Surface plots of the numerical solution ((a) and (b)), numerical solution at different time levels ((c) and (d)), and the error plots ((e) and (f)) for Example 4.5.1

Table 4.2: $e_{1,\varepsilon}^{M_x,M_t}$, $\rho_{1,\varepsilon}^{M_x,M_t}$, $e_1^{M_x,M_t}$, $\rho_1^{M_x,M_t}$, and $C_1^{M_x,M_t}$ for Example 4.5.2

	Mesh points with $M_x = 2M_t$				
ε	$M_t = 8$	$M_t = 16$	$M_t = 32$	$M_t = 64$	$M_t = 128$
2^{-6}	$3.4056e-03$	$8.5514e-04$	$2.1489e-04$	$5.3729e-05$	$1.3431e-05$
	1.9937	1.9926	1.9998	2.0001	
2^{-10}	$4.5568e-03$	$1.1618e-03$	$2.9003e-04$	$7.2541e-05$	$1.8137e-05$
	1.9717	2.0021	1.9993	1.9999	
2^{-14}	$4.8957e-03$	$1.2712e-03$	$3.1931e-04$	$7.9894e-05$	$1.9958e-05$
	1.9453	1.9932	1.9988	2.0011	
2^{-18}	$4.9857e-03$	$1.2998e-03$	$3.2747e-04$	$8.2054e-05$	$2.0484e-05$
	1.9395	1.9889	1.9967	2.0021	
2^{-22}	$5.0085e-03$	$1.3070e-03$	$3.2941e-04$	$8.2529e-05$	$2.0476e-05$
	1.9381	1.9883	1.9969	2.0110	
2^{-26}	$5.0090e-03$	$1.3072e-03$	$3.2942e-04$	$8.2532e-05$	$2.0476e-05$
	1.9381	1.9883	1.9969	2.0110	
$e_1^{M_x,M_t}$	$5.0090e-03$	$1.3072e-03$	$3.2942e-04$	$8.2532e-05$	$2.0476e-05$
$\rho_1^{M_x,M_t}$	1.9381	1.9883	1.9969	2.0110	
$C_1^{M_x,M_t}$	0.4408	0.4306	0.4304	0.4293	0.4290

Table 4.3: $e_{2,\varepsilon}^{M_x,M_t}$, $\rho_{2,\varepsilon}^{M_x,M_t}$, $e_2^{M_x,M_t}$, $\rho_2^{M_x,M_t}$, and $C_2^{M_x,M_t}$ for Example 4.5.2

	Mesh points with $M_x = 2M_t$				
ε	$M_t = 8$	$M_t = 16$	$M_t = 32$	$M_t = 64$	$M_t = 128$
2^{-6}	$5.7545e-03$	$1.1152e-03$	$2.9459e-04$	$7.1619e-05$	$1.7886e-05$
	2.3674	1.9205	2.0403	2.0015	
2^{-10}	$6.1205e-03$	$1.3985e-03$	$3.5029e-04$	$8.7592e-05$	$2.1872e-05$
	2.1298	1.9973	1.9997	2.1337	
2^{-14}	$6.1539e-03$	$1.5220e-03$	$3.7936e-04$	$9.4775e-05$	$2.3669e-05$
	2.0155	2.0043	2.0010	2.0015	
2^{-18}	$6.1621e-03$	$1.5569e-03$	$3.8822e-04$	$9.7017e-05$	$2.4078e-05$
	1.9847	2.0037	2.0006	2.0105	
2^{-22}	$6.1829e-03$	$1.5664e-03$	$3.9088e-04$	$9.7640e-05$	$2.4230e-05$
	1.9808	2.0027	2.0012	2.0107	
2^{-26}	$6.1832e-03$	$1.5655e-03$	$3.9098e-04$	$9.7640e-05$	$2.4230e-05$
	2.0337	2.0007	2.0036	2.0107	
$e_2^{M_x,M_t}$	$1.3632e-03$	$3.3352e-04$	$8.3044e-05$	$2.0721e-05$	$5.1788e-06$
$\rho_2^{M_x,M_t}$	2.0312	2.0058	2.0028	2.0004	
$C_2^{M_x,M_t}$	0.4408	0.4306	0.4304	0.4293	0.4290

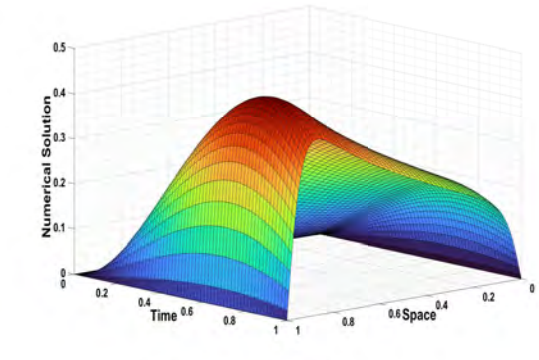

(a) $\varepsilon = 2^{-8}$

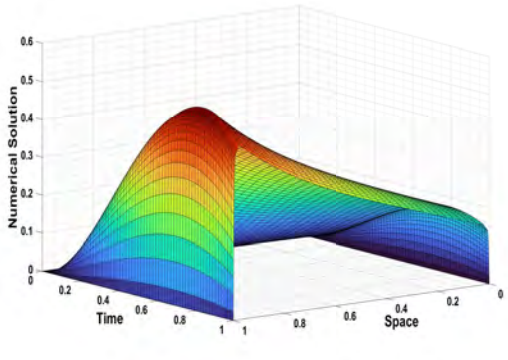

(b) $\varepsilon = 2^{-16}$

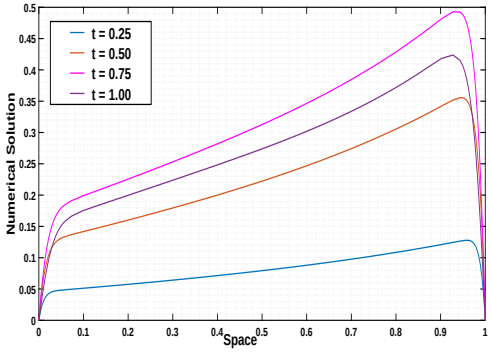

(c) $\varepsilon = 2^{-10}$

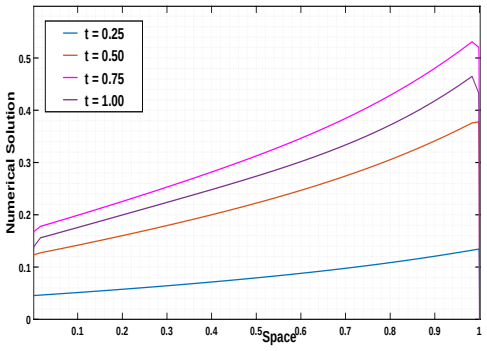

(d) $\varepsilon = 2^{-20}$

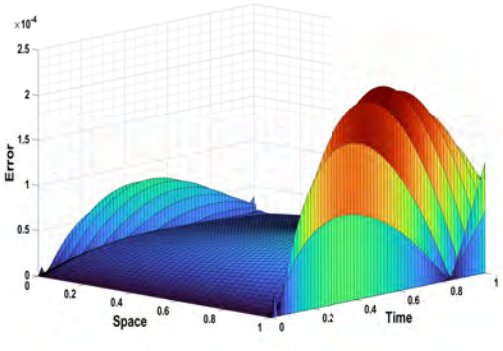

(e) $\varepsilon = 2^{-15}$ and $M_x = M_t = 64$

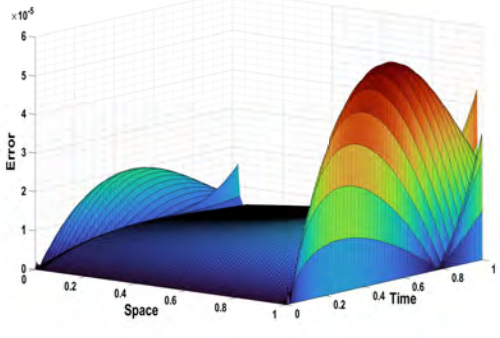

(f) $\varepsilon = 2^{-15}$ and $M_x = M_t = 128$

Figure 4.2: Surface plots of the numerical solution ((a) and (b)), numerical solution at different time levels ((c) and (d)), and the error plots ((e) and (f)) of the first solution component for Example 4.5.2

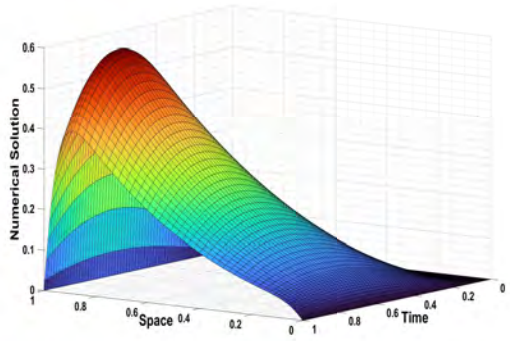

(a) $\varepsilon = 2^{-8}$

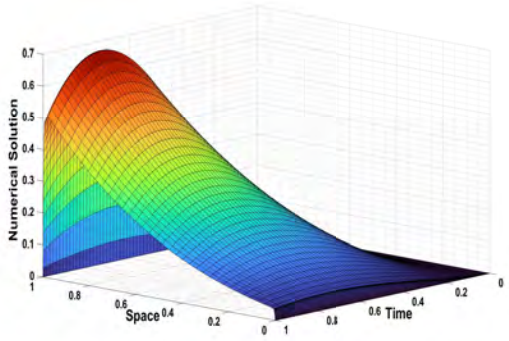

(b) $\varepsilon = 2^{-16}$

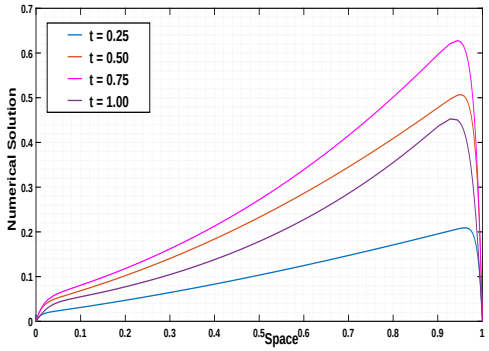

(c) $\varepsilon = 2^{-10}$

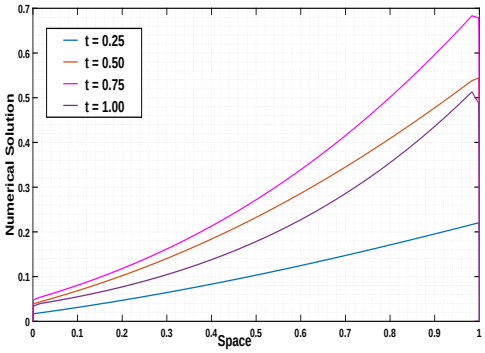

(d) $\varepsilon = 2^{-20}$

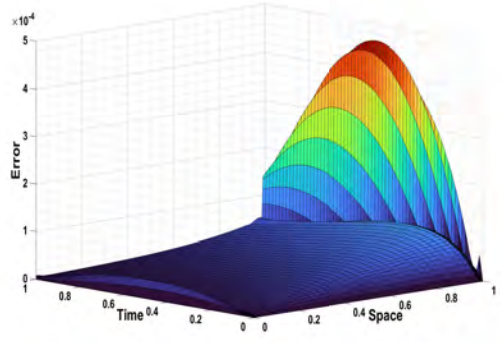

(e) $\varepsilon = 2^{-15}$ and $M_x = M_t = 64$

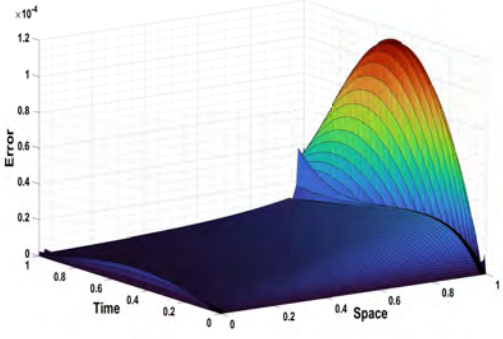

(f) $\varepsilon = 2^{-15}$ and $M_x = M_t = 128$

Figure 4.3: Surface plots of the numerical solution ((a) and (b)), numerical solution at different time levels ((c) and (d)), and error plots ((e) and (f)) of the second solution component for Example 4.5.2

Table 4.4: $e_{1,\varepsilon}^{M_x,M_t}$, $\rho_{1,\varepsilon}^{M_x,M_t}$, $e_1^{M_x,M_t}$, $\rho_1^{M_x,M_t}$, and $C_1^{M_x,M_t}$ for Example 4.5.3

	Mesh points with $M_x = 2M_t$				
ε	$M_t = 8$	$M_t = 16$	$M_t = 32$	$M_t = 64$	$M_t = 128$
2^{-6}	$1.3632e-03$	$3.3352e-04$	$8.3044e-05$	$2.0721e-05$	$5.1788e-06$
	2.0312	2.0058	2.0028	2.0004	
2^{-10}	$1.2981e-03$	$3.1621e-04$	$7.8991e-05$	$1.9703e-05$	$4.4898e-06$
	2.0374	2.0011	2.0033	2.1337	
2^{-14}	$1.2937e-03$	$3.1558e-04$	$7.8824e-05$	$1.9659e-05$	$4.4704e-06$
	2.0354	2.0013	2.0034	2.1367	
2^{-18}	$1.2919e-03$	$3.1544e-04$	$7.8815e-05$	$1.9654e-05$	$4.4451e-06$
	2.0341	2.0008	2.0036	2.1445	
2^{-22}	$1.2915e-03$	$3.1541e-04$	$7.8815e-05$	$1.9654e-05$	$4.4445e-06$
	2.0337	2.0007	2.0036	2.1447	
2^{-26}	$1.2915e-03$	$3.1541e-04$	$7.8815e-05$	$1.9654e-05$	$4.4445e-06$
	2.0337	2.0007	2.0036	2.1447	
$e_1^{M_x,M_t}$	$1.3632e-03$	$3.3352e-04$	$8.3044e-05$	$2.0721e-05$	$5.1788e-06$
$\rho_1^{M_x,M_t}$	2.0312	2.0058	2.0028	2.0004	
$C_1^{M_x,M_t}$	0.4408	0.4306	0.4304	0.4293	0.4290

Table 4.5: $e_{2,\varepsilon}^{M_x,M_t}$, $\rho_{2,\varepsilon}^{M_x,M_t}$, $e_2^{M_x,M_t}$, $\rho_2^{M_x,M_t}$, and $C_2^{M_x,M_t}$ for Example 4.5.3

	Mesh points with $M_x = 2M_t$				
ε	$M_t = 8$	$M_t = 16$	$M_t = 32$	$M_t = 64$	$M_t = 128$
2^{-6}	$1.1148e-03$	$2.8781e-04$	$7.1200e-05$	$1.7627e-05$	$4.3787e-06$
	1.9536	2.0152	2.0141	2.0091	
2^{-10}	$1.2537e-03$	$3.1912e-04$	$7.9966e-05$	$1.9862e-05$	$4.4898e-06$
	1.9740	1.9966	2.0094	2.1453	
2^{-14}	$1.2617e-03$	$3.2006e-04$	$8.0186e-05$	$2.0067e-05$	$4.4920e-06$
	1.9790	1.9969	1.9985	2.1594	
2^{-18}	$1.2647e-03$	$3.2010e-04$	$8.0258e-05$	$2.0062e-05$	$4.4998e-06$
	1.9822	1.9958	2.0002	2.1565	
2^{-22}	$1.2647e-03$	$3.2010e-04$	$8.0260e-05$	$2.0068e-05$	$4.5001e-06$
	1.9822	1.9958	1.9998	2.1569	
2^{-26}	$1.2647e-03$	$3.2010e-04$	$8.0260e-05$	$2.0068e-05$	$4.5001e-06$
	1.9822	1.9958	1.9998	2.1569	
$e_2^{M_x,M_t}$	$1.2647e-03$	$3.2010e-04$	$8.0260e-05$	$2.0068e-05$	$4.5001e-06$
$\rho_2^{M_x,M_t}$	1.9822	1.9958	1.9998	2.1569	
$C_2^{M_x,M_t}$	0.7145	0.8919	0.9140	0.9101	0.9100

Table 4.6: $e_{3,\varepsilon}^{M_x,M_t}$, $\rho_{3,\varepsilon}^{M_x,M_t}$, $e_3^{M_x,M_t}$, $\rho_3^{M_x,M_t}$, and $C_3^{M_x,M_t}$ for Example 4.5.3

	Mesh points with $M_x = 2M_t$				
ε	$M_t = 8$	$M_t = 16$	$M_t = 32$	$M_t = 64$	$M_t = 128$
2^{-6}	$2.2753e-03$	$5.7419e-04$	$1.4203e-04$	$3.5413e-05$	$8.8434e-06$
	1.9865	2.0153	2.0038	2.0016	
2^{-10}	$2.2017e-03$	$5.4998e-04$	$1.3598e-04$	$3.3965e-05$	$8.4798e-06$
	2.0012	2.0160	2.0013	2.0019	
2^{-14}	$2.1949e-03$	$5.4846e-04$	$1.3564e-04$	$3.3888e-05$	$8.4704e-06$
	2.0007	2.0156	2.0009	2.0003	
2^{-18}	$2.1923e-03$	$5.4832e-04$	$1.3564e-04$	$3.3883e-05$	$8.4621e-06$
	1.994	2.0152	2.0011	2.0015	
2^{-22}	$2.1917e-03$	$5.4830e-04$	$1.3564e-04$	$3.3883e-05$	$8.4625e-06$
	1.990	2.0152	2.0011	2.0014	
2^{-26}	$2.1917e-03$	$5.4830e-04$	$1.3564e-04$	$3.3883e-05$	$8.4625e-06$
	1.990	2.0152	2.0011	2.0014	
$e_3^{M_x,M_t}$	$2.2753e-03$	$5.7419e-04$	$1.4203e-04$	$3.5413e-05$	$8.8434e-06$
$\rho_3^{M_x,M_t}$	1.9865	2.0153	2.0038	2.0016	
$C_3^{M_x,M_t}$	0.7480	0.7486	0.7408	0.7402	0.7401

Table 4.7: Uniform maximum pointwise errors comparison in the solution for Example 4.5.3 on different meshes

	Mesh points with $M_x = 2M_t$					
Mesh		$M_t = 8$	$M_t = 16$	$M_t = 32$	$M_t = 64$	$M_t = 128$
eXp	$\boldsymbol{e}^{M_x,M_t}$	$2.27e-03$	$5.74e-04$	$1.42e-04$	$3.54e-05$	$8.84e-06$
	$\boldsymbol{\rho}^{M_x,M_t}$	1.98	2.01	2.00	2.00	-
	$\boldsymbol{C}^{M_x,M_t}$	0.74	0.74	0.74	0.74	0.74
Shishkin	$\boldsymbol{e}^{M_x,M_t}$	$2.52e-03$	$1.15e-03$	$4.25e-04$	$1.45e-04$	$4.48e-05$
	$\boldsymbol{\rho}^{M_x,M_t}$	1.13	1.43	1.55	1.69	-
	$\boldsymbol{C}^{M_x,M_t}$	0.10	0.10	0.08	0.09	0.09
B-S	$\boldsymbol{e}^{M_x,M_t}$	$2.25e-03$	$5.70e-04$	$1.39e-04$	$3.52e-05$	$8.81e-06$
	$\boldsymbol{\rho}^{M_x,M_t}$	1.98	2.01	2.00	2.00	-
	$\boldsymbol{C}^{M_x,M_t}$	0.72	0.72	0.72	0.72	0.72

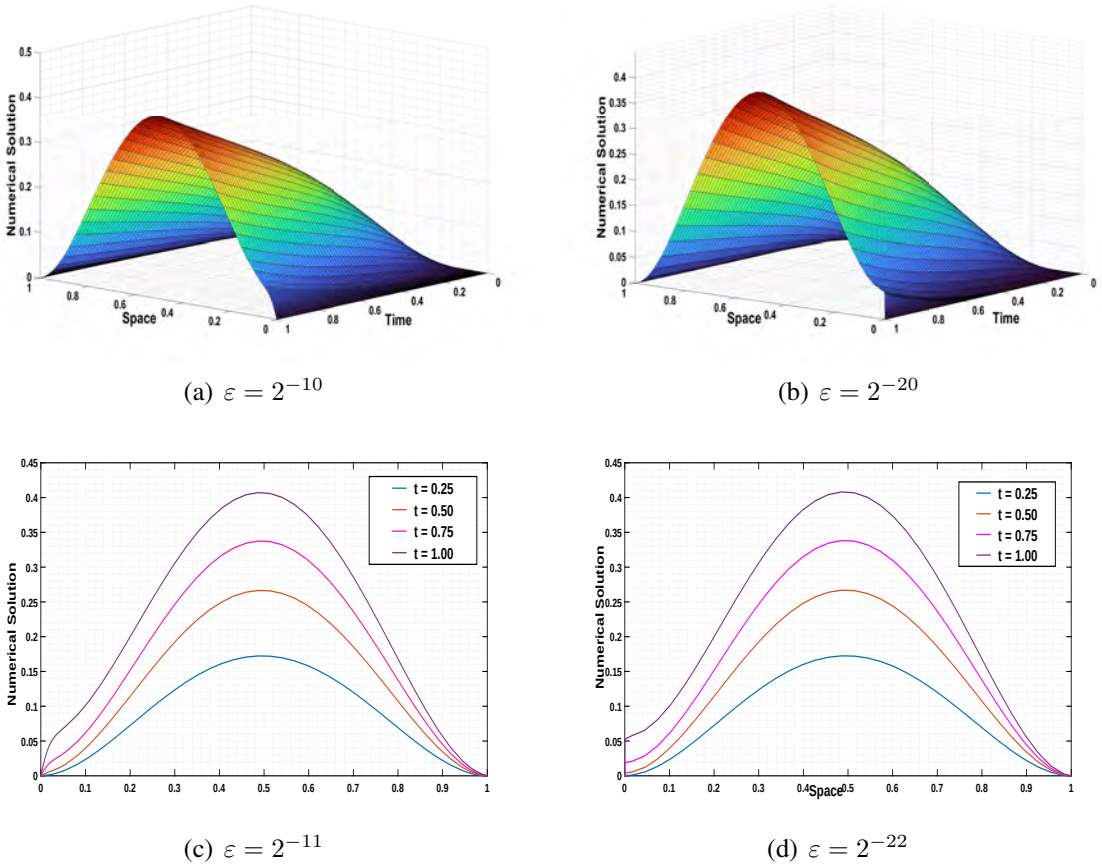

(a) $\varepsilon = 2^{-10}$ (b) $\varepsilon = 2^{-20}$

(c) $\varepsilon = 2^{-11}$ (d) $\varepsilon = 2^{-22}$

Figure 4.4: Surface plots of the numerical solution ((a) and (b)) and numerical solution at different time levels ((c) and (d)) of the first solution component for Example 4.5.3

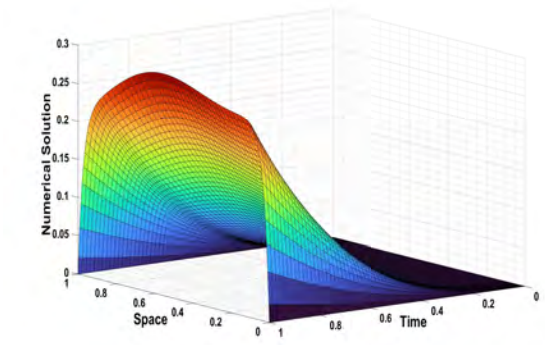

(a) $\varepsilon = 2^{-8}$

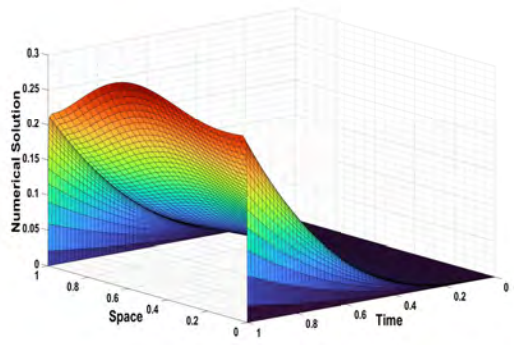

(b) $\varepsilon = 2^{-16}$

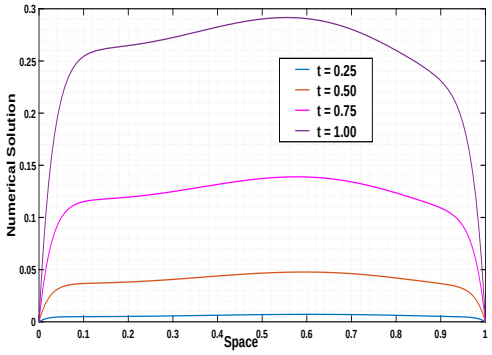

(c) $\varepsilon = 2^{-8}$

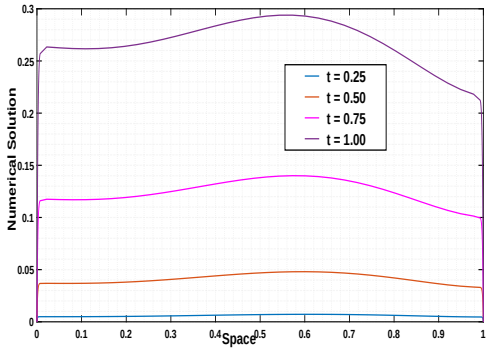

(d) $\varepsilon = 2^{-16}$

Figure 4.5: Surface plots of the numerical solution ((a) and (b)) and numerical solution at different time levels ((c) and (d)) of the second solution component for Example 4.5.3

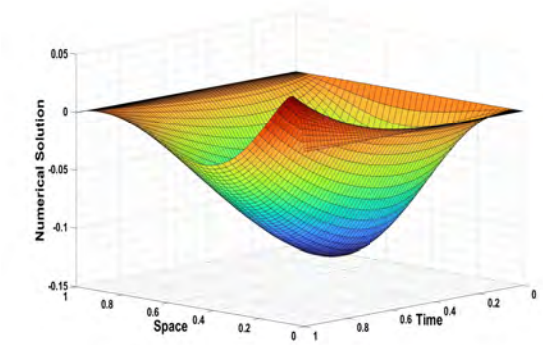

(a) $\varepsilon = 2^{-10}$

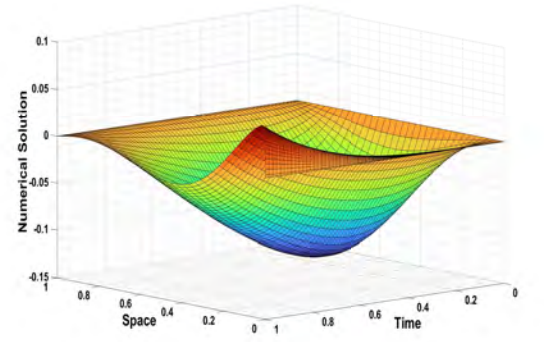

(b) $\varepsilon = 2^{-20}$

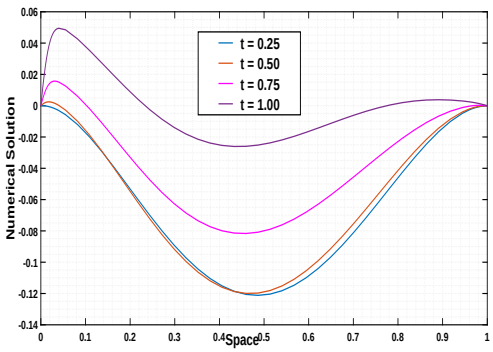

(c) $\varepsilon = 2^{-11}$

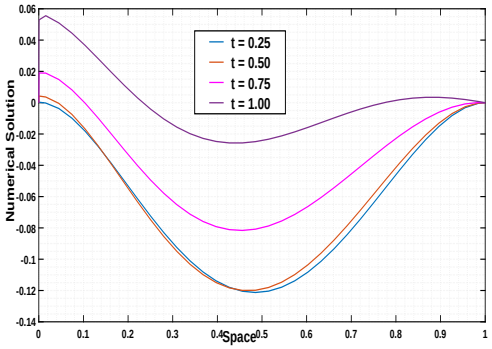

(d) $\varepsilon = 2^{-22}$

Figure 4.6: Surface plots of the numerical solution ((a) and (b)) and numerical solution at different time levels ((c) and (d)) of the third solution component for Example 4.5.3

Chapter 5

Spline-based parameter-uniform scheme for fourth-order singularly perturbed differential equations

---

Fourth-order singularly perturbed differential equations of reaction-diffusion type stand out from the maze of mathematical equations as intriguing enigmas that pique the interest of scientists and mathematicians. These equations blend the beauty of higher-order derivatives with the complexness of chemical reactions and diffusive processes. Higher-order derivatives build a tapestry of intricate dynamics, which encourages us to grasp subtle behaviors and spatial nuances that are not accessible to models with lower-order derivatives. Boundary layers are of great interest, as they exhibit dynamic behavior and give rise to novel occurrences, presenting a visually and mathematically exciting display.

The work of this chapter has been published in the following publication:

S. Singh, D. Kumar, "Spline-based parameter-uniform scheme for fourth-order singularly perturbed differential equations." J. Math. Chem., 60 (2022), 1872–1902.

5.1 Problem statement

Higher-order SPPs are divided into two classes, and this classification is based on reducing the order of the original differential equation if one puts $\mu = 0$ [35]. Here, μ is referred to as the perturbation parameter, appearing in the multiplication of the highest-order derivative of the differential equation. If the order of the differential equation is reduced by one, then SPPs are of convection-diffusion type, whereas if it is reduced by two, then SPPs are of reaction-diffusion type. Motivated by the work in [35], in this chapter, we have taken the stability problems related to fluid dynamics when a specified load is attached to an elastic beam (with a small flexural rigidity) that shows a deflection due to the tension force of the load. The modeling of these problems leads to the Orr-Sommerfield equation [4, 5]

$$\mathcal{E}\mathcal{I}z^{(4)}(t) - \left(\mathcal{N}_0\frac{\mathcal{E}\mathcal{A}}{2L}\int_0^L (z'(t))^2 dt\right)z'' = f(t),\ 0 \le t \le L,$$

where A, $L \rightarrow$ cross-sectional area and length of the beam, $E \rightarrow$ Young's modulus, $I \rightarrow$ moment of inertia, $N_0 \rightarrow$ initial axial tension in the beam. After rescaling all the parameters, we get the following singularly perturbed fourth-order differential equation, whose order is reduced by two for the unperturbed problem (when $\mu = 0$):

$$-\mu z^{(4)}(t) + a(t)z''(t) - b(t)z(t) = -f(t), \quad t \in \mathcal{D} = (0,1), \tag{5.1.1a}$$

subject to the following BCs

$$z(0) = q_1,\ z(1) = q_3,\ z''(0) = -q_2,\ z''(1) = -q_4, \tag{5.1.1b}$$

where $0 < \mu \ll 1$ is referred to as the perturbation parameter. We consider a particular type of BCs influenced by [35], which helps us to set up uniform stability estimates and other results. To extend the maximum principle theory, we transform (5.1.1a)-(5.1.1b) into a system of two weakly coupled second-order ODEs with Dirichlet BCs. We assume $a(t)$, $b(t)$, and $f(t)$ to be sufficiently smooth that satisfy the following conditions

$$\zeta^* \geqslant a(t) \geqslant \zeta > 0, \tag{5.1.2a}$$

$$0 \geqslant b(t) \geqslant -\beta,\ \beta > 0, \tag{5.1.2b}$$

$$\zeta - 2\beta \geqslant \eta > 0,\ \text{for some } \eta, \tag{5.1.2c}$$

for $t \in \overline{\mathcal{D}}$. The above assumptions (5.1.2a)-(5.1.2c) guarantee the existence of a unique solution $z(t) \in C^4(\mathcal{D}) \cap C^2(\overline{\mathcal{D}})$ (see [118]). We transform the BVP (5.1.1a)-(5.1.1b) into a simpler form

$$\begin{aligned} \boldsymbol{\mathcal{L}}\boldsymbol{z}(t) &= \boldsymbol{f}(t),\ t \in \mathcal{D}, \\ \boldsymbol{z}(0) &= (q_1, q_2)^T,\ \boldsymbol{z}(1) = (q_3, q_4)^T, \end{aligned}$$

which is equivalent to

$$\mathcal{L}_1\boldsymbol{z}(t) \equiv -z_1''(t) - z_2(t) = 0,\ t \in \mathcal{D}, \tag{5.1.3a}$$

$$\mathcal{L}_2\boldsymbol{z}(t) \equiv -\mu z_2''(t) + a(t)z_2(t) + b(t)z_1(t) = f(t),\ t \in \mathcal{D}, \tag{5.1.3b}$$

$$z_1(0) = q_1,\ z_1(1) = q_3,\ z_2(0) = q_2,\ z_2(1) = q_4, \tag{5.1.3c}$$

where $\boldsymbol{z}(t) = (z_1(t), z_2(t))^T$, $\boldsymbol{\mathcal{L}} = (\mathcal{L}_1, \mathcal{L}_2)^T$, and $\boldsymbol{f}(t) = (0, f(t))^T$. In the rest of the chapter, we consider the system (5.1.3) in place of (5.1.1) in our analysis.

Remark 5.1.1. *The condition (5.1.2a) implies that (5.1.1) is a non-turning point problem and the condition (5.1.2b) assures that the system (5.1.3) is quasi-monotone (see definition 2.3 in [119]). The conditions (5.1.2a) and (5.1.2b) will be used to establish the maximum principle for the system (5.1.3). Furthermore, the stability estimates will be derived using the condition (5.1.2c) and the maximum principle.*

These types of systems have been less examined in the past. To cite a few, Shanthi and Ramanujam [118] devised a first-order convergent numerical method combining classical and exponentially fitted finite difference schemes. Das and Natesan [120] proposed a second-order finite difference method on a non-uniform mesh generated by the equidistribution principle. Recently, Cen *et al.* [121] proposed an almost fourth-order finite difference scheme on Vulanović-Shishkin mesh. They demonstrated parameter-uniform convergence through their

hybrid method.

The chapter's construction is as follows: Section 5.2 explains the solution's continuous properties, such as maximum principle and stability estimates. The decomposition of the solution into regular and singular components (left and right components) is also given. Furthermore, the bounds on their derivatives are also provided in this section. Section 5.3 illustrates the mesh construction and the implementation of the scheme to solve the system (5.1.3). The interpolation error estimates in S_2^0 and S_2^1 interpolations are given in Section 5.4, using the bounds of Section 5.2 and Section 5.3. The parameter-uniform convergence results established in Section 5.4 are verified in Section 5.5 through two test examples. Section 5.6 presents some concluding remarks about our study.

Throughout the chapter, we use the following notations: $C^k(\mathcal{D})$ is the set of all k times continuously differentiable functions in a domain $\mathcal{D}$ whereas $C^k(\mathcal{D})^2$ is the set of all k times continuously differentiable vector-valued functions with two components in $\mathcal{D}$; C denotes a positive generic constant that can take different values at different places whereas the subscripted C (such as C_j for some j) is a fixed constant. The constant vector $\boldsymbol{C}$ is given as $\boldsymbol{C} = C(1,1)^T$ and the vector $\boldsymbol{z}$ is given as $\boldsymbol{z} = (z_1, z_2)^T$.

5.2 Analytical results

In this section, first, we establish a maximum principle for the system (5.1.3). Then, a stability estimate is derived for the solution to the system (5.1.3) using the maximum principle. Some theoretical bounds for the solution and its derivatives are also given in this section.

Lemma 5.2.1 (Maximum principle)**.** *For the system (5.1.3) assume that* $\mathcal{L}_1\boldsymbol{z}(t) \geqslant 0$, $\mathcal{L}_2\boldsymbol{z}(t) \geqslant 0$ *in* $\mathcal{D}$, $z_1(0) \geqslant 0$, $z_1(1) \geqslant 0$, $z_2(0) \geqslant 0$, *and* $z_2(1) \geqslant 0$. *Then* $\boldsymbol{z}(t) \geqslant 0,\ \forall\, t \in \overline{\mathcal{D}}$.

Proof. To prove the lemma, we define $\boldsymbol{y}(t) = (y_1(t), y_2(t))^T = \left((1+\sigma)\left(\frac{2-t^2}{2}\right), 1\right)^T$ where $0 < \sigma < 1$. Since $\boldsymbol{y}(t) > 0,\ \forall\, t \in \overline{\mathcal{D}}$, so

$$\mathcal{L}_1\boldsymbol{y}(t) = \sigma > 0,$$
$$\mathcal{L}_2\boldsymbol{y}(t) = a(t) + b(t)\left[(1+\sigma)\left(\frac{2-t^2}{2}\right)\right] > \zeta - 2\beta \geqslant \eta > 0.$$

For contrary assume that $\boldsymbol{z}(t) < 0$ and define $\alpha = \max_{t\in\overline{\mathcal{D}}}\{-z_1(t)/y_1(t), -z_2(t)/y_2(t)\}$ which gives $(z_j + \alpha y_j)(t) \geqslant 0,\ j = 1, 2,\ t \in \overline{\mathcal{D}}$. Also, there exists a point $t_0 \in \overline{\mathcal{D}}$ such that either $-z_1(t_0)/y_1(t_0) = \alpha$ or $-z_2(t_0)/y_2(t_0) = \alpha$. In the first case, we get $-z_1(t_0)/y_1(t_0) = \alpha$ *i.e.,* $(z_1 + \alpha y_1)(t_0) = 0$. It means $z_1 + \alpha y_1$ has a minima at $t = t_0$ and so

$$\mathcal{L}_1(\boldsymbol{z} + \alpha\boldsymbol{y})(t_0) = -(z_1 + \alpha y_1)''(t_0) - (z_2 + \alpha y_2)(t_0) < 0,$$

which is a contradiction. Similarly, in the second case, we get $-z_2(t_0)/y_2(t_0) = \alpha$ *i.e.,* $(z_2 + \alpha y_2)(t_0) = 0$. It means $z_2 + \alpha y_2$ has a minima at $t = t_0$ and so

$$\mathcal{L}_2(\boldsymbol{z} + \alpha\boldsymbol{y})(t_0) = -\mu(z_2 + \alpha y_2)''(t_0) + a(t_0)(z_2 + \alpha y_2)(t_0) + b(t_0)(z_1 + \alpha y_1)(t_0) < 0,$$

which is again a contradiction. Hence, the result is obtained. □

Lemma 5.2.2 (Stability estimates)**.** *The solution $\boldsymbol{z}(t)$ of the system (5.1.3) satisfies*

$$\|\boldsymbol{z}(t)\| \leqslant C \max\left\{\|\boldsymbol{z}(0)\|, \|\boldsymbol{z}(1)\|, \max_{t\in\overline{\mathcal{D}}}|\mathcal{L}_1\boldsymbol{z}|, \max_{t\in\overline{\mathcal{D}}}|\mathcal{L}_2\boldsymbol{z}|\right\},\ \forall\, t \in \overline{\mathcal{D}},$$

where $\|\boldsymbol{z}(t)\| = \max\{|z_1(t)|, |z_2(t)|\}$.

Proof. For the proof, refer to [118, 122]. □

Lemma 5.2.3. *The components of the solution of (5.1.3) and its derivatives satisfy the following bounds*

$$|z_1^{(k)}(t)| \leqslant C(1 + \mu^{1-k/2}\mathcal{B}_\mu(t)),\ \textit{for}\ k = 0, 1, \ldots, 4,$$
$$|z_2^{(k)}(t)| \leqslant C(1 + \mu^{-k/2}\mathcal{B}_\mu(t)),\ \textit{for}\ k = 0, 1, \ldots, 4,$$

where $\mathcal{B}_\mu(t) = \exp(-t\sqrt{\zeta/\mu}) + \exp(-(1-t)\sqrt{\zeta/\mu})$.

Proof. Follow the approach given in [118] for the descriptive proof. □

To prove the parameter-uniform convergence, we require more precise bounds for the

exact solution of the system (5.1.3). For this, we decompose the solution $\boldsymbol{z}(t)$ into three parts

$$\boldsymbol{z}(t) = \boldsymbol{v}(t) + \boldsymbol{w}^L(t) + \boldsymbol{w}^R(t), \tag{5.2.1}$$

where $\boldsymbol{v}(t) = (v_1, v_2)^T$, $\boldsymbol{w}^L(t) = (w_1^L(t), w_2^L(t))^T$, and $\boldsymbol{w}^R(t) = (w_1^R(t), w_2^R(t))^T$ are regular, left singular, and right singular components of $\boldsymbol{z}(t)$. The regular component satisfies the following problem

$$\begin{aligned} &\boldsymbol{\mathcal{L}}\boldsymbol{v}(t) = \boldsymbol{f}(t),\ t \in \mathcal{D}, \\ &\boldsymbol{v}(0) = (z_1(0), (f(0) - b(0)z_1(0))/a(0))^T,\ \boldsymbol{v}(1) = (z_1(1), (f(1) - b(1)z_1(1))/a(1))^T, \end{aligned} \tag{5.2.2}$$

and the singular components are solutions of the following BVPs

$$\boldsymbol{\mathcal{L}}\boldsymbol{w}^L(t) = 0,\ t \in \mathcal{D}, \quad \boldsymbol{w}^L(0) = \boldsymbol{z}(0) - \boldsymbol{v}(0),\ \boldsymbol{w}^L(1) = 0, \tag{5.2.3}$$

$$\boldsymbol{\mathcal{L}}\boldsymbol{w}^R(t) = 0,\ t \in \mathcal{D},\ \boldsymbol{w}^R(0) = 0,\ \boldsymbol{w}^R(1) = \boldsymbol{z}(1) - \boldsymbol{v}(1). \tag{5.2.4}$$

Theorem 5.2.1. *If $a(t)$, $b(t)$, and $f(t) \in C^2(\overline{\mathcal{D}})$, then the components $\boldsymbol{v}(t)$, $\boldsymbol{w}^L(t)$, $\boldsymbol{w}^R(t)$, and their derivatives satisfy the following bounds*

$$\begin{aligned} &|v_1^{(k)}(t)| \leqslant C, \quad |v_2^{(k)}(t)| \leqslant C(1 + \mu^{(2-k)/2}), \quad t \in \overline{\mathcal{D}},\ 0 \leqslant k \leqslant 4, \\ &|(w_1^L)^{(k)}(t)| \leqslant C\mu^{1-k/2} \exp(-t\sqrt{a(0)/\mu}),\ 0 \leqslant k \leqslant 4 \\ &|(w_1^R)^{(k)}(t)| \leqslant C\mu^{1-k/2} \exp(-(1-t)\sqrt{a(1)/\mu}),\ 0 \leqslant k \leqslant 4, \\ &|(w_2^L)^{(k)}(t)| \leqslant C\mu^{-k/2} \exp(-t\sqrt{a(0)/\mu}),\ 0 \leqslant k \leqslant 4 \\ &|(w_2^R)^{(k)}(t)| \leqslant C\mu^{-k/2} \exp(-(1-t)\sqrt{a(1)/\mu}),\ 0 \leqslant k \leqslant 4. \end{aligned}$$

Proof. These bounds can be established by following the arguments in [120, 121]. □

Lemma 5.2.4. *The zero-order asymptotic expansion $\boldsymbol{z}_{as}$ of the solution $\boldsymbol{z}$ of (5.1.3) satisfies*

$$\|\boldsymbol{z} - \boldsymbol{z}_{as}\| \leqslant C\sqrt{\mu}.$$

Proof. Refer to Theorem 2.2 given in [118] for the proof. □

5.3 The proposed scheme

In this section, we provide a detailed structure of the non-uniform mesh followed by the scheme analysis to solve the problem (5.1.3).

5.3.1 The mesh construction

It is well-known that standard numerical methods on a uniform mesh give unsatisfactory results because they fail to provide efficient and oscillations-free solutions near the layer region(s). Additionally, it is easier to construct a scheme on a uniform mesh that is uniformly convergent in the diffusion parameter if one uses a significantly large number of mesh points. For computational purposes, it is practically impossible. Thus, we feel the requirement of non-uniform meshes to resolve the layer(s). In this section, we will construct an eXp mesh that generates more mesh points in the layer region than in the other part of the domain.

To construct the eXp mesh $\Delta = \{t_j | \, 0 \leqslant j \leqslant M\}$, we divide the interval $[0, 1]$ into $M > 4$ (multiple of 4) subintervals $I_j = [t_{j-1}, t_j]$. We denote by $\Pi_{\mathfrak{p}}$, the space of all polynomials of degree $\leqslant \mathfrak{p}$. While constructing the mesh, we use a monotonically increasing, continuous, and piecewise continuously differentiable mesh generating function $\Psi(\varrho)$, which is defined as

$$\Psi(\varrho) = -\ln(1 - 2\phi_{\mathfrak{p},\mu}\varrho), \ \varrho \in [0, 1/2 - 1/M], \tag{5.3.1}$$

where $\phi_{\mathfrak{p},\mu} = 1 - \exp\left(-\frac{1}{(\mathfrak{p}+1)\sqrt{\mu}}\right) \in \mathbb{R}^+$. We split the interval $[0, 1]$ as the union of three subintervals $[0, t_{\frac{M}{4}-1}]$, $[t_{\frac{M}{4}-1}, t_{\frac{3M}{4}+1}]$ and $[t_{\frac{3M}{4}+1}, 1]$ *i.e.,* $[0, 1] = [0, t_{\frac{M}{4}-1}] \cup [t_{\frac{M}{4}-1}, t_{\frac{3M}{4}+1}] \cup [t_{\frac{3M}{4}+1}, 1]$, where $t_{\frac{M}{4}-1}$ and $t_{\frac{3M}{4}+1}$ are the transition points. The nodal points can be written in the following form

$$t_j = \begin{cases} (\mathfrak{p}+1)\sqrt{\mu}\Psi(\varrho_j), & j = 0, 1, \ldots, \frac{M}{4} - 1, \\ t_{\frac{M}{4}-1} + \left(\frac{t_{\frac{3M}{4}+1} - t_{\frac{M}{4}-1}}{\frac{M}{2}+2}\right)(j - M/4 + 1), & j = \frac{M}{4}, \ldots, \frac{3M}{4}, \\ 1 - (\mathfrak{p}+1)\sqrt{\mu}\Psi(1 - \varrho_j), & j = \frac{3M}{4} + 1, \ldots, M, \end{cases}$$

where $\varrho_j = \frac{j}{M}$, and $h_j = t_j - t_{j-1}$ for $j = 1, 2, \ldots, M$. The mesh points are equidistantly distributed in $[t_{\frac{M}{4}-1}, t_{\frac{3M}{4}+1}]$ with $M/2 + 2$ elements and these are exponentially graded distributed in $[0, t_{\frac{M}{4}-1}] \cup [t_{\frac{3M}{4}+1}, 1]$, respectively. The mesh step length h_j satisfies the following inequalities utilizing the mesh characterizing function $\Phi = \exp(-\Psi)$ (see [91] for more details)

$$h_j \leqslant \begin{cases} C(\mathfrak{p}+1)\sqrt{\mu}M^{-1} \max \Psi'(\varrho_j), & j = 1, 2, \ldots, \frac{M}{4} - 1, \\ CM_t^{-1}, & j = \frac{M}{4}, \ldots, \frac{3M}{4} + 1, \\ C(\mathfrak{p}+1)\sqrt{\mu}M^{-1} \max \Psi'(1 - \varrho_j), & j = \frac{3M}{4} + 2, \ldots, M, \end{cases}$$

further

$$h_j \leqslant \begin{cases} C(\mathfrak{p}+1)\sqrt{\mu}M^{-1} \max |\Phi'| \exp\left(\frac{t_j}{(\mathfrak{p}+1)\sqrt{\mu}}\right), & j = 1, 2, \ldots, \frac{M}{4} - 1, \\ CM_t^{-1}, & j = \frac{M}{4}, \ldots, \frac{3M}{4} + 1, \\ C(\mathfrak{p}+1)\sqrt{\mu}M^{-1} \max |\Phi'| \exp\left(\frac{1-t_j}{(\mathfrak{p}+1)\sqrt{\mu}}\right), & j = \frac{3M}{4} + 2, \ldots, M. \end{cases}$$

As $\max |\Phi'| \leqslant 2$, we can simply write the above inequalities as

$$h_j \leqslant \begin{cases} C\sqrt{\mu}M^{-1} \exp\left(\frac{t_j}{(\mathfrak{p}+1)\sqrt{\mu}}\right), & j = 1, 2, \ldots, \frac{M}{4} - 1, \\ CM_t^{-1}, & j = \frac{M}{4}, \ldots, \frac{3M}{4} + 1, \\ C\sqrt{\mu}M^{-1} \exp\left(\frac{1-t_j}{(\mathfrak{p}+1)\sqrt{\mu}}\right), & j = \frac{3M}{4} + 2, \ldots, M, \end{cases} \tag{5.3.2}$$

and this adaptive mesh satisfies the following estimate

$$|h_{j+1} - h_j| \leqslant C \begin{cases} \sqrt{\mu}M^{-2}, & j = 1, 2, \ldots, \frac{M}{4} - 1, \\ 0, & j = \frac{M}{4}, \ldots, \frac{3M}{4}, \\ \sqrt{\mu}M^{-2}, & j = \frac{3M}{4} + 1, \ldots, M. \end{cases} \tag{5.3.3}$$

Remark 5.3.1. *The Shishkin and Bakhvalov meshes violate the inequality* $|h_{j+1} - h_j| \leqslant CM^{-2}$ *near the transition points. Thus, we cannot extend our analysis to these meshes.*

5.3.2 Implementation of the collocation scheme

To discretize (5.1.3) we seek the quadratic splines $\mathfrak{B}_j(t) \in S_2^1(\Delta),\ j = 0, 1, \ldots, M+1$ that satisfies the BVP (5.1.3) at certain points as follows:

$$\mathfrak{B}_0(t) = \begin{cases} \dfrac{(t_1 - t)^2}{h_1^2}, & t_0 \leqslant t \leqslant t_1, \\ 0, & \text{otherwise}, \end{cases}$$

$$\mathfrak{B}_1(t) = \begin{cases} \dfrac{h_1^2 - (t_1 - t)^2}{h_1^2} - \dfrac{(t - t_0)^2}{h_1(h_1 + h_2)}, & t_0 \leqslant t \leqslant t_1, \\ \dfrac{(t_2 - t)^2}{h_1(h_1 + h_2)}, & t_1 \leqslant t \leqslant t_2, \\ 0, & \text{otherwise}, \end{cases}$$

and for $j = 2, 3, \ldots, M-1$,

$$\mathfrak{B}_j(t) = \begin{cases} \dfrac{(t - t_{j-2})^2}{h_{j-1}(h_{j-1} + h_j)}, & t_{j-2} \leqslant t \leqslant t_{j-1}, \\ \dfrac{(t - t_{j-2})(t_j - t)}{h_j(h_{j-1} + h_j)} + \dfrac{(t_{j+1} - t)(t - t_{j-1})}{h_j(h_j + h_{j+1})}, & t_{j-1} \leqslant t \leqslant t_j, \\ \dfrac{(t_{j+1} - t)^2}{h_{j+1}(h_j + h_{j+1})}, & t_j \leqslant t \leqslant t_{j+1}, \\ 0, & \text{otherwise}, \end{cases}$$

while for $j = M,\ M+1$ these are given as

$$\mathfrak{B}_M(t) = \begin{cases} \dfrac{(t - t_{M-2})^2}{h_{M-1}(h_{M-1} + h_M)}, & t_{M-2} \leqslant t \leqslant t_{M-1}, \\ \dfrac{h_M^2 - (t - t_{M-1})^2}{h_M^2} - \dfrac{(t_M - t)^2}{h_M(h_{M-1} + h_M)}, & t_{M-1} \leqslant t \leqslant t_M, \\ 0, & \text{otherwise}, \end{cases}$$

$$\mathfrak{B}_{M+1}(t) = \begin{cases} \dfrac{(t - t_{M-1})^2}{h_M^2}, & t_{M-1} \leqslant t \leqslant t_M, \\ 0, & \text{otherwise}. \end{cases}$$

The midpoints of $I_j,\ j = 1, 2, \ldots, M$ are the best choices for collocation with quadratic C^1-splines for regularly perturbed BVPs (see [110]), we take the collocation points ξ_j as the

average of endpoints of the intervals I_j *i.e.,*

$$\xi_j = t_{j-1/2} := \frac{t_{j-1}+t_j}{2} = t_{j-1} + \frac{h_j}{2} = t_j - \frac{h_j}{2}, \quad \text{for } j = 1, 2, \ldots, M.$$

For $\mathfrak{m}, \mathfrak{p} \in \mathbb{N}\,(\mathfrak{m} < \mathfrak{p})$, we define

$$S_{\mathfrak{p}}^{\mathfrak{m}}(\Delta) := \{r \in C^{\mathfrak{m}}[0,1] : \ r|_{I_j} \in \Pi_{\mathfrak{p}}, \text{ for } j = 1, 2, \ldots, M\},$$

as a polynomial space and

$$S_{\mathfrak{p},0}^{\mathfrak{m}}(\Delta) := \{r \in S_{\mathfrak{p}}^{\mathfrak{m}}(\Delta) : \ r(0) = r(1) = 0\}.$$

For the discretization of (5.1.3) we find $\tilde{\boldsymbol{z}} \in S_2^1(\Delta)$ such that

$$\tilde{\boldsymbol{z}}(0) = (q_1, q_2)^T, \quad (\boldsymbol{\mathcal{L}}\tilde{\boldsymbol{z}})_{j-1/2} = \boldsymbol{f}_{j-1/2}, \quad \tilde{\boldsymbol{z}}(1) = (q_3, q_4)^T, \quad j = 1, 2, \ldots, M. \tag{5.3.4}$$

We rewrite (5.3.4) in the component form as

$$\tilde{z}_1(0) = q_1, \quad (\mathcal{L}_1\tilde{\boldsymbol{z}})_{j-1/2} = 0, \quad \tilde{z}_1(1) = q_3, \ j = 1, 2, \ldots, M, \tag{5.3.5a}$$

$$\tilde{z}_2(0) = q_2, \quad (\mathcal{L}_2\tilde{\boldsymbol{z}})_{j-1/2} = f_{j-1/2}, \quad \tilde{z}_2(1) = q_4, \ j = 1, 2, \ldots, M. \tag{5.3.5b}$$

The collocation solution $\tilde{\boldsymbol{z}}$ is represented by

$$\tilde{z}_k(t) = \sum_{j=0}^{M+1} \alpha_{j,k}\mathfrak{B}_j(t), \quad k = 1, 2. \tag{5.3.6}$$

Using (5.3.6) in (5.3.4) and (5.3.5), we obtain the following system

$$\alpha_{0,k} = q_k, \quad [\boldsymbol{L}\boldsymbol{\alpha}]_{j-1/2} = \boldsymbol{f}_{j-1/2}, \ j = 1, 2, \ldots, M, \quad \alpha_{M+1,k} = q_{k+2}, \ k = 1, 2, \tag{5.3.7}$$

which is equivalent to

$$\alpha_{0,1} = q_1, \quad [L_1\boldsymbol{\alpha}]_{j-1/2} = 0, \quad \alpha_{M+1,1} = q_3,\ j = 1, 2, \ldots, M, \tag{5.3.8a}$$

$$\alpha_{0,2} = q_2, \quad [L_2\boldsymbol{\alpha}]_{j-1/2} = f_{j-1/2}, \quad \alpha_{M+1,2} = q_4,\ j = 1, 2, \ldots, M, \tag{5.3.8b}$$

with $\boldsymbol{\alpha} := (\alpha_{0,1}, \alpha_{1,1}, \ldots, \alpha_{M+1,1}, \alpha_{0,2}, \alpha_{1,2}, \ldots, \alpha_{M+1,2})^T \in \mathbb{R}^{2M+4}$, $\boldsymbol{L} := (L_1, L_2)^T$. The operators in (5.3.8) can be simplified as

$$\begin{aligned}
[L_1\boldsymbol{\alpha}]_{j-1/2} :=& -\left[\frac{2(\alpha_{j+1,1} - \alpha_{j,1})}{h_j(h_j + h_{j+1})} - \frac{2(\alpha_{j,1} - \alpha_{j-1,1})}{h_j(h_j + h_{j-1})}\right] - \left[\widetilde{q}_j^{+}\alpha_{j+1,2} + \left(1 - \widetilde{q}_j^{+} - \widetilde{q}_j^{-}\right)\alpha_{j,2}\right. \\
&\left. + \widetilde{q}_j^{-}\alpha_{j-1,2}\right], \\
[L_2\boldsymbol{\alpha}]_{j-1/2} :=& -\mu\left[\frac{2(\alpha_{j+1,2} - \alpha_{j,2})}{h_j(h_j + h_{j+1})} - \frac{2(\alpha_{j,2} - \alpha_{j-1,2})}{h_j(h_j + h_{j-1})}\right] + a_{j-1/2}\left[\widetilde{q}_j^{+}\alpha_{j+1,2} + \left(1 - \widetilde{q}_j^{+}\right.\right. \\
&\left.\left. - \widetilde{q}_j^{-}\right)\alpha_{j,2} + \widetilde{q}_j^{-}\alpha_{j-1,2}\right] + b_{j-1/2}\left[\widetilde{q}_j^{+}\alpha_{j+1,1} + \left(1 - \widetilde{q}_j^{+} - \widetilde{q}_j^{-}\right)\alpha_{j,1} + \widetilde{q}_j^{-}\alpha_{j-1,1}\right],
\end{aligned}$$

where $\widetilde{q}_j^{+} := \frac{h_j}{4(h_j+h_{j+1})}$ and $\widetilde{q}_j^{-} := \frac{h_j}{4(h_j+h_{j-1})}$. Combining all the equations, we get the system

$$\mathfrak{A}\boldsymbol{\alpha} = \mathfrak{G},$$

where

$$\mathfrak{A} = \begin{bmatrix} A & B \\ C & D \end{bmatrix}, \quad \mathfrak{G} = \Big(\underbrace{q_1, 0, \ldots, 0, q_3}_{1^{\text{st}}\text{component}}, \underbrace{q_2, f(\xi_1), \ldots, f(\xi_M), q_4}_{2^{\text{nd}}\text{component}}\Big)^T,$$

$$\boldsymbol{\alpha} = \Big(\underbrace{\alpha_{0,1}, \alpha_{1,1}, \ldots, \alpha_{M,1}, \alpha_{M+1,1}}_{1^{\text{st}}\text{component}}, \underbrace{\alpha_{0,2}, \alpha_{1,2}, \ldots, \alpha_{M,2}, \alpha_{M+1,2}}_{2^{\text{nd}}\text{component}}\Big)^T.$$

The matrices A, B, C, and D are given by

$$A = \begin{bmatrix} 1 & 0 & 0 & 0 & \dots & \dots & 0 \\ a_{21} & a_{22} & a_{23} & 0 & \dots & \dots & 0 \\ 0 & a_{32} & a_{33} & a_{34} & \dots & \dots & 0 \\ \vdots & \ddots & \ddots & \ddots & \vdots & \vdots & \vdots \\ \dots & \dots & \dots & 0 & a_{M+1M} & a_{M+1M+1} & a_{M+1M+2} \\ \dots & \dots & \dots & 0 & 0 & 0 & 1 \end{bmatrix}_{(M+2)\times(M+2)},$$

$$B = \begin{bmatrix} 0 & 0 & 0 & 0 & \dots & \dots & 0 \\ b_{21} & b_{22} & b_{23} & 0 & \dots & \dots & 0 \\ 0 & b_{32} & b_{33} & b_{34} & \dots & \dots & 0 \\ \vdots & \ddots & \ddots & \ddots & \vdots & \vdots & \vdots \\ \dots & \dots & \dots & 0 & b_{M+1M} & b_{M+1M+1} & b_{M+1M+2} \\ \dots & \dots & \dots & 0 & 0 & 0 & 0 \end{bmatrix}_{(M+2)\times(M+2)},$$

$$C = \begin{bmatrix} 0 & 0 & 0 & 0 & \dots & \dots & 0 \\ c_{21} & c_{22} & c_{23} & 0 & \dots & \dots & 0 \\ 0 & c_{32} & c_{33} & c_{34} & \dots & \dots & 0 \\ \vdots & \ddots & \ddots & \ddots & \vdots & \vdots & \vdots \\ \dots & \dots & \dots & 0 & c_{M+1M} & c_{M+1M+1} & c_{M+1M+2} \\ \dots & \dots & \dots & 0 & 0 & 0 & 0 \end{bmatrix}_{(M+2)\times(M+2)},$$

$$D = \begin{bmatrix} 1 & 0 & 0 & 0 & \dots & \dots & 0 \\ d_{21} & d_{22} & d_{23} & 0 & \dots & \dots & 0 \\ 0 & d_{32} & d_{33} & d_{34} & \dots & \dots & 0 \\ \vdots & \ddots & \ddots & \ddots & \vdots & \vdots & \vdots \\ \dots & \dots & \dots & 0 & d_{M+1M} & d_{M+1M+1} & d_{M+1M+2} \\ \dots & \dots & \dots & 0 & 0 & 0 & 1 \end{bmatrix}_{(M+2)\times(M+2)},$$

where for $j = 1, 2, \dots, M$

$$\begin{aligned}
a_{j+1,j} &= -\frac{2}{h_j(h_j + h_{j-1})}, \quad c_{j+1,j} = \widetilde{q}_j^{-} b_{j-1/2}, \\
a_{j+1,j+1} &= \frac{2}{h_j(h_j + h_{j-1})} + \frac{2}{h_j(h_j + h_{j+1})}, \quad c_{j+1,j+1} = b_{j-1/2}(1 - \widetilde{q}_j^{+} - \widetilde{q}_j^{-}), \\
a_{j+1,j+2} &= -\frac{2}{h_j(h_j + h_{j+1})}, \quad c_{j+1,j+2} = \widetilde{q}_j^{+} b_{j-1/2}, \\
b_{j+1,j} &= -\widetilde{q}_j^{-}, \quad d_{j+1,j} = -\frac{2\mu}{h_j(h_j + h_{j-1})} + \widetilde{q}_j^{-} a_{j-1/2}, \\
b_{j+1,j+1} &= -(1 - \widetilde{q}_j^{+} - \widetilde{q}_j^{-}), \quad b_{j+1,j+2} = -\widetilde{q}_j^{+}, \quad d_{j+1,j+2} = -\frac{2\mu}{h_j(h_j + h_{j+1})} + \widetilde{q}_j^{+} a_{j-1/2}, \\
d_{j+1,j+1} &= \frac{2\mu}{h_j(h_j + h_{j-1})} + \frac{2\mu}{h_j(h_j + h_{j+1})} + a_{j-1/2}(1 - \widetilde{q}_j^{+} - \widetilde{q}_j^{-}).
\end{aligned}$$

5.4 Convergence analysis

5.4.1 S_2^0-interpolation

To obtain the interpolation $I_2^0 z_k \in S_2^0(\Delta)$ for an arbitrary function $z_k \in C^0[0,1]$, we find the solution of the following interpolation problem

$$(I_2^0 z_k)_j = (z_k)_j,\ j = 0, 1, \dots, M, \quad \text{and} \quad (I_2^0 z_k)_{j-1/2} = (z_k)_{j-1/2},\ j = 1, 2, \dots, M,$$

where $(z_k)_j = z_k(t_j),\ (z_k)_{j-1/2} = z_k(\xi_j),\ k = 1, 2.$

Theorem 5.4.1. *Assuming $a(t), b(t),\ f(t) \in C^2[0,1]$, the interpolation error $\boldsymbol{z} - I_2^0 \boldsymbol{z}$ of the*

solution $\boldsymbol{z}$ *of (5.1.3) satisfies the following bounds:*

$$\|\boldsymbol{z} - I_2^0 \boldsymbol{z}\| \leqslant \boldsymbol{C} M^{-3}, \quad \textit{and} \quad \boldsymbol{\mu} \max_{j=1,2,\ldots,M} |(\boldsymbol{z} - I_2^0 \boldsymbol{z})''_{j-1/2}| \leqslant \boldsymbol{C} M^{-2},$$

where $\boldsymbol{\mu} = \textit{diag}(1, \mu)$.

Proof. First, we employ the Lagrange representation of the interpolation polynomial and Taylor expansions to confirm that for any $\boldsymbol{z} \in C^4[0,1]^2$, the interpolation error on each I_j satisfies

$$\left\| z_k - I_2^0 z_k \right\|_{I_j} \leqslant \frac{h_j^3}{24} \left\| z_k^{(3)} \right\|_{I_j}, \quad \left| (z_k - I_2^0 z_k)''_{j-1/2} \right| \leqslant \frac{h_j^2}{48} \left\| z_k^{(4)} \right\|_{I_j}, \quad k = 1, 2. \tag{5.4.1}$$

Making use of the linearity of I_2^0, we decompose the solution components z_k into three parts as follows

$$z_k - I_2^0 z_k = (v_k - I_2^0 v_k) + \left(w_k^L - I_2^0 w_k^L \right) + \left(w_k^R - I_2^0 w_k^R \right).$$

Since the bounds for both the components are different, therefore we analyze both components separately.

Analysis for first component z_1**:** We start with finding the interpolation error in the regular component. For $I_j \subset [t_0, t_{M/4-1}]$, we make use of the bounds given in Theorem 5.2.1, to obtain

$$\begin{aligned}
\frac{h_j^3}{24} \left| v_1^{(3)} \right|_{I_j} &\leqslant C \mu^{3/2} M^{-3} \exp\left(\frac{3 t_j}{(\mathfrak{p}+1)\sqrt{\mu}} \right) \\
&\leqslant C M^{-3} \exp\left(\frac{t_j}{\sqrt{\mu}} \right) \\
&\leqslant C M^{-3} \exp\Big((\mathfrak{p}+1) \Psi(\varrho_j) \Big) \\
&\leqslant C M^{-3}.
\end{aligned}$$

Similarly, we employ the same analysis in the right layer region $I_j \subset [t_{3M/4+2}, t_M]$, to obtain $\|v_1 - I_2^0 v_1\|_{I_j} \leqslant C M^{-3}$. Also, for $I_j \subset [t_{M/4}, t_{3M/4+1}]$, the bounds for h_j (using the

inequality (5.3.2)) trivially gives $\|v_1 - I_2^0 v_1\|_{I_j} \leqslant CM^{-3}$. Thus, on consolidating all the estimates for the regular component, we perceive

$$\|v_1 - I_2^0 v_1\| \leqslant CM^{-3}.$$

Next, we consider the left singular component w_1^L in $I_j \subset [t_0, t_{M/4-1}]$. Using Theorem 5.2.1 and the inequality (5.3.2), we get

$$\begin{aligned}
\frac{h_j^3}{24}\left|(w_1^L)^{(3)}\right|_{I_j} &\leqslant C\mu^{3/2}M^{-3}\exp\left(\frac{3t_j}{(\mathfrak{p}+1)\sqrt{\mu}}\right)\mu^{-1/2}|\exp(-t\sqrt{a(0)/\mu})|_{I_j} \\
&\leqslant CM^{-3}\exp\left[C_1\left(\frac{t_j}{\sqrt{\mu}} - \frac{t_{j-1}}{\sqrt{\mu}}\right)\right] \\
&\leqslant CM^{-3}\exp\left(C_1\frac{h_j}{\sqrt{\mu}}\right) \\
&\leqslant CM^{-3}\exp\left(C_1(\mathfrak{p}+1)M^{-1}\max\Psi'(\varrho_j)\right) \\
&\leqslant CM^{-3}.
\end{aligned}$$

Now for $I_j \subset [t_{M/4}, t_{3M/4+1}]$, we obtain

$$\begin{aligned}
\frac{h_j^3}{24}\left|(w_1^L)^{(3)}\right|_{I_j} &\leqslant CM^{-3}\mu^{-1/2}|\exp(-t\sqrt{a(0)/\mu})|_{I_j} \\
&\leqslant CM^{-3}\mu^{-1/2}\exp\left(-\frac{\sqrt{a(0)}t_{j-1}}{\sqrt{\mu}}\right).
\end{aligned}$$

Since $\mu^{-1/2}\exp\left(-\frac{\sqrt{a(0)}t_{j-1}}{\sqrt{\mu}}\right)$ is bounded in $[t_{M/4}, t_{3M/4+1}]$, the above inequality gives

$$\frac{h_j^3}{24}\left|(w_1^L)^{(3)}\right|_{I_j} \leqslant CM^{-3}.$$

We can derive the same bounds for $I_j \subset [t_{3M/4+2}, t_M]$ analogous to $[t_0, t_{M/4-1}]$. Thus,

$$\|w_1^L - I_2^0 w_1^L\| \leqslant CM^{-3}.$$

Now for w_1^R in $I_j \subset [t_0, t_{M/4-1}]$ (using Theorem 5.2.1 and the inequality (5.3.2)), we get

$$\begin{aligned}
\frac{h_j^3}{24}\left|(w_1^R)^{(3)}\right|_{I_j} &\leqslant C\mu^{3/2}M^{-3}\exp\left(\frac{3t_j}{(\mathfrak{p}+1)\sqrt{\mu}}\right)\mu^{-1/2}|\exp(-(1-t)\sqrt{a(1)/\mu})|_{I_j} \\
&\leqslant CM^{-3}\exp\left(\frac{C_2 t_j}{\sqrt{\mu}}\right)\exp\left(-\frac{C_3(1-t_{j-1})}{\sqrt{\mu}}\right) \\
&\leqslant CM^{-3}\exp\left(C_4\frac{t_j-(1-t_{j-1})}{\sqrt{\mu}}\right) \\
&\leqslant CM^{-3}\exp\left(C_4\frac{h_j-1-2t_{j-1}}{\sqrt{\mu}}\right) \\
&\leqslant CM^{-3}\exp\left(C_4(\mathfrak{p}+1)M^{-1}\max\Psi'(\varrho_j)\right) \\
&\leqslant CM^{-3}.
\end{aligned}$$

Following the same approach, one can deduce the bounds for w_1^R in the intervals $[t_{M/4}, t_{3M/4+1}]$ and $[t_{3M/4+2}, t_M]$ as

$$\|w_1^R - I_2^0 w_1^R\| \leqslant CM^{-3}.$$

Now to obtain the bound for $\max\limits_{j=1,2,\ldots,M}|(z_1 - I_2^0 z_1)''_{j-1/2}|$, first, we consider v_1 in $I_j \subset [t_0, t_{M/4-1}]$ as follows

$$\begin{aligned}
\frac{h_j^2}{48}\left|v_1^{(4)}\right|_{I_j} &\leqslant C\mu M^{-2}\exp\left(\frac{2t_j}{(\mathfrak{p}+1)\sqrt{\mu}}\right) \text{ (using Theorem 5.2.1 and the inequality (5.3.2))} \\
&\leqslant CM^{-2}\exp\left(\frac{2t_j}{(\mathfrak{p}+1)\sqrt{\mu}}\right) \\
&\leqslant CM^{-2}\exp\left(2\Psi(\varrho_j)\right) \\
&\leqslant CM^{-2}.
\end{aligned}$$

Use similar approach for v_1 the intervals $[t_{M/4}, t_{3M/4+1}]$ and $[t_{3M/4+2}, t_M]$. Now for the w_1^L in $I_j \subset [t_0, t_{M/4-1}]$, we have

$$\begin{aligned}
\frac{h_j^2}{48}\left|(w_1^L)^{(4)}\right|_{I_j} &\leqslant C\mu M^{-2}\exp\left(\frac{2t_j}{(\mathfrak{p}+1)\sqrt{\mu}}\right)\mu^{-1}|\exp(-t\sqrt{a(0)/\mu})|_{I_j} \\
&\leqslant CM^{-2}\exp\left(\frac{C_5 t_j}{\sqrt{\mu}}\right)\exp\left(\frac{-C_6 t_{j-1}}{\sqrt{\mu}}\right)
\end{aligned}$$

$$
\begin{aligned}
&\leqslant CM^{-2}\exp\left(\frac{C_7(t_j - t_{j-1})}{\sqrt{\mu}}\right)\\
&\leqslant CM^{-2}\exp\left(\frac{C_7 h_j}{\sqrt{\mu}}\right)\\
&\leqslant CM^{-2}\exp\left(C_3(\mathfrak{p}+1)M^{-1}\max\Psi'(\varrho_j)\right)\\
&\leqslant CM^{-2}.
\end{aligned}
$$

For the intervals $[t_{M/4}, t_{3M/4+1}]$ and $[t_{3M/4+2}, t_M]$, we perform the same analysis to obtain

$$\max_{j=1,2,\ldots,M} |(w_1^L - I_2^0 w_1^L)''_{j-1/2}| \leqslant CM^{-2}.$$

Furthermore, analogously, we find the bounds for w_1^R. Subsequently, the effective use of triangle inequality guides us to complete the proof.

Analysis for second component z_2: We start with finding the interpolation error in the regular component. For $I_j \subset [t_0, t_{M/4-1}]$, we make use of the bounds given in Theorem 5.2.1, to obtain

$$
\begin{aligned}
\frac{h_j^3}{24}\left|v_2^{(3)}\right|_{I_j} &\leqslant C\mu^{3/2}(1+\mu^{-1/2})M^{-3}\exp\left(\frac{3t_j}{(\mathfrak{p}+1)\sqrt{\mu}}\right)\\
&\leqslant CM^{-3}\exp\left(\frac{t_j}{\sqrt{\mu}}\right)\\
&\leqslant CM^{-3}\exp\left((\mathfrak{p}+1)\Psi(\varrho_j)\right)\\
&\leqslant CM^{-3}.
\end{aligned}
$$

Similarly, we employ the above analysis in the right layer region $I_j \subset [t_{3M/4+2}, t_M]$, to obtain $\|v_2 - I_2^0 v_2\|_{I_j} \leqslant CM^{-3}$. Also, for $I_j \subset [t_{M/4}, t_{3M/4+1}]$, the bounds for h_j (using inequality (5.3.2)) trivially gives $\|v_2 - I_2^0 v_2\|_{I_j} \leqslant CM^{-3}$. Thus, on consolidating all the estimates for the regular component, we perceive

$$\|v_2 - I_2^0 v_2\| \leqslant CM^{-3}.$$

Next, we consider the left singular component w_2^L in $I_j \subset [t_0, t_{M/4-1}]$. Using Theorem 5.2.1

and the inequality (5.3.2), we get

$$\begin{aligned}\frac{h_j^3}{24}\left|(w_2^L)^{(3)}\right|_{I_j} &\leqslant C\mu^{3/2}M^{-3}\exp\left(\frac{3t_j}{(\mathfrak{p}+1)\sqrt{\mu}}\right)\mu^{-3/2}|\exp(-t\sqrt{a(0)/\mu})|_{I_j}\\ &\leqslant CM^{-3}\exp\left[C_8\left(\frac{t_j}{\sqrt{\mu}}-\frac{t_{j-1}}{\sqrt{\mu}}\right)\right]\\ &\leqslant CM^{-3}\exp\left(C_8\frac{h_j}{\sqrt{\mu}}\right)\\ &\leqslant CM^{-3}\exp\left(C_8(\mathfrak{p}+1)M^{-1}\max\Psi'(\varrho_j)\right)\\ &\leqslant CM^{-3}.\end{aligned}$$

Now for $I_j \subset [t_{M/4}, t_{3M/4+1}]$, we obtain

$$\begin{aligned}\frac{h_j^3}{24}\left|(w_2^L)^{(3)}\right|_{I_j} &\leqslant CM^{-3}\mu^{-3/2}|\exp(-t\sqrt{a(0)/\mu})|_{I_j}\\ &\leqslant CM^{-3}\mu^{-3/2}\exp\left(-\frac{\sqrt{a(0)}t_{j-1}}{\sqrt{\mu}}\right).\end{aligned}$$

The term $\mu^{-3/2}\exp\left(-\frac{\sqrt{a(0)}t_{j-1}}{\sqrt{\mu}}\right)$ is bounded in $[t_{M/4}, t_{3M/4+1}]$, by employing the L'Hôpital rule. Hence, the above inequality gives

$$\frac{h_j^3}{24}\left|(w_2^L)^{(3)}\right|_{I_j} \leqslant CM^{-3}.$$

Similarly, we can derive the bound for $I_j \subset [t_{3M/4+2}, t_M]$ as we obtained for $[t_0, t_{M/4-1}]$. Thus,

$$\|w_2^L - I_2^0 w_2^L\| \leqslant CM^{-3}.$$

Now for w_2^R in $I_j \subset [t_0, t_{M/4-1}]$ (using Theorem 5.2.1 and the inequality (5.3.2)), we get

$$\begin{aligned}\frac{h_j^3}{24}\left|(w_2^R)^{(3)}\right|_{I_j} &\leqslant C\mu^{3/2}M^{-3}\exp\left(\frac{3t_j}{(\mathfrak{p}+1)\sqrt{\mu}}\right)\mu^{-3/2}|\exp(-(1-t)\sqrt{a(1)/\mu})|_{I_j}\\ &\leqslant CM^{-3}\exp\left(\frac{C_9 t_j}{\sqrt{\mu}}\right)\exp\left(-\frac{C_{10}(1-t_{j-1})}{\sqrt{\mu}}\right)\\ &\leqslant CM^{-3}\exp\left(C_{11}\frac{t_j-(1-t_{j-1})}{\sqrt{\mu}}\right)\end{aligned}$$

$$\leqslant CM^{-3}\exp\left(C_{11}\frac{h_j-1-2t_{j-1}}{\sqrt{\mu}}\right)$$
$$\leqslant CM^{-3}\exp\left(C_{11}(\mathfrak{p}+1)M^{-1}\max\Psi'(\varrho_j)\right)$$
$$\leqslant CM^{-3}.$$

Following the same approach one can deduce the bounds for w_2^R in the intervals $[t_{M/4}, t_{3M/4+1}]$ and $[t_{3M/4+2}, t_M]$ as

$$\|w_2^R - I_2^0 w_2^R\| \leqslant CM^{-3}.$$

Now to obtain the bound for $\max\limits_{j=1,2,\ldots,M}|(z_2 - I_2^0 z_2)''_{j-1/2}|$, first, we consider v_2 in $I_j \subset [t_0, t_{M/4-1}]$ as follows

$$\frac{h_j^2}{48}\left|v_2^{(4)}\right|_{I_j} \leqslant C\mu(1+\mu^{-1})M^{-2}\exp\left(\frac{2t_j}{(\mathfrak{p}+1)\sqrt{\mu}}\right) \text{ (using Theorem 5.2.1 and the inequality (5.3.2))}$$
$$\leqslant CM^{-2}\exp\left(\frac{2t_j}{(\mathfrak{p}+1)\sqrt{\mu}}\right)$$
$$\leqslant CM^{-2}\exp\left(2\Psi(\varrho_j)\right)$$
$$\leqslant CM^{-2}.$$

The similar approach can be used for v_2 in the intervals $[t_{M/4}, t_{3M/4+1}]$ and $[t_{3M/4+2}, t_M]$. Now for the w_2^L in $I_j \subset [t_0, t_{M/4-1}]$, we have

$$\frac{h_j^2}{48}\left|(w_2^L)^{(4)}\right|_{I_j} \leqslant C\mu M^{-2}\exp\left(\frac{2t_j}{(\mathfrak{p}+1)\sqrt{\mu}}\right)\mu^{-2}|\exp(-t\sqrt{a(0)/\mu})|_{I_j}$$
$$\leqslant C\mu^{-1}M^{-2}\exp\left(\frac{C_{12}t_j}{\sqrt{\mu}}\right)\exp\left(\frac{-C_{13}t_{j-1}}{\sqrt{\mu}}\right)$$
$$\leqslant C\mu^{-1}M^{-2}\exp\left(\frac{C_{14}(t_j-t_{j-1})}{\sqrt{\mu}}\right)$$
$$\leqslant C\mu^{-1}M^{-2}\exp\left(\frac{C_{14}h_j}{\sqrt{\mu}}\right)$$
$$\leqslant C\mu^{-1}M^{-2}\exp\left(C_{14}(\mathfrak{p}+1)M^{-1}\max\Psi'(\varrho_j)\right)$$
$$\leqslant C\mu^{-1}M^{-2}.$$

For the intervals $[t_{M/4}, t_{3M/4+1}]$ and $[t_{3M/4+2}, t_M]$, we perform the same analysis to obtain

$$\max_{j=1,2,\ldots,M} |(w_2^L - I_2^0 w_2^L)''_{j-1/2}| \leqslant C\mu^{-1}M^{-2}.$$

Furthermore, analogously, we find the bounds for w_2^R. Subsequently, the effective use of triangle inequality guides us to complete the proof. □

Lemma 5.4.1. *Let* $\mathfrak{s}_k \in S_2^0(\Delta)$ *with* $(\mathfrak{s}_k)_{j-1/2} = 0,\ j = 1, 2, \ldots, M,\ k = 1, 2,$ *then*

$$\|\mathfrak{s}_k\|_{I_j} \leqslant \max_j\{|(\mathfrak{s}_k)_{j-1}|, |(\mathfrak{s}_k)_j|\}, \quad \|\mathfrak{s}_k''\|_{I_j} \leqslant \frac{8}{h_j^2}\max_j\{|(\mathfrak{s}_k)_{j-1}|, |(\mathfrak{s}_k)_j|\}.$$

Proof. The result follows using the approach given in [103]. □

5.4.2 S_2^1-interpolation

To obtain the interpolation $I_2^1 z_k \in S_2^1(\Delta)$ for an arbitrary function $z_k \in C^1[0, 1]$ we find the solution of the following interpolation problem

$$(I_2^1 z_k)_0 = (z_k)_0, \quad (I_2^1 z_k)_{j-1/2} = (z_k)_{j-1/2},\ j = 1, 2, \ldots, M, \quad (I_2^1 z_k)_M = (z_k)_M, \tag{5.4.2}$$

where $(z_k)_{j-1/2} = z_k(\xi_j),$ for $k = 1, 2.$

From [93, 111], we have

$$[\Lambda\mathfrak{s}_k]_j \equiv a_j(\mathfrak{s}_k)_{j-1} + 3(\mathfrak{s}_k)_j + c_j(\mathfrak{s}_k)_{j+1},\ j = 1, 2, \ldots, M-1, \tag{5.4.3a}$$

or

$$[\Lambda\mathfrak{s}_k]_j \equiv 4a_j(\mathfrak{s}_k)_{j-1/2} + 4c_j(\mathfrak{s}_k)_{j+1/2},\ j = 1, 2, \ldots, M-1, \tag{5.4.3b}$$

where $(\mathfrak{s}_k)_{j+1/2} = \mathfrak{s}_k\left(t_j + \dfrac{h_{j+1}}{2}\right) = \mathfrak{s}_k\left(\dfrac{t_j + t_{j+1}}{2}\right)$, $a_j = \dfrac{h_{j+1}}{h_j + h_{j+1}}$ and $c_j = 1 - a_j = \dfrac{h_j}{h_j + h_{j+1}}$.

Lemma 5.4.2. *For all vectors* $\mathfrak{s}_k \in \mathbb{R}^{M+1}$ *with* $(\mathfrak{s}_k)_0 = (\mathfrak{s}_k)_M = 0$, *the operator* Λ *is stable* i.e.,

$$\max_{j=1,2,\ldots,M-1} |(\mathfrak{s}_k)_j| \leqslant \frac{1}{2}\max_{j=1,2,\ldots,M-1} |[\Lambda\mathfrak{s}_k]_j|, \quad k = 1, 2.$$

Proof. Refer to Lemma 3 given in [94] for the detailed proof. □

Theorem 5.4.2. *Assume that $a(t), b(t), f(t) \in C^2[0,1]$, then the interpolation error $\boldsymbol{z} - I_2^1\boldsymbol{z}$ of the solution $\boldsymbol{z}$ of (5.1.3) satisfies*

$$\max_{j=0,1,\ldots,M} |(\boldsymbol{z} - I_2^1\boldsymbol{z})_j| \leqslant \boldsymbol{C}M^{-4}, \tag{5.4.4a}$$

$$\|\boldsymbol{z} - I_2^1\boldsymbol{z}\| \leqslant \boldsymbol{C}M^{-3}, \tag{5.4.4b}$$

$$\boldsymbol{\mu} \max_{j=1,2,\ldots,M} |(\boldsymbol{z} - I_2^1\boldsymbol{z})''_{j-1/2}| \leqslant \boldsymbol{C}M^{-2}. \tag{5.4.4c}$$

Proof. To find the interpolation error $z_k - I_2^1 z_k$, we examine an arbitrary function z_k such that

$$(z_k - I_2^1 z_k)_0 = (z_k - I_2^1 z_k)_M = 0, \quad k = 1, 2.$$

Using the definitions of S_2^1-interpolation and the operator Λ, we have

$$\tau_{z_k,j} = [\Lambda(z_k - I_2^1 z_k)]_j = a_j(z_k)_{j-1} - 4a_j(z_k)_{j-1/2} + 3(z_k)_j - 4c_j(z_k)_{j+1/2} + c_j(z_k)_{j+1}, \tag{5.4.5}$$

for $j = 1, 2, \ldots, M,\ k = 1, 2$. Moreover, we use the Taylor series expansions to get

$$|\tau_{z_k,j}| \leqslant \frac{1}{12} h_j h_{j+1} |h_{j+1} - h_j| |(z_k^{(3)})_j|_{I_j} + \frac{5}{96} \max\{h_j^4, h_{j+1}^4\} \|(z_k^{(4)})_j\|_{I_j \cup I_{j+1}}. \tag{5.4.6}$$

Promptly, we decompose the interpolation error into three parts

$$z_k - I_2^1 z_k = (v_k - I_2^1 v_k) + \left(w_k^L - I_2^1 w_k^L\right) + \left(w_k^R - I_2^1 w_k^R\right),$$

or

$$\tau_{z_k,j} = \tau_{v_k,j} + \tau_{w_k^L,j} + \tau_{w_k^R,j}.$$

Analysis for first component z_1: We begin with finding the error in the regular component. For $I_j \subset [t_0, t_{M/4-1}]$, we employ Theorem 5.2.1 and the inequality (5.4.6), to get

$$|\tau_{v_1,j}| \leqslant C\left(h_j h_{j+1} |h_{j+1} - h_j| + \max\{h_j^4, h_{j+1}^4\}\right).$$

In $[t_0, t_{M/4-1}]$ which gives

$$\begin{aligned}
|\tau_{v_1,j}| &\leqslant C\bigg(h_{j+1}^2|h_{j+1}-h_j| + h_{j+1}^4\bigg) \text{ as } h_j < h_{j+1}\\
&\leqslant C\bigg(\mu^{3/2}M^{-4}\exp\bigg(\frac{2t_{j+1}}{(\mathfrak{p}+1)\sqrt{\mu}}\bigg) + \mu^2 M^{-4}\exp\bigg(\frac{4t_{j+1}}{(\mathfrak{p}+1)\sqrt{\mu}}\bigg)\bigg)\\
&\leqslant CM^{-4}\exp\bigg(\frac{4t_{j+1}}{(\mathfrak{p}+1)\sqrt{\mu}}\bigg)\\
&\leqslant CM^{-4}\exp\bigg(4\Psi(\varrho_{j+1})\bigg)\\
&\leqslant CM^{-4}.
\end{aligned}$$

Moreover, for $t_j \in [t_{M/4}, t_{3M/4+1}]$, it is easy to prove $|\tau_{v_1,j}| \leqslant CM^{-4}$. Similarly, for $t_j \in [t_{3M/4+2}, t_M]$ we get $|\tau_{v_1,j}| \leqslant CM^{-4}$. Therefore, using the application of Lemma 5.4.2, we obtain

$$\max_{j=0,1,\ldots,M} |(v_1 - I_2^1 v_1)_j| \leqslant CM^{-4}.$$

Now to find the bounds for w_1^L, we use the fact that $h_j < h_{j+1}$ for $t_j \in [t_0, t_{M/4-1}]$, which yields

$$\begin{aligned}
|\tau_{w_1^L,j}| &\leqslant \frac{1}{12}h_j h_{j+1}|h_{j+1}-h_j||(w_{1,j}^L)'''|_{I_j} + \frac{5}{96}\max\{h_j^4, h_{j+1}^4\}\|(w_{1,j}^L)^{(4)}\|_{I_j\cup I_{j+1}}\\
&\leqslant C\bigg(h_{j+1}^2|h_{j+1}-h_j|\mu^{-1/2}|\exp(-t\sqrt{a(0)/\mu})|_{I_j} + h_{j+1}^4\mu^{-1}||\exp(-t\sqrt{a(0)/\mu})|_{I_j}|_{I_j\cup I_{j+1}}\bigg)\\
&\leqslant CM^{-4}\bigg(\exp\bigg(\frac{2t_{j+1}}{(\mathfrak{p}+1)\sqrt{\mu}}\bigg)\bigg|\exp\bigg(-t\sqrt{\frac{a(0)}{\mu}}\bigg)\bigg|_{I_j}\\
&\quad + \exp\bigg(\frac{4t_{j+1}}{(\mathfrak{p}+1)\sqrt{\mu}}\bigg)\bigg|\exp\bigg(-t\sqrt{\frac{a(0)}{\mu}}\bigg)\bigg|_{I_j\cup I_{j+1}}\bigg)\\
&\leqslant CM^{-4}\exp\bigg(\frac{C_{15}h_{j+1}}{\sqrt{\mu}}\bigg)\\
&\leqslant CM^{-4}\exp\bigg(C_{15}(\mathfrak{p}+1)M^{-1}\max\Psi'(\varrho_{j+1})\bigg)\\
&\leqslant CM^{-4}.
\end{aligned}$$

In the right layer region $[t_{3M/4+1}, t_M]$, we obtain the same bounds. Furthermore, one can easily prove $|\tau_{w_1^L,j}| \leqslant CM^{-4}$ for $t_j \in [t_{M/4-1}, t_{3M/4+1}]$. An application of Lemma 5.4.2

provides

$$\max_{j=0,1,\ldots,M} |(w_1^L - I_2^1 w_1^L)_j| \leqslant CM^{-4}.$$

The same theory can be used to derive the bounds for the right singular component w_1^R (skipping the analysis here).

Analysis for the second component z_2: As the analysis is analogous to the study for the first component in S_2^1-interpolation, we are not providing the details here.

The estimate in (5.4.4a) can be achieved immediately by consolidating all the interpolation errors for three components. To show (5.4.4b), we use triangle inequality as

$$\begin{aligned}\|\boldsymbol{z} - I_2^1\boldsymbol{z}\| &\leqslant \|\boldsymbol{z} - I_2^0\boldsymbol{z}\| + \|I_2^0\boldsymbol{z} - I_2^1\boldsymbol{z}\| \\ &\leqslant \|\boldsymbol{z} - I_2^0\boldsymbol{z}\| + \max_{j=0,1,\ldots,M} |(\boldsymbol{z} - I_2^1\boldsymbol{z})_j|.\end{aligned}$$

Now using $(I_2^1\boldsymbol{z})_j = (\boldsymbol{z})_j,\ j = 0, 1, \ldots, M$, Lemma 5.4.1, Theorem 5.4.1, and (5.4.4a), we obtain the estimate (5.4.4b). Moreover, to obtain the inequality (5.4.4c), we use the identical approach as we have done for (5.4.4b). For this goal, we write

$$\begin{aligned}|(z_k - I_2^1 z_k)''_{j-1/2}| &\leqslant |(z_k - I_2^0 z_k)''_{j-1/2}| + |(I_2^0 z_k - I_2^1 z_k)''_{j-1/2}| \\ &\leqslant |(z_k - I_2^0 z_k)''_{j-1/2}| + \max_{j=0,1,\ldots,M} \frac{8}{h_j^2} |(z_k - I_2^1 z_k)_j|.\end{aligned}$$

Hence, the proof is accomplished by utilizing Theorem 5.4.1 and inequality (5.4.4a). □

Lemma 5.4.3. *If there exists a constant* $\mu_1 > 0$ *such that*

$$\max\{h_{j+1}, h_{j-1}\} \geqslant \mu_1 h_j, \quad j = 1, 2, \ldots, M-1,\ h_1 \geqslant \mu_1 h_2,\ \textit{and}\ h_M \geqslant \mu_1 h_{M-1},$$

then the operator $\boldsymbol{L}$ *is stable in the infinity-norm* i.e.,

$$\|\boldsymbol{\gamma}\| \leqslant 2\frac{(1+\mu_1)}{\mu_1\zeta}\|\boldsymbol{L\gamma}\|, \textit{ for all } \boldsymbol{\gamma} = (\gamma_1, \gamma_2)^T, \gamma_k \in \mathbb{R}_0^{M+2} = \{r \in \mathbb{R}^{M+2} : r_0 = r_{M+1} = 0\}.$$

Proof. Following the approach of [94], we obtain the required result. □

Theorem 5.4.3. *Let* $\boldsymbol{z}$ *and* $\tilde{\boldsymbol{z}}$ *are the exact and approximate solutions to (5.1.3), respectively,*

on the eXp mesh, then

$$\|\boldsymbol{z} - \tilde{\boldsymbol{z}}\| \leqslant CM^{-2}.$$

Proof. The use of triangle inequality yields

$$\|z_k - \tilde{z}_k\| \leqslant \|z_k - I_2^1 z_k\| + \|I_2^1 z_k - \tilde{z}_k\|,$$

for $k = 1, 2$. Now making use of $\mathfrak{B}$-spline functions, we write the interpolant $I_2^1 z_k$ as

$$I_2^1 z_k(x) = \sum_{j=0}^{M+1} \beta_{j,k} \mathfrak{B}_j(x), \quad \text{for } k = 1, 2.$$

$$[\boldsymbol{L}(\boldsymbol{\alpha} - \boldsymbol{\beta})]_{j-1/2} = \boldsymbol{\mu}(I_2^1 \boldsymbol{z} - \boldsymbol{z})''_{j-1/2},\ j = 1, 2, \ldots, M,\ k = 1, 2.$$

Finally, Theorem 5.4.2 and Lemma 5.4.3 give

$$\|\boldsymbol{\alpha} - \boldsymbol{\beta}\| \leqslant CM^{-2}.$$

Since each $\mathfrak{B}_j \geqslant 0$ and the sum of all basis functions equals 1, so

$$\|I_2^1 \boldsymbol{z} - \tilde{\boldsymbol{z}}\| \leqslant \|\boldsymbol{\alpha} - \boldsymbol{\beta}\| \leqslant CM^{-2}.$$

The proof is finally completed by applying Theorem 5.4.2. □

5.5 Numerical illustrations

In this section, we verify the theoretical results obtained in the previous section by implementing our numerical method on two test problems. The exact solution for both test problems is unavailable, so we use the double-mesh principle [112] to calculate the error estimates and orders of convergence. We define a maximum pointwise error as

$$E_{k,\mu}^M = \max_j |\widetilde{z}_k(t_{2j-1}) - \hat{z}_k(t_{j-1/2})|, \quad k = 1, 2,$$

taking M and $2M$ intervals in consideration, $\hat{z}_k$ and $\widetilde{z}_k$ denote the computed solutions on these intervals respectively. The following formula gives the associated orders of convergence

$$\chi_{k,\mu}^{M} = \log_2 \left(\frac{E_{k,\mu}^{M}}{E_{k,\mu}^{2M}} \right), \quad k = 1, 2.$$

Uniform errors E_k^M, for each fixed M are obtained by taking the maximum of $E_{k,\mu}^M$ over a finite range of μ values ranging over $S = \{\mu | \mu = 2^{-8}, 2^{-12}, \ldots, 2^{-30}\}$,

$$E_k^M = \max_{\mu \in S} E_{k,\mu}^M, \quad k = 1, 2,$$

Moreover, the associated orders of parameter uniform convergence χ_k^M are given by

$$\chi_{k}^{M} = \log_2 \left(\frac{E_{k}^{M}}{E_{k}^{2M}} \right), \quad k = 1, 2.$$

We have also calculated the overall error $\boldsymbol{E}^M$ and corresponding orders of convergence as follows:

$$\begin{aligned} \boldsymbol{E}^M &= \max_k (\max_{\mu \in S} E_{k,\mu}^M), \\ \boldsymbol{\chi}^M &= \log_2 \left(\frac{\boldsymbol{E}^M}{\boldsymbol{E}^{2M}} \right). \end{aligned}$$

Additionally, we have also determined μ-uniform error constants C_1^M, C_2^M (see [113], Chapter 8, page 166, for the computational algorithm) to confirm this analogy. The exact and numerical solutions components are denoted as z_k and $\widetilde{z}_k$, respectively. Moreover, the solution in the vector form is represented by bold letters.

Example 5.5.1. *In this example, we consider the following fourth-order, two-point BVP:*

$$\begin{aligned} &-\mu z^{(4)}(t) + (6 - t^2) z''(t) + 2z(t) = -(10t + 1), \quad t \in (0, 1), \\ &z(0) = 1, z(1) = 1, \ z''(0) = -1, \ z''(1) = -1. \end{aligned}$$

Example 5.5.2. *In this example, we consider the following two-point BVP:*

$$-\mu z^{(4)}(t) + 5\exp(1-t)z''(t) + (1+t^3)z(t) = -2\exp(t), \quad t \in (0,1),$$
$$z(0) = 1, z(1) = 1,\ z''(0) = -1,\ z''(1) = -1.$$

As the first equation of the system (second-order differential equation in the first component z_1) is independent of the perturbation parameter, we do not observe steep boundary layers in the first component (refer to [120]). In contrast, the second component exhibits twin boundary layers in the neighborhood of the left and right ends of the domain. As mentioned earlier, the uniform mesh is not a good choice to resolve these boundary layers, which is also confirmed by the results of the test problems for which we obtain negative orders of convergence (refer to Tables 5.1 and 5.2). One cannot procure their aim of obtaining parameter uniform measures on this mesh. So, here, we preferred eXp mesh to obtain the numerical results for both problems. Tables 5.3, 5.4, 5.5, and 5.6 validate the parameter-uniform results for the solutions $\widetilde{z}_1$ and $\widetilde{z}_2$ in Examples 5.5.1 and 5.5.2, which are uniformly convergent of $O(M^{-2})$. These tables confirm the theoretical fact that μ-uniform errors show monotonically decreasing behavior as the number of mesh intervals M increases. Additionally, we have also determined μ-uniform orders of convergence $\boldsymbol{\chi}^M$ and μ-uniform error constants ($\boldsymbol{C}^M = \max_k C_k^M$) to confirm this analogy.

A comparison of computed results between three meshes (eXp, Shishkin, and Bakhvalov-Shishkin (B-S) mesh) is provided in Tables 5.7 and 5.8. One can observe that results on the Shishkin mesh are almost second-order convergent (which is $O(M^{-2}\ln^2 M)$), whereas on the eXp mesh and B-S mesh, obtained results give second-order accuracy with lesser errors compared to the Shishkin mesh.

Furthermore, we display combined plots of described meshes (eXp, Shishkin, and B-S meshes) in Fig. 5.1 for different values of μ, which shows the distribution of mesh points in different regions (layer and regular) of the domain. As mentioned in [91], eXp mesh and B-S mesh are both excellent choices for these types of problems, differ by a slight variation in the selection of mesh generating function $\Psi(\varrho)$. We have demonstrated the appearance of the boundary layer in the solution component $\widetilde{z}_2$ by plotting the graphs of the solution. From

Table 5.1: Maximum pointwise errors in the solutions on uniform mesh for $\mu = 2^{-28}$ for Examples 5.5.1

	$\widetilde{z}_1$		$\widetilde{z}_2$	
M	$E^M_{1,\mu}$	$\chi^M_{1,\mu}$	$E^M_{2,\mu}$	$\chi^M_{2,\mu}$
32	$3.222e-06$	2.021	$7.437e-06$	-2.045
64	$7.933e-07$	2.011	$3.071e-05$	-2.001
128	$1.967e-07$	2.005	$1.230e-04$	-1.995
256	$4.899e-08$	2.002	$4.906e-04$	-1.978
512	$1.222e-08$	2.001	$1.933e-03$	-1.913
1024	$3.052e-09$	-	$7.283e-03$	-

Table 5.2: Maximum pointwise errors in the solutions on uniform mesh for $\mu = 2^{-28}$ for Examples 5.5.2

	$\widetilde{z}_1$		$\widetilde{z}_2$	
M	$E^M_{1,\mu}$	$\chi^M_{1,\mu}$	$E^M_{2,\mu}$	$\chi^M_{2,\mu}$
32	$9.993e-06$	2.010	$9.994e-06$	0.109
64	$2.480e-06$	2.006	$9.261e-06$	-2.012
128	$6.172e-07$	2.003	$3.737e-05$	-1.997
256	$1.539e-07$	2.001	$1.492e-04$	-1.979
512	$3.844e-08$	2.000	$5.884e-04$	-1.914
1024	$9.604e-09$	-	$2.218e-03$	-

Fig. 5.2, it is noticed that the boundary layers for $\mu = 10^{-6}$ are stiffer (refer Figs. 5.2(b) and 5.2(d)) as compared to boundary layers for $\mu = 10^{-3}$ (refer Figs. 5.2(a) and 5.2(c)) which validates the theory, that for SPBVPs the width of the boundary layer decreases as μ decreases.

Remark 5.5.1. *In Fig. 5.2, z_k^{Δ} represents the k^{th} component of the numerical solution on the partition Δ.*

5.6 Concluding remarks

A numerical scheme comprising the quadratic $\mathfrak{B}$-splines on the eXp mesh is investigated for the fourth-order singularly perturbed BVPs. The primary motivation to adopt the exponentially graded mesh is that it does not need prior knowledge about the transition parameter *i.e.,* it is independent of the transition point(s). In contrast, other meshes like Bakhvalov and Shishkin-

Table 5.3: Maximum pointwise errors $E^M_{1,\mu}$ in the solution $\widetilde{z}_1$ for Example 5.5.1

	M					
μ	32	64	128	256	512	1024
2^{-8}	$2.3461e-05$	$6.5592e-06$	$1.7130e-06$	$4.3602e-07$	$1.0987e-07$	$2.7845e-08$
	1.8387	1.9370	1.9741	1.9886	1.9803	
2^{-12}	$1.7630e-05$	$5.4024e-06$	$1.4923e-06$	$3.9199e-07$	$1.0048e-07$	$2.5456e-08$
	1.7064	1.8561	1.9286	1.9639	1.9808	
2^{-16}	$7.8702e-06$	$2.2170e-06$	$6.0518e-07$	$1.6076e-07$	$4.1381e-08$	$1.0460e-08$
	1.8278	1.8732	1.9125	1.9579	1.9841	
2^{-20}	$9.4327e-06$	$2.5722e-06$	$6.7291e-07$	$1.7210e-07$	$4.3556e-08$	$1.0792e-08$
	1.8747	1.9345	1.9672	1.9823	2.0129	
2^{-24}	$1.0122e-05$	$2.7735e-06$	$7.2530e-07$	$1.8550e-07$	$4.6697e-08$	$1.1990e-08$
	1.8677	1.9351	1.9672	1.9900	1.9615	
2^{-28}	$1.0332e-05$	$2.8294e-06$	$7.4052e-07$	$1.8912e-07$	$4.7259e-08$	$9.9457e-09$
	1.8368	1.9657	1.9692	2.0006	2.2484	
2^{-30}	$1.0367e-05$	$2.8387e-06$	$7.4314e-07$	$1.9022e-07$	$4.8853e-08$	$1.1572e-08$
	1.8687	1.9335	1.9660	1.9611	2.0778	
E^M_1	$2.3461e-05$	$6.5592e-06$	$1.7130e-06$	$4.3602e-07$	$1.0987e-07$	$2.7845e-08$
χ^M_1	1.8387	1.9370	1.9741	1.9886	1.9803	
C^M_1	0.0142	0.0155	0.0162	0.0166	0.0171	0.0162

Table 5.4: Maximum pointwise errors $E^M_{2,\mu}$ in the solution $\widetilde{z}_2$ for Example 5.5.1

	M					
μ	32	64	128	256	512	1024
2^{-8}	$8.2846e-03$	$2.4950e-03$	$6.4062e-04$	$1.5738e-04$	$3.8850e-05$	$9.6341e-06$
	1.7314	1.9615	2.0252	2.0183	2.0117	
2^{-12}	$8.4202e-03$	$2.5451e-03$	$6.5380e-04$	$1.6060e-04$	$3.9655e-05$	$9.8330e-06$
	1.7261	1.9608	2.0254	2.0179	2.0118	
2^{-16}	$8.4448e-03$	$2.5521e-03$	$6.5572e-04$	$1.6108e-04$	$3.9774e-05$	$9.8626e-06$
	1.7264	1.9605	2.0253	2.0179	2.0118	
2^{-20}	$8.4513e-03$	$2.5539e-03$	$6.5621e-04$	$1.6120e-04$	$3.9805e-05$	$9.8702e-06$
	1.7265	1.9605	2.0253	2.0179	2.0118	
2^{-24}	$8.4530e-03$	$2.5543e-03$	$6.5634e-04$	$1.6124e-04$	$3.9812e-05$	$9.8721e-06$
	1.7261	1.9604	2.0252	2.0179	2.0117	
2^{-28}	$8.4534e-03$	$2.5545e-03$	$6.5637e-04$	$1.6124e-04$	$3.9814e-05$	$9.8726e-06$
	1.7265	1.9605	2.0253	2.0179	2.0118	
2^{-30}	$8.4535e-03$	$2.5545e-03$	$6.5638e-04$	$1.6125e-04$	$3.9815e-05$	$9.8727e-06$
	1.7265	1.9605	2.0253	2.0179	2.0118	
E^M_2	$8.4535e-03$	$2.5545e-03$	$6.5638e-04$	$1.6125e-04$	$3.9815e-05$	$9.8727e-06$
χ^M_2	1.7265	1.9605	2.0253	2.0179	2.0118	
C^M_2	11.5418	13.9509	14.3388	14.0898	13.9163	13.8031

Table 5.5: Maximum pointwise errors $E_{1,\mu}^M$ in the solution $\widetilde{z}_1$ for Example 5.5.2

	M					
μ	32	64	128	256	512	1024
2^{-8}	$2.7497e-05$	$7.3428e-06$	$1.8792e-06$	$4.7392e-07$	$1.1890e-07$	$2.9804e-08$
	1.9049	1.9662	1.9874	1.9949	1.9962	
2^{-12}	$1.4878e-05$	$4.5389e-06$	$1.2507e-06$	$3.2812e-07$	$8.3969e-08$	$2.1297e-08$
	1.7128	1.8596	1.9304	1.9663	1.9792	
2^{-16}	$2.4553e-05$	$6.6558e-06$	$1.7312e-06$	$4.4143e-07$	$1.1145e-07$	$2.7981e-08$
	1.8832	1.9428	1.9715	1.9858	1.9939	
2^{-20}	$2.9922e-05$	$8.2465e-06$	$2.1653e-06$	$5.5497e-07$	$1.4049e-07$	$3.5223e-08$
	1.8594	1.9292	1.9641	1.9819	1.9959	
2^{-24}	$3.1399e-05$	$8.6892e-06$	$2.2890e-06$	$5.8722e-07$	$1.4843e-07$	$3.8089e-08$
	1.8534	1.9245	1.9627	1.9841	1.9623	
2^{-28}	$3.1776e-05$	$8.8037e-06$	$2.3207e-06$	$5.9564e-07$	$1.5037e-07$	$3.7029e-08$
	1.8518	1.9235	1.9620	1.9859	2.0218	
2^{-30}	$3.1839e-05$	$8.8233e-06$	$2.3259e-06$	$5.9755e-07$	$1.5375e-07$	$3.3171e-08$
	1.8514	1.9234	1.9607	1.9585	2.2126	
E_1^M	$3.1839e-05$	$8.8233e-06$	$2.3259e-06$	$5.9755e-07$	$1.5375e-07$	$3.3171e-08$
χ_1^M	1.8514	1.9234	1.9607	1.9585	2.2126	
C_1^M	0.0435	0.0482	0.0508	0.0522	0.0537	0.0526

Table 5.6: Maximum pointwise errors $E_{2,\mu}^M$ in the solution $\widetilde{z}_2$ for Example 5.5.2

	M					
μ	32	64	128	256	512	1024
2^{-8}	$7.3662e-03$	$3.3448e-03$	$9.2219e-04$	$2.3204e-04$	$5.7190e-05$	$1.4139e-05$
	1.1390	1.8588	1.9907	2.0205	2.0161	
2^{-12}	$7.2268e-03$	$3.3181e-03$	$9.1534e-04$	$2.3040e-04$	$5.6795e-05$	$1.4039e-05$
	1.1230	1.8580	1.9902	2.0203	2.0163	
2^{-16}	$7.1859e-03$	$3.3049e-03$	$9.1156e-04$	$2.2943e-04$	$5.6553e-05$	$1.3979e-05$
	1.1206	1.8582	1.9903	2.0204	2.0163	
2^{-20}	$7.1757e-03$	$3.3016e-03$	$9.1061e-04$	$2.2918e-04$	$5.6492e-05$	$1.3964e-05$
	1.1200	1.8583	1.9904	2.0204	2.0163	
2^{-24}	$7.1731e-03$	$3.3008e-03$	$9.1038e-04$	$2.2912e-04$	$5.6477e-05$	$1.3961e-05$
	1.1198	1.8583	1.9904	2.0204	2.0163	
2^{-28}	$7.1725e-03$	$3.3006e-03$	$9.1032e-04$	$2.2911e-04$	$5.6473e-05$	$1.3960e-05$
	1.1197	1.8582	1.9903	2.0204	2.0163	
2^{-30}	$7.1724e-03$	$3.3006e-03$	$9.1031e-04$	$2.2910e-04$	$5.6472e-05$	$1.3960e-05$
	1.1197	1.8582	1.9903	2.0204	2.0163	
E_2^M	$7.3662e-03$	$3.3448e-03$	$9.2219e-04$	$2.3204e-04$	$5.7190e-05$	$1.4139e-05$
χ_2^M	1.1390	1.8588	1.9907	2.0205	2.0161	
C_2^M	9.7927	18.0255	19.8860	20.0194	19.7385	19.5169

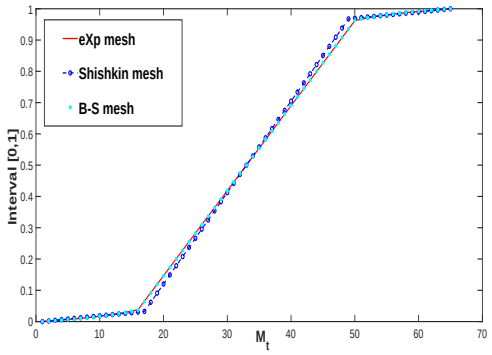

(a) $\mu = 2^{-8}$

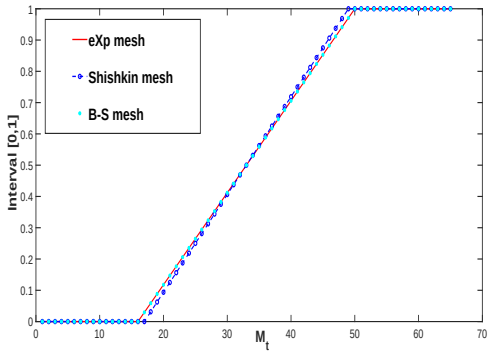

(b) $\mu = 2^{-20}$

Figure 5.1: Mesh comparison of eXp mesh, Shishkin mesh, and B-S mesh for $M = 64$

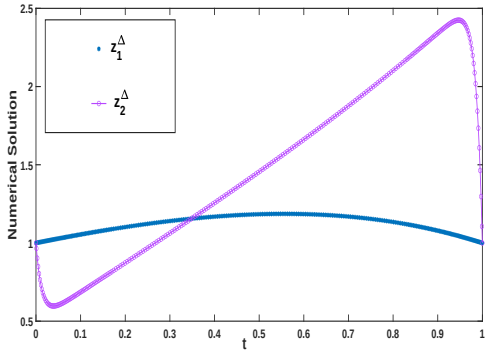

(a) $M = 256,\ \mu = 10^{-3}$

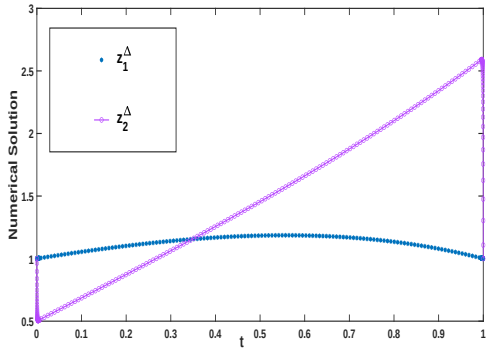

(b) $M = 256,\ \mu = 10^{-6}$

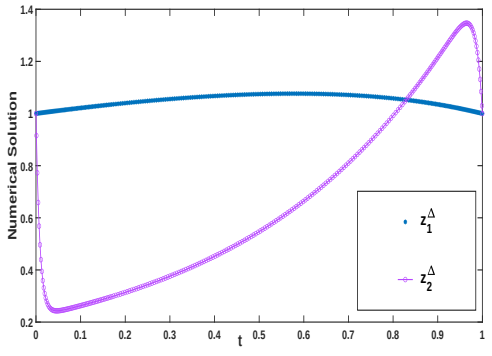

(c) $M = 256,\ \mu = 10^{-3}$

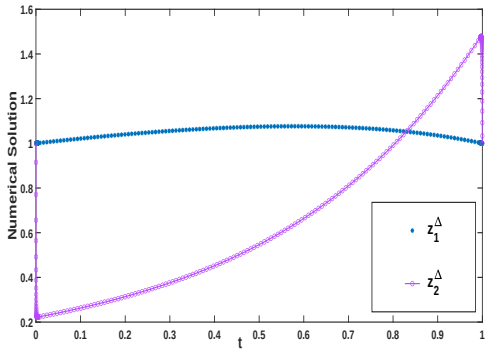

(d) $M = 256,\ \mu = 10^{-6}$

Figure 5.2: Numerical solution plots of Example 5.5.1 (subfigures (a) and (b)), and Example 5.5.2 (subfigures (c) and (d))

Table 5.7: Uniform maximum pointwise errors comparison in the solution for Example 5.5.1

	eXp mesh			Shishkin mesh			B-S mesh		
M	$\boldsymbol{E}^M$	$\boldsymbol{\chi}^M$	$\boldsymbol{C}^M$	$\boldsymbol{E}^M$	$\boldsymbol{\chi}^M$	$\boldsymbol{C}^M$	$\boldsymbol{E}^M$	$\boldsymbol{\chi}^M$	$\boldsymbol{C}^M$
32	$8.453e-03$	1.726	11.54	$1.681e-02$	0.727	5.75	$8.104e-03$	1.713	11.06
64	$2.554e-03$	1.960	13.95	$1.015e-02$	1.252	10.28	$2.472e-03$	1.936	13.49
128	$6.564e-04$	2.025	14.33	$4.261e-03$	1.565	12.77	$6.460e-04$	2.013	14.11
256	$1.612e-04$	2.017	14.08	$1.440e-03$	1.667	12.77	$1.600e-04$	2.012	13.98
512	$3.981e-05$	2.011	13.91	$4.534e-04$	1.715	11.90	$3.966e-05$	2.009	13.86
1024	$9.873e-06$	-	13.80	$1.381e-04$	-	10.72	$9.853e-06$	-	13.77

Table 5.8: Uniform maximum pointwise errors comparison in the solution for Example 5.5.2

	eXp mesh			Shishkin mesh			B-S mesh		
M	$\boldsymbol{E}^M$	$\boldsymbol{\chi}^M$	$\boldsymbol{C}^M$	$\boldsymbol{E}^M$	$\boldsymbol{\chi}^M$	$\boldsymbol{C}^M$	$\boldsymbol{E}^M$	$\boldsymbol{\chi}^M$	$\boldsymbol{C}^M$
32	$7.172e-03$	1.139	9.79	$9.955e-03$	0.300	1.72	$7.019e-03$	1.713	9.58
64	$3.301e-03$	1.858	18.02	$8.127e-03$	0.791	3.57	$3.220e-03$	1.936	17.58
128	$9.103e-04$	1.990	19.88	$4.695e-03$	1.343	5.23	$8.973e-04$	2.013	19.60
256	$2.291e-04$	2.020	20.01	$1.850e-03$	1.620	5.23	$2.273e-04$	2.012	19.86
512	$5.467e-05$	2.016	19.73	$6.018e-04$	1.706	4.31	$5.625e-05$	2.009	19.66
1024	$1.396e-05$	-	19.51	$1.844e-04$	-	3.35	$1.393e-05$	-	19.47

type meshes need this information in advance. The computed theoretical bounds on the spline interpolation error reveal that the method is second-order parameter-uniformly convergent. The numerical outcomes displayed in the tables verify the theoretical estimates on the orders of convergence and the errors evaluated in Section 5.4.

Chapter 6

Uniformly convergent scheme for fourth-order singularly perturbed convection-diffusion ODE

Convection-diffusion with fourth-order singular perturbation ODEs cross theoretical borders to have a tangible impact on various fields. Their solutions shed light on the mysterious subtleties that lie dormant inside nature and give us a glimpse into the fundamental principles that regulate different physical processes. The appearance of boundary layers is one of the defining characteristics of these equations. These layers provide locations in which the solutions undergo abrupt changes. This intricate feature offers an ideal foundation for research, with their analysis revealing how the system navigates steep gradients and evolves.

6.1 Introduction

Motivated by the work of Shanthi and Ramanujam [123, 124], in this chapter, the following singularly perturbed convection-diffusion type fourth-order boundary value problem (BVP) will be in consideration

---

The work of this chapter has been published in the following publication:
S. Singh, D. Kumar, V. Shanthi, "Uniformly convergent scheme for fourth-order singularly perturbed convection-diffusion ODE." Appl. Numer. Math., 186 (2023), 334–357.

$$-\varepsilon y^{(4)}(x) - a(x)y'''(x) + b(x)y''(x) + c(x)y'(x) - d(x)y(x) = -f(x), \quad x \in \mathfrak{D} = (0,1), \tag{6.1.1a}$$

subject to the following boundary conditions (BCs)

$$y(0) = q_1,\ y(1) = q_3,\ y''(0) = -q_2,\ y''(1) = -q_4. \tag{6.1.1b}$$

Choosing a particular type of BCs motivated by [35] helps us to establish uniform stability estimates and other results. To extend the maximum principle theory, we transform (6.1.1a)-(6.1.1b) into a system of two strongly/weakly coupled singularly perturbed systems (depending on the coefficient of the first order derivative) of second-order ordinary differential equations (ODEs) (refer [125] for the definition of strongly/weakly coupled systems) with Dirichlet BCs. We assume $a(x)$, $b(x)$, $c(x)$, $d(x)$, and $f(x)$ to be sufficiently smooth that satisfy the following conditions

$$a(x) \geqslant \alpha^* > 0,\ b(x) \geqslant \beta^* > 0, \tag{6.1.2a}$$

$$c(x) \geqslant \gamma^* > 0,\ 0 \geqslant d(x) \geqslant -\delta^*,\ \delta^* > 0, \tag{6.1.2b}$$

$$\alpha^* - \delta^*(1+\zeta^*) \geqslant \eta^* > 0, \text{ for some } \eta^* \text{ and } \zeta^* > 0, \tag{6.1.2c}$$

for $x \in \overline{\mathfrak{D}}$.

Under these assumptions the BVP (6.1.1a)-(6.1.1b) has a unique solution $y(x)$ exhibiting a less severe boundary layer at $x = 0$ [35, 112]. The 'less severe' means the solution $y(x)$ of the BVP (6.1.1a)-(6.1.1b) and its first derivative are bounded uniformly, for all ε on the interval $[0, 1]$. It may be noted that the reduced problem satisfies the boundary condition at $x = 0$ exactly [35]. The applications of the problem mentioned above can be seen in reactor theory [126], traveling of water waves [127], pattern formation in second-order materials, and traveling waves in suspension bridges [128]. Fourth-order differential equations like extended Fisher-Kolmogorov equations [129], Swift-Hohenberg equation [130], Euler-Bernoulli beam equation [131], and Benjamin-Ono equation appear in different fields and explains several

mathematical and physical phenomena.

Existence of a unique solution $y(x) \in C^4(\mathfrak{D}) \cap C^2(\overline{\mathfrak{D}})$ guaranteed by the assumptions made in the equations (6.1.2a)-(6.1.2c) (see [132]). We convert the BVP (6.1.1a)-(6.1.1b) into a simpler form as follows

$$\begin{aligned} \boldsymbol{\mathcal{L}}\boldsymbol{y}(x) &= \boldsymbol{f}(x),\ x \in \mathfrak{D}, \\ \boldsymbol{y}(0) &= (q_1, q_2)^T,\ \boldsymbol{y}(1) = (q_3, q_4)^T, \end{aligned}$$

which is equivalent to

$$\mathcal{L}_1\boldsymbol{y}(x) \equiv -y_1''(x) - y_2(x) = 0,\ x \in \mathfrak{D}, \tag{6.1.3a}$$

$$\mathcal{L}_2\boldsymbol{y}(x) \equiv -\varepsilon y_2''(x) - a(x)y_2'(x) - c(x)y_1'(x) + b(x)y_2(x) + d(x)y_1(x) = f(x),\ x \in \mathfrak{D}, \tag{6.1.3b}$$

$$y_1(0) = q_1,\ y_1(1) = q_3,\ y_2(0) = q_2,\ y_2(1) = q_4, \tag{6.1.3c}$$

which can be written in a simpler way as

$$\boldsymbol{\mathcal{L}}\boldsymbol{y}(x) \equiv \begin{bmatrix} \mathcal{L}_1\boldsymbol{y}(x) \\ \mathcal{L}_2\boldsymbol{y}(x) \end{bmatrix} \equiv \begin{bmatrix} -\dfrac{d^2}{dx^2} & 0 \\ 0 & -\varepsilon\dfrac{d^2}{dx^2} \end{bmatrix} \boldsymbol{y} - \mathcal{A}(x)\boldsymbol{y}' + \mathcal{B}(x)\boldsymbol{y} = \boldsymbol{f}(x),$$

where $\mathcal{A}(x) = \begin{bmatrix} 0 & 0 \\ c(x) & a(x) \end{bmatrix}$, $\mathcal{B}(x) = \begin{bmatrix} 0 & -1 \\ d(x) & b(x) \end{bmatrix}$, $\boldsymbol{y}(x) = (y_1(x), y_2(x))^T$, $\boldsymbol{\mathcal{L}} = (\mathcal{L}_1, \mathcal{L}_2)^T$, and $\boldsymbol{f}(x) = (0, f(x))^T$. The system (6.1.3) will be in consideration in place of (6.1.1) in our analysis in the remaining chapter.

Remark 6.1.1. *The fourth-order ODEs are reduced into a system of two second-order ODEs using the given BCs of the kind (6.1.1b). According to the condition, the singularly perturbed problem is a non-turning point issue (6.1.2a). Condition (6.1.2b) is applied to ensure that the aforementioned system (6.1.3a)-(6.1.3c) is "quasi-monotone" (see definition 2.3 in [119]). To obtain the maximum principle for the SPBVP (6.1.3a)-(6.1.3c), the conditions (6.1.2a)-(6.1.2c) are adequate. The last criterion (6.1.2c) is combined with the maximum principle to*

arrive at a stable outcome.

In current years, constructing the numerical techniques for fourth-order SPODEs has been successfully attempted by several researchers. For the reaction-diffusion class of fourth-order ODEs in 2002, Shanthi and Ramanujam suggested an exponentially fitted finite difference method (EFFDM) for linear and nonlinear BVPs. In [124], the authors used the boundary value technique (BVT), which includes EFFDM in the layer region and classical FDM away from the layer region. In [133], Shanthi and Ramanujam used the fitted operator method (FOM), fitted mesh method (FMM), and BVT for the respective class of BVP. Das and Natesan [120] used the adaptive mesh via equidistribution of a monitor function and developed a second-order uniformly convergent scheme. Using the Vulanović-Shishkin mesh, Cen *et al.* [121] constructed an almost fourth-order hybrid FDM combining non-equidistant generalized Numerov and the central difference schemes. Recently, Singh and Kumar [134] analyzed quadratic $\mathfrak{B}$-splines-based technique using eXp mesh and showed second-order parameter uniform convergent results.

For the convection-diffusion type SPBVPs in [123], the authors employed BVT to find the numerical solution. In 2016, Chandru and Shanthi [135] considered fourth-order SPBVP with a turning point in the domain. They converted the considered problem into a weakly coupled system of two second-order ODEs and implemented their asymptotic numerical scheme on linear and nonlinear problems. After going through the cited literature and their references, spline approximations are not new for singular perturbation, but currently, it is less explored for the higher order singularly perturbed problems. In most cases, we see the presence of a logarithmic factor in the convergence part of the method, but here, the use of quadratic $\mathfrak{B}$-spline with a graded mesh provides a second-order convergence (without logarithmic factor). We intend to construct a parameter uniform approximation for the problem (6.1.1) by applying $\mathfrak{B}$-spline's collocation technique on the eXp mesh. Along with this, we also explore the proposed method for nonlinear problems.

The present piece of work is systematized as follows. Section 6.2 contains the analytic properties of the continuous solution of SPBVP (6.1.1) and its equivalent form (6.1.3) and derivatives bounds of the components. The execution and construction of the numerical scheme are given in Section 6.3, along with the properties of the eXp mesh. Section 6.4

examines the convergence estimates in detail and offers second-order uniform accuracy. Section 6.5 is devoted to the nonlinear BVPs, which include the quasilinearization technique for nonlinear problems. After linearizing, it is easy to implement the proposed method. In supporting the provided convergence, we give computational results in Section 6.6. The present manuscript completes with concluding comments in Section 6.7.

Throughout the chapter, we denote C as a positive generic constant that takes different values at different places and $\boldsymbol{C} = (C, C)$. Moreover, $C_i,\ i = 1, 2, \ldots, 11$ are fixed constants.

6.2 Analytical results

6.2.1 Maximum principle and stability result

Here, we state some basic results without proofs for the BVP (6.1.3a)-(6.1.3c). These results can be proved using the procedures adopted in [124, 132].

Theorem 6.2.1. *Consider the BVP (6.1.3a)-(6.1.3c), assume that* $\mathcal{L}_1\boldsymbol{y} \geq 0$, $\mathcal{L}_2\boldsymbol{y} \geq 0$ *in* $\mathfrak{D}$, $y_1(0) \geq 0$, $y_1(1) \geq 0$, $y_2(0) \geq 0$, *and* $y_2(1) \geq 0$. *Then,* $\boldsymbol{y}(x) \geq 0$, *in* $\overline{\mathfrak{D}}$.

Proof. Follow the approach of [132] for the proof. □

Lemma 6.2.1. *Consider the BVP (6.1.3a)-(6.1.3c). If* $\boldsymbol{y}$ *is a smooth function, then*

$$\|\boldsymbol{y}\| \leq C \max\{|y_1(0)|, |y_2(0)|, |y_1(1)|, |y_2(1)|, \max_{x\in\mathfrak{D}} |\mathcal{L}_1\boldsymbol{y}|, \max_{x\in\mathfrak{D}} |\mathcal{L}_2\boldsymbol{y}|\},$$

where $\|\boldsymbol{y}\| = \max\{|y_1(x)|, |y_2(x)|\}$.

Lemma 6.2.2. *For* $k = 1, 2$, *we have the following bounds*

$$|y_1^{(k)}| \leq C,\ |y_2^{(k)}| \leq C(1 + \varepsilon^{-k}),$$

and

$$|y_1^{(k+2)}| \leq C(1 + \varepsilon^{-k}),\ |y_2^{(k+2)}| \leq C\varepsilon^{-2}(1 + \varepsilon^{-k}).$$

Proof. We have the required proof by using the result of Lemma 6.2.1 and applying the arguments of [112, 113]. □

The proof of parameter-uniform convergence requires sharper bounds for the exact solution and its derivatives of the system (6.1.3). For this, we decompose the solution $\boldsymbol{y}(x)$ into two parts

$$\boldsymbol{y}(x) = \boldsymbol{v}(x) + \boldsymbol{w}(x), \tag{6.2.1}$$

where $\boldsymbol{v}(x) = (v_1, v_2)^T$, $\boldsymbol{w}(x) = (w_1(x), w_2(x))^T$ are the regular and singular components of $\boldsymbol{y}(x)$, respectively.

Theorem 6.2.2. *If $a(x)$, $b(x)$, $c(x)$, $d(x)$, and $f(x) \in C^4(\overline{\mathfrak{D}})$. Then the components $\boldsymbol{v}(x)$, $\boldsymbol{w}(x)$, and their derivatives have the following bounds*

$$|v_1^{(k)}(x)| \leqslant C, \quad |v_2^{(k)}(x)| \leqslant C(1+\varepsilon^{4-k}), \quad x \in \overline{\mathfrak{D}},\ 0 \leqslant k \leqslant 4,$$
$$|w_1^{(k)}(x)| \leqslant C\varepsilon^{2-k}\exp(-x\alpha^*/\varepsilon), \quad |w_2^{(k)}(x)| \leqslant C\varepsilon^{-k}\exp(-x\alpha^*/\varepsilon), \quad x \in \overline{\mathfrak{D}},\ 0 \leqslant k \leqslant 4.$$

Proof. We use the minimum regularity of the coefficient functions a, b, c, d, and f to prove a higher-order decomposition of the analytical solution. The regular component can be written in the form $\boldsymbol{v} = \boldsymbol{v}_0 + \varepsilon\boldsymbol{v}_1 + \varepsilon^2\boldsymbol{v}_2 + \varepsilon^3\boldsymbol{v}_3 + \varepsilon^4\boldsymbol{v}_4$, where $\boldsymbol{v}_0 = (v_{01}, v_{02})^T$, $\boldsymbol{v}_1 = (v_{11}, v_{12})^T$, $\boldsymbol{v}_2 = (v_{21}, v_{22})^T$, $\boldsymbol{v}_3 = (v_{31}, v_{32})^T$, $\boldsymbol{v}_4 = (v_{41}, v_{42})^T$ and satisfies the following problems

$$\begin{bmatrix} -\dfrac{d^2}{dx^2} & 0 \\ 0 & 0 \end{bmatrix} \boldsymbol{v}_0 - \mathcal{A}(x)\boldsymbol{v}_0' + \mathcal{B}(x)\boldsymbol{v}_0 = \boldsymbol{f}(x),\ \boldsymbol{v}_0(1) = \boldsymbol{y}(1),$$
$$\begin{bmatrix} -\dfrac{d^2}{dx^2} & 0 \\ 0 & 0 \end{bmatrix} \boldsymbol{v}_1 - \mathcal{A}(x)\boldsymbol{v}_1' + \mathcal{B}(x)\boldsymbol{v}_1 = \begin{bmatrix} 0 & 0 \\ 0 & \dfrac{d^2}{dx^2} \end{bmatrix} \boldsymbol{v}_0,\ \boldsymbol{v}_1(1) = \boldsymbol{0},$$
$$\begin{bmatrix} -\dfrac{d^2}{dx^2} & 0 \\ 0 & 0 \end{bmatrix} \boldsymbol{v}_2 - \mathcal{A}(x)\boldsymbol{v}_2' + \mathcal{B}(x)\boldsymbol{v}_2 = \begin{bmatrix} 0 & 0 \\ 0 & \dfrac{d^2}{dx^2} \end{bmatrix} \boldsymbol{v}_1,\ \boldsymbol{v}_2(1) = \boldsymbol{0},$$
$$\begin{bmatrix} -\dfrac{d^2}{dx^2} & 0 \\ 0 & 0 \end{bmatrix} \boldsymbol{v}_3 - \mathcal{A}(x)\boldsymbol{v}_3' + \mathcal{B}(x)\boldsymbol{v}_3 = \begin{bmatrix} 0 & 0 \\ 0 & \dfrac{d^2}{dx^2} \end{bmatrix} \boldsymbol{v}_2,\ \boldsymbol{v}_3(1) = \boldsymbol{0},$$
$$\boldsymbol{\mathcal{L}v_4} = \begin{bmatrix} 0 & 0 \\ 0 & \dfrac{d^2}{dx^2} \end{bmatrix} \boldsymbol{v}_3,\ \boldsymbol{v}_4(0) = \boldsymbol{0},\ \boldsymbol{v}_4(1) = \boldsymbol{0}.$$

Thus

$$\boldsymbol{\mathcal{L}}\boldsymbol{v}(x) = \boldsymbol{f}(x),\ x \in \mathfrak{D}, \tag{6.2.2}$$

for suitably chosen $\boldsymbol{v}(0)$ and $\boldsymbol{v}(1)$. Moreover, the singular component is the solution to the following BVP

$$\boldsymbol{\mathcal{L}}\boldsymbol{w}(x) = 0,\ x \in \mathfrak{D}, \quad \boldsymbol{w}(0) = \boldsymbol{y}(0) - \boldsymbol{v}(0),\ \boldsymbol{w}(1) = 0. \tag{6.2.3}$$

We can apply the approach of [136] (by putting $\mu = 1$). For more details on this approach, one can refer [132, 137, 138]. With the mentioned decomposition and Lemma 6.2.2 the following bounds hold for $\boldsymbol{v}$

$$|v_1^{(k)}(x)| \leqslant C, \quad |v_2^{(k)}(x)| \leqslant C(1 + \varepsilon^{4-k}). \tag{6.2.4}$$

The appropriate choice of barrier function gives the following bounds on the components of $\boldsymbol{w}$

$$|w_1(x)| \leqslant C_1\varepsilon^2(1 - \exp(-x\alpha^*/\varepsilon)), \tag{6.2.5a}$$

$$|w_2(x)| \leqslant C_1\varepsilon^2(1 - \exp(-x\alpha^*/\varepsilon)) + C_2\alpha^* \exp(-x\alpha^*/\varepsilon). \tag{6.2.5b}$$

Using the argument of [112, 113, 136], the first order derivatives satisfy

$$|w_1'(x)| \leqslant C_1\varepsilon \exp(-x\alpha^*/\varepsilon), \tag{6.2.6a}$$

$$|w_2'(x)| \leqslant C_1\varepsilon \exp(-x\alpha^*/\varepsilon) + C_2\varepsilon^{-1}\alpha^* \exp(-x\alpha^*/\varepsilon), \tag{6.2.6b}$$

$$\leqslant C\varepsilon^{-1} \exp(-x\alpha^*/\varepsilon). \tag{6.2.6c}$$

We use differential equations to get the bounds for second-order derivatives

$$|w_1''(x)| \leqslant C \exp(-x\alpha^*/\varepsilon), \tag{6.2.7a}$$

$$|w_2''(x)| \leqslant C(1 - \exp(-x\alpha^*/\varepsilon)) + C\varepsilon^{-2} \exp(-x\alpha^*/\varepsilon). \tag{6.2.7b}$$

The third and fourth-order derivatives satisfy

$$|w_1'''(x)| \leqslant C\varepsilon^2(1+\varepsilon^{-3}\exp(-x\alpha^*/\varepsilon)), \tag{6.2.8a}$$

$$|w_2'''(x)| \leqslant C\varepsilon^{-1}(1+\varepsilon^{-2}\exp(-x\alpha^*/\varepsilon)), \tag{6.2.8b}$$

$$|w_1''''(x)| \leqslant C(1+\varepsilon^{-2}\exp(-x\alpha^*/\varepsilon)), \tag{6.2.8c}$$

$$|w_2''''(x)| \leqslant C\varepsilon^{-2}(1+\varepsilon^{-2}\exp(-x\alpha^*/\varepsilon)). \tag{6.2.8d}$$

Thus, we have obtained the required bounds. The asymptotic expansion approach of [132] can also be used. In [138], a third-order convection-diffusion type problem is considered, but the approach of proving the bounds can be followed. □

6.3 The suggested numerical method

This section includes the construction of the eXp mesh, pursued by the construction and implementation of the method to the problem (6.1.3).

6.3.1 Construction of the mesh

A combination of standard numerical techniques with a uniform mesh delivers unsatisfactory results (not parameter-uniform) because of the solution oscillations near the layer region unless a large number of mesh points is considered; that is practically impossible. Thus, one feels the necessity of layer-resolving mesh, and non-uniform meshes are suitable for this purpose. This section will produce a particular type of eXp mesh that generates more mesh points in the layer region (in the neighborhood of the left part of the domain) than the regular part.

To construct the eXp mesh $\Delta^{N_x} = \{x_j |\ 0 \leqslant j \leqslant N_x\}$, the interval $[0,1]$ can be divided into $N_x > 2$ (multiple of 2) subintervals $I_j = [x_{j-1}, x_j]$. Construction of the mesh requires a piecewise continuously differentiable, monotonically increasing, and continuous mesh generating function $\Upsilon(\varrho)$, which is characterized as

$$\Upsilon(\varrho) = -\ln(1-2\phi_{\mathcal{P},\varepsilon}\varrho),\ \varrho \in [0, 1/2 - 1/N_x], \tag{6.3.1}$$

where $\mathcal{P}$ is the degree of the polynomial, $\phi_{\mathcal{P},\varepsilon} = 1 - \exp\left(-\frac{1}{(\mathcal{P}+1)\varepsilon}\right) \in \mathbb{R}^+$. We divide the interval $[0,1]$ as $[0,1] = [0, x_{\frac{N_x}{2}-1}] \cup [x_{\frac{N_x}{2}-1}, 1]$, where $x_{\frac{N_x}{2}-1}$ is the transition point. We write the grid points in the following format

$$x_j = \begin{cases} (\mathcal{P}+1)\varepsilon\Upsilon(\varrho_j), & j = 0, 1, \ldots, \frac{N_x}{2} - 1, \\ x_{\frac{N_x}{2}-1} + \left(\dfrac{1 - x_{\frac{N_x}{2}-1}}{\frac{N_x}{2}+1}\right), & j = \frac{N_x}{2}, \ldots, N_x, \end{cases}$$

where $\varrho_j = \frac{j}{N_x}$ for $j = 0, 1, \ldots, N_x$. The mesh points are distributed equidistantly in $[x_{\frac{N_x}{2}-1}, 1]$ with $N_x/2 + 1$ elements and exponentially graded in $[0, x_{\frac{N_x}{2}-1}]$ with $N_x/2 - 1$ elements. The step size $\hat{h}_j = x_j - x_{j-1}$, $j = 1, 2, \ldots, N_x$ fulfills the following inequalities using the function $\Theta = \exp(-\Upsilon)$, known as the mesh characterizing function (see [91] for more details)

$$\hat{h}_j \leqslant \begin{cases} C(\mathcal{P}+1)\varepsilon N_x^{-1} \max \Upsilon'(\varrho_j), & j = 1, 2, \ldots, \frac{N_x}{2} - 1, \\ C N_x^{-1}, & j = \frac{N_x}{2}, \ldots, N_x, \end{cases}$$

further on simplification

$$\hat{h}_j \leqslant \begin{cases} C(\mathcal{P}+1)\varepsilon N_x^{-1} \max |\Theta^{'}| \exp\left(\frac{x_j}{(\mathcal{P}+1)\varepsilon}\right), & j = 1, 2, \ldots, \frac{N_x}{2} - 1, \\ C N_x^{-1}, & j = \frac{N_x}{2}, \ldots, N_x. \end{cases}$$

As $\max |\Theta^{'}| \leqslant 2$, the above inequalities can be simplified as

$$\hat{h}_j \leqslant \begin{cases} C\varepsilon N_x^{-1} \exp\left(\frac{x_j}{(\mathcal{P}+1)\varepsilon}\right), & j = 1, 2, \ldots, \frac{N_x}{2} - 1, \\ C N_x^{-1}, & j = \frac{N_x}{2}, \ldots, N_x, \end{cases} \tag{6.3.2}$$

and for the mesh Δ^{N_x}, $\hat{h}_j$ also holds

$$|\hat{h}_{j+1} - \hat{h}_j| \leqslant C \begin{cases} \varepsilon N_x^{-2}, & j = 1, 2, \ldots, \frac{N_x}{2} - 1, \\ 0, & j = \frac{N_x}{2}, \ldots, N_x - 1. \end{cases} \tag{6.3.3}$$

Remark 6.3.1. *This analysis cannot be given for the meshes provided by Shishkin and Bakhvalov because of the violation of the condition* $|\hat{h}_{j+1} - \hat{h}_j| \leqslant CN_x^{-2}$ *in the vicinity of transition points (refer [94]).*

6.3.2 Execution of the collocation technique

In this section, we demonstrate the execution of our collocation technique to find the solution to the problem (6.1.3) using piecewise quadratic C^1-splines. We denote by χ_j, the collocation points obtained by taking an average of x_{j-1} and x_j *i.e.,*

$$\chi_j = x_{j-1/2} := \frac{x_{j-1} + x_j}{2} = x_{j-1} + \frac{\hat{h}_j}{2} = x_j - \frac{\hat{h}_j}{2}, \quad \text{for } j = 1, 2, \ldots, N_x.$$

For $\mathfrak{m}, \mathcal{P} \in \mathbb{N}\,(\mathfrak{m} < \mathcal{P})$, we define the following spaces

$$S_{\mathcal{P}}^{\mathfrak{m}}(\Delta^{N_x}) := \{r \in C^{\mathfrak{m}}[0,1] : \ r|_{I_j} \in \Pi_{\mathcal{P}}, \text{ for } j = 1, 2, \ldots, N_x\},$$

where $\Pi_{\mathcal{P}}$ is the set of all polynomials of degree $\leqslant \mathcal{P}$.

For the discretization of (6.1.3), we seek the quadratic splines $\mathfrak{B}_j(x) \in S_2^1(\Delta^{N_x}),\ j = 0, 1, \ldots, N_x + 1$ defined below that constitute the solution of BVP (6.1.3)

$$\mathfrak{B}_0(x) = \begin{cases} \dfrac{(x_1 - x)^2}{\hat{h}_1^2}, & x_0 \leqslant x \leqslant x_1, \\ 0, & \text{otherwise}, \end{cases}$$

$$\mathfrak{B}_1(x) = \begin{cases} \dfrac{\hat{h}_1^2 - (x_1 - x)^2}{\hat{h}_1^2} - \dfrac{(x - x_0)^2}{\hat{h}_1(\hat{h}_1 + \hat{h}_2)}, & x_0 \leqslant x \leqslant x_1, \\ \dfrac{(x_2 - x)^2}{\hat{h}_1(\hat{h}_1 + \hat{h}_2)}, & x_1 \leqslant x \leqslant x_2, \\ 0, & \text{otherwise}, \end{cases}$$

and for $j = 2, 3, \ldots, N_x - 1$,

$$\mathfrak{B}_j(x) = \begin{cases} \dfrac{(x - x_{j-2})^2}{\hat{h}_{j-1}(\hat{h}_{j-1} + \hat{h}_j)}, & x_{j-2} \leqslant x \leqslant x_{j-1}, \\ \dfrac{(x - x_{j-2})(x_j - x)}{\hat{h}_j(\hat{h}_{j-1} + \hat{h}_j)} + \dfrac{(x_{j+1} - x)(x - x_{j-1})}{\hat{h}_j(\hat{h}_j + \hat{h}_{j+1})}, & x_{j-1} \leqslant x \leqslant x_j, \\ \dfrac{(x_{j+1} - x)^2}{\hat{h}_{j+1}(\hat{h}_j + \hat{h}_{j+1})}, & x_j \leqslant x \leqslant x_{j+1}, \\ 0, & \text{otherwise}, \end{cases}$$

while for $j = N_x,\ N_x + 1$ these are defined as

$$\mathfrak{B}_{N_x}(x) = \begin{cases} \dfrac{(x - x_{N_x-2})^2}{\hat{h}_{N_x-1}(\hat{h}_{N_x-1} + \hat{h}_{N_x})}, & x_{N_x-2} \leqslant x \leqslant x_{N_x-1}, \\ \dfrac{\hat{h}_{N_x}^2 - (x - x_{N_x-1})^2}{\hat{h}_{N_x}^2} - \dfrac{(x_{N_x} - x)^2}{\hat{h}_{N_x}(\hat{h}_{N_x-1} + \hat{h}_{N_x})}, & x_{N_x-1} \leqslant x \leqslant x_{N_x}, \\ 0, & \text{otherwise}, \end{cases}$$

$$\mathfrak{B}_{N_x+1}(x) = \begin{cases} \dfrac{(x - x_{N_x-1})^2}{\hat{h}_{N_x}^2}, & x_{N_x-1} \leqslant x \leqslant x_{N_x}, \\ 0, & \text{otherwise}. \end{cases}$$

To discretize the Equation (6.1.3), we seek $\tilde{\boldsymbol{y}} \in S_2^1(\Delta^{N_x})$ such that

$$\tilde{\boldsymbol{y}}(0) = (q_1, q_2)^T, \quad (\boldsymbol{\mathcal{L}}\tilde{\boldsymbol{y}})_{j-1/2} = \boldsymbol{f}_{j-1/2}, \quad \tilde{\boldsymbol{y}}(1) = (q_3, q_4)^T, \quad j = 1, 2, \ldots, N_x. \tag{6.3.4}$$

Equation (6.3.4) can be rewritten in the components form as

$$\tilde{y}_1(0) = q_1, \quad (\mathcal{L}_1\tilde{\boldsymbol{y}})_{j-1/2} = 0, \quad \tilde{y}_1(1) = q_3,\ j = 1, 2, \ldots, N_x, \tag{6.3.5a}$$

$$\tilde{y}_2(0) = q_2, \quad (\mathcal{L}_2\tilde{\boldsymbol{y}})_{j-1/2} = f_{j-1/2}, \quad \tilde{y}_2(1) = q_4,\ j = 1, 2, \ldots, N_x. \tag{6.3.5b}$$

We represent the collocation solution $\tilde{\boldsymbol{y}}$ as

$$\tilde{y}_k(x) = \sum_{j=0}^{N_x+1} \lambda_{j,k}\mathfrak{B}_j(x), \quad k = 1, 2. \tag{6.3.6}$$

Use of (6.3.6) in (6.3.4) and (6.3.5) give the following system

$$\lambda_{0,k} = q_k, \quad [\boldsymbol{L\lambda}]_{j-1/2} = \boldsymbol{f}_{j-1/2},\ j = 1, 2, \ldots, N_x, \quad \lambda_{N_x+1,k} = q_{k+2},\ k = 1, 2, \tag{6.3.7}$$

which represent the same system given by the following equations

$$\lambda_{0,1} = q_1, \quad [L_1\boldsymbol{\lambda}]_{j-1/2} = 0, \quad \lambda_{N_x+1,1} = q_3,\ j = 1, 2, \ldots, N_x, \tag{6.3.8a}$$

$$\lambda_{0,2} = q_2, \quad [L_2\boldsymbol{\lambda}]_{j-1/2} = f_{j-1/2}, \quad \lambda_{N_x+1,2} = q_4,\ j = 1, 2, \ldots, N_x, \tag{6.3.8b}$$

with $\boldsymbol{\lambda} := (\lambda_{0,1}, \lambda_{1,1}, \ldots, \lambda_{N_x+1,1}, \lambda_{0,2}, \lambda_{1,2}, \ldots, \lambda_{N_x+1,2})^T \in \mathbb{R}^{2N_x+4}$, $\boldsymbol{L} := (L_1, L_2)^T$. The operators in (6.3.8) can be written in a simple way as

$$\begin{aligned}
[L_1\boldsymbol{\lambda}]_{j-1/2} :=& -\left[\frac{2(\lambda_{j+1,1} - \lambda_{j,1})}{\hat{h}_j(\hat{h}_j + \hat{h}_{j+1})} - \frac{2(\lambda_{j,1} - \lambda_{j-1,1})}{\hat{h}_j(\hat{h}_j + \hat{h}_{j-1})}\right] - \left[\widetilde{q}_j^{+}\lambda_{j+1,2} + \left(1 - \widetilde{q}_j^{+} - \widetilde{q}_j^{-}\right)\lambda_{j,2}\right.\\
&\left. + \widetilde{q}_j^{-}\lambda_{j-1,2}\right],\\
[L_2\boldsymbol{\lambda}]_{j-1/2} :=& -\varepsilon\left[\frac{2(\lambda_{j+1,2} - \lambda_{j,2})}{\hat{h}_j(\hat{h}_j + \hat{h}_{j+1})} - \frac{2(\lambda_{j,2} - \lambda_{j-1,2})}{\hat{h}_j(\hat{h}_j + \hat{h}_{j-1})}\right] + b_{j-1/2}\left[\widetilde{q}_j^{+}\lambda_{j+1,2} + \left(1 - \widetilde{q}_j^{+} - \widetilde{q}_j^{-}\right)\lambda_{j,2}\right.\\
&\left. + \widetilde{q}_j^{-}\lambda_{j-1,2}\right] - a_{j-1/2}\left[-\frac{\lambda_{j-1,2}}{\hat{h}_j + \hat{h}_{j-1}} + \lambda_{j,2}\left(\frac{1}{\hat{h}_j + \hat{h}_{j-1}} - \frac{1}{\hat{h}_j + \hat{h}_{j+1}}\right) + \frac{\lambda_{j+1,2}}{\hat{h}_j + \hat{h}_{j+1}}\right]\\
&- c_{j-1/2}\left[-\frac{\lambda_{j-1,1}}{\hat{h}_j + \hat{h}_{j-1}} + \lambda_{j,1}\left(\frac{1}{\hat{h}_j + \hat{h}_{j-1}} - \frac{1}{\hat{h}_j + \hat{h}_{j+1}}\right) + \frac{\lambda_{j+1,1}}{\hat{h}_j + \hat{h}_{j+1}}\right]\\
&+ d_{j-1/2}\left[\widetilde{q}_j^{+}\lambda_{j+1,1} + \left(1 - \widetilde{q}_j^{+} - \widetilde{q}_j^{-}\right)\lambda_{j,1} + \widetilde{q}_j^{-}\lambda_{j-1,1}\right],
\end{aligned}$$

where $\widetilde{q}_j^{+} := \dfrac{\hat{h}_j}{4(\hat{h}_j + \hat{h}_{j+1})}$ and $\widetilde{q}_j^{-} := \dfrac{\hat{h}_j}{4(\hat{h}_j + \hat{h}_{j-1})}$. Merging all the equations delivers the following system

$$\mathfrak{A}\boldsymbol{\lambda} = \mathfrak{G},$$

where

$$\mathfrak{A} = \begin{bmatrix} \hat{A} & \hat{B} \\ \hat{C} & \hat{D} \end{bmatrix}, \quad \mathfrak{G} = \Big(\underbrace{q_1, 0, \ldots, 0, q_3}_{1^{\text{st}}\text{component}}, \underbrace{q_2, f(\chi_1), \ldots, f(\chi_{N_x}), q_4}_{2^{\text{nd}}\text{component}}\Big)^T,$$

$$\boldsymbol{\lambda} = \Big(\underbrace{\lambda_{0,1}, \lambda_{1,1}, \ldots, \lambda_{N_x,1}, \lambda_{N_x+1,1}}_{1^{\text{st}}\text{component}}, \underbrace{\lambda_{0,2}, \lambda_{1,2}, \ldots, \lambda_{N_x,2}, \lambda_{N_x+1,2}}_{2^{\text{nd}}\text{component}} \Big)^T .$$

The matrices $\hat{A}, \hat{B}, \hat{C}$ and $\hat{D}$ are given by

$$\hat{A} = \begin{bmatrix} 1 & 0 & 0 & 0 & \ldots & \ldots & 0 \\ \hat{a}_{21} & \hat{a}_{22} & \hat{a}_{23} & 0 & \ldots & \ldots & 0 \\ 0 & \hat{a}_{32} & \hat{a}_{33} & \hat{a}_{34} & \ldots & \ldots & 0 \\ \vdots & \ddots & \ddots & \ddots & \vdots & \vdots & \vdots \\ \ldots & \ldots & \ldots & 0 & \hat{a}_{N_x+1N_x} & \hat{a}_{N_x+1N_x+1} & \hat{a}_{N_x+1N_x+2} \\ \ldots & \ldots & \ldots & 0 & 0 & 0 & 1 \end{bmatrix}_{(N_x+2)\times(N_x+2)},$$

$$\hat{B} = \begin{bmatrix} 0 & 0 & 0 & 0 & \ldots & \ldots & 0 \\ \hat{b}_{21} & \hat{b}_{22} & \hat{b}_{23} & 0 & \ldots & \ldots & 0 \\ 0 & \hat{b}_{32} & \hat{b}_{33} & \hat{b}_{34} & \ldots & \ldots & 0 \\ \vdots & \ddots & \ddots & \ddots & \vdots & \vdots & \vdots \\ \ldots & \ldots & \ldots & 0 & \hat{b}_{N_x+1N_x} & \hat{b}_{N_x+1N_x+1} & \hat{b}_{N_x+1N_x+2} \\ \ldots & \ldots & \ldots & 0 & 0 & 0 & 0 \end{bmatrix}_{(N_x+2)\times(N_x+2)},$$

$$\hat{C} = \begin{bmatrix} 0 & 0 & 0 & 0 & \ldots & \ldots & 0 \\ \hat{c}_{21} & \hat{c}_{22} & \hat{c}_{23} & 0 & \ldots & \ldots & 0 \\ 0 & \hat{c}_{32} & \hat{c}_{33} & \hat{c}_{34} & \ldots & \ldots & 0 \\ \vdots & \ddots & \ddots & \ddots & \vdots & \vdots & \vdots \\ \ldots & \ldots & \ldots & 0 & \hat{c}_{N_x+1N_x} & \hat{c}_{N_x+1N_x+1} & \hat{c}_{N_x+1N_x+2} \\ \ldots & \ldots & \ldots & 0 & 0 & 0 & 0 \end{bmatrix}_{(N_x+2)\times(N_x+2)},$$

$$\hat{D} = \begin{bmatrix} 1 & 0 & 0 & 0 & \dots & \dots & 0 \\ \hat{d}_{21} & \hat{d}_{22} & \hat{d}_{23} & 0 & \dots & \dots & 0 \\ 0 & \hat{d}_{32} & \hat{d}_{33} & \hat{d}_{34} & \dots & \dots & 0 \\ \vdots & \ddots & \ddots & \ddots & \vdots & \vdots & \vdots \\ \dots & \dots & \dots & 0 & \hat{d}_{N_x+1N_x} & \hat{d}_{N_x+1N_x+1} & \hat{d}_{N_x+1N_x+2} \\ \dots & \dots & \dots & 0 & 0 & 0 & 1 \end{bmatrix}_{(N_x+2)\times(N_x+2)},$$

where for $j = 1, 2, \dots, N_x$

$$\begin{aligned}
\hat{a}_{j+1,j} =& -\frac{2}{\hat{h}_j(\hat{h}_j+\hat{h}_{j-1})}, \quad \hat{a}_{j+1,j+1} = \frac{2}{\hat{h}_j(\hat{h}_j+\hat{h}_{j-1})} + \frac{2}{\hat{h}_j(\hat{h}_j+\hat{h}_{j+1})}, \\
\hat{a}_{j+1,j+2} =& \frac{2}{\hat{h}_j(\hat{h}_j+\hat{h}_{j+1})}, \quad \hat{b}_{j+1,j} = -\widetilde{q}_j^-, \quad \hat{b}_{j+1,j+1} = -(1-\widetilde{q}_j^+ - \widetilde{q}_j^-),\ \hat{b}_{j+1,j+2} = -\widetilde{q}_j^+, \\
\hat{c}_{j+1,j} =& \frac{c_{j-1/2}}{\hat{h}_j+\hat{h}_{j-1}} + \widetilde{q}_j^- d_{j-1/2}, \quad \hat{c}_{j+1,j+2} = -\frac{c_{j-1/2}}{\hat{h}_j+\hat{h}_{j-1}} + \widetilde{q}_j^+ d_{j-1/2}, \\
\hat{c}_{j+1,j+1} =& -c_{j-1/2}\left(\frac{1}{\hat{h}_j+\hat{h}_{j-1}} - \frac{1}{\hat{h}_j+\hat{h}_{j+1}}\right) + d_{j-1/2}(1-\widetilde{q}_j^+ - \widetilde{q}_j^-), \\
\hat{d}_{j+1,j} =& \frac{2\varepsilon}{\hat{h}_j(\hat{h}_j+\hat{h}_{j-1})} + \widetilde{q}_j^- b_{j-1/2} + \frac{a_{j-1/2}}{\hat{h}_j+\hat{h}_{j-1}}, \\
\hat{d}_{j+1,j+1} =& 2\varepsilon\left(\frac{1}{\hat{h}_j+\hat{h}_{j-1}} + \frac{1}{\hat{h}_j+\hat{h}_{j+1}}\right) + b_{j-1/2}(1-\widetilde{q}_j^+ - \widetilde{q}_j^-) \\
& a_{j-1/2}\left(\frac{1}{\hat{h}_j+\hat{h}_{j-1}} - \frac{1}{\hat{h}_j+\hat{h}_{j+1}}\right), \\
\hat{d}_{j+1,j+2} =& -\frac{2\varepsilon}{\hat{h}_j(\hat{h}_j+\hat{h}_{j+1})} + \widetilde{q}_j^+ b_{j-1/2} - \frac{a_{j-1/2}}{\hat{h}_j+\hat{h}_{j+1}}.
\end{aligned}$$

6.4 Convergence analysis

6.4.1 S_2^0-interpolation

We solve the following interpolation problem to find the interpolation $I_2^0 y_k \in S_2^0(\Delta^{N_x})$ for an arbitrary function $y_k \in C^0[0,1]$

$$(I_2^0 y_k)_j = (y_k)_j,\ j = 0, 1, \dots, N_x, \quad \text{and} \quad (I_2^0 y_k)_{j-1/2} = (y_k)_{j-1/2},\ j = 1, 2, \dots, N_x,$$

where $(y_k)_j = y_k(x_j),\ (y_k)_{j-1/2} = y_k(\chi_j),\ k = 1, 2.$

Theorem 6.4.1. *Assuming $a(x),\ b(x),\ c(x),\ d(x),\ f(x) \in C^4[0,1]$, the interpolating error $\boldsymbol{y} - I_2^0\boldsymbol{y}$ of the solution $\boldsymbol{y}$ of (6.1.3) satisfies the following bounds:*

$$\|\boldsymbol{y} - I_2^0\boldsymbol{y}\| \leqslant CN_x^{-3}, \quad \boldsymbol{\varepsilon} \max_{j=1,2,\ldots,N_x} |(\boldsymbol{y} - I_2^0\boldsymbol{y})'_{j-1/2}| \leqslant \boldsymbol{C}N_x^{-2},$$
$$\boldsymbol{\varepsilon}^2 \max_{j=1,2,\ldots,N_x} |(\boldsymbol{y} - I_2^0\boldsymbol{y})''_{j-1/2}| \leqslant \boldsymbol{C}N_x^{-2},$$

where $\boldsymbol{\varepsilon} = diag(1, \varepsilon)$.

Proof. First, we utilize the Lagrange representation of the interpolating polynomial and Taylor series expansions to verify that for any $\boldsymbol{y} \in C^4[0,1]^2$, the interpolating error on each subinterval satisfies

$$\left\|y_k - I_2^0 y_k\right\|_{I_j} \leqslant \frac{\hat{h}_j^3}{24}\left\|y_k^{(3)}\right\|_{I_j}, \ \left|(y_k - I_2^0 y_k)'_{j-1/2}\right| \leqslant \frac{\hat{h}_j^2}{24}\left\|y_k^{(3)}\right\|_{I_j}, \ \left|(y_k - I_2^0 y_k)''_{j-1/2}\right| \leqslant \frac{\hat{h}_j^2}{48}\left\|y_k^{(4)}\right\|_{I_j}, \tag{6.4.1}$$

for $k = 1, 2$. Applying the linearity property of I_2^0, decomposition of the solution components y_k into two parts is given by

$$y_k - I_2^0 y_k = (v_k - I_2^0 v_k) + (w_k - I_2^0 w_k).$$

Since the nature of both solution components is distinct, we give individual analyses for both solution components.

Analysis for first component y_1: We start our analysis by finding the interpolating error in the regular component. For $I_j \subset [0, x_{N_x/2-1}]$, we apply the bounds given in Theorem 6.2.2, to obtain

$$\begin{aligned}
\frac{\hat{h}_j^3}{24}\left|v_1^{(3)}\right|_{I_j} &\leqslant C\varepsilon^3 N_x^{-3}\exp\left(\frac{3x_j}{(\mathcal{P}+1)\varepsilon}\right) \\
&\leqslant CN_x^{-3}\exp\left(\frac{x_j}{\varepsilon}\right) \\
&\leqslant CN_x^{-3}\exp\Big((\mathcal{P}+1)\Upsilon(\varrho_j)\Big) \\
&\leqslant CN_x^{-3}.
\end{aligned}$$

Also, for $I_j \subset [x_{N_x/2}, 1]$, the bounds for $\hat{h}_j$ (using (6.3.2)) trivially gives $\|v_1 - I_2^0 v_1\|_{I_j} \leqslant CN_x^{-3}$. Thus, by merging all these estimates, we have

$$\|v_1 - I_2^0 v_1\| \leqslant CN_x^{-3}.$$

Next, we assess the singular component w_1 in $I_j \subset [0, x_{N_x/2-1}]$. Using Theorem 6.2.2 and the inequality (6.3.2), we get

$$\begin{aligned}
\frac{\hat{h}_j^3}{24}\left|w_1^{(3)}\right|_{I_j} &\leqslant C\varepsilon^3 N_x^{-3} \exp\left(\frac{3x_j}{(\mathcal{P}+1)\varepsilon}\right)\varepsilon^{-1}|\exp(-x\alpha^*/\varepsilon)|_{I_j} \\
&\leqslant CN_x^{-3}\exp\left[C_1\left(\frac{x_j}{\varepsilon} - \frac{x_{j-1}}{\varepsilon}\right)\right] \\
&\leqslant CN_x^{-3}\exp\left(C_1\frac{\hat{h}_j}{\varepsilon}\right) \\
&\leqslant CN_x^{-3}\exp\left(C_1(\mathcal{P}+1)N_x^{-1}\max\Upsilon'(\varrho_j)\right) \\
&\leqslant CN_x^{-3}.
\end{aligned}$$

Now for $I_j \subset [x_{N_x/2}, 1]$, we obtain

$$\begin{aligned}
\frac{\hat{h}_j^3}{24}\left|w_1^{(3)}\right|_{I_j} &\leqslant CN_x^{-3}\varepsilon^{-1}|\exp(-x\alpha^*/\varepsilon)|_{I_j} \\
&\leqslant CN_x^{-3}\varepsilon^{-1}\exp\left(-\frac{\alpha^* x_{j-1}}{\varepsilon}\right).
\end{aligned}$$

Since $\varepsilon^{-1}\exp\left(-\frac{\alpha^* x_{j-1}}{\varepsilon}\right)$ is bounded in $[x_{N_x/2}, 1]$, the above inequality gives

$$\frac{\hat{h}_j^3}{24}\left|w_1^{(3)}\right|_{I_j} \leqslant CN_x^{-3}.$$

Thus, for the singular component, we obtain

$$\|w_1 - I_2^0 w_1\| \leqslant CN_x^{-3}.$$

Now to acquire the bound for $\max_{j=1,2,\ldots,N_x} |(y_1 - I_2^0 y_1)'_{j-1/2}|$, first, we assess v_1 in $I_j \subset [0, x_{N_x/2-1}]$ as follows

$$\begin{aligned}\frac{\hat{h}_j^2}{24}\left|v_1^{(3)}\right|_{I_j} &\leqslant C\varepsilon^2 N_x^{-2}\exp\left(\frac{2x_j}{(\mathcal{P}+1)\varepsilon}\right)\\ &\leqslant CN_x^{-2}\exp\left(\frac{2x_j}{(\mathcal{P}+1)\varepsilon}\right)\\ &\leqslant CN_x^{-2}\exp\Big(2\Upsilon(\varrho_j)\Big)\\ &\leqslant CN_x^{-2}.\end{aligned}$$

Also, for $I_j \subset [x_{N_x/2}, 1]$, the bounds for $\hat{h}_j$ (using (6.3.2)) trivially gives $|(v_1 - I_2^0 v_1)'_{j-1/2}| \leqslant CN_x^{-2}$. Thus, by merging all these estimates, we have

$$\left|(v_1 - I_2^0 v_1)'_{j-1/2}\right| \leqslant CN_x^{-2}.$$

Next, we assess the singular component w_1 in $I_j \subset [0, x_{N_x/2-1}]$. Using Theorem 6.2.2 and the inequality (6.3.2), we get

$$\begin{aligned}\frac{\hat{h}_j^2}{24}\left|w_1^{(3)}\right|_{I_j} &\leqslant C\varepsilon^2 N_x^{-2}\exp\left(\frac{2x_j}{(\mathcal{P}+1)\varepsilon}\right)\varepsilon^{-1}|\exp(-x\alpha^*/\varepsilon)|_{I_j}\\ &\leqslant CN_x^{-2}\exp\left[C_2\left(\frac{x_j}{\varepsilon}-\frac{x_{j-1}}{\varepsilon}\right)\right]\\ &\leqslant CN_x^{-2}\exp\left(C_2\frac{\hat{h}_j}{\varepsilon}\right)\\ &\leqslant CN_x^{-2}\exp\Big(C_2(\mathcal{P}+1)N_x^{-1}\max\Upsilon'(\varrho_j)\Big)\\ &\leqslant CN_x^{-2}.\end{aligned}$$

Similar bound can be obtained in $I_j \subset [x_{N_x/2}, 1]$. Now to acquire the bound for $\max_{j=1,2,\ldots,N_x} |(y_1 - I_2^0 y_1)''_{j-1/2}|$, first, we assess v_1 in $I_j \subset [0, x_{N_x/2-1}]$ as follows

$$\frac{\hat{h}_j^2}{48}\left|v_1^{(4)}\right|_{I_j} \leqslant C\varepsilon^2 N_x^{-2}\exp\left(\frac{2x_j}{(\mathcal{P}+1)\varepsilon}\right) \text{ (using Theorem 6.2.2 and the inequality (6.3.2))}$$

$$\leqslant CN_x^{-2}\exp\left(\frac{2x_j}{(\mathcal{P}+1)\varepsilon}\right)$$
$$\leqslant CN_x^{-2}\exp\Big(2\Upsilon(\varrho_j)\Big)$$
$$\leqslant CN_x^{-2}.$$

Use similar approach for v_1 the interval $[x_{N_x/2}, 1]$. Now for the w_1 in $I_j \subset [0, x_{N_x/2-1}]$, we have

$$\begin{aligned}\frac{\hat{h}_j^2}{48}\left|w_1^{(4)}\right|_{I_j} &\leqslant C\varepsilon^2 N_x^{-2}\exp\left(\frac{2x_j}{(\mathcal{P}+1)\varepsilon}\right)\varepsilon^{-2}|\exp(-x\alpha^*/\varepsilon)|_{I_j}\\ &\leqslant CN_x^{-2}\exp\left(\frac{C_3x_j}{\varepsilon}\right)\exp\left(\frac{-C_4x_{j-1}}{\varepsilon}\right)\\ &\leqslant CN_x^{-2}\exp\left(\frac{C_5(x_j-x_{j-1})}{\varepsilon}\right)\\ &\leqslant CN_x^{-2}\exp\left(\frac{C_5\hat{h}_j}{\varepsilon}\right)\\ &\leqslant CN_x^{-2}\exp\Big(C_5(\mathcal{P}+1)N_x^{-1}\max\Upsilon'(\varrho_j)\Big)\\ &\leqslant CN_x^{-2}.\end{aligned}$$

For the interval $[x_{N_x/2}, 1]$

$$\begin{aligned}\frac{\hat{h}_j^2}{48}\left|w_1^{(4)}\right|_{I_j} &\leqslant CN_x^{-2}\varepsilon^{-2}|\exp(-x\alpha^*/\varepsilon)|_{I_j}\\ &\leqslant CN_x^{-2}\varepsilon^{-2}\exp\left(\frac{-\alpha^*x_{j-1}}{\varepsilon}\right).\end{aligned}$$

Since $\varepsilon^{-2}\exp\left(-\frac{\alpha^*x_{j-1}}{\varepsilon}\right)$ is bounded in $[x_{N_x/2}, 1]$, the above inequality gives

$$\frac{\hat{h}_j^2}{48}\left|w_1^{(4)}\right|_{I_j} \leqslant CN_x^{-2}.$$

Analysis for second component y_2: We start our analysis by finding the interpolating error in the regular component. For $I_j \subset [0, x_{N_x/2-1}]$, we apply the bounds given in Theorem

6.2.2, to obtain

$$\begin{aligned}\frac{\hat{h}_j^3}{24}\left|v_2^{(3)}\right|_{I_j} &\leqslant C\varepsilon^3 N_x^{-3}\exp\left(\frac{3x_j}{(\mathcal{P}+1)\varepsilon}\right)\\ &\leqslant CN_x^{-3}\exp\left(\frac{x_j}{\varepsilon}\right)\\ &\leqslant CN_x^{-3}\exp\Big((\mathcal{P}+1)\Upsilon(\varrho_j)\Big)\\ &\leqslant CN_x^{-3}.\end{aligned}$$

Also, for $I_j \subset [x_{N_x/2}, 1]$, the bounds for $\hat{h}_j$ (using (6.3.2)) trivially gives $\|v_2 - I_2^0 v_2\|_{I_j} \leqslant CN_x^{-3}$. Thus, by merging all these estimates, we have

$$\|v_2 - I_2^0 v_2\| \leqslant CN_x^{-3}.$$

Next, we assess the singular component w_2 in $I_j \subset [0, x_{N_x/2-1}]$. Using Theorem 6.2.2 and the inequality (6.3.2), we get

$$\begin{aligned}\frac{\hat{h}_j^3}{24}\left|w_2^{(3)}\right|_{I_j} &\leqslant C\varepsilon^3 N_x^{-3}\exp\left(\frac{3x_j}{(\mathcal{P}+1)\varepsilon}\right)\varepsilon^{-3}|\exp(-x\alpha^*/\varepsilon)|_{I_j}\\ &\leqslant CN_x^{-3}\exp\left[C_6\left(\frac{x_j}{\varepsilon}-\frac{x_{j-1}}{\varepsilon}\right)\right]\\ &\leqslant CN_x^{-3}\exp\left(C_6\frac{\hat{h}_j}{\varepsilon}\right)\\ &\leqslant CN_x^{-3}\exp\Big(C_6(\mathcal{P}+1)N_x^{-1}\max\Upsilon'(\varrho_j)\Big)\\ &\leqslant CN_x^{-3}.\end{aligned}$$

Now for $I_j \subset [x_{N_x/2}, 1]$, we obtain

$$\begin{aligned}\frac{\hat{h}_j^3}{24}\left|w_2^{(3)}\right|_{I_j} &\leqslant CN_x^{-3}\varepsilon^{-3}|\exp(-x\alpha^*/\varepsilon)|_{I_j}\\ &\leqslant CN_x^{-3}\varepsilon^{-3}\exp\left(-\frac{\alpha^* x_{j-1}}{\varepsilon}\right).\end{aligned}$$

Since $\varepsilon^{-3}\exp\left(-\frac{\alpha^* x_{j-1}}{\varepsilon}\right)$ is bounded in $[x_{N_x/2}, 1]$, the above inequality gives

$$\frac{\hat{h}_j^3}{24}\left|w_2^{(3)}\right|_{I_j} \leqslant CN_x^{-3}.$$

Thus, for the singular component, we obtain

$$\|w_2 - I_2^0 w_2\| \leqslant CN_x^{-3}.$$

Now to acquire the bound for $\max\limits_{j=1,2,\ldots,N_x} |(y_2 - I_2^0 y_2)'_{j-1/2}|$, first, we assess v_2 in $I_j \subset [0, x_{N_x/2-1}]$ as follows

$$\begin{aligned}
\frac{\hat{h}_j^2}{24}\left|v_2^{(3)}\right|_{I_j} &\leqslant C\varepsilon^2 N_x^{-2}\exp\left(\frac{2x_j}{(\mathcal{P}+1)\varepsilon}\right)\\
&\leqslant CN_x^{-2}\exp\left(\frac{2x_j}{(\mathcal{P}+1)\varepsilon}\right)\\
&\leqslant CN_x^{-2}\exp\Big(2\Upsilon(\varrho_j)\Big)\\
&\leqslant CN_x^{-2}.
\end{aligned}$$

Also, for $I_j \subset [x_{N_x/2}, 1]$, the bounds for $\hat{h}_j$ (using (6.3.2)) trivially gives $|(v_2 - I_2^0 v_2)'_{j-1/2}| \leqslant CN_x^{-2}$. Thus, by merging all these estimates, we have

$$\left|(v_2 - I_2^0 v_2)'_{j-1/2}\right| \leqslant CN_x^{-2}.$$

Next, we assess the singular component w_2 in $I_j \subset [0, x_{N_x/2-1}]$. Using Theorem 6.2.2 and the inequality (6.3.2), we get

$$\begin{aligned}
\frac{\hat{h}_j^2}{24}\left|w_2^{(3)}\right|_{I_j} &\leqslant C\varepsilon^2 N_x^{-2}\exp\left(\frac{2x_j}{(\mathcal{P}+1)\varepsilon}\right)\varepsilon^{-3}|\exp(-x\alpha^*/\varepsilon)|_{I_j}\\
&\leqslant C\varepsilon^{-1}N_x^{-2}\exp\left[C_7\left(\frac{x_j}{\varepsilon} - \frac{x_{j-1}}{\varepsilon}\right)\right]\\
&\leqslant C\varepsilon^{-1}N_x^{-2}\exp\left(C_7\frac{\hat{h}_j}{\varepsilon}\right)
\end{aligned}$$

$$\leqslant C\varepsilon^{-1}N_x^{-2}\exp\left(C_7(\mathcal{P}+1)N_x^{-1}\max\Upsilon'(\varrho_j)\right)$$
$$\leqslant C\varepsilon^{-1}N_x^{-2}.$$

Similar bound can be obtained in $I_j \subset [x_{N_x/2}, 1]$. Now to acquire the bound for $\max_{j=1,2,\ldots,N_x} |(y_2 - I_2^0 y_2)''_{j-1/2}|$, first, we assess v_2 in $I_j \subset [0, x_{N_x/2-1}]$ as follows

$$\frac{\hat{h}_j^2}{48}\left|v_2^{(4)}\right|_{I_j} \leqslant C\varepsilon^2 N_x^{-2}\exp\left(\frac{2x_j}{(\mathcal{P}+1)\varepsilon}\right) \text{ (using Theorem 6.2.2 and the inequality (6.3.2))}$$
$$\leqslant CN_x^{-2}\exp\left(\frac{2x_j}{(\mathcal{P}+1)\varepsilon}\right)$$
$$\leqslant CN_x^{-2}\exp\left(2\Upsilon(\varrho_j)\right)$$
$$\leqslant CN_x^{-2}.$$

Use similar approach for v_2 the interval $[x_{N_x/2}, 1]$. Now for the w_1 in $I_j \subset [0, x_{N_x/2-1}]$, we have

$$\frac{\hat{h}_j^2}{48}\left|w_2^{(4)}\right|_{I_j} \leqslant C\varepsilon^2 N_x^{-2}\exp\left(\frac{2x_j}{(\mathcal{P}+1)\varepsilon}\right)\varepsilon^{-4}|\exp(-x\alpha^*/\varepsilon)|_{I_j}$$
$$\leqslant C\varepsilon^{-2}N_x^{-2}\exp\left(\frac{C_8 x_j}{\varepsilon}\right)\exp\left(\frac{-C_9 x_{j-1}}{\varepsilon}\right)$$
$$\leqslant C\varepsilon^{-2}N_x^{-2}\exp\left(\frac{C_{10}(x_j - x_{j-1})}{\varepsilon}\right)$$
$$\leqslant C\varepsilon^{-2}N_x^{-2}\exp\left(\frac{C_{10}\hat{h}_j}{\varepsilon}\right)$$
$$\leqslant C\varepsilon^{-2}N_x^{-2}\exp\left(C_{10}(\mathcal{P}+1)N_x^{-1}\max\Upsilon'(\varrho_j)\right)$$
$$\leqslant C\varepsilon^{-2}N_x^{-2}.$$

For the interval $[x_{N_x/2}, 1]$

$$\frac{\hat{h}_j^2}{48}\left|w_2^{(4)}\right|_{I_j} \leqslant CN_x^{-2}\varepsilon^{-4}|\exp(-x\alpha^*/\varepsilon)|_{I_j}$$
$$\leqslant C\varepsilon^{-2}N_x^{-2}\varepsilon^{-2}\exp\left(\frac{-\alpha^* x_{j-1}}{\varepsilon}\right).$$

Since $\varepsilon^{-2}\exp\left(-\frac{\alpha^* x_{j-1}}{\varepsilon}\right)$ is bounded in $[x_{N_x/2}, 1]$, the above inequality gives

$$\frac{\hat{h}_j^2}{48}\left|w_2^{(4)}\right|_{I_j} \leqslant C\varepsilon^{-2}N_x^{-2}.$$

□

Lemma 6.4.1. *Let $z \in S_2^0(\Delta^{N_x})$ with $z_{j-1/2} = 0$, $j = 1, 2, \ldots, N_x$, then*

$$\|z\|_{I_j} \leqslant \max_j\{|z_{j-1}|, |z_j|\},\ \|z'\|_{I_j} \leqslant \frac{4}{\hat{h}_j}\max_j\{|z_{j-1}|, |z_j|\},\ \|z''\|_{I_j} \leqslant \frac{8}{\hat{h}_j^2}\max_j\{|z_{j-1}|, |z_j|\}.$$

Proof. From [93] we know that,

$$z(x) = \frac{2}{\hat{h}_j^2}(x - x_{j-1/2})[z_{j-1}(x - x_j) + z_j(x - x_{j-1})],\ x \in I_j,$$

which implies

$$|z(x)| = \frac{2}{\hat{h}_j^2}|x - x_{j-1/2}|\max\{|z_{j-1}|, |z_j|\}(|x - x_j| + |x - x_{j-1}|).$$

Using the relations $|x - x_{j-1/2}| \leqslant \frac{\hat{h}_j}{2}$ and $|x - x_j| + |x - x_{j-1}| = \hat{h}_j$, so

$$\|z\|_{I_j} \leqslant \max_j\{|z_{j-1}|, |z_j|\}.$$

Differentiating the function $z(x)$, we get

$$z'(x) = \frac{2}{\hat{h}_j^2}(z_{j-1} + z_j)(x - x_{j-1/2}) + \frac{2}{\hat{h}_j^2}[z_{j-1}(x - x_j) + z_j(x - x_{j-1})],$$

By taking the absolute value, we get

$$|z'(x)| = \frac{2}{\hat{h}_j^2}(|z_{j-1}| + |z_j|)|x - x_{j-1/2}| + \frac{2}{\hat{h}_j^2}\max\{|z_{j-1}|, |z_j|\}(|x - x_j| + |x - x_{j-1}|).$$

Using the above relations gives

$$\|z'\|_{I_j} \leqslant \frac{4}{\hat{h}_j} \max_j\{|z_{j-1}|, |z_j|\}.$$

A similar approach can easily obtain the bound on z''. □

6.4.2 S_2^1-interpolation

We solve the following interpolation problem to find the interpolation $I_2^1 y_k \in S_2^1(\Delta^{N_x})$ for an arbitrary function $y_k \in C^1[0,1]$

$$(I_2^1 y_k)_0 = (y_k)_0, \quad (I_2^1 y_k)_{j-1/2} = (y_k)_{j-1/2},\ j = 1, 2, \ldots, N_x, \quad (I_2^1 y_k)_{N_x} = (y_k)_{N_x}, \tag{6.4.2}$$

where $(y_k)_{j-1/2} = y_k(\chi_j),$ for $k = 1, 2.$

From [93, 111], we have

$$[\Lambda \mathcal{R}_k]_j \equiv r_j(\mathcal{R}_k)_{j-1} + 3(\mathcal{R}_k)_j + s_j(\mathcal{R}_k)_{j+1} = 4r_j(\mathcal{R}_k)_{j-1/2} + 4s_j(\mathcal{R}_k)_{j+1/2},\ j = 1, 2, \ldots, N_x - 1, \tag{6.4.3}$$

where $r_j = \frac{\hat{h}_{j+1}}{\hat{h}_j + \hat{h}_{j+1}}$ and $s_j = 1 - r_j = \frac{\hat{h}_j}{\hat{h}_j + \hat{h}_{j+1}}$.

Lemma 6.4.2. *For all vectors $\mathcal{R}_k \in \mathbb{R}^{N_x+1}$ with $(\mathcal{R}_k)_0 = (\mathcal{R}_k)_{N_x} = 0$, the operator Λ is stable* i.e.,

$$\max_{j=1,2,\ldots,N_x-1} |(\mathcal{R}_k)_j| \leqslant \frac{1}{2} \max_{j=1,2,\ldots,N_x-1} |[\Lambda \mathcal{R}_k]_j|, \quad k = 1, 2.$$

Proof. For the proof, refer to [94]. □

Theorem 6.4.2. *Assume that $a(x),\ b(x),\ c(x),\ d(x),\ f(x) \in C^4[0,1]$, then the interpolating error $\boldsymbol{y} - I_2^1 \boldsymbol{y}$ of the solution $\boldsymbol{y}$ of (6.1.3) satisfies*

$$\max_{j=0,1,\ldots,N_x} |(\boldsymbol{y} - I_2^1 \boldsymbol{y})_j| \leqslant \boldsymbol{C} N_x^{-4}, \tag{6.4.4a}$$

$$\|\boldsymbol{y} - I_2^1 \boldsymbol{y}\| \leqslant C N_x^{-3}, \tag{6.4.4b}$$

$$\boldsymbol{\varepsilon} \max_{j=1,2,\ldots,N_x} |(\boldsymbol{y} - I_2^1 \boldsymbol{y})'_{j-1/2}| \leqslant \boldsymbol{C} N_x^{-2}, \tag{6.4.4c}$$

$$\boldsymbol{\varepsilon}^2 \max_{j=1,2,\ldots,N_x} |(\boldsymbol{y} - I_2^1 \boldsymbol{y})''_{j-1/2}| \leqslant \boldsymbol{C} N_x^{-2}. \tag{6.4.4d}$$

Proof. To find the interpolating error $y_k - I_2^1 y_k$, we examine an arbitrary function y_k such that

$$(y_k - I_2^1 y_k)_0 = (y_k - I_2^1 y_k)_{N_x} = 0, \quad k = 1, 2.$$

Using the definitions of S_2^1-interpolation and the operator Λ, we have

$$\hat{\tau}_{y_k,j} = [\Lambda(y_k - I_2^1 y_k)]_j = r_j(y_k)_{j-1} - 4r_j(y_k)_{j-1/2} + 3(y_k)_j - 4s_j(y_k)_{j+1/2} + s_j(y_k)_{j+1}, \tag{6.4.5}$$

for $j = 1, 2, \ldots, N_x,\ k = 1, 2$. Moreover, we utilize the Taylor series expansions to bring

$$|\hat{\tau}_{y_k,j}| \leqslant \frac{1}{12}\hat{h}_j\hat{h}_{j+1}|\hat{h}_{j+1} - \hat{h}_j||(y_k^{(3)})_j|_{I_j} + \frac{5}{96}\max\{\hat{h}_j^4, \hat{h}_{j+1}^4\}\|(y_k^{(4)})_j\|_{I_j \cup I_{j+1}}. \tag{6.4.6}$$

We decompose the interpolating error into two parts as

$$y_k - I_2^1 y_k = (v_k - I_2^1 v_k) + (w_k - I_2^1 w_k),$$

or

$$\hat{\tau}_{y_k,j} = \hat{\tau}_{v_k,j} + \hat{\tau}_{w_k,j}.$$

Analysis for first component y_1: We start with the regular component. For $I_j \subset [0, x_{N_x/2-1}]$, we employ Theorem 6.2.2 and the inequality (6.4.6), to get

$$|\hat{\tau}_{v_1,j}| \leqslant C\bigg(\hat{h}_j\hat{h}_{j+1}|\hat{h}_{j+1} - \hat{h}_j| + \max\{\hat{h}_j^4, \hat{h}_{j+1}^4\}\bigg).$$

In $[0, x_{N_x/2-1}]$ we obtain

$$\begin{aligned}
|\hat{\tau}_{v_1,j}| &\leqslant C\bigg(\hat{h}_{j+1}^2|\hat{h}_{j+1} - \hat{h}_j| + \hat{h}_{j+1}^4\bigg) \text{ as } \hat{h}_j < \hat{h}_{j+1} \\
&\leqslant C\bigg(\varepsilon^3 N_x^{-4}\exp\bigg(\frac{2x_{j+1}}{(\mathcal{P}+1)\varepsilon}\bigg) + \varepsilon^4 N_x^{-4}\exp\bigg(\frac{4x_{j+1}}{(\mathcal{P}+1)\varepsilon}\bigg)\bigg) \\
&\leqslant CN_x^{-4}\exp\bigg(\frac{4x_{j+1}}{(\mathcal{P}+1)\varepsilon}\bigg) \\
&\leqslant CN_x^{-4}\exp\bigg(4\Upsilon(\varrho_{j+1})\bigg)
\end{aligned}$$

$$\leqslant CN_x^{-4}.$$

Moreover, for $x_j \in [x_{N_x/2}, 1]$, it is straightforward to verify $|\hat{\tau}_{v_1,j}| \leqslant CN_x^{-4}$. Therefore, Lemma 6.4.2 gives

$$\max_{j=0,1,\ldots,N_x} |(v_1 - I_2^1 v_1)_j| \leqslant CN_x^{-4}.$$

Now to find the bounds for w_1, we employ the attribute that $\hat{h}_j < \hat{h}_{j+1}$ for $x_j \in [0, x_{N_x/2-1}]$, which yields

$$\begin{aligned}
|\hat{\tau}_{w_1,j}| &\leqslant \frac{1}{12}\hat{h}_j\hat{h}_{j+1}|\hat{h}_{j+1} - \hat{h}_j||(w_{1,j})'''|_{I_j} + \frac{5}{96}\max\{\hat{h}_j^4, \hat{h}_{j+1}^4\}\|(w_{1,j})^{(4)}\|_{I_j\cup I_{j+1}} \\
&\leqslant C\left(\hat{h}_{j+1}^2|\hat{h}_{j+1} - \hat{h}_j|\varepsilon^{-1}|\exp(-x\alpha^*/\varepsilon)|_{I_j} + \hat{h}_{j+1}^4\varepsilon^{-2}|\exp(-x\alpha^*/\varepsilon)|_{I_j\cup I_{j+1}}\right) \\
&\leqslant CN_x^{-4}\left(\exp\left(\frac{2x_{j+1}}{(\mathcal{P}+1)\varepsilon}\right)|\exp(-x\alpha^*/\varepsilon)|_{I_j} + \exp\left(\frac{4x_{j+1}}{(\mathcal{P}+1)\varepsilon}\right)|\exp(-x\alpha^*/\varepsilon)|_{I_j\cup I_{j+1}}\right) \\
&\leqslant CN_x^{-4}\exp\left(\frac{C_{11}\hat{h}_{j+1}}{\varepsilon}\right) \\
&\leqslant CN_x^{-4}\exp\left(C_{11}(\mathcal{P}+1)N_x^{-1}\max\Upsilon'(\varrho_{j+1})\right) \\
&\leqslant CN_x^{-4}.
\end{aligned}$$

In the regular region $[x_{N_x/2}, 1]$ we acquire the identical bounds. An application of Lemma 6.4.2 delivers

$$\max_{j=0,1,\ldots,N_x} |(w_1 - I_2^1 w_1)_j| \leqslant CN_x^{-4}.$$

Analysis for the second component y_2: The examination is analogous to the first component in S_2^1-interpolation. We are not delivering the details here.

The estimation given in (6.4.4a) can be acquired instantly by combining all the interpolating errors for both components. To show (6.4.4b), we utilize triangle inequality as

$$\begin{aligned}
\|\boldsymbol{y} - I_2^1\boldsymbol{y}\| &\leqslant \|\boldsymbol{y} - I_2^0\boldsymbol{y}\| + \|I_2^0\boldsymbol{y} - I_2^1\boldsymbol{y}\| \\
&\leqslant \|\boldsymbol{y} - I_2^0\boldsymbol{y}\| + \max_{j=0,1,\ldots,N_x} |(\boldsymbol{y} - I_2^1\boldsymbol{y})_j|.
\end{aligned}$$

Now using $(I_2^1\boldsymbol{y})_j = (\boldsymbol{y})_j,\ j = 0, 1, \ldots, N_x$, Lemma 6.4.1, Theorem 6.4.1, and (6.4.4a), we

get the estimate (6.4.4b). Moreover, to obtain the inequality (6.4.4c) and (6.4.4d), we employ a similar procedure as we have accomplished for (6.4.4b). For this, we have

$$\begin{aligned}
|(y_k - I_2^1 y_k)'_{j-1/2}| &\leqslant |(y_k - I_2^0 y_k)'_{j-1/2}| + |(I_2^0 y_k - I_2^1 y_k)'_{j-1/2}| \\
&\leqslant |(y_k - I_2^0 y_k)''_{j-1/2}| + \max_{j=0,1,\ldots,N_x} \frac{4}{\hat{h}_j} |(y_k - I_2^1 y_k)_j|, \\
|(y_k - I_2^1 y_k)''_{j-1/2}| &\leqslant |(y_k - I_2^0 y_k)''_{j-1/2}| + |(I_2^0 y_k - I_2^1 y_k)''_{j-1/2}| \\
&\leqslant |(y_k - I_2^0 y_k)''_{j-1/2}| + \max_{j=0,1,\ldots,N_x} \frac{8}{\hat{h}_j^2} |(y_k - I_2^1 y_k)_j|.
\end{aligned}$$

Hence, we complete the proof by using the Theorem 6.4.1 and inequality (6.4.4a). □

Lemma 6.4.3. *If there exists a constant* $\mu_1 > 0$ *such that*

$$\max\{\hat{h}_{j+1}, \hat{h}_{j-1}\} \geqslant \mu_1 \hat{h}_j, \quad j = 1, 2, \ldots, N_x - 1, \ \hat{h}_1 \geqslant \mu_1 \hat{h}_2, \ \textit{and}\ \hat{h}_{N_x} \geqslant \mu_1 \hat{h}_{N_x - 1}.$$

Then the operator $\boldsymbol{L}$ *is stable in the infinity-norm* i.e.,

$$\|\boldsymbol{\gamma}\| \leqslant C \frac{(1+\mu_1)}{\mu_1 \alpha^*} \|\boldsymbol{L\gamma}\|, \textit{ for all } \boldsymbol{\gamma} = (\gamma_1, \gamma_2)^T, \gamma_k \in \mathbb{R}_0^{N_x+2} = \{z \in \mathbb{R}^{N_x+2} : z_0 = z_{N_x+1} = 0\}.$$

Proof. Set $(m_1)_{j-1/2} = \left(1 - \widetilde{q}_j^+ - \widetilde{q}_j^-\right)$, $(m_2)_{j-1/2} = b_{j-1/2}\left(1 - \widetilde{q}_j^+ - \widetilde{q}_j^-\right)$, $j = 1, 2, \ldots, N_x$ and $\widetilde{q}_j^+, \widetilde{q}_j^- \in (0, 1/4)$, therefore $(m_1)_{j-1/2}$, $(m_2)_{j-1/2} > 0$. For arbitrary γ_1 and γ_2, we define

$$\begin{aligned}
[\Lambda_1 \boldsymbol{\gamma}]_{j-1/2} :=& -\frac{1}{(m_1)_{j-1/2}} \left[\frac{2(\gamma_{j+1,1} - \gamma_{j,1})}{\hat{h}_j(\hat{h}_j + \hat{h}_{j+1})} - \frac{2(\gamma_{j,1} - \gamma_{j-1,1})}{\hat{h}_j(\hat{h}_j + \hat{h}_{j-1})} \right] - \gamma_{j,2}, \\
[\Lambda_2 \boldsymbol{\gamma}]_{j-1/2} :=& \frac{1}{(m_2)_{j-1/2}} \Bigg\{ -\varepsilon \left[\frac{2(\gamma_{j+1,2} - \gamma_{j,2})}{\hat{h}_j(\hat{h}_j + \hat{h}_{j+1})} - \frac{2(\gamma_{j,2} - \gamma_{j-1,2})}{\hat{h}_j(\hat{h}_j + \hat{h}_{j-1})} \right] + d_{j-1/2} \Bigg[\widetilde{q}_j^+ \gamma_{j+1,1} \\
&+ \left(1 - \widetilde{q}_j^+ - \widetilde{q}_j^-\right) \gamma_{j,1} + \widetilde{q}_j^- \gamma_{j-1,1} \Bigg] - a_{j-1/2} \Bigg[-\frac{\gamma_{j-1,2}}{\hat{h}_j + \hat{h}_{j-1}} + \gamma_{j,2} \Bigg(\frac{1}{\hat{h}_j + \hat{h}_{j-1}} \\
&- \frac{1}{\hat{h}_j + \hat{h}_{j+1}} \Bigg) + \frac{\gamma_{j+1,2}}{\hat{h}_j + \hat{h}_{j+1}} \Bigg] - c_{j-1/2} \Bigg[-\frac{\gamma_{j-1,1}}{\hat{h}_j + \hat{h}_{j-1}} + \gamma_{j,1} \Bigg(\frac{1}{\hat{h}_j + \hat{h}_{j-1}} \\
&- \frac{1}{\hat{h}_j + \hat{h}_{j+1}} \Bigg) + \frac{\gamma_{j+1,1}}{\hat{h}_j + \hat{h}_{j+1}} \Bigg] \Bigg\} + \gamma_{j,2}.
\end{aligned}$$

The operators Λ_1 and Λ_2 are well defined because $(m_1)_{j-1/2}$ and $(m_2)_{j-1/2}$ are positive. The

M-criterion [139] implies that $\|\Lambda_k^{-1}\| \leqslant 1$. Next, we have

$$[\Lambda_1 \boldsymbol{\gamma}]_{j-1/2} = \frac{[L_1 \boldsymbol{\gamma}]_{j-1/2} + \left[\widetilde{q_j^+}\lambda_{j+1,2} + \widetilde{q_j^-}\lambda_{j-1,2}\right]}{(m_1)_{j-1/2}},$$
$$[\Lambda_2 \boldsymbol{\gamma}]_{j-1/2} = \frac{[L_2 \boldsymbol{\gamma}]_{j-1/2} - b_{j-1/2}\left[\widetilde{q_j^+}\lambda_{j+1,2} + \widetilde{q_j^-}\lambda_{j-1,2}\right]}{(m_2)_{j-1/2}}.$$

We obtain the desired proof by applying the [94] analogy. □

Theorem 6.4.3. *Let $\tilde{\boldsymbol{y}}$ and $\boldsymbol{y}$ are the solutions to the problems (6.3.4) and (6.1.3), respectively, on the eXp mesh, then*

$$\|\boldsymbol{y} - \tilde{\boldsymbol{y}}\| \leqslant C N_x^{-2}.$$

Proof. The triangle inequality yields

$$\|y_k - \tilde{y}_k\| \leqslant \|y_k - I_2^1 y_k\| + \|I_2^1 y_k - \tilde{y}_k\|,$$

for $k = 1, 2$. The interpolant $I_2^1 y_k$ can be written as follows by using $\mathfrak{B}$-spline functions

$$I_2^1 y_k(x) = \sum_{j=0}^{N_x+1} \beta_{j,k} \mathfrak{B}_j(x), \quad \text{for } k = 1, 2.$$

Use of Theorem 6.4.2 and Lemma 6.4.3 give

$$\|\boldsymbol{\lambda} - \boldsymbol{\beta}\| \leqslant C N_x^{-2}.$$

Since each $\mathfrak{B}_j \geqslant 0$ and the sum of all basis functions is equal to 1, so

$$\|I_2^1 \boldsymbol{y} - \tilde{\boldsymbol{y}}\| \leqslant \|\boldsymbol{\lambda} - \boldsymbol{\beta}\| \leqslant C N_x^{-2}.$$

An application of Theorem 6.4.2 completes the proof. □

6.5 Nonlinear BVPs

Now, we look into the following nonlinear class of BVPs

$$\varepsilon y^{(4)}(x) = \mathcal{F}(x, y', y'', y'''), \quad x \in \mathfrak{D} = (0, 1), \tag{6.5.1a}$$

subject to the following BCs

$$y(0) = q_1,\ y(1) = q_3,\ y''(0) = -q_2,\ y''(1) = -q_4, \tag{6.5.1b}$$

where $\mathcal{F}(x, y', y'', y''')$ is a sufficiently smooth function with respect to its arguments and satisfies the following requirements

$$\mathcal{F}_{y'''} \geqslant \alpha^* > 0,\ \mathcal{F}_{y''} \geqslant \beta^* > 0, \tag{6.5.2a}$$

$$\mathcal{F}_{y'} \geqslant \gamma^* > 0,\ 0 \geqslant \mathcal{F}_y \geqslant -\delta^*,\ \delta^* > 0, \tag{6.5.2b}$$

$$\alpha^* - \delta^*(1 + \zeta^*) \geqslant \eta^* > 0, \text{ for some } \eta^* \text{ and } \zeta^* > 0, \tag{6.5.2c}$$

for $x \in \overline{\mathfrak{D}}$. Putting $\varepsilon = 0$, we obtain the following reduced problem

$$\mathcal{F}(x, y', y'', y''') = 0,\ y(0) = q_1,\ y(1) = q_3,\ y''(1) = -q_4, \tag{6.5.3}$$

which has a solution $y_0 \in C^4(\mathfrak{D})$. With these assumptions, there exists a unique solution to the problem (6.5.1) and exhibits a boundary layer of width $O(\varepsilon)$ in the neighborhood of $x = 0$. Other analytical aspects like uniqueness, existence, and asymptotical analysis can be seen in [140, 141]. In the process of finding the numerical solution for (6.5.1), we use Newton's technique of quasilinearization [112]. We have the following linearized form of (6.5.1)

$$\begin{aligned} -\varepsilon y^{(4)[p+1]}(x) - a^{[p]}(x) y'''^{[p+1]}(x) + b^{[p]}(x) y''^{[p+1]}(x) + c^{[p]}(x) y'^{[p+1]}(x) \\ - d^{[p]}(x) y^{[p+1]}(x) = -f^{[p]}(x), \quad x \in \mathfrak{D} = (0, 1), \end{aligned} \tag{6.5.4a}$$

$$y^{[p+1]}(0) = q_1,\ y^{[p+1]}(1) = q_3,\ y''^{[p+1]}(0) = -q_2,\ y''^{[p+1]}(1) = -q_4, \tag{6.5.4b}$$

where

$$\begin{aligned}
a^{[p]}(x) &= \mathcal{F}_{y'''}(x, y'^{[p]}, y''^{[p]}, y'''^{[p]}),\ b^{[p]}(x) = \mathcal{F}_{y''}(x, y'^{[p]}, y''^{[p]}, y'''^{[p]}),\\
c^{[p]}(x) &= \mathcal{F}_{y'}(x, y'^{[p]}, y''^{[p]}, y'''^{[p]}),\ d^{[p]}(x) = \mathcal{F}_{y}(x, y'^{[p]}, y''^{[p]}, y'''^{[p]}),\\
-f^{[p]}(x) &= \mathcal{F}(x, y'^{[p]}, y''^{[p]}, y'''^{[p]}) - y^{[p]}\mathcal{F}_{y}(x, y'^{[p]}, y''^{[p]}, y'''^{[p]}) + y'^{[p]}\mathcal{F}_{y'}(x, y'^{[p]}, y''^{[p]}, y'''^{[p]})\\
&\quad - y''^{[p]}\mathcal{F}_{y''}(x, y'^{[p]}, y''^{[p]}, y'''^{[p]}) + y'''^{[p]}\mathcal{F}_{y'''}(x, y'^{[p]}, y''^{[p]}, y'''^{[p]}).
\end{aligned}$$

We have the following mentions

1. For each p, from (6.5.2) we get

$$a^{[p]}(x) \geqslant \alpha^* > 0,\ b^{[p]}(x) \geqslant \beta^* > 0,\ c^{[p]}(x) \geqslant \gamma^* > 0,\ 0 \geqslant d^{[p]}(x) \geqslant -\delta^*,\ \delta^* > 0.$$

2. The linearized form (6.5.4) can be solved using the numerical technique discussed in Section 3.

6.6 Numerical illustrations

This section verifies the theoretical outcomes by executing our numerical approach on three test problems. Due to the unavailability of the analytic solution for all test problems, we use the double-mesh principle [112] to compute the error estimates and orders of convergence. We determine maximum pointwise error (MPE) as

$$E_{k,\varepsilon}^{N_x} = \max_j |\widetilde{y}_k(x_{2j-1}) - \hat{y}_k(x_{j-1/2})|, \quad k = 1, 2,$$

taking N_x and $2N_x$ mesh intervals into consideration, $\hat{y}_k$ and $\widetilde{y}_k$ denote the numerical solutions on these mesh intervals, respectively. After obtaining the MPEs, we calculate the associated orders of convergence using the formula

$$\chi_{k,\varepsilon}^{N_x} = \log_2\left(\frac{E_{k,\varepsilon}^{N_x}}{E_{k,\varepsilon}^{2N_x}}\right), \quad k = 1, 2.$$

For each fixed N_x, uniform errors $E_k^{N_x}$ are obtained as

$$E_k^{N_x} = \max_{\varepsilon \in S} E_{k,\varepsilon}^{N_x}, \quad k = 1, 2,$$

where $S = \{\varepsilon | \varepsilon = 2^{-10}, 2^{-14}, \ldots, 2^{-28}\}$. Moreover, the associated orders of parameter uniform convergence $\chi_k^{N_x}$ are given by

$$\chi_k^{N_x} = \log_2 \left(\frac{E_k^{N_x}}{E_k^{2N_x}} \right), \quad k = 1, 2.$$

The overall error $\boldsymbol{E}^{N_x}$ and corresponding orders of convergence $\boldsymbol{\chi}^{N_x}$ are given by

$$\begin{aligned} \boldsymbol{E}^{N_x} &= \max\{E_1^{N_x}, E_2^{N_x}\}, \\ \boldsymbol{\chi}^{N_x} &= \log_2 \left(\frac{\boldsymbol{E}^{N_x}}{\boldsymbol{E}^{2N_x}} \right). \end{aligned}$$

We denote y_k and $\widetilde{y}_k$ as the solution components of the exact and numerical solutions, respectively. Moreover, the bold notation represents the solution in vector form.

Example 6.6.1. *First, we solve the following fourth-order BVP*

$$\begin{aligned} &-\varepsilon y^{(4)}(x) - 2(2x+1)y'''(x) + xy''(x) + 4y'(x) + y(x) = -\cos x, \quad x \in (0,1), \\ &y(0) = 1, y(1) = 1,\ y''(0) = -1,\ y''(1) = -1. \end{aligned}$$

Example 6.6.2. *Next, we solve the following fourth-order BVP*

$$\begin{aligned} &-\varepsilon y^{(4)}(x) - \exp(1-x)y'''(x) + y''(x) + y(x) = -\exp(x), \quad x \in (0,1), \\ &y(0) = 1, y(1) = 1,\ y''(0) = -1,\ y''(1) = -1. \end{aligned}$$

Example 6.6.3. *Last, we solve the following nonlinear fourth-order BVP*

$$\begin{aligned} &-\varepsilon y^{(4)}(x) - \exp(2x+1)y'''(x) + y''^2(x) + y(x) = 0, \quad x \in (0,1), \\ &y(0) = 1, y(1) = 1,\ y''(0) = -1,\ y''(1) = -1. \end{aligned}$$

As we notice, the perturbation parameter does not appear in the first equation of the system (6.1.3), so we do not observe any sharp boundary layer in the first solution component. While the second solution component exhibits a boundary layer near the left end of the domain. As cited before, the uniform mesh is unsuitable for resolving the boundary layers. One cannot accomplish the purpose of getting parameter uniform estimations on this mesh. So, in the present chapter, we preferred the eXp mesh to obtain the numerical outcomes for all problems. Tables 6.1, 6.2, 6.4, and 6.5 validate the parameter-uniform results for the solutions $\widetilde{y}_1$ and $\widetilde{y}_2$ in Examples 6.6.1 and 6.6.2, which are uniformly convergent of $O(N_x^{-2})$. These tables prove that ε-uniform errors monotonically decrease as the number of mesh intervals N_x increases. Further, we have also determined ε-uniform orders of convergence and ε-uniform error constants $\boldsymbol{C}^{N_x}$ (see [113], Chapter 8, page 166 for the computation of $\boldsymbol{C}^{N_x}$) to verify this analogy.

A comparison of numerical results between eXp, Shishkin, and Bakhvalov-Shishkin (B-S) mesh is given in Tables 6.3 and 6.6. One can notice that results on Shishkin mesh provide almost second-order accuracy (which is of $O(N_x^{-2}\ln^2 N_x)$). While on B-S and eXp mesh, the acquired results give second-order accuracy with reduced errors compared to the Shishkin mesh.

As mentioned in [91], B-S and eXp meshes are suitable choices for these class problems, varying by a small variation in the selection of mesh generating function $\Upsilon(\varrho)$. We have illustrated the formation of the boundary layer in the solution component $\widetilde{y}_2$ by plotting the graphs of the numerical solution. From Figs. 6.1 and 6.2, it can be noticed that the layer at $x = 0$, for $\varepsilon = 10^{-4}$ (refer Figs. 6.1(b) and 6.2(b)) is stiffer as compared to $\varepsilon = 10^{-2}$ (refer Figs. 6.1(a) and 6.2(a)) which confirm the aspect, decreasing the ε results in the decreasement of the width of the layer. We have considered a nonlinear fourth-order BVP in Example 6.6.3. After converting into a system (like (6.1.3)), we see that nonlinearity appears in the second equation. For Example 6.6.3, we provide the uniform results of $O(N_x^{-2})$ in Tables 6.7 and 6.8. In Figure 6.3, it is easy to see the boundary layer in the second component, whose width decreases as ε decreases.

Table 6.1: $E_{1,\varepsilon}^{N_x}$, $\chi_{1,\varepsilon}^{N_x}$, $E_1^{N_x}$, $\chi_1^{N_x}$, and CPU time (in seconds) for Example 6.6.1

	N_x				
ε	32	64	128	256	512
2^{-10}	$9.2932e-06$	$2.2039e-06$	$6.6282e-07$	$1.8114e-07$	$4.6799e-08$
	2.0761	1.7334	1.8715	1.9526	
2^{-14}	$1.3729e-05$	$3.4945e-06$	$8.7867e-07$	$2.1961e-07$	$5.4710e-08$
	1.9741	1.9917	2.0004	2.0051	
2^{-18}	$1.4070e-05$	$3.6006e-06$	$9.1120e-07$	$2.2926e-07$	$5.7483e-08$
	1.9663	1.9824	1.9908	1.9958	
2^{-22}	$1.4092e-05$	$3.6072e-06$	$9.1325e-07$	$2.2986e-07$	$5.7654e-08$
	1.9659	1.9818	1.9903	1.9953	
2^{-26}	$1.4101e-05$	$3.6077e-06$	$9.1338e-07$	$2.2990e-07$	$5.7666e-08$
	1.9666	1.9818	1.9902	1.9952	
2^{-28}	$1.4125e-05$	$3.6077e-06$	$9.1338e-07$	$2.2990e-07$	$5.7667e-08$
	1.9691	1.9818	1.9902	1.9952	
CPU time	0.0992	0.1282	0.1693	0.2021	0.5095
$E_1^{N_x}$	$1.4125e-05$	$3.6077e-06$	$9.1338e-07$	$2.2990e-07$	$5.7667e-08$
$\chi_1^{N_x}$	1.9691	1.9818	1.9902	1.9952	
$C_1^{N_x}$	0.0193	0.0197	0.0200	0.0201	0.0202

Table 6.2: $E_{2,\varepsilon}^{N_x}$, $\chi_{2,\varepsilon}^{N_x}$, $E_2^{N_x}$, $\chi_2^{N_x}$, and CPU time (in seconds) for Example 6.6.1

	N_x				
ε	32	64	128	256	512
2^{-10}	$1.2311e-02$	$3.1789e-03$	$7.9747e-04$	$1.9888e-04$	$4.9551e-05$
	1.9533	1.9950	2.0035	2.0049	
2^{-14}	$1.2231e-02$	$3.1554e-03$	$7.9098e-04$	$1.9716e-04$	$4.9158e-05$
	1.9546	1.9961	2.0043	2.0039	
2^{-18}	$1.2225e-02$	$3.1538e-03$	$7.9052e-04$	$1.9704e-04$	$4.9071e-05$
	1.9547	1.9962	2.0043	2.0055	
2^{-22}	$1.2225e-02$	$3.1537e-03$	$7.9050e-04$	$1.9700e-04$	$4.7323e-05$
	1.9547	1.9962	2.0046	2.0576	
2^{-26}	$1.2225e-02$	$3.1537e-03$	$7.9046e-04$	$1.9703e-04$	$4.7301e-05$
	1.9547	1.9963	2.0043	2.0585	
2^{-28}	$1.2225e-02$	$3.1537e-03$	$7.9046e-04$	$1.9703e-04$	$4.7300e-05$
	1.9547	1.9963	2.0043	2.0585	
CPU time	0.0937	0.1313	0.1507	0.1994	0.5096
$E_2^{N_x}$	$1.2311e-02$	$3.1789e-03$	$7.9747e-04$	$1.9888e-04$	$4.9551e-05$
$\chi_2^{N_x}$	1.9533	1.9950	2.0035	2.0049	
$C_2^{N_x}$	16.6912	17.2237	17.2695	17.3002	17.3000

Table 6.3: Uniform MPEs comparison in the solution for Example 6.6.1

	eXp mesh			Shishkin mesh			B-S mesh		
N_x	$\boldsymbol{E}^{N_x}$	$\boldsymbol{\chi}^{N_x}$	$\boldsymbol{C}^{N_x}$	$\boldsymbol{E}^{N_x}$	$\boldsymbol{\chi}^{N_x}$	$\boldsymbol{C}^{N_x}$	$\boldsymbol{E}^{N_x}$	$\boldsymbol{\chi}^{N_x}$	$\boldsymbol{C}^{N_x}$
32	$1.231e-02$	1.953	16.69	$9.280e-02$	1.625	31.10	$1.169e-02$	1.921	15.96
64	$3.178e-03$	1.995	17.22	$3.007e-02$	1.558	29.67	$3.086e-03$	1.975	16.85
128	$7.974e-04$	2.003	17.26	$1.021e-02$	1.617	29.65	$7.849e-04$	1.992	17.14
256	$1.988e-04$	2.004	17.30	$3.328e-03$	1.649	28.47	$1.972e-04$	1.997	17.23
512	$4.955e-05$	-	17.30	$1.061e-03$	-	28.40	$4.938e-05$	-	17.25

Table 6.4: $E_{1,\varepsilon}^{N_x}$, $\chi_{1,\varepsilon}^{N_x}$, $E_1^{N_x}$, $\chi_1^{N_x}$, and CPU time (in seconds) for Example 6.6.2

	N_x				
ε	32	64	128	256	512
2^{-10}	$8.4932e-05$	$2.2161e-05$	$5.6284e-06$	$1.4107e-06$	$3.5092e-07$
	1.9383	1.9772	1.9963	2.0072	
2^{-14}	$8.9221e-05$	$2.3507e-05$	$6.0327e-06$	$1.5268e-06$	$3.8391e-07$
	1.9243	1.9622	1.9823	1.9917	
2^{-18}	$8.9495e-05$	$2.3593e-05$	$6.0593e-06$	$1.5344e-06$	$3.8606e-07$
	1.9234	1.9611	1.9815	1.9908	
2^{-22}	$8.9513e-05$	$2.3599e-05$	$6.0609e-06$	$1.5349e-06$	$3.8620e-07$
	1.9234	1.9611	1.9815	1.9908	
2^{-26}	$8.9518e-05$	$2.3599e-05$	$6.0610e-06$	$1.5349e-06$	$3.8621e-07$
	1.9234	1.9611	1.9815	1.9907	
2^{-28}	$8.9531e-05$	$2.3599e-05$	$6.0610e-06$	$1.5349e-06$	$3.8621e-07$
	1.9234	1.9611	1.9815	1.9908	
CPU time	0.1789	0.1995	0.2334	0.3429	0.7541
$E_1^{N_x}$	$8.9531e-05$	$2.3599e-05$	$6.0610e-06$	$1.5349e-06$	$3.8621e-07$
$\chi_1^{N_x}$	1.9234	1.9611	1.9815	1.9908	
$C_1^{N_x}$	0.1222	0.1284	0.1324	0.1341	0.1350

Table 6.5: $E_{2,\varepsilon}^{N_x}$, $\chi_{2,\varepsilon}^{N_x}$, $E_2^{N_x}$, $\chi_2^{N_x}$, and CPU time (in seconds) for Example 6.6.2

	N_x				
ε	32	64	128	256	512
2^{-10}	$3.9384e-02$	$1.0381e-02$	$2.4893e-03$	$6.2139e-04$	$1.5487e-04$
	1.9237	2.0601	2.0022	2.0044	
2^{-14}	$3.9429e-02$	$1.0389e-02$	$2.4912e-03$	$6.2176e-04$	$1.5494e-04$
	1.9242	2.0601	2.0024	2.0045	
2^{-18}	$3.9432e-02$	$1.0390e-02$	$2.4913e-03$	$6.2179e-04$	$1.5499e-04$
	1.9242	2.0602	2.0024	2.0043	
2^{-22}	$3.9432e-02$	$1.0390e-02$	$2.4913e-03$	$6.2172e-04$	$1.5472e-04$
	1.9242	2.0602	2.0026	2.0066	
2^{-26}	$3.9432e-02$	$1.0390e-02$	$2.4909e-03$	$6.2073e-04$	$1.5368e-04$
	1.9242	2.0605	2.0046	2.0140	
2^{-28}	$3.9432e-02$	$1.0390e-02$	$2.4905e-03$	$6.2073e-04$	$1.5367e-04$
	1.9242	2.0607	2.0047	2.0141	
CPU time	0.1544	0.2096	0.2169	0.3190	0.9111
$E_2^{N_x}$	$3.9432e-02$	$1.0390e-02$	$2.4913e-03$	$6.2179e-04$	$1.5499e-04$
$\chi_2^{N_x}$	1.9242	2.0606	2.0024	2.0043	
$C_2^{N_x}$	53.8381	56.7417	54.3831	53.8494	53.8420

Table 6.6: Uniform MPEs comparison in the solution for Example 6.6.2

	eXp mesh			Shishkin mesh			B-S mesh		
N_x	$\boldsymbol{E}^{N_x}$	$\boldsymbol{\chi}^{N_x}$	$\boldsymbol{C}^{N_x}$	$\boldsymbol{E}^{N_x}$	$\boldsymbol{\chi}^{N_x}$	$\boldsymbol{C}^{N_x}$	$\boldsymbol{E}^{N_x}$	$\boldsymbol{\chi}^{N_x}$	$\boldsymbol{C}^{N_x}$
32	$3.943e-02$	1.924	53.83	$6.733e-02$	1.614	30.08	$3.647e-02$	1.858	49.78
64	$1.039e-02$	2.060	56.74	$2.196e-02$	1.422	30.78	$1.006e-02$	2.037	54.92
128	$2.491e-03$	2.002	54.38	$8.190e-03$	1.650	36.04	$2.450e-04$	1.984	53.51
256	$6.217e-04$	2.004	53.84	$2.608e-03$	1.641	36.01	$6.191e-04$	2.008	54.09
512	$1.549e-04$	-	53.84	$8.360e-04$	-	36.23	$1.539e-04$	-	53.78

Table 6.7: $E_{1,\varepsilon}^{N_x}$, $\chi_{1,\varepsilon}^{N_x}$, $E_1^{N_x}$, $\chi_1^{N_x}$, and CPU time (in seconds) for Example 6.6.3

	N_x				
ε	32	64	128	256	512
2^{-10}	$9.3838e-07$	$3.1206e-07$	$9.7593e-08$	$2.8182e-08$	$6.9874e-09$
	1.5883	1.6770	1.7920	2.0119	
2^{-14}	$1.3668e-06$	$3.5111e-07$	$8.8247e-08$	$2.2015e-08$	$5.4701e-09$
	1.9608	1.9923	2.0031	2.0088	
2^{-18}	$1.4074e-06$	$3.6409e-07$	$9.2215e-08$	$2.3172e-08$	$5.8045e-09$
	1.9507	1.9812	1.9926	1.9971	
2^{-22}	$1.4279e-06$	$3.6491e-07$	$9.2465e-08$	$2.3247e-08$	$5.8270e-09$
	1.9683	1.9806	1.9919	1.9962	
2^{-26}	$1.4280e-06$	$3.6490e-07$	$9.2464e-08$	$2.3246e-08$	$5.8270e-09$
	1.9683	1.9806	1.9919	1.9962	
2^{-28}	$1.4280e-06$	$3.6490e-07$	$9.2464e-08$	$2.3246e-08$	$5.8270e-09$
	1.9691	1.9818	1.9902	1.9952	
CPU time	0.2997	0.4162	0.6000	1.2170	4.4456
$E_1^{N_x}$	$1.4280e-06$	$3.6490e-07$	$9.7593e-08$	$2.8182e-08$	$6.9874e-09$
$\chi_1^{N_x}$	1.9684	1.9027	1.7920	2.0119	
$C_1^{N_x}$	0.0023	0.0020	0.0020	0.0020	0.0020

Table 6.8: $E_{2,\varepsilon}^{N_x}$, $\chi_{2,\varepsilon}^{N_x}$, $E_2^{N_x}$, $\chi_2^{N_x}$, and CPU time (in seconds) for Example 6.6.3

	N_x				
ε	32	64	128	256	512
2^{-10}	$1.6945e-02$	$3.6257e-03$	$9.3528e-04$	$2.3547e-04$	$5.8666e-05$
	2.2245	1.9548	1.9899	2.0049	
2^{-14}	$1.6935e-02$	$3.6247e-03$	$9.3488e-04$	$2.3536e-04$	$5.8630e-05$
	2.2241	1.9550	1.9899	2.0052	
2^{-18}	$1.6934e-02$	$3.6246e-03$	$9.3486e-04$	$2.3537e-04$	$5.8712e-05$
	2.2240	1.9550	1.9898	2.0032	
2^{-22}	$1.6934e-02$	$3.6246e-03$	$9.3485e-04$	$2.3527e-04$	$5.9486e-05$
	2.2241	1.9550	1.9904	1.9837	
2^{-26}	$1.6934e-02$	$3.6246e-03$	$9.3485e-04$	$2.3527e-04$	$5.9486e-05$
	2.2241	1.9550	1.9904	1.9837	
2^{-28}	$1.6934e-02$	$3.6246e-03$	$9.3485e-04$	$2.3527e-04$	$5.9486e-05$
	2.2241	1.9550	1.9904	1.9837	
CPU time	0.2880	0.4400	0.4940	1.2604	4.2056
$E_2^{N_x}$	$1.6945e-02$	$3.6257e-03$	$9.3528e-04$	$2.3547e-04$	$5.9486e-05$
$\chi_2^{N_x}$	2.2245	1.9548	1.9899	1.9849	
$C_2^{N_x}$	23.1150	19.7949	20.4110	20.6940	20.3641

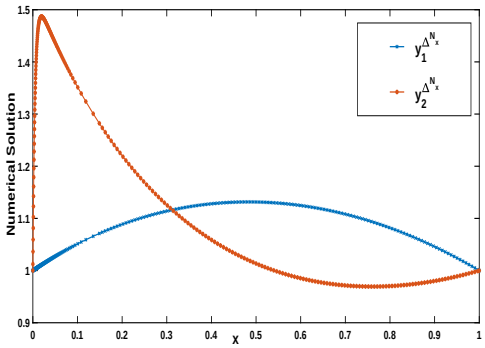

(a) $N_x = 256,\ \varepsilon = 10^{-2}$

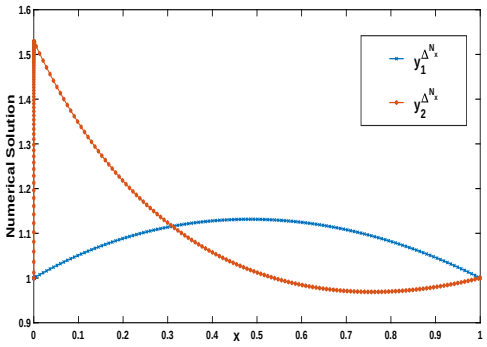

(b) $N_x = 256,\ \varepsilon = 10^{-4}$

Figure 6.1: Numerical solution plots (subfigures (a) and (b)) of Example 6.6.1

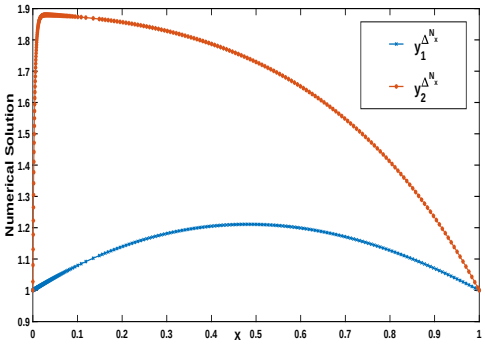

(a) $N_x = 256,\ \varepsilon = 10^{-2}$

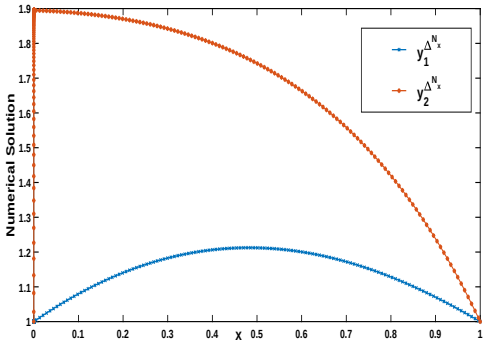

(b) $N_x = 256,\ \varepsilon = 10^{-4}$

Figure 6.2: Numerical solution plots (subfigures (a) and (b)) of Example 6.6.2

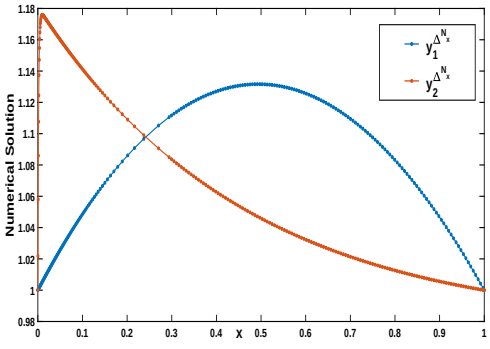

(a) $N_x = 256,\ \varepsilon = 10^{-2}$

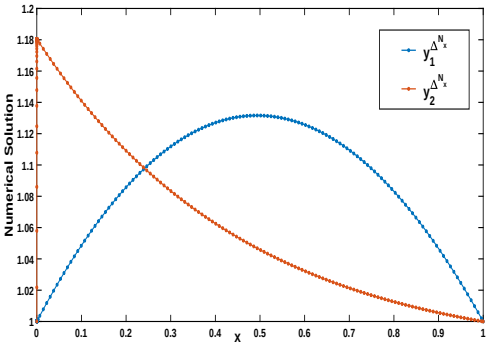

(b) $N_x = 256,\ \varepsilon = 10^{-4}$

Figure 6.3: Numerical solution plots (subfigures (a) and (b)) of Example 6.6.3

6.7 Concluding comments

A numerical method incorporating the quadratic $\mathfrak{B}$-splines on the eXp mesh is analyzed for the fourth-order convection-diffusion type linear and nonlinear singularly perturbed BVPs. Since eXp mesh does not require prior knowledge about the transition parameter, this is our primary motivation to adopt this mesh. In contrast, different meshes given by Bakhvalov and Shishkin need these details in advance. The nonlinear differential equations are linearized through Newton's method. The calculated theoretical bounds on the spline interpolation error demonstrate that the present method shows second-order parameter-uniform accuracy. The numerical results in the tables ensure the theoretical estimations in Section 6.4.

Chapter 7

Conclusions

The most important findings gained throughout this thesis are gathered in this section. In addition, it addresses the various paths that may be taken to build upon the existing study and dives into further investigating these directions.

7.1 Summary

The results of this thesis, along with some significant remarks, are broken down into their essential components as follows:

- The first chapter discusses the analytical and mathematical foundations of singular perturbation theory. This thesis is devoted to developing robust numerical techniques to resolve the challenges associated with the computational treatment of singularly perturbed problems. The first chapter of this research attempts to discuss most of these difficulties in greater depth.

- Chapter 2 offers a novel numerical method for solving degenerate parabolic problems of the convection-diffusion type subject to singular perturbations. We present a computation framework that combines the Crank-Nicolson scheme with the quadratic spline collocation method in time and spatial direction, respectively. This hybrid approach has been meticulously crafted to handle the complexities of solving the concerned class of singularly perturbed problems. In conjunction with this, an exponentially graded mesh

is employed precisely, which brings about resolution inside the boundary layer domain. The comprehensive examination of error and rigorous analysis confirms that the suggested technique provides second-order parameter-uniform convergence. Remarkably, the proposed approach outperforms current methods in terms of effectiveness.

- As we progressed through Chapter 3, we examined a more challenging topic, a weakly coupled system of ℓ singularly perturbed reaction-diffusion equations. These systems typically result in double-layer structures because of parameters (commonly denoted by ε) that multiply the highest-order derivative term. The decision to use an exponentially graded mesh was driven substantially by the specific benefits offered by this method over other approaches to meshing, such as the Shishkin and Bakhvalov-type meshes. The theoretical bounds of the spline interpolation error have been calculated by carefully examining the underlying methodology. These second-order robustly convergent results of the suggested approach are remarkable because they hold regardless of the size of the perturbation parameter. In a complete review of the various physical and numerical characteristics of singularly perturbed systems, this suggested collocation approach is practical and easily implementable.

- The complex dynamical interaction between diffusion and reaction processes in complex systems is illustrated in Chapter 4 as we discuss a class of models referred to as weakly coupled systems of parabolic singularly perturbed reaction-diffusion equations. We provide a robust numerical technique based on splines to solve the problem of a singularly perturbed system consisting of equations with the same diffusion parameter. The theoretical background verifies that the suggested method converges uniformly and achieves second-order spatial precision. In addition, the Crank-Nicolson approach is used to confirm the temporal accuracy of second-order. The execution practice of the conceived system substantiates the unchanging credibility of both the theoretical bounds and the tabulated outcomes.

- In addition, the current thesis contributes toward developing an efficient numerical technique for the fourth-order singularly perturbed problems in Chapters 5 and 6. The solutions presented by the researchers illuminate the enigmatic intricacies inherent in

natural phenomena, offering us a look into the underlying principles governing a diverse range of physical processes. As mentioned above, the presence of boundary layers is a fundamental attribute of the equations. Spline techniques have yet to be explored in the literature for these problems. The complex nature of the problem can be made easier to handle by reformulating it into a system of reaction-diffusion/convection-diffusion problems of the second order in which one equation is free from perturbation parameters. To address these boundary value problems, we investigate a numerical method that applies quadratic B-splines across an exponentially graded mesh. The computed theoretical bounds on the spline interpolation error reveal that the technique is second-order parameter-uniformly convergent. Later on, in Chapter 6, we also considered the non-linear boundary value problem. The detailed tabulation of numerical data validates the theoretical estimates about convergence orders and errors.

7.2 Future scopes

Examining the complexities of numerical methods based on quadratic spline for singularly perturbed problems, we explore a fascinating terrain of less explored paths and promising directions for future development in this area. The results of this study provide new avenues for investigation and creativity in addition to adding to the corpus of existing knowledge. The possible paths for further research are described in this section, emphasizing the areas that call for more in-depth investigation and methodological advancements.

1. Singularly perturbed integro-differential equations arising in finance, electrostatics, chemistry, biology, theory of elasticity, potential theory, heat and mass transfer, astronomy, and fluid dynamics [142].

2. Higher dimensional singularly perturbed differential equations [143].

3. Time fractional singularly perturbed PDEs [144].

4. Delay differential equations and delay integro-differential equations [145, 146].

Bibliography

[1] S. Singh, D. Kumar, and J. Vigo-Aguiar. A robust numerical technique for weakly coupled system of parabolic singularly perturbed reaction–diffusion equations. *J. Math. Chem.*, 61:1313–1350, 2023.

[2] A. C. Fowler. Convective diffusion of an enzyme reaction. *SIAM J. Appl. Math.*, 33: 289–297, 1977.

[3] R. Dillon, P. K. Maini, and H. G. Othmer. Pattern formation in generalized turing systems. *J. Math. Biol.*, 32:345–393, 1994.

[4] R. E. O'Malley. *Singular Perturbation Methods for Ordinary Differential Equations*. Springer-Verlag, New York, 1990.

[5] B. Semper. Locking in finite-element approximations to long thin extensible beams. *IMA J. Numer. Anal.*, 14:97–109, 1994.

[6] K. W. Morton. *Numerical Solution of Convection-Diffusion Problems*. Chapman & Hall, London, 1996.

[7] C. V. Pao. *Nonlinear parabolic and elliptic equations*. Plenum Press, New York, 1992.

[8] T. Linß. *Layer-Adapted Meshes for Reaction-Convection-Diffusion Problems*. Springer-Verlag, Berlin, 2010.

[9] H. G. Roos, M. Stynes, and L. Tobiska. *Robust Numerical Methods for Singularly Perturbed Differential Equations: Convection-Diffusion-Reaction and Flow Problems*. Springer, Berlin, 2008.

[10] L. Prandtl. Uber flussigkeits-bewegung bei kleiner reibung. in verhandlungen. pages 484–491, 1905.

[11] W. Wasow. *On Boundary Layer Problems in the Theory of Ordinary Differential Equations*. PhD thesis, New York University, New York, U.S.A., 1941.

[12] K. O. Friedrichs and W. R. Wasow. Singular perturbations of nonlinear oscillations. *Duke Math. J.*, 13:367–381, 1946.

[13] J. J. H. Miller, E. O. Riordan, and G. I. Shishkin. *Fitted numerical methods for singular perturbation problems*. Word Scientific, Singapore, 1996.

[14] H. G. Roos, M. Stynes, and L. Tobiska. *Numerical Methods for Singularly Perturbed Differential Equations*. Springer-Verlag, Berlin, 2008.

[15] A. H. Nayfeh. *Introduction to Perturbation Techniques*. John Wiley & Sons, New York, 1993.

[16] R. E. O'Malley Jr. *Introduction to Singular Perturbations*. Academic Press, New York, 1974.

[17] R. E. O'Malley Jr. *Singular Perturbation Methods for Ordinary Differential Equations*. Springer, New York, 1991.

[18] R. Bellman. *Perturbation Techniques in Mathematics, Physics and Engineering*. Holt, Rinehart, Winston, New York, 1964.

[19] D. R. Smith. *Singular Perturbation Theory*. Cambridge University Press, Cambridge, UK, 1985.

[20] C. E. Pearson. On a differential equation of boundary layer type. *J. Math. Phys.*, 47: 134–154, 1968.

[21] C. E. Pearson. On nonlinear ordinary differential equations of boundary layer type. *J. Math. Phys.*, 47:351–358, 1968.

[22] M. K. Kadalbajoo and V. Gupta. A brief survey on numerical methods for solving singularly perturbed problems. *Appl. Math. Comput.*, 217:3641–3716, 2010.

[23] M. K. Kadalbajoo and K. C. Patidar. A survey of numerical techniques for solving singularly perturbed ordinary differential equations. *Appl. Math. Comput.*, 130:457–510, 2002.

[24] M. K. Kadalbajoo and K. C. Patidar. Singularly perturbed problems in partial differential equations: a survey. *Appl. Math. Comput.*, 134:371–429, 2003.

[25] M. K. Kadalbajoo and Y. N. Reddy. Asymptotic and numerical analysis of singular perturbation problems: a survey. *Appl. Math. Comput.*, 30:223–259, 1989.

[26] R. Vulanović and P. A. Farrell. Continuous and numerical analysis of a multiple boundary turning point problem. *SIAM J. Numer. Anal.*, 30:1400–1418, 1993.

[27] S. Natesan and N. Ramanujam. A computational method for solving singularly perturbed turning point problems exhibiting twin boundary layers. *Appl. Math. Comput.*, 93:259–275, 1998.

[28] S. Natesan, J. Jayakumar, and J. Vigo-Aguiar. Parameter uniform numerical method for singularly perturbed turning point problems exhibiting boundary layers. *J. Comput. Appl. Math.*, 158:121–134, 2003.

[29] K. K. Sharma, P. Rai, and K. C. Patidar. A review on singularly perturbed differential equations with turning points and interior layers. *Appl. Math. Comput.*, 219:10575–10609, 2013.

[30] D. Kumar. A collocation method for singularly perturbed differential-difference turning point problems exhibiting boundary/interior layers. *J. Differ. Equ. Appl.*, 24:1847–1870, 2018.

[31] D. Kumar. A parameter-uniform method for singularly perturbed turning point problems exhibiting interior or twin boundary layers. *Int. J. Comput. Math.*, 96:865–882, 2019.

[32] M. P. Alam, D. Kumar, and A. Khan. Trigonometric quintic b-spline collocation method for singularly perturbed turning point boundary value problems. *Int. J. Comput. Math.*, 98:1029–1048, 2021.

[33] N. S. Bakhvalov. On the optimization of methods for solving boundary value problems in the presence of boundary layers. *Zh. Vychisl. Mat. Mat. Fiz.*, 9:841–859, 1969.

[34] E. O'Riordan and M. Stynes. A uniformly accurate finite-element method for a singularly perturbed one-dimensional reaction-diffusion problem. *Math. Comp.*, 47: 555–570, 1986.

[35] H. G. Roos, M. Stynes, and L. Tobiska. *Numerical Methods for Singularly Perturbed Differential Equations, Convection-Diffusion and Flow Problems*. Springer-Verlag, New York, 1996.

[36] G. I. Shishkin. Mesh approximation of singularly perturbed boundary-value problems for systems of elliptic and parabolic equations. *Comput. Maths. Math. Phys.*, 35: 429–446, 1995.

[37] N. Madden. *Numerical methods for wave-current interactions*. National University of Ireland, Cork, 2000.

[38] S. Matthews. *Parameter robust methods for a system of coupled singularly perturbed ordinary differential reaction-diffusion equations*. School of Mathematical Sciences, Dublin City University, 2000.

[39] S. Matthews, J. J. H. Miller, E. O'Riordan, and G. I. Shishkin. Parameter-robust numerical methods for a system of reaction-diffusion problems with boundary layers. In J.J.H. Miller, G. I. Shishkin, and L. Vulkov, editors, *Analytical and Numerical Methods for Convection-Dominated and Singularly Perturbed Problems*, pages 219–224. Nova Science Publishers Inc., New York, USA, 2000.

[40] S. Matthews, E. O'Riordan, and G. I. Shishkin. A numerical method for a system of singularly perturbed reaction-diffusion equations. *J. Comput. Appl. Math.*, 145: 151–166, 2002.

[41] N. Madden and M. Stynes. A uniformly convergent numerical method for a coupled system of singularly perturbed linear reaction-diffusion problems. *IMA J. Numer. Anal*, 23:627–644, 2003.

[42] T. Valanarasu and N. Ramanujam. An asymptotic initial value method for boundary value problems for a system of singularly perturbed second order ordinary differential equations. *Appl. Math. Comput.*, 147:227–240, 2004.

[43] T. Linß and N. Madden. Accurate solution of a system of coupled singularly perturbed reaction-diffusion equations. *Computing*, 73:121–133, 2004.

[44] T. Linß and N. Madden. A finite element analysis of a coupled system of singularly perturbed reaction-diffusion equations. *Appl. Math. Comput.*, 148:869–880, 2004.

[45] S. Natesan and B. S. Deb. A robust computational method for singularly perturbed coupled system of reaction-diffusion boundary-value problems. *Appl. Math. Comput.*, 188:353–364, 2007.

[46] C. Clavero, J. L. Gracia, and F. J. Lisbona. High order schemes for reaction-diffusion singularly perturbed systems. *Lect. Notes Comput. Sci. Eng.*, 69:107–115, 2009.

[47] C. Clavero, J. L. Gracia, and F. J. Lisbona. An almost third order finite difference scheme for singularly perturbed reaction-diffusion systems. *J. Comput. Appl. Math.*, 234:2501–2515, 2010.

[48] P. Das and S. Natesan. Optimal error estimate using mesh equidistribution technique for singularly perturbed system of reaction-diffusion boundary-value problems. *Appl. Math. Comput.*, 249:265–277, 2014.

[49] R. Lin and M. Stynes. A balanced finite element method for a system of singularly perturbed reaction-diffusion two-point boundary value problems. *Numer. Algorithms*, 70:691–707, 2015.

[50] P. Das and J. Vigo-Aguiar. Parameter uniform optimal order numerical approximation of a class of singularly perturbed system of reaction diffusion problems involving a small perturbation parameter. *J. Comput. Appl. Math.*, 354:533–544, 2019.

[51] G. Singh and S. Natesan. A uniformly convergent numerical scheme for a coupled system of singularly perturbed reaction-diffusion equations. *Numer. Funct. Anal. Opti.*, 41:1172–1189, 2020.

[52] T. Linß and N. Madden. Layer-adapted meshes for a linear system of coupled singularly perturbed reaction-diffusion problems. *IMA J. Numer. Anal.*, 29:109–125, 2009.

[53] J. L. Gracia, F. J. Lisbona, and E. O'Riordan. A coupled system of singularly perturbed parabolic reaction-diffusion equations. *Adv. Comput. Math.*, 32:43–61, 2008.

[54] R. B. Kellogg, T. Linß and M. Stynes. A finite difference method on layer-adapted meshes for an elliptic reaction-diffusion system in two dimensions. *Math. Comp.*, 77: 2085–2096, 2008.

[55] R. B. Kellogg, N. Madden, and M. Stynes. A parameter-robust numerical method for a system of reaction-diffusion equations in two dimensions. *Numer. Methods Partial Differential Equations*, 24:312–334, 2008.

[56] P. Das, S. Rana, and J. Vigo-Aguiar. Higher order accurate approximations on equidistributed meshes for boundary layer originated mixed type reaction-diffusion systems with multiple scale nature. *Appl. Numer. Math.*, 148:79–97, 2020.

[57] P. Das. Comparison of a priori and a posteriori meshes for singularly perturbed nonlinear parameterized problems. *J. Comput. Appl. Math.*, 290:16–25, 2015.

[58] P. Das. An a posteriori based convergence analysis for a nonlinear singularly perturbed system of delay differential equations on an adaptive mesh. *Numer. Algor.*, 81:465–487, 2019.

[59] D. Shakti, J. Mohapatra, P. Das, and J. Vigo-Aguiar. A moving mesh refinement based optimal accurate uniformly convergent computational method for a parabolic system of boundary layer originated reaction-diffusion problems with arbitrary small diffusion terms. *J. Comput. Appl. Math.*, 404(113167), 2022.

[60] P. Das and S. Natesan. Higher-order parameter uniform convergent schemes for robin type reaction-diffusion problems using adaptively generated grid. *Int J. Comput. Methods*, 9(1250052), 2012.

[61] C. Clavero and J. L. Gracia. An improved uniformly convergent scheme in space for 1d parabolic reaction-diffusion systems. *Appl. Math. Comput.*, 243:57–73, 2014.

[62] S. C. S. Rao and S. Kumar. An almost fourth order uniformly convergent domain decomposition method for a coupled system of singularly perturbed reaction-diffusion equations. *J. Comput. Appl. Math.*, 235:3342–3354, 2011.

[63] M. Kumar and S. Kumar. High order robust approximations for singularly perturbed semilinear systems. *Appl. Math. Model.*, 36:3570–3579, 2012.

[64] P. Das and S. Natesan. A uniformly convergent hybrid scheme for singularly perturbed system of reaction-diffusion robin type boundary-value problems. *J. Appl. Math. Comput.*, 41:447–471, 2013.

[65] M. Chandru, T. Prabha, P. Das, and V. Shanthi. A numerical method for solving boundary and interior layers dominated parabolic problems with discontinuous convection coefficient and source terms. *Diff. Equ. Dyn. Syst.*, 27:91–112, 2019.

[66] P. Das and V. Mehrmann. Numerical solution of singularly perturbed convection-diffusion-reaction problems with two small parameters. *BIT Numer. Math.*, 56:51–76, 2016.

[67] M. Chandru, P. Das, and H. Ramos. Numerical treatment of two-parameter singularly perturbed parabolic convection diffusion problems with non-smooth data. *Math. Meth. Appl. Sci.*, 41:5359–5387, 2018.

[68] B. Semper. Conforming finite element approximations for a fourth-order singular perturbation problem. *SIAM J. Numer. Anal*, 29:1043–1058, 1992.

[69] S. Franz and H. G. Roos. Robust error estimation in energy and balanced norms for singularly perturbed fourth order problems. *Comput. Math. Appl.*, 72:233–247, 2016.

[70] A. Gupta and A. Kaushik. A higher-order hybrid finite difference method based on grid equidistribution for fourth-order singularly perturbed differential equations. *J. Appl. Math. Comput.*, 68:1163–1191, 2022.

[71] P. Panaseti, A. Zouvani, N. Madden, and C. Xenophontos. A c^1-conforming *hp* finite element method for fourth order singularly perturbed boundary value problems. *Appl. Numer. Math.*, 104:81–97, 2016.

[72] P. Constantinou, C. Varnava, and C. Xenophontos. An *hp* finite element method for 4th order singularly perturbed problems. *Numer. Algorithms*, 73:567–590, 2016.

[73] C. Xenophontos. A parameter robust finite element method for fourth order singularly perturbed problems. *Comput. Methods Appl. Math.*, 17:337–349, 2017.

[74] T. C. Hanks. Model relating heat-flow values near, and vertical velocities of mass transport beneath, oceanic rises. *J. Geophysical Research*, 76:537–544, 1971.

[75] H. Schlichting and K. Gersten. *Boundary-Layer Theory*. MacGraw Hill, New York, 1979.

[76] V. Gupta and M. K. Kadalbajoo. A layer adaptive b-spline collocation method for singularly perturbed one-dimensional parabolic problem with a boundary turning point. *Numer. Methods Partial Differential Equations*, 27:1143–1164, 2010.

[77] S. K. Sahoo and V. Gupta. Second-order parameter-uniform finite difference scheme for singularly perturbed parabolic problem with a boundary turning point. *J. Diff. Equ. Appl.*, 27:223–240, 2021.

[78] R. K. Dunne, E. O'Riordan, and G. I. Shishkin. A fitted mesh method for a class of singularly perturbed parabolic problems with a boundary turning point. *Comput. Methods Appl. Math.*, 3:361–372, 2003.

[79] C. C. Christara, T. Chen, and D. M. Dang. Quadratic spline collocation for one-dimensional linear parabolic partial differential equations. *Numer. Algorithms*, 53: 511–553, 2010.

[80] M. Viscor and M. Stynes. A robust finite difference method for a singularly perturbed degenerate parabolic problem, part i. *Int. J. Numer. Anal. Model.*, 7:549–566, 2010.

[81] C. Clavero, J. L. Gracia, G. I. Shishkin, and L. P. Shishkina. Schemes convergent ε-uniformly for parabolic singularly perturbed problems with a degenerating convective term and a discontinuous source. *Math. Model. Anal.*, 20:641–657, 2015.

[82] A. Majumdar and S. Natesan. Second-order uniformly convergent richardson extrapolation method for singularly perturbed degenerate parabolic pdes. *Int. J. Appl. Comput. Math.*, 3:31–53, 2017.

[83] A. Majumdar and S. Natesan. An ε-uniform hybrid numerical scheme for a singularly perturbed degenerate parabolic convection-diffusion problem. *Int. J. Comput. Math.*, 96:1313–1334, 2019.

[84] S. Yadav, P. Rai, and K. K. Sharma. A higher order uniformly convergent method for singularly perturbed parabolic turning point problems. *Numer. Methods Partial Differential Equations*, 36:342–368, 2020.

[85] S. Kumar and J. Vigo-Aguiar. A parameter-uniform grid equidistribution method for singularly perturbed degenerate parabolic convection-diffusion problems. *J. Comput. Appl. Math.*, 2020. URL https://doi.org/10.1016/j.cam.2020.113273.

[86] O. A. Ladyzhenskaia, V. A. Solonnikov, and N. N. Uratseva. *Linear and Quasi-Linear Equations of Parabolic Type*. American Mathematical Society, USA, 1968.

[87] L. Bobisud. Second-order linear parabolic equations with a small parameter. *Arch. Ration. Mech. Anal*, 27:385–397, 1968.

[88] M. Stynes and E. O'Riordan. Uniformly convergent difference schemes for singularly perturbed parabolic diffusion-convection problems without turning points. *Numer. Math.*, 55:521–544, 1989.

[89] C. Clavero, J. L. Gracia, and J. C. Jorge. High-order numerical methods for one-dimensional parabolic singularly perturbed problems with regular layers. *Numer. Methods Partial Differential Equations*, 21:149–169, 2005.

[90] C. Clavero and J. L. Gracia. A high order hodie finite difference scheme for 1d parabolic singularly perturbed reaction-diffusion problems. *Appl. Math. Comput.*, 218: 5067–5080, 2012.

[91] P. Constantinou and C. Xenophontos. Finite element analysis of an exponentially graded mesh for singularly perturbed problems. *Comput. Methods Appl. Math.*, 15: 135–143, 2015.

[92] M. Shivhare, P. C. Podila, H. Ramos, and J. Vigo-Aguiar. Quadratic b-spline collocation method for time dependent singularly perturbed differential-difference equation arising in the modeling of neuronal activity. *Numer. Methods Partial Differential Equations*, 39:1805–1826, 2023.

[93] W. J. Kammerer, G. W. Reddien, and R. S. Varga. Quadratic interpolatory splines. *Numer. Math.*, 22:241–259, 1974.

[94] T. Linß G. Radojev, and H. Zarin. Approximation of singularly perturbed reaction-diffusion problems by quadratic c^1-splines. *Numer. Algorithms*, 61:35–55, 2012.

[95] Y. Kan-On and M. Mimura. Singular perturbation approach to a 3-component reaction-diffusion system arising in population dynamics. *SIAM J. Math. Anal.*, 29:1519–1536, 1998.

[96] W. Rodi. *Turbulence Models and Their Applications in Hydraulics*. (A. A. Balkema ed.) IAHR Monograph Series, 3rd edition, Rotterdam, 1993.

[97] G. P. Thomas. Towards an improved turbulence model for wave-current interactions. *in: Second Annual Report to EU MAST-III Project "The Kinematics and Dynamics of Wave-Current Interactions"*, 1998.

[98] W. H. Ruan and C. V. Pao. Asymptotic behavior and positive solutions of a chemical reaction diffusion system. *J. Math. Anal. Appl.*, 159:157–178, 1992.

[99] G. I. Barenblatt, I. P. Zheltov, and I. N. Kochina. Basic concepts in the theory of seepage of homogeneous liquids in fissured rocks. *J. Appl. Math. Mech.*, 24:1286–1303, 1960.

[100] S. C. Cowin. Bone poroelasiticity. *J. Biomech.*, 32:217–238, 1999.

[101] D. S. Naidu and A. Calise. Singular perturbations and time scales in guidance and control of aerospace systems: a survey. *J. Guid. Control Dyn.*, 24:1057–1078, 2001.

[102] M. Stephens and N. Madden. A parameter-uniform schwarz method for a coupled system of reaction-diffusion equations. *J. Comput. Appl. Math.*, 230:360–370, 2009.

[103] M. Shivhare, P. C. Podila, and D. Kumar. A uniformly convergent quadratic b-spline collocation method for singularly perturbed parabolic partial differential equations with two small parameters. *J. Math. Chem.*, 59:186–215, 2021.

[104] H. Zarin. Exponentially graded mesh for singularly perturbed problem with two small parameters. *Appl. Numer. Math.*, 120:233–242, 2017.

[105] S. Singh, D. Kumar, and H. Ramos. A uniformly convergent quadratic b-spline based scheme for singularly perturbed degenerate parabolic problems. *Math. Comput. Simulation*, 195:88–106, 2022.

[106] M. H. Protter and H. F. Weinberger. On the spectrum of general second-order operators. *Bull. Amer. Math. Soc.*, 72:251–255, 1966.

[107] T. Linß. Layer-adapted meshes for one-dimensional reaction-convection-diffusion problems. *J. Numer. Math.*, 12:193–205, 2004.

[108] T. Linß. Analysis of a fem for a coupled system of singularly perturbed reaction-diffusion equations. *Numer. Algorithms*, 50:283–291, 2009.

[109] O. A. Ladyzhenskaya, N. N., and Ural'tseva. *Linear and quasilinear elliptic equations*. Leon Ehrenpreis Academic Press, New York, 1968.

[110] C. De Boor and B. Swartz. Collocation at gaussian points. *SIAM J. Numer. Anal.*, 10: 582–606, 1973.

[111] M. J. Marsden. Quadratic spline interpolation. *Bull. Amer. Math. Soc.*, 80:903–906, 1974.

[112] E. P. Doolan, J. J. H. Miller, and W. H. A. Schilders. *Uniform Numerical Methods for Problems with Initial and Boundary Layers*, volume 1. Boole Press, Dublin, 1980.

[113] P. Farrell, A. Hegarty, J. M. Miller, E. O'Riordan, and G. I. Shishkin. *Robust Computational Techniques for Boundary Layers*. CRC Press, New York, 2000.

[114] J. L. Gracia and F. J. Lisbona. A uniformly convergent scheme for a system of reaction-diffusion equations. *J. Comput. Appl. Math.*, 206:1–16, 2007.

[115] L. Shishkina and G. Shishkin. Robust numerical method for a system of singularly perturbed parabolic reaction-diffusion equations on a rectangle. *Math. Model. Anal.*, 13:251–261, 2008.

[116] C. Clavero, J. L. Gracia, and F. Lisbona. Second order uniform approximations for the solution of time dependent singularly perturbed reaction-diffusion systems. *Int. J. Numer. Anal. Model.*, 7:428–443, 2010.

[117] S. Kumar and S. C. S. Rao. A robust overlapping schwarz domain decomposition algorithm for time-dependent singularly perturbed reaction-diffusion problems. *J. Comput. Appl. Math.*, 261:127–138, 2014.

[118] V. Shanthi and N. Ramanujam. A numerical method for boundary value problems for singularly perturbed fourth-order ordinary differential equations. *Appl. Math. Comput.*, 129:269–294, 2002.

[119] N. Ramanujam and U. N. Srivastava. Singular perturbation problems for systems of partial differential equations of parabolic type. *Funkcialaj Ekvacioj*, 23:245–258, 1980.

[120] P. Das and S. Natesan. Adaptive mesh generation for singularly perturbed fourth-order ordinary differential equations. *Int. J. Comput. Math.*, 92:562–578, 2015.

[121] Z. Cen, A. Xu, and A. Le. A high-order finite difference scheme for a singularly perturbed fourth-order ordinary differential equation. *Int. J. Comput. Math.*, 95:1806–1819, 2018.

[122] C. De Boor. Good approximation by splines with variable knots. ii. In *Conference on the Numerical Solution of Differential Equations, Lecture Notes in Mathematics Vol. 363*, pages 12–20, Berlin, 1974. Springer.

[123] V. Shanthi and N. Ramanujam. Computational methods for reaction-diffusion problems for fourth order ordinary differential equations with a small parameter at the highest derivative. *Appl. Math. Comput.*, 147:97–113, 2002.

[124] V. Shanthi and N. Ramanujam. A boundary value technique for boundary value problems for singularly perturbed fourth-order ordinary differential equations. *Comput. Math. Appl.*, 47:1673–1688, 2004.

[125] T. Linss. Analysis of a system of singularly perturbed convection-diffusion equations with strong coupling. *SIAM J. Numer. Anal.*, 47:1847–1862, 2009.

[126] R. E. Ewing. *The Mathematics of Reservoir Simulation*. SIAM, Philadelphia, 1983.

[127] B. Buffoni, A. R. Champneys, and J. F. Toland. Bifurcation and coalescence of a plethora of homoclinic orbits for a hamiltonian system. *J. Dyn. Differ. Equ.*, 8:221–279, 1996.

[128] Y. Chen and P. J. McKenna. Traveling waves in a nonlinearly suspended beam: theoretical results and numerical observations. *J. Differ. Equ.*, 136:325–355, 1997.

[129] G. T. Dee and W. van Saarloos. Bistable systems with propagating fronts leading to pattern formation. *Phys. Rev. Lett.*, 60:2641–2644, 1988.

[130] J. Swift and P. C. Hohenberg. Hydrodynamic fluctuations at the convective instability. *Phys. Rev. A*, 15:319–328, 1977.

[131] C. W. Soh. Euler-bernoulli beams from a symmetry standpoint-characterization of equivalent equations. *J. Math. Anal.*, 345:387–395, 2008.

[132] V. Shanthi and N. Ramanujam. Asymptotic numerical methods for singularly perturbed fourth order ordinary differential equations of convection-diffusion type. *Appl. Math. Comput.*, 133:559–579, 2002.

[133] V. Shanthi and N. Ramanujam. Asymptotic numerical methods for singularly perturbed fourth-order ordinary differential equations of reaction-diffusion type. *Comput. Math. Appl.*, 46:463–478, 2003.

[134] S. Singh and D. Kumar. Spline-based parameter-uniform scheme for fourth-order singularly perturbed differential equations. *J. Math. Chem.*, 60:1872–1902, 2022.

[135] M. Chandru and V. Shanthi. An asymptotic numerical method for singularly perturbed fourth order ode of convection-diffusion type turning point problem. *Neural Parallel Sci. Comput.*, 24:473–488, 2016.

[136] Z. Cen. Parameter-uniform finite difference scheme for a system of coupled singularly perturbed convection–diffusion equations. *Int. J. Comput. Math.*, 82:177–192, 2005.

[137] R. M. Priyadharshini, N. Ramanujam, and V. Shanthi. Approximation of derivative in a system of singularly perturbed convection-diffusion equations. *J. Appl. Math. Comput.*, 29:137–151, 2009.

[138] S. Valarmathi and N. Ramanujam. An asymptotic numerical method for singularly perturbed third-order ordinary differential equations of convection-diffusion type. *Comput. Math. Appl.*, 44:693–710, 2002.

[139] J. M. Ortega and W. C. Rheinboldt. *Iterative Solution of Nonlinear Equations in Several Variables*. SIAM, Philadelphia, 2000.

[140] F. A. Howes. The asymptotic solution of a class of third-order boundary value problem arising in the theory of thin film flow. *SIAM J. Appl. Math.*, 43:993–1004, 1983.

[141] M. Feckan. Singularly perturbed higher order boundary value problems. *J. Differ. Equ.*, 3:79–102, 1994.

[142] A. A. Bobodzhanov and V. F. Safonov. Singularly perturbed integro-differential equations with diagonal degeneration of the kernel in reverse time. *Differential Equ.*, 40:120–127, 2004.

[143] M. Shivhare and P. C. Podila. Numerical study of two-parameter singularly perturbed problem in two dimensions on an exponentially graded mesh. *Comput. Appl. Math.*, 41:81, 2022.

[144] K. Kumar, P. C. Podila, and J. Vigo-Aguiar. Numerical solution of time-fractional singularly perturbed convection–diffusion problems with a delay in time. *Math. Methods Appl. Sci.*, 44:3080–3097, 2021.

[145] D. Kumar and P. Kumari. Parameter-uniform numerical treatment of singularly perturbed initial-boundary value problems with large delay. *Appl. Numer. Math.*, 153: 412–429, 2020.

[146] M. Kudu, I. Amirali, and G. M.Amiraliyev. A finite-difference method for a singularly perturbed delay integro-differential equation. *J. Comput. Appl. Math.*, 308:379–390, 2016.

List of research publications

Publications from the Thesis

1. S. Singh, D. Kumar, H. Ramos, A uniformly convergent quadratic B-spline based scheme for singularly perturbed degenerate parabolic problems, Math. Comput. Simul., 195 (2022), 88–106.

2. S. Singh, D. Kumar, H. Ramos, An efficient parameter uniform spline-based technique for singularly perturbed weakly coupled reaction-diffusion systems, J. Appl. Anal. Comput., 2023, 13 (4): 2203–l2228. doi: 10.11948/20220446

3. S. Singh, D. Kumar, Spline-based parameter-uniform scheme for fourth-order singularly perturbed differential equations, J. Math. Chem., 60 (2022), 1872–1902.

4. S. Singh, D. Kumar, J. Vigo-Aguiar, A robust numerical technique for weakly coupled system of parabolic singularly perturbed reaction-diffusion equations, J. Math. Chem., (2023). https://doi.org/10.1007/s10910-023-01464-w.

5. S. Singh, D. Kumar, V. Shanthi, Uniformly convergent scheme for fourth-order singularly perturbed convection-diffusion ODE, Appl. Numer. Math., 186 (2023), 334–357.

Other Publications

1. S. Singh, D. Kumar, Parameter uniform numerical method for a system of singularly perturbed parabolic convection–diffusion equations, Math. Comput. Simul., 212 (2023), 360–381.

2. S. Singh, R. Choudhary, D. Kumar, An efficient numerical technique for two-parameter singularly perturbed problems having discontinuity in convection coefficient and source term, Comp. Appl. Math., 42 (2023), https://doi.org/10.1007/s40314-023-02196-y

3. S. Singh, D. Kumar, K. Deswal, Trigonometric B-spline based ε-uniform scheme for singularly perturbed problems with Robin boundary conditions, J. Difference Equ. Appl., 28 (2022), 924–945.

4. R. Choudhary, D. Kumar, S. Singh, Second-order convergent scheme for time-fractional partial differential equations with a delay in time, J. Math. Chem., 61 (2023), 21–46.

5. D. Kumar, K. Deswal, S. Singh, Wavelet-based approximation with nonstandard finite difference scheme for singularly perturbed partial integrodifferential equations, Comp. Appl. Math., 41, 341 (2022).

6. R. Choudhary, S. Singh, D. Kumar, A second-order numerical scheme for the time-fractional partial differential equations with a time delay, Comp. Appl. Math., 41, 114 (2022).

7. R. Choudhary, S. Singh, D. Kumar, A high-order numerical technique for generalized time-fractional Fisher's equation, Math. Methods Appl. Sci., 46, 16050–16071 (2023).

8. D. Kumar, K. Deswal, S. Singh, A highly accurate algorithm for retrieving the predicted behavior of problems with piecewise-smooth initial data, Appl. Numer. Math., 173 (2022), 279–294.

9. S. Singh, P. Kumari, D. Kumar, An effective numerical approach for two parameter time-delayed singularly perturbed problems, Comput. Appl. Math., 41, 337 (2022).

10. R. Choudhary, S. Singh, P. Das, D. Kumar, A higher-order stable numerical approximation for time-fractional non-linear Kuramoto-Sivashinsky equation based on quintic $\mathfrak{B}$-spline, Math. Methods Appl. Sci. (Accepted).

11. R. Chawla, D. Kumar, S. Singh, A second-order scheme for the generalized time-fractional Burgers' equation, J. Comput. Nonlinear Dynam., 2023 (Accepted).

Conferences /Workshops attended

Conferences

1. International Conference on Advances in Mechanics, Modelling, Computing and Statistics held at Department of Mathematics, BITS Pilani, Pilani Campus in 2022. **(Presented)**

2. International conference on Mathematical Modelling, Applied Analysis and Computation held at Department of Mathematics, JECRC University, Jaipur in 2022. **(Presented)**

3. International Conference on Dynamical Systems and Numerical Methods, Department of Mathematics, Jamia Millia Islamia, New Delhi in 2022. **(Presented)**

4. International Conference on Differential Equations and Control Problems, held at Department of Mathematics, IIT Mandi, Mandi in 2023. **(Presented)**

Workshops

1. One week online course on "Computational Mathematical Software (Mathematica, Maxima, & R)" organized by the department of mathematics, Atma Ram Sanatan Dharma College, University of Delhi in 2022.

2. A five days workshop on "Advanced Topics in Mathematics-2021", organized by the centre for applied mathematics, Dr. SPM International Institute of Information Technology, Naya Raipur in 2021.

3. One week online faculty developement programme on "Mathematical Analysis and its Applications" organized by Vivekananda College, University of Delhi in collaboration with Mahatma Hansraj Faculty Development Centre Hansraj College, University of Delhi in 2021.

4. International workshop on “Wavelets and its Applications: Image Processing, Data Sciences and PDEs” organized by the department of mathematics Manav Rachna University, Faridabad in collaboration with department of mathematics IIT Indore in 2021.

5. International webinar on “Numerical Explosive Combustion Models: Multiplicity and Simulations” organized by the department of mathematics Manav Rachna University, Faridabad in 2022.

Biography of the Candidate

Mr. Satpal Singh received his B.Sc. degree from Jai Narain Vyas University, Jodhpur and M.Sc. degree in Mathematics from Maharishi Dayanand Saraswati University, Ajmer. In 2020, he joined as a full-time Ph.D. scholar in the Department of Mathematics at Birla Institute of Technology and Science (BITS) Pilani, India under the supervision of Prof. Devendra Kumar. His research interests include numerical approaches for linear, non-linear, and free boundary PDEs in singular perturbation theory. He's also working on fractional order PDEs. He has served as a teaching assistant for the various courses of mathematics at BITS Pilani, Pilani Campus. More about his research contributions can be found at `scholar.google.com`. Contact him at `p20190425@pilani.bits-pilani.ac.in`.

Biography of the Supervisor

Dr. Devendra Kumar is the current head and professor in the Department of Mathematics at Birla Institute of Technology and Science Pilani, Pilani campus. He has earned his Ph.D. degree from the Department of Mathematics of Indian Institute of Technology Kanpur. His research interests include the development of numerical methods for initial/boundary value problems for ordinary differential equations, partial differential equations, delay/advanced differential equations, singularly perturbed problems, fractional-order differential equations, etc. More on his research contributions can be found at
`https://www.bits-pilani.ac.in/pilani/dkumar/Profile`.
Contact him at `dkumar@pilani.bits-pilani.ac.in`.